

**LIPOSOMES: FORMULATION AND CHARACTERISATION AS CONTRAST
AGENTS AND AS VACCINE DELIVERY SYSTEMS**

RANDIP KAUR

Doctor of Philosophy

ASTON UNIVERSITY

April 2011

This copy of the thesis has been supplied on condition that anyone who consults it is understood to recognise that its copyright rests with its author and that no quotation from the thesis and no information derived from it may be published without proper acknowledgement.

Aston University
**LIPOSOMES: FORMULATION AND CHARACTERISATION AS CONTRAST AGENTS AND AS
VACCINE DELIVERY SYSTEMS**

Randip Kaur
Doctor of Philosophy
2011

Abstract

Liposome systems are well reported for their activity as vaccine adjuvants; however novel lipid-based microbubbles have also been reported to enhance the targeting of antigens into dendritic cells (DCs) in cancer immunotherapy (Suzuki et al 2009). This research initially focused on the formulation of gas-filled lipid coated microbubbles and their potential activation of macrophages using *in vitro* models. Further studies in the thesis concentrated on aqueous-filled liposomes as vaccine delivery systems.

Initial work involved formulating and characterising four different methods of producing lipid-coated microbubbles (sometimes referred to as gas-filled liposomes), by homogenisation, sonication, a gas-releasing chemical reaction and agitation/pressurisation in terms of stability and physico-chemical characteristics. Two of the preparations were tested as pressure probes in MRI studies. The first preparation composed of a standard phospholipid (DSPC) filled with air or nitrogen (N₂), whilst in the second method the microbubbles were composed of a fluorinated phospholipid (*F*-GPC) filled with a fluorocarbon saturated gas. The studies showed that whilst maintaining high sensitivity, a novel contrast agent which allows stable MRI measurements of fluid pressure over time, could be produced using lipid-coated microbubbles. The *F*-GPC microbubbles were found to withstand pressures up to 2.6 bar with minimal damage as opposed to the DSPC microbubbles, which were damaged at above 1.3 bar. However, it was also found that DSPC-filled with N₂ microbubbles were also extremely robust to pressure and their performance was similar to that of *F*-GPC based microbubbles. Following on from the MRI studies, the DSPC-air and N₂ filled lipid-based microbubbles were assessed for their potential activation of macrophages using *in vitro* models and compared to equivalent aqueous-filled liposomes. The microbubble formulations did not stimulate macrophage uptake, so studies thereafter focused on aqueous-filled liposomes.

Further studies concentrated on formulating and characterising, both physico-chemically and immunologically, cationic liposomes based on the potent adjuvant dimethyldioctadecylammonium (DDA) and immunomodulatory trehalose dibehenate (TDB) with the addition of polyethylene glycol (PEG). One of the proposed hypotheses for the mechanism behind the immunostimulatory effect obtained with DDA:TDB is the 'depot effect' in which the liposomal carrier helps to retain the antigen at the injection site thereby increasing the time of vaccine exposure to the immune cells. The depot effect has been suggested to be primarily due to their cationic nature. Results reported within this thesis demonstrate that higher levels of PEG i.e. 25 % were able to significantly inhibit the formation of a liposome depot at the injection site and also severely limit the retention of antigen at the site. This therefore resulted in a faster drainage of the liposomes from the site of injection.

The versatility of cationic liposomes based on DDA:TDB in combination with different immunostimulatory ligands including, polyinosinic-polycytidylic acid (poly (I:C), TLR 3 ligand), and CpG (TLR 9 ligand) either entrapped within the vesicles or adsorbed onto the liposome surface was investigated for immunogenic capacity as vaccine adjuvants. Small unilamellar (SUV) DDA:TDB vesicles (20-100 nm native size) with protein antigen adsorbed to the vesicle surface were the most potent in inducing both T cell (7-fold increase) and antibody (up to 2 log increase) antigen specific responses. The addition of TLR agonists poly(I:C) and CpG to SUV liposomes had small or no effect on their adjuvanticity.

Finally, threitol ceramide (ThrCer), a new immunostimulatory agent, was incorporated into the bilayers of liposomes composed of DDA or DSPC to investigate the uptake of ThrCer, by dendritic cells (DCs), and presentation on CD1d molecules to invariant natural killer T cells. These systems were prepared both as multilamellar vesicles (MLV) and Small unilamellar (SUV). It was demonstrated that the IFN- γ secretion was higher for DDA SUV liposome formulation ($p < 0.05$), suggesting that ThrCer encapsulation in this liposome formulation resulted in a higher uptake by DCs.

Key words: liposome; lipid-coated microbubbles; contrast agent; vaccine; protein; immunostimulatory.

Acknowledgements

Firstly, I would like to express my sincere gratitude to my supervisor Prof Yvonne Perrie for the continuous support of my PhD study and research. Her guidance helped me in all the time of research and writing of this thesis.

I would also like to acknowledge the support of our collaborators, Dr Anita Milicic at the Jenner Institute, University of Oxford, Dr Martin Bencsik from the School of Science and Technology, Nottingham Trent University and Prof Gurdyal Besra from the School of Biosciences, University of Birmingham.

I would like to thank all the others in the drug delivery group at Aston University for their support, the lab technicians, Jiteen, Chris and also Mel and Brian from the biomedical facility for the enormous help they have given with regard to all the equipment and materials I needed throughout this project. I would also like to thank Dr Vincent Bramwell for his invaluable help and support, particularly with regards to the immunological assays and interpretation aspects of this study.

Last but by no means least, I would like to thank my family and friends; you have all been so supportive throughout the years, thank you so much. I am truly and earnestly grateful for all your support, encouragement, love and praise. I would like to particularly thank my brother Amanjit for all the computer and diagram rescue assistance and my sister's Rumjit and Satdip for providing encouragement. Lastly, and most importantly, I wish to thank my parents, Kamaljit Sunner and Tarlochan Sunner. They have always supported and encouraged me to do my best in all matters of life. To them I dedicate this thesis.

Publications resulting from this and related work

Kaur, R., Bramwell, V., Perrie, Y. (2011) Steric stabilisation of the DDA:TDB delivery system using polyethylene glycol. (*in preparation*).

Kaur, R., Milicic, A., Reyes-Sandoval, A., Hill, A., Perrie, Y. (2011) Incorporation of immunostimulatory components to the DDA:TDB adjuvant delivery. (*in preparation*).

Kaur, R., Chen, J., Dawoodji, A., Cerundolo, V., Garcia-Diaz, Y. R., Wojno, J., Cox, L. R., Besra, G. S., Moghaddam, B., Perrie, Y. (2011) Preparation, characterisation and entrapment of a non-glycosidic threitol ceramide into liposomes for presentation to invariant natural killer T cells. *Journal of Pharmaceutical Sciences*. Accepted.

Bibi, S., **Kaur, R.**, Henriksen-Lacey, M., McNeil, S.E., Wilkhu, J., Lattmann, E., Christensen, D., Mohammed, A.R., Perrie, Y. (2010) Microscopy imaging of liposomes: From coverslips to environmental SEM. *International Journal of Pharmaceutics*. Accepted.

Kaur, R., Morris, R., Bencsik, M., Vangala, A., Rades, T., Perrie, Y. (2009) Development of a novel magnetic resonance imaging contrast agent for pressure measurements using lipid-coated microbubbles. *Journal of Biomedical Nanotechnology*. 5: 1-9.

Related abstracts, posters and presentations

Kaur, R., Chen, J., Dawoodji, A., Cerundolo, V., Garcia-Diaz, Y. R., Wojno, J., Cox, L. R., Besra, G. S., Moghaddam, B., Perrie, Y. (2011) Preparation, characterisation and entrapment of a non-glycosidic threitol ceramide into liposomes for presentation to invariant natural killer T cells. *38th Annual Meeting & Exposition of the Controlled Release Society Conference, Maryland, USA*. Abstract #100129. Podium presentation.

Kaur, R., Bramwell, V., Perrie, Y. (2011) Steric stabilisation of the DDA:TDB delivery system using polyethylene glycol. *New TBVac, Copenhagen, Denmark*. Podium presentation.

Milicic, A., **Kaur, R.**, Reyes-Sandoval, A., Honeycutt, J., Perrie, Y., Hill, A. V. S. (2010) DDA:TDB cationic liposomes as protein vaccine adjuvants. *British Society for Immunology, Liverpool*.

Kaur, R., Milicic, A., Reyes-Sandoval, A., Hill, A. V. S., Perrie, Y. (2010) Incorporation of immunostimulatory components to the DDA:TDB adjuvant delivery. *37th Annual Meeting and Exposition of the Controlled Release Society Conference, Portland Oregon, USA*. Abstract #503.

Kaur, R., Morris, R., Bencsik, M., Vangala, A., Rades, T., Perrie, Y. (2009) Development of a novel magnetic resonance imaging contrast agent for pressure measurements using lipid-coated microbubbles: effect of the filling gas. *4th International Liposome Society Conference, London*.

Kaur, R., Morris, R., Bencsik, M., Vangala, A., Rades, T., Perrie, Y. (2009) Development of a novel magnetic resonance imaging contrast agent for pressure measurements using lipid coated gas filled microbubbles. *36th Annual Meeting and Exposition of the Controlled Release Society Conference, Copenhagen, Denmark*. Abstract #811.

Kaur, R., Morris, R., Bencsik, M., Vangala, A., Rades, T., Perrie, Y. (2009) Investigating the potential of gas-filled lipid-coated microbubbles as vaccine adjuvants. *Pharm. Pharmacol.* 61: (Supp/1) A-44.

Kaur, R., Morris, R., Bencsik, M., Vangala, A., Rades, T., Perrie, Y. (2009) Lipid-coated gas filled microbubbles in the development of a novel magnetic resonance imaging contrast agent for pressure measurements. *15th UKICRS Symposium, Kings College London*.

Kaur, R., Morris, R., Bencsik, M., Vangala, A., Rades, T., Perrie, Y. (2009) Development of a novel magnetic resonance imaging contrast agent for pressure measurements using lipid-coated microbubbles: effect of air and N₂ as filling gas. *Elsinore meetings on Infection Immunity. Helsingor, Denmark*.

Kaur, R., Morris, R., Bencsik, M., Vangala, A., Rades, T., Perrie, Y. (2009) Development of a novel magnetic resonance imaging contrast agent for pressure measurements using lipid-coated microbubbles: effect of the filling gas. *Young Pharmaceutical Scientist, Nice, France*.

Morris, R., Bencsik, M., Nestle, N., **Kaur, R.**, Galvosas, P., Perrie, Y. (2008) MRI Pressure Measurement in Novel homogeneous soft solids. *9th Magnetic Resonance in Porous Media conference (MRPM9), Boston*.

Kaur, R., Morris, R., Cave, G., Bencsik, M., Krafft, M. P., Waton, G., Rades, T., Perrie, Y. (2008) Development of novel magnetic resonance imaging contrast agent for pressure measurements using microbubbles. *NHS Pharmaceutical Quality Assurance Service Conference, Manchester*.

Kaur, R., Morris, R., Cave, G., Bencsik, M., Krafft, M. P., Waton, G., Rades, T., Perrie, Y. (2008) Gas-filled liposomes: development and optimisation as ultrasound contrast agents. *Pharm. Pharmacol.* 60: (Supp/1) A-56.

Contents

Title	Page
Abstract	2
Acknowledgments	3
List of publications	4
Contents	6
List of figures	14
List of tables	19
Abbreviations	21
Chapter 1 General introduction	23
1.1 Liposomes	24
1.2 Structure and biophysical properties	26
1.2.1 Liposome composition	29
1.2.2 Liposome morphology	31
1.2.2.1 Lipid hydration method	31
1.2.2.2 Sonication	31
1.2.2.3 Reverse-phase evaporation method	32
1.2.2.4 Ether vaporisation method	32
1.2.2.5 Dehydration-rehydration method	33
1.3 Application of liposomes	33
1.3.1 Liposomes as radiodiagnostic carriers	34
1.3.1.1 Lipid-coated microbubbles in magnetic resonance imaging	34
1.3.2 Liposomes as vaccine adjuvants	35
1.3.2.1 Vaccines	35
1.3.2.2 Innate and adaptive immune responses	36
1.3.3 Types of Vaccines	38
1.3.3.1 Live Attenuated Vaccines	38
1.3.3.2 Inactivated Vaccines	38
1.3.3.3 Toxoids	39
1.3.3.4 Subunit Vaccines	39
1.3.4 Improvement of the potency of subunit vaccines	39

1.3.5 Adjuvants	40
<i>1.3.5.1 Role of adjuvants in the immune responses</i>	41
1.3.6 Classification of adjuvants	41
<i>1.3.6.1 Alum</i>	42
<i>1.3.6.2 Freund's adjuvant</i>	43
<i>1.3.6.3 CpG (cytidine-phosphate-guanosine)</i>	43
<i>1.3.6.4 Liposomes</i>	44
1.4 Liposomes delivery of protein antigens	44
1.4.1 Liposome composition: cationic lipids and immunomodulators	45
1.4.2 Liposome preparation: surface adsorbed versus entrapped antigen	46
1.5 Aims and objectives	48

Chapter 2 Formulation, characterisation and application of lipid-coated

microbubbles	49
2.1 Introduction	50
2.1.1 Microbubbles and ultrasound	51
<i>2.1.1.1 Classification of ultrasound contrast agents</i>	53
2.1.2 Microbubbles and magnetic resonance imaging (MRI)	56
2.2 Aims and objectives	58
2.3 Materials and Methods	59
2.3.1 Materials	59
2.3.2 Methods	60
<i>2.3.2.1 Preparation of air-filled microbubbles by homogenisation</i>	60
<i>2.3.2.2 Preparation of N₂-filled microbubbles by homogenisation</i>	61
<i>2.3.2.3 Morphological analysis using microscopic imaging analysis</i>	61
<i>2.3.2.4 Fluorescent staining of microbubbles</i>	61
<i>2.3.2.5 Production of multilamellar vesicles (MLV)</i>	61
<i>2.3.2.6 Production of small unilamellar vesicles (SUV)</i>	63
<i>2.3.2.7 Preparation of microbubbles by a gas releasing chemical reaction</i>	63
<i>2.3.2.8 Preparation of microbubbles by sonication</i>	63
<i>2.3.2.9 Preparation of bubble liposomes</i>	64
<i>2.3.2.10 Determination of size and zeta potential</i>	65

2.3.2.11 <i>Colloidal stability and Polyelectrolyte theory</i>	66
2.3.2.12 <i>MRI studies - preparation of microbubbles as pressure probes for MRI</i>	68
2.3.2.13 <i>Statistical analysis</i>	69
2.4 Results and discussion	70
2.4.1 Particle size analysis of lipid-coated microbubbles	70
2.4.2 Preparation of microbubbles by homogenisation	71
2.4.2.1 <i>Stability of microbubbles prepared by homogenisation</i>	75
2.4.3 Preparation of microbubbles by a gas-releasing chemical reaction	79
2.4.4 Preparation of microbubbles by sonication	85
2.4.5 Preparation of ‘bubble liposomes’	86
2.4.6 Formulations to proceed forward into subsequent studies	92
2.4.7 MRI studies - stability of the microbubbles as pressure probes	93
2.4.7.1 <i>Comparison of stability of air-filled DSPC and F-GPC microbubbles</i>	93
2.4.7.2 <i>Comparison of air-filled and N₂-filled DSPC microbubbles as pressure probes</i>	95
2.5 Conclusion	98

Chapter 3 Cellular responses of macrophages to liposomes and lipid-coated

microbubbles: <i>in vitro</i> studies	100
3.1 Introduction	101
3.1.1 Mononuclear phagocyte system (MPS)	101
3.1.2 Uptake of liposomes by macrophages	102
3.2 Aims and objectives	103
3.3 Materials and methods	106
3.3.1 Materials	106
3.3.2 Methods	107
3.3.2.1 <i>Resuscitation of frozen BALB/c cell line</i>	107
3.3.2.2 <i>Cell quantification</i>	107
3.3.2.3 <i>Optimisation of cell number</i>	107
3.3.2.4 <i>Optimisation of liposome concentration</i>	108
3.3.2.5 <i>Preparation for assays</i>	108

3.3.2.6 <i>Cell proliferation</i>	109
3.3.2.7 <i>Phagocytic activities</i>	109
3.2.2.8 <i>Statistical analyses</i>	111
3.4 Results and discussion	112
3.4.1 Optimisation of cell number	112
3.4.2 Optimisation of liposome concentration	113
3.4.3 Characterisation of liposomes	114
3.4.4 Effect of liposome composition on cell viability	116
3.4.5 Effect of microbubbles on cell viability	121
3.4.6 Phagocytic activities	122
3.5 Conclusion	125
Chapter 4 Investigating the use of liposomes as vaccine adjuvants	126
4.1 Introduction	127
4.1.1 Dimethyldioctadecylammonium and α,α' -trehalose 6, 6'-dibehenate	127
4.1.2 Antigen delivery system and immunostimulator	130
4.1.3 Improving immunogenicity through modification of the liposomes composition	131
4.1.4 Steric stabilisation using polyethylene glycol (PEG)	132
4.2 Aims and objectives	134
4.3 Materials and methods	135
4.3.1 Materials	135
4.3.2 Method	137
4.3.2.1 <i>Lipid-hydration method</i>	137
4.3.2.2 <i>Small unilamellar vesicles</i>	138
4.3.2.3 <i>Dehydration-rehydration method</i>	138
4.3.2.4 <i>Determination of vesicle size and zeta potential</i>	140
4.3.2.5 <i>Sodium dodecyl sulphate polyacrylamide gel-electrophoresis</i>	140
4.3.2.6 <i>Quantification of non-adsorbed antigen via the BCA Assay</i>	141
4.3.2.7 <i>Radiolabeling of Ag85B-ESAT-6 antigen</i>	141
4.3.2.8 <i>Ag85B-ESAT-6 antigen adsorption / entrapment to cationic liposomes</i>	142

4.3.2.9 <i>Ag85B-ESAT-6 antigen retention in simulated in vivo conditions</i>	143
4.3.2.10 <i>Biodistribution of cationic liposomes adsorbing and entrapping Ag85B-ESAT-6 antigen</i>	143
4.3.2.11 <i>Immunological analysis of liposome formulations</i>	144
4.3.2.12 <i>Analysis of Ag85B-ESAT-6 specific antibody isotypes</i>	144
4.3.2.13 <i>Spleen cell culture preparation</i>	146
4.3.2.14 <i>Analysis of spleen cell proliferation</i>	146
4.3.2.15 <i>Analysis of cytokine production</i>	147
4.3.2.16 <i>Freeze-fracture microscopy</i>	148
4.3.2.17 <i>Statistical analyses</i>	149
4.4 Results and discussion	150
4.4.1 The effect of PEGylation DDA:TDB MLV characteristics	150
4.4.2 The effect of antigen adsorption onto MLV DDA:TDB	152
4.4.3 Adsorption of antigen to MLV DDA:TDB	154
4.4.3.1 <i>Adsorption of OVA</i>	154
4.4.3.2 <i>Adsorption of Ag85B-ESAT-6 antigen</i>	159
4.4.4 Interactions of MLV liposomes with serum proteins	160
4.4.4.1 <i>Particle size and zeta potential</i>	160
4.4.4.2 <i>Antigen retention in the presence of biological moieties</i>	162
4.4.5 Entrapment of antigen within DRV cationic liposomes	165
4.4.5.1 <i>Comparison of size and zeta potential of pegylated DRV</i>	167
4.4.5.2 <i>The effect of PEGylation DDA:TDB SUV characteristics</i>	170
4.4.5.3 <i>Comparison of MLV, SUV and DRV antigen loading and retentions</i>	171
4.4.5.4 <i>Addition of cryoprotectant: a modified DRV procedure for the formation of small liposomes</i>	176
4.4.6 Biodistribution studies of liposomes and their associated antigens	178
4.4.6.1 <i>The effect of PEGylation on MLV retention at the site of injection</i>	179
4.4.6.2 <i>The effect of PEGylation on SUV retention at the site of injection</i>	181

4.4.6.3 <i>The effect of entrapping antigen within the liposomal systems on their biodistribution</i>	185
4.4.7 Detection of vaccine components in the popliteal lymph nodes	190
4.4.7.1 <i>Monocyte influx to the SOI as determined by pontamine blue staining</i>	193
4.4.8 Synopsis of the biodistribution data	195
4.4.9 Testing the potential of the formulations as vaccine adjuvants	195
4.4.9.1 <i>Antibody production</i>	196
4.4.9.2 <i>Cytokine production</i>	198
4.4.9.3 <i>Cell proliferation</i>	203
4.5 Conclusion	205

Chapter 5 Incorporation of immunostimulatory components to the DDA:TDB adjuvant delivery system	207
5.1 Introduction	208
5.1.1 Toll like receptors (TLRs)	208
5.1.1.1 <i>Poly(I:C) - TLR 3 agonist</i>	209
5.1.1.2 <i>Unmethylated CpG DNA - TLR 9 agonist</i>	210
5.2 Aims and objectives	211
5.3 Materials and Methods	212
5.3.1 Materials	212
5.3.2 Methods	213
5.3.2.1 <i>Lipid hydration method</i>	213
5.3.2.2 <i>Small unilamellar vesicles</i>	213
5.3.2.3 <i>Dehydration-rehydration method</i>	214
5.3.2.4 <i>Determination of vesicle size and zeta potential</i>	214
5.3.2.5 <i>Trypsination experiment</i>	214
5.3.2.6 <i>OVA antigen adsorption/entrapment to cationic liposomes</i>	215
5.3.2.7 <i>OVA antigen retention in simulated in vivo conditions</i>	216
5.3.2.8 <i>Oligreen assay</i>	216
5.3.2.9 <i>Immunisation studies</i>	217
5.3.2.10 <i>Analysis of anti-OVA antibody production following vaccination with the liposomal formulations</i>	218

5.3.2.11 <i>Spleen ELISpot assay</i>	218
5.3.2.12 <i>Statistical analyses</i>	218
5.4 Results and discussion	219
5.4.1 Quantification of entrapped protein	219
5.4.2 Incorporation of immunostimulating compounds	222
5.4.2.1 <i>Multilamellar vesicles (MLV)</i>	222
5.4.2.2 <i>Dehydration-rehydration vesicles (DRV)</i>	224
5.4.2.3 <i>Small unilamellar vesicles (SUV)</i>	224
5.4.2.4 <i>Quantification of OVA adsorption and entrapment</i>	227
5.4.2.5 <i>Quantification of CpG using the OliGreen assay</i>	228
5.4.3 Immunisation studies	231
5.4.3.1 <i>Antigen-specific CD4⁺ T-cells in the spleen and peripheral blood</i>	231
5.4.3.2 <i>Antibody responses</i>	235
5.5 Conclusion	237

Chapter 6 Preparation, characterisation and entrapment of a non-glycosidic threitol ceramide into liposomes for presentation to invariant natural killer T cells	238
6.1 Introduction	239
6.1.1 Incorporation of ThrCer into liposomes	241
6.2 Aims and objectives	242
6.3 Materials and Methods	243
6.3.1 Materials	243
6.3.2 Methods	244
6.3.2.1 <i>Preparation of liposomes</i>	244
6.3.2.2 <i>Measuring entrapment of ThrCer in DSPC and DDA liposomes</i>	244
6.3.2.3 <i>ThrCer retention in simulated in vivo conditions</i>	245
6.3.2.4 <i>Determination of liposome size</i>	245
6.3.2.5 <i>Langmuir-Blodgett isotherms</i>	246
6.3.2.6 <i>Liposome presentation to invariant natural killer T cells</i>	247

6.3.2.7 <i>IFN-γELISA</i>	247
6.3.2.8 <i>Phenotyping of APC</i>	248
6.3.2.9 <i>Injection of ThrCer liposome to assess DC maturation in vivo</i>	248
6.3.2.10 <i>Statistical analysis</i>	249
6.4 Results and discussion	250
6.4.1 Characterisation of ThrCer liposomes	250
6.4.2 Determination of vesicle stability over time	252
6.4.3 ThrCer is retained in liposomes under simulated <i>in vivo</i> conditions	255
6.4.4 Langmuir-Blodgett isotherms	257
6.4.5 Maturation effect on DCs	262
6.4.6 Uptake of ThrCer by DCs	262
6.4.7 DC maturation <i>in vivo</i>	265
6.5 Conclusion	267
Chapter 7 General discussion	269
7.1 Magnetic resonance imaging (MRI) contrast agent for imaging of fluid pressure	270
7.2 Lipid-coated microbubbles as vaccine adjuvants	272
7.3 Aqueous-filled liposomes as vaccine adjuvants	272
7.4 Addition of immunostimulatory components CpG and poly(I:C)	274
7.5 Incorporation of ThrCer into liposomes for presentation to <i>i</i> NKT cells	274
7.6 Further studies	275
Chapter 8 References	276

List of figures

Chapter 1	General introduction	Page
Figure 1.1	Schematic representation of a liposome	27
Figure 1.2	Schematic representation of three types of liposomes	30
Figure 1.3	Schematic representation of the immune response	37
Chapter 2	Formulation, characterisation and application of lipid-coated microbubbles	
Figure 2.1	Schematic representation of a lipid-coated microbubble	51
Figure 2.2	Schematic representation of recovery of oil from porous rock	57
Figure 2.3	Schematic representation of microbubble formation by the homogenisation process	60
Figure 2.4	Schematic representation of microbubble formation by the sonication process	64
Figure 2.5	Potential energy as a function of separation between the surfaces of charged colloidal particles	67
Figure 2.6	Schematic representation of the MRI experiment	69
Figure 2.7	Schematic representation of phase transition temperature of lipids	72
Figure 2.8	Microscopic images of microbubbles	74
Figure 2.9	Fluorescent staining of microbubbles	75
Figure 2.10	Size (μm) of DSPC based microbubbles supplemented with cholesterol and/or PEG-distearate at 5 % and 10 % over 28 days	77
Figure 2.11	Foam volume (ml) of DSPC based microbubbles supplemented with cholesterol and/or PEG-distearate at 5% and 10% over 28 days	78
Figure 2.12	Observation of foam volume (ml) of DSPC based microbubbles supplemented with cholesterol and/or PEG-distearate at 5 % and 10 % over 28 days	79
Figure 2.13	Images of microbubbles before and after pressurisation	80
Figure 2.14	Images of CO_2 microbubbles of various liposome formulations	82
Figure 2.15	Optical image of <i>F</i> -GPC (PFC) based microbubbles	86

Figure 2.16	Preparation of bubble liposomes	87
Figure 2.17	Images of various bubble liposome formulations	91
Figure 2.18	Comparison of stability of air-filled DSPC and <i>F</i> -GPC microbubbles	95
Figure 2.19	(A) Size (μm) and (B) foam volume (ml) of air-filled and N_2 -filled DSPC microbubbles over 28 days	96
Figure 2.20	Observation of foam volume (ml) of N_2 -filled DSPC microbubbles over 28 days	97
Figure 2.21	A comparison of the time course of the signal sensitivity for air and N_2 -filled DSPC microbubbles	98
Chapter 3	Cellular responses of macrophages to liposomes and lipid-coated microbubbles: <i>in vitro</i> studies	
Figure 3.1	A diagram of phagocytosis of particulate carriers by macrophages	103
Figure 3.2	Structure of MTS tetrazolium and its formazan product	104
Figure 3.3	Reaction of NAG assay and relative compounds	105
Figure 3.4	Effect of cell number of macrophages on absorbance	113
Figure 3.5	Effect of liposome concentration on cell viability	114
Figure 3.6	The effect of liposome composition on cell viability	118
Figure 3.7	The effect of cationic liposomes on cell viability	121
Figure 3.8	The effect of microbubbles on cell viability	122
Figure 3.9	Phagocytic activity (units/ml) measured for aqueous-filled liposomes	124
Figure 3.10	Phagocytic activity (units/ml) measured for microbubbles	124
Chapter 4	Investigating the use of liposomes as vaccine adjuvants	
Figure 4.1	Structure of dimethyldioctadecylammonium (DDA)	129
Figure 4.2	Structure of $\alpha\alpha'$ -trehalose 6,6'-dibehenate (TDB)	130
Figure 4.3	Chemical structures of distearoylphosphatidylcholine (DSPC), distearoylphosphatidylethanolamine after conjugation with poly (ethylene glycol) (PEG) (DSPE-PEG)	133
Figure 4.4	Schematic representation of the lipid-hydration method	138
Figure 4.5	Schematic representation of the dehydration-rehydration method	139

Figure 4.6	Time-points for the biodistribution study, days 1, 4 and 14 post injection (p.i)	144
Figure 4.7	Schematic representation of analysis of antibody production by enzyme-linked immunosorbent assay (ELISA)	145
Figure 4.8	Schematic representation spleen cell proliferation analysis	147
Figure 4.9	Schematic representation of cytokine detection using DuoSet [®] capture ELISA kits	148
Figure 4.10	(A) Vesicle size (nm) (bars) and polydispersity (values) and (B) zeta-potential (mV) of DDA:TDB, 5, 10, 25 % PEG liposomes	150
Figure 4.11	(A) Vesicle size (nm) and (B) zeta-potential (mV) of DDA:TDB, 5, 10, 25 % PEG liposomes following the addition of OVA	155
Figure 4.12	Adsorption of OVA	158
Figure 4.13	Quantification of antigen adsorption of DDA:TDB, 5, 10, 25 % PEG liposomes using ¹²⁵ I-labelled Ag85B-ESAT-6	160
Figure 4.14	(A) Vesicle size (nm) and (B) zeta-potential (mV) of DDA:TDB, 5, 10, 25 % PEG liposomes upon exposure to stimulated <i>in vivo</i> conditions represented by storage at 37 °C in 50 % FCS	163
Figure 4.15	Adsorbed Ag85B-ESAT-6 antigen retention profile	165
Figure 4.16	(A) Vesicle size (nm) and (B) zeta-potential (mV) of DDA:TDB, 5, 10, 25 % PEG liposomes following the entrapment of OVA	169
Figure 4.17	Quantification of antigen entrapment of DDA:TDB, 5, 10, 25 % PEG liposomes using ¹²⁵ I-labelled Ag85B-ESAT-6	173
Figure 4.18	Ag85B-ESAT-6 antigen release profile	175
Figure 4.19	Effect of sucrose on (A) vesicle size (nm) (B) zeta potential (mV) within DRV liposomes	177
Figure 4.20	Quantification of antigen entrapment of DDA:TDB and 10 % PEG liposomes with addition of sucrose	178
Figure 4.21	Pharmacokinetic profile of liposome and antigen MLV and SUV	183

Figure 4.22	Pharmacokinetic profile of liposome and antigen DRV and mDRV	188
Figure 4.23	Draining of liposomes and Ag85B-ESAT-6 to the PLN after	192
Figure 4.24	Pontamine blue staining at the site of injection (quadriceps)	194
Figure 4.25	Ag85B-ESAT-6 specific antibody titres	200
Figure 4.26	Ag85B-ESAT-6 specific cytokine production	202
Figure 4.27	Spleen cell proliferation in response to stimulation/re-stimulation with Ag85B-ESAT-6 antigen	204
Chapter 5	Incorporation of immunostimulatory components to the DDA:TDB adjuvant delivery system	
Figure 5.1	Immunisation study timeline	217
Figure 5.2	SDS page of DDA:TDB MLV and DRV liposomes exposed to trypsin	219
Figure 5.3	Percentage (%) of OVA (A) adsorption and (B) entrapment following exposure to trypsin	221
Figure 5.4	(A) Vesicle size (nm) and (B) zeta-potential (mV) of DDA:TDB MLV liposomes	223
Figure 5.5	(A) Vesicle size (nm) and (B) zeta-potential (mV) of DDA:TDB DRV liposomes	225
Figure 5.6	(A) Vesicle size (nm) and (B) zeta-potential (mV) of DDA:TDB SUV liposomes	226
Figure 5.7	OVA retention profile	230
Figure 5.8	Spleen T-cell responses	233
Figure 5.9	Peripheral blood T-cell responses	234
Figure 5.10	Total IgG antibody responses	236
Chapter 6	Preparation, characterisation and entrapment of a non-glycosidic threitol ceramide into liposomes for presentation to invariant natural killer T cells	
Figure 6.1	CD1d agonists α GalCer and ThrCer	240

Figure 6.2	Size (nm) of (A) DSPC liposomes and (B) DDA liposomes over time of sonication	250
Figure 6.3	Size (nm) of (A) MLV and (B) SUV of DSPC and DDA liposomes with and without the inclusion of ThrCer represented by storage at 25 °C	254
Figure 6.4	Entrapped ThrCer release profile of DSPC and DDA (A) MLV and (B) SUV	256
Figure 6.5	Surface pressure - area isotherm	258
Figure 6.6	The surface pressure-area isotherms of mixed and pure monolayers at the air/water interface	260
Figure 6.7	The maturation status of APC in response to different liposomes was assessed 36 hours after addition of the liposomes	263
Figure 6.8	IFN- γ release from <i>i</i> NKT cells co-cultured with DCs pulsed with liposomes prepared as MLV or SUV with and without the inclusion of ThrCer	264
Figure 6.9	Mean fluorescence intensity	266

List of tables

Chapter 1 General introduction

Table 1.1	Liposome-based products that have been either approved or licensed for use in humans	25
Table 1.2	Examples of bilayer-forming lipids	28
Table 1.3	A selection of immunomodulators, which could enhance the immunogenicity of liposome systems	46

Chapter 2 Formulation, characterisation and application of lipid-coated microbubbles

Table 2.1	General classification of ultrasound contrast agents	53
Table 2.2	Physical characteristics of materials used for making microbubbles and emulsions	55
Table 2.3	Details of the formulations, the concentration and the volumes used in the preparation of microbubbles	62
Table 2.4	Comparison of sizes produced by laser diffraction and by microscopic imaging analysis	71
Table 2.5	Size (nm) and zeta potential (mV) of microbubbles formed by gas-releasing chemical reaction	81
Table 2.6	Size (nm) of <i>F</i> -GPC based microbubbles	86
Table 2.7	Size (nm) and zeta potential (mV) before and after pressurisation with perfluoropropane	87
Table 2.8	Summary of the characterisation data	92

Chapter 3 Cellular responses of macrophages to liposomes and lipid-coated microbubbles: *in vitro* studies

Table 3.1	Summary table of the formulations tested	109
Table 3.2	Characterisation data for the various formulations	116

Chapter 4	Investigating the use of liposomes as vaccine adjuvants	
Table 4.1	Weight (mg) and moles of DDA:TDB and 5 %, 10 % and 25 % PEG	140
Table 4.2	Description table of the bands and corresponding formulations including the result of the BCA assay	158
Table 4.3	Characterisation data for the SUV based liposomes with 2 µg of Ag85B-ESAT-6	170
Table 4.4	Summary of the percentage (%) of liposome and antigen retention at the SOI for MLV and SUV formulations	185
Table 4.5	Summary of the percentage (%) of liposome and antigen retention at the SOI for DRV and mDRV formulations	187
Table 4.6	Summary table of the effect of PEG, on a number of characteristics	206
Chapter 5	Incorporation of immunostimulatory components to the DDA:TDB adjuvant delivery system	
Table 5.1	Adjuvants and their corresponding TLR receptors	210
Table 5.2	Quantification of CpG using the OliGreen assay	228
Chapter 6	Preparation, characterisation and entrapment of a non-glycosidic threitol ceramide into liposomes for presentation to invariant natural killer T cells	
Table 6.1	Characterisation of MLV or SUV liposomes prepared from DSPC or DDA with and without the inclusion of ThrCer	251
Table 6.2	The experimental extrapolated area and area compressibility of mixed and pure monolayers at the air/water interface (at 20 °C) by DSPC, DDA and ThrCer in ddH ₂ O	259

Abbreviations list

α-gal	α -galactose
ANOVA	analysis of variance
APC	antigen presenting cell
CD4	cluster of differentiation 4
Chol	cholesterol
CO₂	carbon dioxide
DC	dendritic cell
DC-Chol	3 β -[N-(N',N'-(dimethylaminoethane)-carbamoyl)- cholesterol (DC-Chol)
ddH₂O	double distilled water
DDA	dimethyldioctadecylammonium
DOPE	1,2-dioleoyl- <i>sn</i> -glycero-3-phosphoethanolamine
DMEM	dulbecco's modified eagle medium
DNA	deoxyribose nucleic acid
DSPC	1,2-distearoyl- <i>sn</i> -glycero-3-phosphocholine
ELISA	enzyme linked immunosorbent assay
FCA	freund's complete adjuvant
FCS	fetal calf serum
GM-CSF	granulocyte monocyte colony stimulating factor
H₂SO₄	sulfuric acid
IFN-γ	gamma-interferon
iNKT	invariant natural killer T cell
MHC	major histocompatibility complex
MLV	multilamellar vesicles
MPS	mononuclear phagocyte system
MRI	magnetic resonance imaging
N₂	nitrogen
NaCl	sodium chloride
NaHCO₃	sodium bicarbonate
OVA	ovalbumin
PBS	phosphate buffered saline

PCS	photon correlation spectroscopy
PEG	polyethylene glycol
PEG-distearate	polyethylene-glycol distearate
PI	polydispersity index
Poly(I:C)	polyinosinic-polycytidylic acid
PSG	penicillin-streptomycin-glutamine
SD	standard deviation
SDS	sodium dodecyl sulphate
SOI	site of injection
SUV	small unilamellar vesicles
TB	tuberculosis
T_c	phase transition temperature
TDB	trehalose 6,6'-dibehenate
Th₁	t-helper type 1
Th₂	t-helper type 2
ThrCer	threitol ceramide
TLR	toll-like receptor
US	ultrasound
ZP	zeta potential

Chapter 1

General introduction

1.1 Liposomes

Liposomes are defined as microscopic spherical vesicles that form when phospholipids are hydrated or exposed to an aqueous environment (Bangham et al 1965). Liposomes were first discovered by Alec D. Bangham in the early 1960s while studying cell membranes (Bangham et al 1965). It was shown that amphiphiles, which are molecules that consist of a hydrophobic and a hydrophilic part such as phospholipids spontaneously form closed structures when they are hydrated in aqueous solutions (Chrai et al 2002). Since then, research in this field has expanded enormously. Today, most research into applications of liposomes is in the field of drug delivery (Gregoriadis & Florence 1993).

Table 1.1 lists some liposomal products that have been approved in the past 15 years (Zhang et al 2008). Doxil was the first liposomal-based product approved for use in humans by the United States Food and Drug Administration (FDA) in 1995 (Northfelt et al 1998). This liposomal drug formulation is used in the treatment of AIDS associated with Kaposi's sarcoma. Doxil has considerably extended the circulation half-life of doxorubicin, a drug used in anticancer chemotherapy, and furthermore it has increased the delivery of the drug into tumour tissues, thus resulting in an enhanced response (Northfelt et al 1998). This has been achieved by coating doxorubicin with stealth liposome carriers. Such carriers are composed of hydrogenated soy phosphatidylcholine, cholesterol, and PEGylated phosphoethanolamine. Other liposomal drugs used in clinical practice today include DaunoXome (daunorubicin liposomes) which is also a chemotherapy drug that is given to treat AIDS-related Kaposi's sarcoma, AmBisome (amphotericin B liposomes) in the treatment of fungal infections and DepoCyt (cytarabine liposomes) used to treat lymphomatous meningitis. The pharmacokinetic behaviour of a drug varies considerably *in vivo* when the drug is in its free state and when it is

encapsulated in liposomes. The benefits of such encapsulation are numerous. Liposome carriers can decrease drug toxicity by ensuring specificity to target organs and reducing any risks associated with the drug reaching organs that could be adversely affected (e.g. doxorubicin) (Rahman et al 1980). Additionally, the half-life of the drug is considerably increased *in vivo*, where the drug can remain stable in organs for prolonged periods (e.g. cytarabine). Furthermore, liposome carriers can often reduce the effective dose of the drug (cytarabine, methotrexate) (Zee-Cheng & Cheng 1989). Liposomes are also good vehicles for lipophilic drugs, which would otherwise be difficult to administer (Ali et al 2010).

Table 1.1 Liposome-based products either approved or licensed for use in humans.

<i>Marketed product</i>	<i>Drug used</i>	<i>Target diseases</i>	<i>Company</i>
Doxil™ or Caelyx™	Doxorubicin	Kaposi's sarcoma	SEQUUS, USA
DaunoXome™	Daunorubicin	Kaposi's sarcoma, breast & lung cancer	NeXstar, USA
Amphotec™	Amphotericin-B	Fungal infections, Leishmaniasis	SEQUUS, USA
Fungizone®	Amphotericin-B	Fungal infections, Leishmaniasis	Bristol-squibb, Netherland
Avian retrovirus vaccine	Killed avian retrovirus	Chicken pox	Vineland lab, USA
Epaxal –Berna Vaccine	Inactivated hepatitis-A Virions	Hepatitis A	Berna Biotech
Depocyt	Cytarabine	Cancer therapy	Skye Pharm, USA
Doxil®	Doxorubicin Hcl	Refractory ovarian cancer	ALZA, USA
Evacet™	Doxorubicin	Metastatic breast cancer	The liposome company, USA
Autragen™	Tretinoin	Kaposi's sarcoma	Aronex Pharm, USA
Nyotran™	Nystatin	Systemic fungal infections	Aronex Pharm, USA
Mikasome®	Amikacin	Bacterial infection	NeXstar, USA
Verteporfin	Visudyne	Age-related macular degeneration	Novartis

Liposomes are considered to be good candidates for drug carriers because they are relatively easy to prepare, exhibit little or no immunogenicity and toxicity by themselves, are biodegradable and can carry a diverse range of compounds, either encapsulated in the water phase (hydrophilic compounds) or incorporated in the lipid bilayer (hydrophobic compounds) (Chrai et al 2002) (Figure 1.1). Furthermore, liposome properties can be easily modified by changing the liposomal lipid composition, the charge or particle size, or chemical modification of the liposomal surface (Poste 1983; Gregoriadis 1985). Liposomes provide a unique opportunity to deliver pharmaceuticals into cells or even inside individual cellular compartments (Torchilin et al 1993). In many cases, therapeutic applicability was shown to improve through the use of liposomes as a drug carrier system (Chrai et al 2002).

1.2 Structure and biophysical properties of liposomes

Phospholipids are the main component of naturally occurring bilayers (O'Doherty 2004) and are amphipathic moieties with a hydrophilic head group and generally fatty acid two hydrophobic chains (tails) (Figure 1.1). When these lipids are exposed to an aqueous environment, intermolecular interactions between lipid molecules (hydrophilic interactions between polar head groups and van der Waals interactions between hydrocarbon chains) and with water molecules (hydrophilic interactions between the head groups) lead to spontaneous formation of closed bilayers (Uhumwangho & Okor 2005). As shown in Figure 1.1, the polar head groups contact water and the hydrophobic alkyl chains form a non-polar interior. The phospholipid molecules can move around within their lateral side bilayer, but there is a significant energy barrier preventing migration/flipping of the lipid molecules to the other side of the bilayer (Alberts et al 2002).

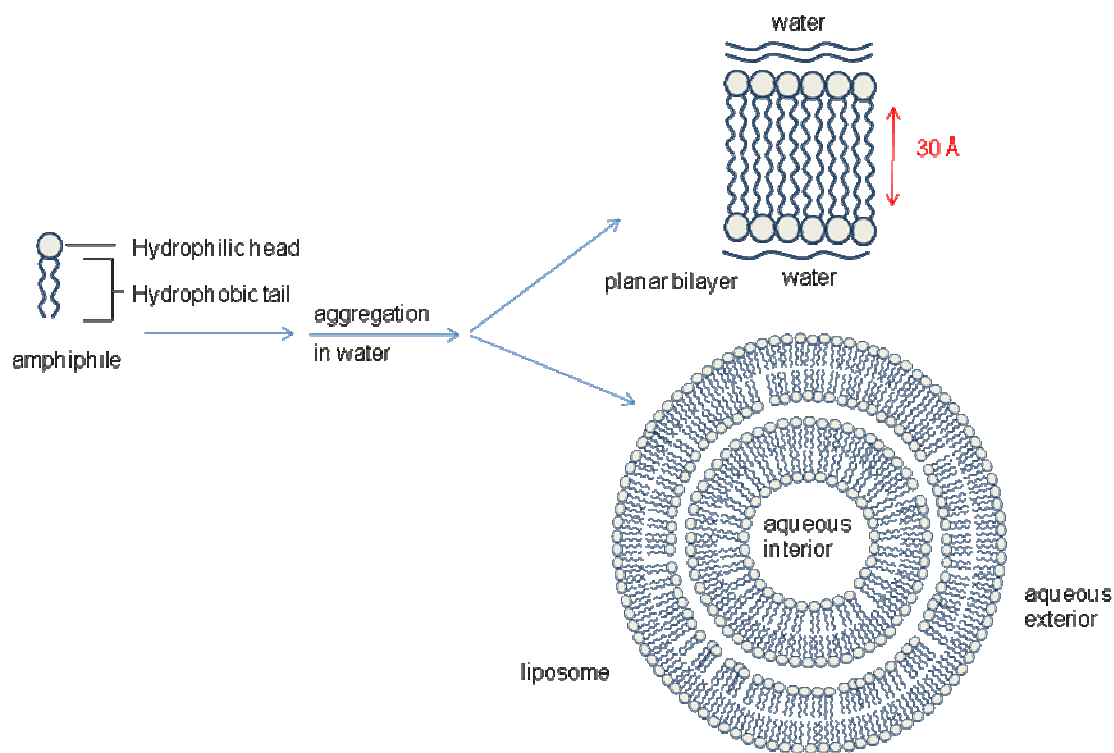
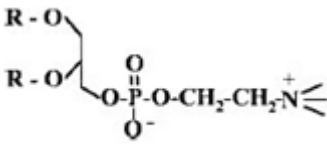
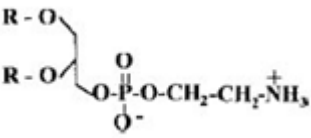
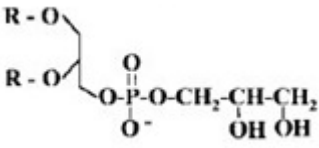


Figure 1.1 Schematic representation of a liposome. When these lipids are exposed to an aqueous environment, intermolecular interactions between lipid molecules and with water molecules lead to spontaneous formation of closed bilayers.

The two types of phospholipids used within liposome formulations can be classified as natural and synthetic. The most common natural phospholipid is phosphatidylcholine (PC), also known as lecithin and it can be extracted from animal (hen egg) and vegetable (soyabean) sources (Zhang et al 2002). Other natural phospholipids include phosphatidylethanolamine (PE) and phosphatidylserine (PS). These natural phospholipids are heterogeneous with respect to their fatty acid chains and usually have a high degree of polyunsaturation, which can affect liposome characteristics (Frezard 1999). Synthetically prepared phospholipids have well-defined fatty acid compositions and can be obtained with different or identical saturated or unsaturated chains (New et al 1990). The structures of the most commonly used bilayer-forming lipids are illustrated in Table 1.2 (Frezard 1999).

Table 1.2 Examples of bilayer-forming lipids.

Lipid family Structural formula	Hydrophobic chains (R) (name)	Abbreviation of lipid name (T_c)
Phosphatidyl choline 	$\text{CH}_3\text{-(CH}_2\text{)}_7\text{-CH=CH-(CH}_2\text{)}_7\text{-C(O)-}$ (oleyl) $\text{CH}_3\text{-(CH}_2\text{)}_{12}\text{-C(O)-}$ (myristoyl) $\text{CH}_3\text{-(CH}_2\text{)}_{14}\text{-C(O)-}$ (palmitoyl) $\text{CH}_3\text{-(CH}_2\text{)}_{16}\text{-C(O)-}$ (stearoyl)	DOPC ($< 0^\circ\text{C}$) DMPC ($+ 23^\circ\text{C}$) DPPC ($+ 42^\circ\text{C}$) DSPC ($+ 55^\circ\text{C}$)
Phosphatidyl ethanolamine 	$\text{CH}_3\text{-(CH}_2\text{)}_7\text{-CH=CH-(CH}_2\text{)}_7\text{-C(O)-}$ (oleyl)	DOPE ($< 0^\circ\text{C}$)
Phosphatidyl glycerol 	$\text{CH}_3\text{-(CH}_2\text{)}_{12}\text{-C(O)-}$ (myristoyl) $\text{CH}_3\text{-(CH}_2\text{)}_{14}\text{-C(O)-}$ (palmitoyl)	DMPG ($+ 13^\circ\text{C}$) DPPG ($+ 35^\circ\text{C}$)

Phosphatidylcholine is the major component of most biological membranes and is often used as bulk lipid for the preparation of liposomes due to its non-toxic biodegradable profile (Zhang et al 2002). Depending on the nature of the phospholipid component, the lipid bilayer of the liposomal vesicles can exist within a fluid or rigid state at ambient temperature. The state and characteristics of amphiphiles is dependent on the lipids gel-liquid crystalline phase transition temperature (T_c). This means that the liposome bilayers can be in fluid or rigid state, in which the transition temperature is below or above ambient temperature, respectively (Gregoriadis et al 1998). The phase transition temperature of phospholipids is influenced by numerous factors including the lipids alkyl hydrocarbon chain length and degree of saturation. As the alkyl chain increases in length, the van der Waal interactions between the lipid chains become stronger, thereby in order to disrupt the stringent and rigid lipid packing of the

liposome bilayer, more energy needs to be applied, thus increasing the phase transition temperature. For example, dimyristoylphosphatidylcholine (DMPC) has a hydrocarbon chain length of C₁₄ and a phase transition temperature of 23 °C, whereas 1,2-distearoyl-*sn*-glycero-3-phosphocholine (DSPC) has a hydrocarbon chain length of C₁₈, resulting in a higher phase transition temperature of 55 °C, as more energy is required to disrupt the ordered packing and to subsist in a fluid state. In terms of liposomal drug delivery, the phase transition temperature is important as it can dictate the stability and drug release profile of the systems. For example early work by Gregoriadis and Ryman (1971) showed that liposomes formulated with DSPC had higher drug retention and longer circulation times than liposomes formulated with lower transition temperature lipids.

1.2.1 Liposome composition

Liposomes are often classified into groups by size and number of membranes (lamellarity) (Rongen et al 1997) (Figure 1.2):

- Multilamellar vesicles (MLV) are onion-like structures that have series of substantially spherical shells, formed of five to twenty lipid bilayers, interspersed with aqueous layers and range in diameter from around 100 - 4000 nm (Rongen et al 1997).
- Large unilamellar vesicles (LUV) are vesicles that have a size above 100 nm, and normally consist of one concentric lamella (New 1990).
- Small unilamellar vesicles (SUV) are defined as the smallest phospholipid vesicles approximately 45 nm, with a maximum size of up to 100 nm. The size depends on the ionic strength of the aqueous medium and the lipid composition in the membrane. They usually consist of one lamella (Rongen et al 1997).

Depending on its physico-chemical properties, a drug can either be incorporated in the lipid bilayer (for lipophilic drugs) or encapsulated in the water phase of the liposome (for hydrophilic drugs). A lipophilic drug will be accommodated between the lipid molecules of the bilayer (Weiner et al 1989; Scherphof et al 1987) and thus the amount of drug that can be incorporated will depend on how well the drug fits in between the bilayer molecules and on the strength of the lipid interaction (Zhang et al 2002). This will also determine the stability of the drug-liposome complex *in vivo*. Because of the relatively large amount of lipid in the lipid bilayers of MLV, they are considered best for encapsulation or transportation of lipophilic materials, whereas for LUV because of their large aqueous/lipid volume ratio, they are considered best for encapsulation of hydrophilic molecules, particularly macromolecules (Szoka & Papahadjopoulos 1978). SUV have the advantage of a small size, which allows relatively easy access to the cells of tissue, but their small volume limits delivery of hydrophilic aqueous materials to trace amounts (Waalkes 1992). However, SUV may be useful in the transportation of lipophilic materials (Keller & Lasic 2005; Mohammed & Perrie 2005).



Figure 1.2 Schematic representation of three types of liposomes. These are small unilamellar (SUV), large unilamellar vesicles (LUV) and multilamellar (MLV). SUV have diameters of less than 100 nm, LUV have a lipid bilayer surrounding a large, unstructured aqueous phase. MLV have a series of substantially spherical shells formed of five to twenty lipid bilayers interspersed with aqueous layers.

1.2.2 Liposome morphology

There are numerous ways to generate liposomes and the number of lipid bilayers present within the liposomal vesicle is dependent on the method of preparation.

1.2.2.1 Lipid hydration method

MLV are the simplest liposomal vesicles to make and can be prepared by the established lipid hydration method (Bangham et al 1965). This involves mixing of the selected lipid components within a solvent (i.e. chloroform/methanol) mixture, which is then evaporated by rotary evaporation. Once the solvent is completely removed, a dry lipid film forms and as the aqueous solution (i.e. water) is added to hydrate the film, the lipid components begin to break away gradually forming large spherical liposomes, with each consisting of numerous concentric lipid bilayers entrapping water. As these vesicles form, the lipid components arrange themselves in a random manner and the size of MLV liposomes cannot be controlled. Therefore within the liposomal solution there are heterogeneous population of MLV sizes, ranging from as small as 100 nm to a few microns in size (Gregoriadis et al 2002).

1.2.2.2 Sonication

After preparation of MLV liposomes, these large liposomal structures can be dramatically reduced in size and their morphology can be modified by probe or bath sonication of the MLV suspension, generating SUV (Huang 1969; Johnson et al 1971). For larger volumes and dilute samples, bath sonication is more suitable. Normally, a 5 to 10 minute sonication above the T_c of lipids is sufficient for producing SUV of 100 nm or even smaller (Zhang et al 2002). The advantages of bath sonication include a controllable operating temperature, freedom from contamination, and no loss of lipid material. Probe sonication on the other hand, dissipates

more energy into the sample and therefore is often used for achieving the smallest size possible, for concentrated samples or suspension in more viscous aqueous solutions (Zhang et al 2002).

LUVs can be produced using a range of methods including reverse-phase evaporation and ether vaporisation method (Frezard 1999).

1.2.2.3 Reverse-phase evaporation method

In reverse-phase evaporation, several phospholipids (pure/mixed with cholesterol) can be used. The lipid mixture is added to a round bottom flask and the solvent is removed under reduced pressure by a rotary evaporator. The system is purged with nitrogen and the lipids are re-dissolved in the organic phase. This is the point when the reverse phase vesicles will form (O'Doherty 2004). Diethyl ether and isopropyl ether are the usual solvents of choice. After the lipids are re-dissolved, the aqueous phase (contains compound to be encapsulated) is added. The system is kept under continuous nitrogen and the two-phase system is sonicated until the mixture becomes a clear one-phase dispersion. The mixture is then placed on the rotary evaporator and the organic solvent removed until a gel is formed. The resulting liposomes are called reverse-phase evaporation vesicles (REV). The large unilamellar vesicles formed have the ability to encapsulate large macromolecular vesicles with high efficiency (Szoka & Papahadjopoulos 1978).

1.2.2.4 Ether vaporisation method

In the ether vaporisation method, osmotically active unilamellar vesicles are produced following the slow injection of a lipid mixture in organic phase into a warm aqueous solution.

Such vesicles have a well-defined size distribution (O'Doherty 2004). Additionally in comparison to sonicated and hand shaken preparations, vesicles formed using the ether vaporisation method have a ten times greater high volume trapping efficiency (Deamer & Bangham 1976).

1.2.2.5 Dehydration-rehydration method

In a bid to enhance the efficiency of drug incorporation within liposomes, Kirby and Gregoriadis (1984a) developed a method of producing liposomes known as the dehydration-rehydration procedure. The method produces vesicles that undergo various transformations in physical characterisation, in order to generate the ideal completed liposomes. The procedure involves mixing the material to be entrapped together with the SUV before freeze-drying. In this way all of the lipid can be brought into contact with all of the solute in the anhydrous state. During the dehydration-rehydration procedure, the concentration of vesicles combined with the reduction in hydrophobic forces causes loss of vesicle stability. This promotes fusion of these destabilised SUV into larger multilamellar vesicles entrapping solute as they form (Deamer & Barchfield 1982) into dehydration-rehydration vesicles (DRV).

1.3 Application of liposomes

As noted, liposomes have a wide range of biomedical applications such as carriers for controlled drug release of tumours therapeutic agents and antibiotic, for gene and antisense therapy through nucleic acid sequence delivery, immunisation through antigen delivery and as radiodiagnostic carriers. In this thesis, liposomes have been investigated as radiodiagnostic contrast agents and as vaccine adjuvants, these applications will be explored in detail in the following sections.

1.3.1 Liposomes as radiodiagnostic carriers

Liposomes have been recognised as promising carriers for diagnostic agents and contrast agents to locate sites specifically (Torchilin 1997). Contrast agents are defined as substances used to enhance the contrast of structures or fluids within the body in medical imaging (Torchilin 1996). These agents are used in imaging to increase the signal difference between the area of interest (e.g. the blood pool) and the background (Gregoriadis 1988; Torchilin 1985). The ability of liposomes to entrap different substances into both the aqueous phase and the liposome membrane compartment made them suitable for carrying the diagnostic moieties used with all imaging modalities: gamma-scintigraphy, magnetic resonance (MR) imaging, computer tomography (CT) imaging and even sonography (Torchilin 1997). The different chemical nature of reporter moieties used in different modalities requires different protocols to load liposomes with the given contrast agent. Such characteristics of liposomal contrast agents led to the development of an entire family to be used in various settings such as tumours, liver and spleen, infection and inflammation sites, the cardiovascular system, and other regions of interest in the clinical field (Torchilin 1997).

1.3.1.1 Lipid-coated microbubbles in magnetic resonance imaging (MRI)

In medicine, MRI is used as a diagnostic tool where cross-sectional images of soft tissue can be produced. Water molecules in tissues absorb and transmit high frequency radiowaves when placed in strong magnetic fields, which is analysed using MRI (Vangala et al 2007a). The MRI signal from different water densities within the biological material is used to create images on the basis of the difference in relaxation time (Vangala et al 2007a).

In addition to its application in medical imaging, a study by Vangala and co-workers (2007a) have investigated the potential of MRI to quantify and map the oil content in rock by measuring the different relaxation times of the MRI signal coming from oil and water. It was suggested that this technology could be enhanced by the application of gas filled lipid-coated microbubbles (Vangala et al 2007a). Lipid-coated microbubbles are liposomes that are prepared with entrapped gases, such as air, oxygen or fluorinated gases, rather than with an aqueous core (Perrie 2005). Lipid-coated microbubbles can act as MRI pressure probes, as when these microbubbles are present in a pressure-varying medium, changes in liposome size (resulting from changes in pressure) would cause a change in the MRI signal allowing an accurate three-dimensional image of the pressure changes in porous rock (Vangala et al 2007a). Indeed, pressure sensitive MRI systems have already been suggested for applications in health care. For example, they have been used to measure haemodynamic pressures for evaluating cardiovascular function and arterial pressure and for such applications, lipid-coated microbubbles have been tested as pressure sensitive contrasting agents (Perrie 2005).

1.3.2 Liposomes as vaccine adjuvants

1.3.2.1 Vaccines

Vaccines have been defined as ‘any preparation made from a pathogen that is used for vaccination and provides protective immunity against infection with the pathogen’ (Parham 2009). The ultimate goal of a vaccine is to develop long-lived immunological protection, whereby the first encounter with a pathogen is ‘remembered’ by the immune system (Pashine 2005).

1.3.2.2 Innate and adaptive immune responses

The immune system has two main functions; to recognise invading pathogens and then to trigger pathways that will destroy them (Hames & Hooper 2000). Such pathogens are controlled and terminated by the innate immune response and is ready to react quickly. Most components of innate immunity, are present before the onset of infection and constitute a set of disease-resistance mechanisms that are not specific to a particular pathogen that include cellular and molecular components that recognise classes of molecules different to frequently encountered pathogens (Goldsby et al 2003). Phagocytic cells such as neutrophils, macrophages, in addition to pattern recognition receptors, NK cells, complement, and variety of antimicrobial compounds synthesised by the host all play important roles in innate immunity (Goldsby et al 2003).

The adaptive immune response is made up of B and T lymphocytes that have unique receptors specific to various microbial antigens (Sudhakar & Subramani 2005), in contrast to the receptors of the innate immune system which are of many different types but not specific to a particular pathogen (Parham 2009). These antigen-specific receptors are encoded by genes generated during a complex process of gene rearrangement that occurs during the course of lymphocyte development. As each B and T lymphocyte contains a unique antigenic receptor, it allows for large and diverse population of cells capable of recognising a wide spectrum of pathogens. This is termed the lymphocyte repertoire (Sudhakar & Subramani 2005). In response to an infection lymphocytes bearing receptors specific for the pathogen are then selected to participate in the immune response. The proliferation and differentiation of these cells, termed clonal selection and expansion, generates a large population of specific effector cells. To assist in future invasion by the same pathogen, some of the lymphocytes persist in

the body and provide long-term immunological memory, thus resulting in a faster and stronger response (Parhan 2009).

A. Innate immune response



B. Adaptive (acquired) immune response



Figure 1.3 Schematic representation of the immune response. (A) **Innate immune response.** Non-self cells are rapidly attacked in the innate immune system. Key players in the innate system are neutrophils, macrophages, pattern recognition receptors, NK cells, and complement. The desired end result is the destruction of the foreign substance, the non-self cell. (B) **Adaptive immune response.** The major players in this response are the B lymphocytes, T lymphocytes, and NK cells. The desired end result is destruction of the non-self cell but through a more complex and tightly orchestrated series of events (Bingham 2008).

1.3.3 Types of Vaccines

There are four types of traditional vaccines: (1) live attenuated, (2) inactivated, (3) toxoids, and (4) subunit vaccines.

1.3.3.1 Live Attenuated Vaccines

Live attenuated vaccines consist of live virus that has mutated so that it has a reduced ability to grow in human cells and is no longer pathogenic to humans (Parhan 2009). These microorganisms are still able to infect their target cells. However, infection is inefficient (mild) and there are limitations in the replication of the microorganisms. Vaccines produced in this manner include the bacillus Calmette-Guérin (BCG) and the measles, mumps, yellow fever vaccines and rubella combination vaccine (MMR) (Harper et al 2003; Nichol et al 1999; Arving & Greenberg 2006), and such vaccines are generally capable of stimulating both a humoral and cell-mediated immune response. However, there is a risk of reversion to virulence, and this type of vaccine is not considered safe for use in immunocompromised individuals.

1.3.3.2 Inactivated Vaccines

Inactivated vaccines consist of microorganisms that have been killed or viruses, usually by heat or chemicals such as formaldehyde, thus destroying infectivity while retaining immunogenicity (Mackett & Williamson 1995). While offering advantages in terms of safety, such vaccines are generally less effective than live attenuated vaccines, usually only stimulating humoral immunity and often requiring booster doses (Mackett & Williamson 1995). Examples of these vaccines include: trivalent inactivated influenza vaccine (TIV), cholera, bubonic plague and hepatitis A vaccines (Fiore et al 2006; Cox et al 2004).

1.3.3.3 Toxoids

Some microorganisms produce toxic compounds that are the responsible for causing the disease (i.e. tetanus toxin and diphtheria toxin). Toxoids are inactivated forms of these toxic compounds. In addition to being successful vaccines in their own right, toxoids may also be used to increase the immunogenicity of some other vaccines, such as the *Haemophilus influenzae* type B (Hib), which contains a polysaccharide unit from the virus conjugated to diphtheria or tetanus toxins (Perrie 2006).

1.3.3.4 Subunit Vaccines

Subunit vaccines initiate strong immune responses using a small part of the organism that could include a gene from the genome. Recombinant DNA technology has greatly facilitated the development of such vaccines, a process where are foreign genes are introduced into yeast or bacteria expression systems. This allows the production of large quantities of antigen that is purified and used as a vaccine (Arvin & Greenberg 2006). The immune response induced by such vaccines is short-lived and thus several boosts are required to achieve protection. For Hepatitis B virus for example, only the surface protein of the virus is used to generate the subunit vaccine. Before recombinant DNA technology, this was extracted from the blood serum of chronically infected patients (Berman et al 1990; Edlich et al 2003).

1.3.4 Improvement of the potency of subunit vaccines

To improve subunit vaccines, the trend now is to produce highly purified recombinant proteins that do not induce strong immune responses and lack natural immunostimulatory substances. However, such vaccines fail to induce an effective immune response despite their increased safety, since they lack immunostimulatory components of whole-cell vaccines key

to activating an innate immune response. Additionally, vaccines need to induce a cell-mediated as well as humoral immune response against pathogens causing chronic infection such as hepatitis C virus, human immunodeficiency virus (HIV), tuberculosis and malaria, but subunit vaccines have been ineffective at inducing such a response (Fearon 1997). In order to make subunit vaccines capable of inducing potent immune responses, adjuvants and novel vaccine strategies are required (Fearon 1997, Janeway 1989).

1.3.5 Adjuvants

Adjuvants (derived from the latin word *adjuvare*, meaning help or aid) are defined as substances used in combination with a specific antigen that produced a robust immune response than the antigen alone (Gupta et al 1993, Vogel 1995). The concept of adjuvants arose in the 1920s from observations such as those of Ramon et al (1926) who noted horses that developed an abscess at the inoculation site of diphtheria toxoid generated higher specific antibody titers (Petrovsky & Aguilar 2004). They subsequently found that an abscess generated by the injection of unrelated substances, along with the diphtheria toxoid, increased the immune response against the toxoid (Ramon 1959). The most appropriate adjuvant for a given vaccine antigen will depend to a large extent on the type of immune response that is required for protective immunity. Moreover, some adjuvants are strikingly potent, but also very harmful to the host. Therefore, the potency of an adjuvant often conflicts with host safety and tolerability. Adjuvants can be used for various purposes, (a) firstly to enhance the immunogenicity of recombinant antigens (McElrath 1995), (b) to reduce the amount of antigens or the number of immunisations needed for protective immunity, (c) to improve the efficacy of vaccine in newborns, the elderly or immunocompromised persons and (d) as

antigen delivery systems for the uptake of antigens by the mucosa (Petrovsky & Aguilar 2004, Marx et al 1993, Douce et al 1995).

1.3.5.1 Role of adjuvants in the immune responses

To date, it is not clear how the immune response is augmented by adjuvants but the immune response to vaccine antigens is improved in more than one way. These include:

- (a) Improve antigen delivery to APCs, increase cellular infiltration, inflammation, and trafficking to the injection site (Aguilar & Rodriguez 2007).
- (b) Promote the activation state of APCs by up regulating co-stimulatory signals or MHC expression, inducing cytokine release (Aguilar & Rodriguez 2007).
- (c) Enhance antigen processing and presentation to the cells of the immune system (Aguilar & Rodriguez 2007).
- (d) Modulate antibody avidity, affinity as well as the magnitude, isotype or subclass induction (Pashine et al 2005).
- (e) Stimulate cell-mediated immunity and lymphocyte proliferation non-specifically (Pashine et al 2005).

1.3.6 Classification of adjuvants

The source, physiochemical properties and mechanism of action are amongst the features that help classify adjuvants (Vogel 1998). Considering their mechanism of action, Edelmann (1991) (reviewed in Allison and Byars 1991) classified adjuvants into three groups: (a) immunostimulatory adjuvants, being substances that increase the immune response to the

antigen by directly activating APCs through specific receptors e.g. TLRs, known as adjuvant receptors (Kaisho and Akira 2002), (b) carriers that provide help to T-cells as immunogenic proteins and, (c) particulate or vehicle adjuvants (vaccine delivery systems), serve as a matrix for antigens, mainly function to localise vaccine components and to target vaccines to APCs (Petrovsky & Aguilar 2004) . So, delivery systems are used to promote the interaction of both antigens and immunostimulators with the key cells of the innate immune system. Immunostimulatory adjuvants provide the inflammatory context necessary for optimal antigen-specific immune activation by activating APCs and amplifying the innate immune response (Aguilar & Rodriguez 2007). Some of the most common adjuvants are described in the following section.

1.3.6.1 Alum

Alum are aluminum-based mineral salts (generically called alum) (Gupta 1998). Aluminium salts are insoluble, gel like precipitates of aluminium hydroxide or aluminium phosphate. Immunogen is bound by electrostatic interactions to pre-formed gel or during gel formation *in situ* (Levine et al 1955). The major mode of action appears to be depot formation at the site of injection. The antigen is only slowly released from the gel, ensuring its sustained exposure to immune surveillance. Alum induces strong Th₂ responses, and work *in vitro* indicated that alum up-regulated co-stimulatory signals on human monocytes and promoted the release of IL-4 (Ulanova et al 2001). Unfortunately, alum is a poor adjuvant for cell-mediated immunity and can induce IgE antibody responses, which are associated with allergic reactions (Gupta 1998).

1.3.6.2 Freund's adjuvants

Freund's complete adjuvant was developed in 1937 and is a powerful immunogenic adjuvant composed of a mixture of paraffin (i.e. mineral) oil, a surfactant (Aracel A), and heat killed *Mycobacterium tuberculosis* (MTB) (Stuart-Harris 1969). This adjuvant functions to prolong antigen persistence. The mycobacterial components in FCA have additional direct immunostimulatory activities making FCA very potent. However, it is not used for human vaccination because of problems associated with its use, mainly ulcerating tissue necrosis (Claassen et al 1992). In contrast, Freund's incomplete adjuvant (FIA) does not contain the mycobacteria component and, consequently displays somewhat less adjuvanticity (Walsh 2007).

1.3.6.3 CpG (cytidine-phosphate-guanosine)

Bacterial components are often potent immune activators; however, these are commonly associated with toxicity, for example, bacterial DNA with immunostimulatory CpG motifs is one of the most potent cellular adjuvants (Weiner et al 1997). Immunostimulatory CpG are unmethylated cytosine-guanine dinucleotides found in bacterial DNA, but absent in mammalian DNA (Petrovsky & Aguilar 2004). These DNA sequences stimulate the immune system through a specific receptor, TLR 9, which is intracellularly expressed in human, and mouse B-cells and plasmacytoid DCs (Krug et al 2001). Within minutes of exposure of B-cells or plasmacytoid DCs to CpG motifs, they interact with TLR 9, leading to the activation of cell signaling pathways. The adjuvant effect of CpG appears to be maximised by the conjugation to plasmid protein antigens (Klinman et al 1999), or their formulation with delivery systems (Singh et al 2001).

1.3.6.4 Liposomes

The immunological role and adjuvant properties of liposomes were first identified by Alison and Gregoriadis (1974) for diphtheria toxoid. Since then the immunological adjuvanticity of liposomes has been well recognised and they have been extensively investigated as potential vaccine adjuvants for more than 20 years for a number of antigens, including tetanus toxoid (Davis & Gregoriadis 1987), *Leishmania major* antigen (Kahl et al 1989) and hepatitis B surface antigen (Brunei et al 1999). Liposomes have been researched for their role in enhancing transfection of DNA plasmids (Perrie et al 2001; Perrie et al 2003), and as efficient adjuvants for subunit vaccine delivery (Davidsen et al 2005; Smith Korsholm et al 2007), with some liposomal based vaccines (i.e. virosomes) having been licensed for human use (i.e. Inflexal vaccine for influenza).

1.4 Liposomes delivery of protein antigens

The use of liposomes as carrier systems has been ongoing for many years. Liposomes are used as a carrier system for various types of substances and thus their versatility, both structural and functional, make them ideal for the delivery of protein antigens. *In vivo*, protein antigens are recognised by major histocompatibility complex (MHC) molecules that are expressed on the surface of APCs. These include dendritic cells and macrophages. There are two different classes of MHC molecules, MHC I and MHC II. MHC molecules process foreign antigens and by transporting it through the cytosol, the peptide and MHC complex is displayed on the surface of the APC. Thus, the complex interacts with the T-cell receptor and facilitates an interaction between APCs and T-cells (Madigan et al 2002). The source of protein antigen however determines which MHC molecule will bind, process and present the antigen. For

instance, the immune system processes subunit protein antigens as exogenous antigens. These antigens can be processed by MHC class II molecules and effectively induce a humoral immune response once presented to the Th₁ pathway CD4⁺ lymphocytes. Such antigens are unable to gain access into the cytosol of the target cell that is important for MHC class I presentation of antigen to cytotoxic T lymphocytes (Spack & Sorgi 2001). The use of a liposomal delivery system, however, can artificially direct exogenous antigen into the cytoplasm of the target cell and induce MHC class I presentation (Rao & Alving 2000). This will also provoke the release of Th₁ cytokines that will additionally stimulate strong CTL responses (Spack & Sorgi 2001).

1.4.1 Liposome composition: cationic lipids and immunomodulators

Liposomal systems can enhance specific immune responses to protein antigens. This has been shown from the introduction of cationic lipids into the lipid bilayer, and from ligand and co-adjuvant incorporation. A possible strategy showing potential in this field is combining liposomal delivery systems with adjuvants and/or immunomodulating molecules such as cytokines (Rao et al 2002). Olsen et al (2001) showed an increase and an induction of protective immunity against tuberculosis when isolated protein antigens, found in mycobacterial culture filtrates, were incorporated within liposomal vesicles combined with dimethyldioctadecylammonium (DDA; when hydrated in an aqueous environment this cationic lipid self assembles into closed bilayers) (Olsen et al 2001). Yet these identified proteins possess low inherent immunogenicity when injected alone (Andersen 1994). The authors reached a conclusion that in order for immune protection to remain high over an extended period, a depot must have been formed at the injection site by DDA (Holten-

Andersen et al 2004; Olsen et al 2001). Holten-Andersen and co-workers conclude DDA may act to increase antigen and immunostimulator uptake into APC when it forms the depot. Table 1.3 highlights other immunomodulators that like DDA when incorporated into liposomal delivery systems act to enhance immunogenicity against tuberculosis and other infectious organisms.

Table 1.3 A selection of immunomodulators, which could enhance the immunogenicity of liposome systems.

Immunomodulator	Description
MPL (monophosphoryl lipid A)	Induces the synthesis and secretion of various cytokines (Ulrich & Myers 1995) and is effective at potentiating mucosal and systemic immune responses to the incorporating antigen. This adjuvant has no observed side effects, other than minor irritation at the injection site (Thoelen et al 1998).
MPD (muramyl dipeptide)	Derived from bacterial cell walls and activates macrophages thus regulates the immune system (Murata et al 1997).
TDM (trehalose 6,6' dimycolate)	Cord factor, which is a glycoprotein present on the cell membrane surface of <i>M. tuberculosis</i> . Activates macrophages and synthesis of cytokines, to drive a Th1 immune response. It is extremely toxic as it induces hypersensitivity granulomas, complex inflammatory events and apoptosis (Yamagami et al 2001).
TDB (trehalose 6,6' dibehenate)	An analogue of trehalose 6,6' dimycolate (TDM) but consists of a shorter fatty acid chains therefore is considered to be less toxic (Davidsen et al 2005). Very immunogenic as a co-adjuvant for eliciting protective immunity against tuberculosis (Holten-Andersen et al 2004; Davidsen et al 2005).

1.4.2 Liposome preparation: surface adsorbed versus entrapped antigen

The preparation method used in producing liposome vesicles may have a strong influence in the way they are processed *in vivo*. Protein antigens can be incorporated into liposome vesicles at a high concentration and this is not influenced by vesicle size, since smaller vesicles with a diameter of 100 – 200 nm are also capable of achieving this (Lima 2004). This therefore suggests liposomal preparation method does not dictate the amount of antigen

entrapped by the liposomal vesicles. Factors that could, however, influence how liposomal vesicles are processed by the immune system include morphology, preparation and location of protein antigen. This could further influence which immune pathway is activated (Therien & Shahum 1996).

Depending on the antigen location and its physical association with the liposomal delivery system, the type and strength of the immune system can vary (Shahum & Therien 1988; Fortin et al 1996). Antigen can either be encapsulated or bound to the surface of the delivery system. These different locations can thus influence the route in which the antigen is processed within APCs, which further dictates the cell populations activated and the immune response initiated (Fortin et al 1996). In contrast, an early study showed that for toxoid delivery via liposomal formulation, antibody responses to the immunopurified tetanus toxoid was no different between toxoid linked to the surface MLV and toxoid entrapped within DRV, implying that the physical location of the antigen has no influential effect on induction of specific immune responses (Davis & Gregoriadis 1987).

Various studies however have shown both encapsulated and surface linked antigens to be beneficial, thus suggesting how the antigen is associated could be antigen specific (Fortin et al 1996). For a range of antigens including e.g. Factor VIII protein, the DRV procedure in terms of high antigen entrapment efficiency has been shown to be highly immunogenic (Kirby & Gregoriadis 1987b).

1.5 Aims and objectives

Given the ability of liposome-based systems to be formulated to deliver a range of moieties their application initially to act as possible contrast agents and then further use these systems as potential vaccine adjuvants was considered. The feasibility of contrast agents as novel antigen delivery tools to dendritic cells has been assessed previously in cancer immunotherapy (Suzuki et al 2009). The authors found that exogenous antigen delivery into cytosol by lipid coated microbubbles could induce antigen-specific CTLs and lead to a strong anti-tumour effect. Therefore the overall aim of this thesis was to investigate the potential of liposomes in the application of contrast agents and as vaccine delivery systems.

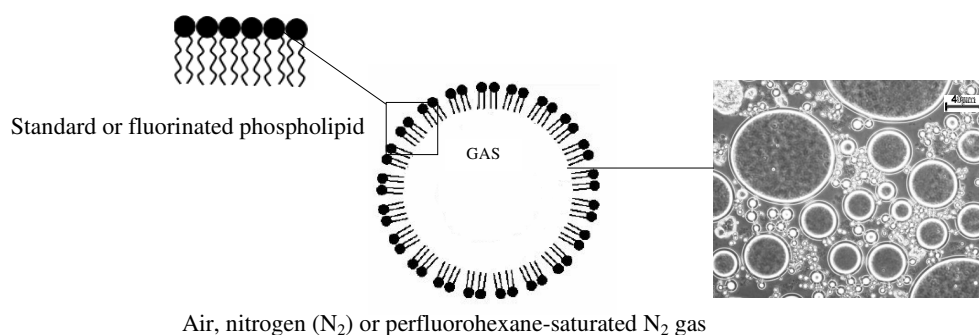
The objectives of this study were:

- To compare and evaluate four different methods of producing lipid-coated microbubbles/gas-filled liposomes and to test the stability and physico-chemical characteristics of these preparations in order for their use as contrast agents to fluid pressure.
- To examine the effect of liposome and microbubble formulations on macrophage cells to assess their potential as possible vaccine adjuvants.
- To investigate the effect of liposome formulation on their biodistribution and adjuvant properties.
- To investigate the versatility of cationic liposomes in combination with immunostimulatory ligands including TLR ligands, polyinosinic-polycytidylic acid (poly(I:C), TLR 3 ligand), and CpG (TLR 9 ligand).
- To prepare delivery systems containing a new immunostimulatory agent threitol ceramide (ThrCer) and test the stability and efficacy of the system.

Chapter 2

Formulation, characterisation and application of lipid-coated microbubbles

Graphical Abstract:



Whilst maintaining high sensitivity a novel contrast agent, which allows stable MRI measurements of fluid pressure over time, can be produced.

Some of the results presented in this chapter have been published in the paper:
Kaur, R., Morris, R., Bencsik, M., Vangala, A., Rades, T., Perrie, Y. (2009) Development of a novel magnetic resonance imaging contrast agent for pressure measurements using lipid-coated microbubbles. *Journal of Biomedical Nanotechnology*. 5: 1-9.

2.1 Introduction

Microbubbles are comprised of shells (commonly surfactant based) encasing spherical voids or cavities filled by a gas. However, it has been shown that gas microbubbles are prone to dissolution, even in gas-saturated solutions as a consequence of the Laplace pressure across the gas-liquid interface (Duncan & Needham 2004). The Laplace pressure is the pressure difference between the inside and the outside of a bubble. The effect is caused by the surface tension of the interface between liquid and gas. The Laplace pressure is given as:

Equation 2.1

$$\Delta P = P_{\text{inside}} - P_{\text{outside}} = \frac{2\gamma}{r},$$

- P_{inside} is the pressure inside the bubble
- P_{outside} is the pressure outside the bubble
- γ (also denoted as σ) is the surface tension
- r is the radius of the bubble

Stabilisation of micron sized gas bubbles (microbubbles) against such dissolution has been shown to be achieved by the creation of a radial shell, typically composed of a polymer or surfactant such as a phospholipid (Fox & Herzfield 1954; Strasberg 1959). The amphiphilic nature of phospholipid molecules results in their accumulation and ordering at the gas-liquid interface with the hydrophilic head-group region exposed to the aqueous phase, whilst the hydrophobic tail region of the lipid is oriented towards the gas phase (Figure 2.1) (Tanford 1980). The phospholipid molecules therefore tend to self-assemble and form a monolayer shell at the surface of a gas bubble at appropriate temperature and concentration. These phospholipid shells are highly flexible and are capable of accommodating surface area changes of at least 40 % for condensed monolayers (Needham & Kim 2001). Such flexibility

may be due to the ability of phospholipid monolayers to expand through multiple phase transitions (i.e. liquid condensed, liquid expanded, as the lateral surface pressure is reduced and the area per lipid molecule is increased) (Needham & Kim 2001).

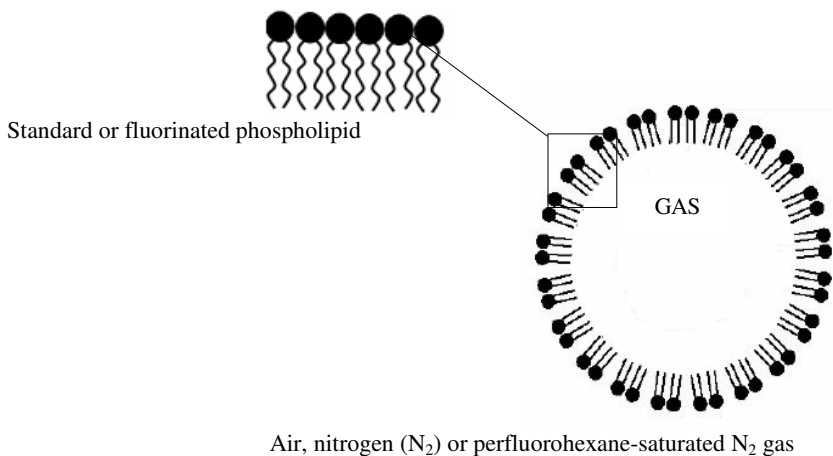


Figure 2.1 Schematic representation of a lipid-coated microbubble. The hydrophilic head-group region exposed to the aqueous phase, whilst the hydrophobic tail region of the lipid is oriented towards the gas phase.

Lipid-coated microbubbles are important in biomedical applications because of their potential as ultrasound contrast agents and drug and gene delivery vehicles. In the following sections, some of the applications of microbubbles are summarised.

2.1.1 Microbubbles and ultrasound

Ultrasound (US) is one of the most common medical imaging methods used therapeutically. US imaging has developed into a very successful modality in clinical diagnosis because it can provide real-time images of soft tissue structures and blood flow without ionising radiation. Ultrasound waves have frequencies greater than 20 KHz (Zagzebski 1996) and above the audible range of humans (which is from 20 Hz to 20 kHz) and diagnostic ultrasound typically operates in the frequency range of 1 - 10 MHz.

Medical ultrasound is now a well-established technique for clinical diagnostics and is likely to play an important role in the foreseeable future (de Jong and Ten Cate 1996). However, ultrasound images do not have a very sharp contrast, and often the area being imaged is buried and shadowed by tissues. This problem can be resolved, in part, by using ultrasound contrast agents when imaging. Ultrasound contrast agents are exogenous substances that can be administered, either in the blood pool or in a cavity, to enhance ultrasonic signals (Ohlerth & O'Brien 2007). These contrast agents can enhance the acoustic backscattering of blood significantly. This has numerous advantages when conducting ultrasound imaging, including the ability to improve blood flow imaging, and enhancing the ability to determine the delineation of organs (Hasik et al 2002). The microbubbles in the contrast agents cause this enhancement of the backscattering signal (Phillip et al 1996). The key factor in the enhancement of acoustic backscattering is the high compressibility of a gas relative to water. Two types of responses are generated when the gas bubble is insonified by a US wave:

1. The surrounding medium and the gas inside the bubble have a very large difference in acoustic impedance, which causes the bubble to reflect the US waves at its surface.
2. However, more importantly the bubble is forced into volume pulsation, causing the bubble to resonate. The significance of this event results from the difference in the orders of magnitude between the wavelength of the US wave and the diameter of the bubble, with the wavelength of the US wave being two to three orders of magnitude greater. The ratio of the scattering cross sections to the physical ratio significantly increases by having the ultrasound signal set to the resonance frequency of the microbubble (Hoff 1996). This increase in scattering cross section results in an

increase in the backscattering of up to three orders of magnitude above the level frequencies (Hoff 1996).

2.1.1.1 Classification of ultrasound contrast agents

There are four classes or generations of ultrasound contrast agents and many of these agents have been approved for clinical use (Table 2.1) (Bauer & Solbiati 2003). Although the approved indications are restricted, ultrasound contrast agents have also been used and tested widely for off-label indications in humans.

Table 2.1 General classification of ultrasound contrast agents (Ohlerth & O'Brien 2007).

Generation	Composition	Characteristics	Commercial agent (Manufacturer)	Clinical approval in humans
0	Free air microbubbles	No lung passage		
1	Air microbubbles covered by a galactose and palmitic acid shell	Lung passage	Levovist (Schering AG)	EU, Canada
2	Coated inert gas microbubbles formed by a perflutren lipid microspheres	Increased stability	Definity (Bristol-Myers Squibb)	USA, Canada
			Imagent (Alliance)	USA
			Optison (Amersham Health, Inc.)	EU, USA, Canada
3	Gas/air microbubbles, hard shell formed by a thin layer of a biodegradable cyanacrylate polymer	Controlled acoustic characteristics	SHU 563 (Schering AG)	–
			Bispheres (Point Biomedical)	–

Initially contrast agents were hand-made through agitating the agents in a physiological saline solution prior to injection. Using this method free air microbubbles are produced however, they cannot pass the capillary bed of the lungs because of their large size (50 μm), but hand-made agents have the capability to diagnose an intra or extracardiac right to left shunt (Ohlerth & O'Brien 2007). The persistence and stability of the microbubbles was increased using two principal methods: 1) the selection of gases with low diffusion coefficient and 2) the encapsulation of the bubble with or without surfactants. This has led to the development of the first generation of transpulmonary contrast agents using air as the gas in the microbubbles covered by a shell. Levovist is one of the first generation contrast agents to be investigated (Quaia 2005; Ohlerth & O'Brien 2007). Levovist has a mean diameter of 2 - 3 μm and is characterised by air microbubbles covered by a galactose and palmitic acid shell. The shell allows the microbubble recirculation and capillary passage in addition to increasing the stability of the microbubble (Ohlerth & O'Brien 2007).

To achieve better stabilisation and lower microbubble diffusion, the second generation of ultrasound contrast agents use insoluble gases. The survival of the microbubble is increased thereby increasing the diagnostic window. In addition, after intravenous (IV) bolus injection the half-life is greater than 5 minutes (Ohlerth & O'Brien 2007). One group of second-generation ultrasound contrast agents is composed of perfluorocarbon-filled (PFC) microbubbles, which have a higher molecular weight and a longer residence time in blood. Table 2.2 lists solubilities and other characteristics of some PFC and other materials useful in making microbubbles.

Table 2.2 Physical characteristics of materials used for making microbubbles and emulsions (Unger et al 2004).

Compound	Molecular weight	Boiling point (°C)	Solubility in water
Nitrogen (N ₂)	28	-195.79	Sparingly
Sulfur hexafluoride (SF ₆)	147.07	-82.7	Sparingly
Perfluoroethane (C ₂ F ₆)	138.01	-78.1	N/A
Perfluoropropane (C ₃ F ₈)	188.02	-36.7	Insoluble
Perfluorobutane (C ₄ F ₁₀)	238.04	-2	Insoluble
Perfluoropentane (C ₅ F ₁₂)	288.05	29.5	Insoluble
Perfluorohexane (C ₆ F ₁₄)	338.06	59-60	Insoluble
Perfluorooctylbromide (C ₈ F ₁₇ Br)	499	143	Insoluble

As shown in the above table, perfluoropropane and perfluorobutane are both relatively insoluble and are gases below room temperature. However, perfluoropentane is a liquid at room temperature and boils to gas at temperatures above 29.5 °C. In the United States, there are currently two perfluoropropane-based microbubble products marketed for diagnostic imaging with ultrasound. One of these products, Definity[®], was developed by ImaRx and is currently marketed by Bristol-Myers Squibb for diagnostic ultrasound imaging. The other currently marketed product is Optison[®], microbubbles stabilised by human serum albumin (Table 2.1).

Second-generation ultrasound contrast agents also have another group composed of sulphur hexafluoride-filled microbubbles, e.g. Sonovue (Table 2.1). Sulphur hexafluoride-filled microbubbles have a number of advantages ranging from the prolonged stability in the vial (up to 6 hours), and the peripheral blood (half-life of 6 minutes), and the uniformity of their size, which improves backscattering and harmonic behaviour at low acoustic power. The

prolonged stability in the peripheral blood maybe due to a high molecular weight gas with low solubility in water which confers a good resistance to pressure changes (Schneider 1999). Sonovue, similar to Levovist at low acoustic pressures, produces a clinically useful signal and a non-linear response limiting microbubble destruction (Ohlerth & O'Brien 2007). Third generation agents (e.g. Bispheres; Table 2.1) use the stabilisation of a hard shell (polymer shells) and contain either air or perfluorocarbons resulting in much longer persistence time (Leen & Horgan 2003).

2.1.2 Microbubbles and magnetic resonance imaging (MRI)

Magnetic resonance imaging (MRI) is frequently used within medicine as a diagnostic tool to produce cross-sectional images of soft tissue. MRI analyses the absorption and transmission of high frequency radio waves by water molecules in tissue placed in strong magnetic fields. Images are then created based on the differences in relaxation times of the MRI signal coming from different water densities within the biological material. Under current proposals, MRI could also be potentially used to quantify and map the oil content in the porous rock by measuring the different relaxation times of the MRI signal coming from oil and water, and this technology could be enhanced by the application of lipid-coated microbubbles. These can act as MRI pressure probes since when these microbubbles are present in a pressure varying medium, the change in microbubble size (resulting from changes in pressure) can cause a change in the MRI signal (Bencsik & Ramanathan 2001; Morris et al 2007). This would allow an accurate three-dimensional image of the pressure changes in porous rock and sandstone, which has particular application in oil recovery. Current techniques for oil recovery include drilling two wells into the non-porous layer. Water and detergents is then pumped into the first hole, which forces the oil out through the second hole (Figure 2.2). In these applications

between half and up to two-thirds of the produced oil returns. The remainder is trapped in the oil reservoir by various means. Therefore, oil recovery using such methods is often low with oil being retained in smaller porosity regions. The combination of MRI and microbubbles could potentially address this by offering the ability to investigate and determine appropriate fluid pressures required to enhance oil recovery from the smaller pore regions of the rock, thus enhancing the efficiency of oil extraction (Figure 2.2).



Figure 2.2 Schematic representation of recovery of oil from porous rock. This usually involves drilling two wells into the non-porous layer. Water and detergents is pumped into the first hole, which forces the oil out through the second hole. Lipid-coated microbubbles can be pumped into porous rock. As the microbubbles flow into porous rock they will change size to fit into the various pores. As they change size the pressure inside will change, so with different pressures there are different MRI signals. Therefore the MRI signal can be measured and information on the porosity of the stone where the oil is trapped can be obtained (Rentech 2009).

Similar microbubbles have also been demonstrated as an effective contrast agent for non-invasive manometry using MRI (Alexander et al 2006). The authors suggested the potential for detecting intravascular pressure with the aid of a lipid-coated microbubble contrast agent.

While the early experimental results *in vitro* have shown this successfully, an *in vivo* use of this technique for early detection of pulmonary hypertension was limited by inadequate sensitivity. Furthermore, it has been shown that using MRI, a gas encapsulated within suspended micrometer-sized phospholipid monolayer spheres (liposomes) causes changes in nuclear magnetic resonance (NMR) signal intensity, as a result of fluid pressure changes (Alexander et al 1996). The technique presented here again relies on compressible microbubbles suspended in a medium containing virtually unrestricted water to generate contrast to pressure. The microbubbles generate perturbations in the static magnetic field, which are dependent on their radii. A change in pressure causes a change in radius, which induces variations in signal intensity and relaxation due to water molecule diffusion (Morris et al 2008).

2.2 Aims and objectives

The aim of the experimental work reported in this chapter was to develop and characterise lipid-based microbubbles as potential contrast agents. To achieve this, the objectives were:

- Initially looking at potential characterisation methods for comparing and evaluating microbubble sizing methods using three techniques. This consisted of two different laser diffraction techniques and microscopic imaging analysis to ensure reproducibility and reliability of sizing data.
- Secondly, four different methods of producing lipid-coated microbubbles were evaluated and compared in terms of stability and physico-chemical characteristics.
- Potential formulations identified from these studies were then further investigated as contrast agents for fluid pressure.

2.3 Materials and Methods

2.3.1 Materials

Chemicals	Supplier
Chloroform	Thermo Fisher Scientific, Loughborough
Cholesterol (Chol)	Sigma-Aldrich, Poole, Dorset, UK
Citric acid	Sigma-Aldrich, Poole, Dorset, UK
Gellan gum (CP Kelco's Kelcogel AFT)	CP Kelco, USA
Headspace vial (beveled top, flat bottom)	Sigma-Aldrich, Poole, Dorset, UK
ISOTON II diluent	Beckman-Coulter, UK
Pluronic-F68	Sigma-Aldrich, Poole, Dorset, UK
Polyethylene-glycol distearate	Sigma-Aldrich, Poole, Dorset, UK
Methanol	Thermo Fisher Scientific, Loughborough
Phosphate buffered saline tablets (PBS)	Sigma-Aldrich, Poole, Dorset, UK
Perfluoropropane	Fluorochem Ltd, Derbyshire, UK
Perfluorohexane	Sigma-Aldrich, Poole, Dorset, UK
Sodium chloride (NaCl)	Sigma-Aldrich, Poole, Dorset, UK
Sodium bicarbonate (NaHCO ₃)	Sigma-Aldrich, Poole, Dorset, UK
Tris (ultra pure)	Biomedicals, Inc. Ohio, USA
Lipids	Supplier
3β-[N-(N',N'-(dimethylaminoethane)- carbamoyl] Cholesterol (DC-Chol)	Avanti lipids, Alabaster, AL, USA
1,2-distearoyl- <i>sn</i> -glycero-3-phosphocholine (DSPC)	Avanti lipids, Alabaster, AL, USA

1,2-dioleoyl-*sn*-glycero-3-
phosphoethanolamine (DOPE)

Avanti lipids, Alabaster, AL, USA

1,2-dipalmitoyl-*sn*-glycero-
phosphoethanolamine-N-(Lissamine
Rhodamine B Sulfonyl) (Ammonium Salt)

Avanti lipids, Alabaster, AL, USA

The perfluoroalkylated phosphatidylcholine (*F*-GPC) was synthesised and obtained from the Institute Charles Sadron, France.

2.3.2 Methods

2.3.2.1 Preparation of air-filled microbubbles by homogenisation

Air-filled microbubbles were prepared by modifying the method previously described by Unger et al (1999). 50 mg of DSPC was transferred into a 50 ml container and was homogenised with 5 ml of double-distilled water in the presence or absence of desired amounts of cholesterol and/or PEG-distearate and homogenised for 4 minutes below the phase transition temperature (T_c) of the lipid using a high-speed homogeniser (Ultra-Turrax T8, UK) (Figure 2.3). A thick foam comprising of air-filled microbubbles was produced over the aqueous medium.

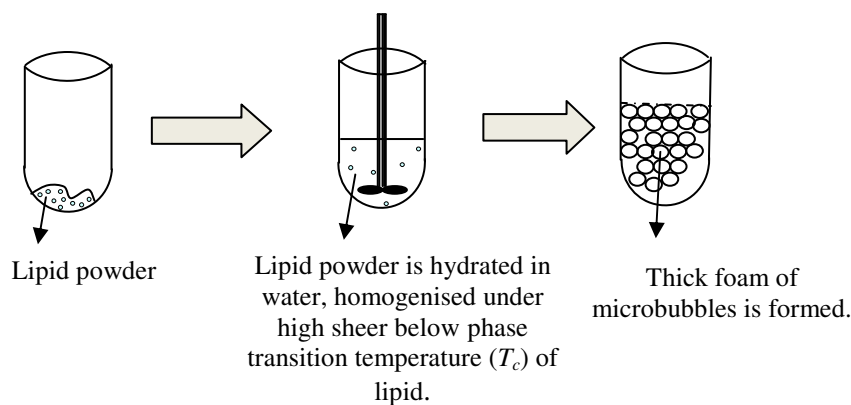


Figure 2.3 Schematic representation of microbubble formation by the homogenisation process. Lipid powder is hydrated in water, homogenised below the phase transition temperature (T_c) of the lipid. Following homogenisation, thick foam of microbubbles was formed.

2.3.2.2 Preparation of nitrogen-filled (N₂) microbubbles by homogenisation

N₂-filled microbubbles were prepared as described above, but during homogenisation the headspace above the dispersion was filled with N₂ gas. The N₂ gas was passed into the container via a syringe needle with the tip of the needle placed at the top of the dispersion. Following homogenisation, a thick foam comprising of N₂-filled microbubbles was produced over the aqueous medium.

2.3.2.3 Morphological analysis using microscopic imaging analysis

Microbubbles were viewed under an optical light microscope (Zeiss Axioskop, Germany) fitted with a colour Axio camera. Photomicrographs were obtained to assess the morphological characteristics such as microbubble size, shape and aggregation.

2.3.2.4 Fluorescent staining of microbubbles

For fluorescent staining either fluorescein sodium was included in the aqueous phase or a lipid based dye 1,2-dipalmitoyl-*sn*-glycero-phosphoethanolamine-N-(Lissamine Rhodamine B Sulfonyl) included to the lipid phase. The resulting fluorescent stained microbubbles were viewed under the optical microscope and photomicrographs taken.

2.3.2.5 Production of multilamellar vesicles (MLV)

MLV were prepared by the lipid-hydration method first observed by Bangham et al (1965). The lipids used throughout these experiments were dissolved in either chloroform:methanol (9:1 v/v) for the preparation of bubble liposomes or only chloroform (10 v/v) for the preparation of microbubbles by gas releasing chemical reaction as detailed in Table 2.3. The

required lipid solutions were placed in a 50 ml round-bottom Quick-fit flask and the solvent was removed by rotary evaporation at 37°C. This yields a thin lipid film on the walls of the flask, which was flushed with oxygen-free nitrogen (N₂) in order to ensure complete removal of all solvent traces. The dry lipid film was hydrated by addition of 2 ml of double distilled water (ddH₂O) or with sodium bicarbonate (NaHCO₃) in the case of microbubbles prepared by gas releasing chemical reaction (as described later) and agitated vigorously until the thin lipid film was completely dissolved and transformed into a milky suspension. The hydration of the lipid film was maintained above the gel-liquid crystal transition temperature T_c of the phospholipid ($>T_c$) 1,2-distearoyl-*sn*-glycero-3-phosphocholine (DSPC), has a T_c above 55 °C. Therefore, the hydration medium added to hydrate the lipid film was pre-warmed to a temperature above 55 °C and the liposome solution was maintained at this temperature during liposome formation.

Table 2.3 The concentration and the volumes used in the preparation of microbubbles in chloroform (10 v/v). Formulations were prepared such that they had a total concentration of 16 μmoles.

Formulation Molar ratio (%)	DSPC (μl) 10 mg/ml	Cholesterol (μl) 10 mg/ml	PEG distearate (μl) 10 mg/ml	DC-Chol (μl) 10 mg/ml	DOPE (μl) 10 mg/ml
DSPC (100 %)	1264 μl				
DSPC: Chol (50:50 %)	632 μl	309 μl			
DSPC: Chol:PEG distearate (47.5:47.5:5 %)	600 μl	294 μl	74.4 μl		
DSPC:Chol:PEG distearate (45:45:10 %)	570 μl	278 μl	149 μl		
DSPC:Chol:DC-Chol (33:33:33%)	417 μl	204 μl		284 μl	
DSPC:DOPE:DC-Chol (33:33:33%)	417 μl			284 μl	393 μl

2.3.2.6 Production of small unilamellar vesicles (SUV)

To generate SUV, the MLV produced were disrupted using sonic energy to fracture the large liposomes into smaller structures (< 100 nm). A probe sonicator (Soniprep 150) was used to produce SUV. The tip of the sonication probe was placed on the surface of the mixture. Table 2.3 provides the details of the formulations, the concentration and the volumes used in the preparation of aqueous liposomes and microbubbles.

2.3.2.7 Preparation of microbubbles by a gas releasing chemical reaction

Formulations were prepared at specific ratios in chloroform (10 v/v) as shown in Table 2.3. MLV were prepared by the lipid-hydration method as discussed previously in section 2.3.2.5. Following hydration of lipid film using an aqueous solution of 0.1 M sodium bicarbonate (NaHCO₃), the flask was briefly sonicated using a water bath sonicator. The liposome suspension was then dialysed against a large volume of 0.1 M sodium chloride (NaCl) solution for about 10 minutes, and then 0.1 M citric acid solution was added into the suspension and incubated for several minutes. By adding acid solvent into liposome suspension, hydrogen ions diffused through the membrane phase of the lipid particles and initiated carbon dioxide (CO₂) formation (Liu et al 2005) (Equation 2.2). The actual product is sodium citrate.



2.3.2.8 Preparation of microbubbles by sonication

Fluorinated microbubbles were prepared using the method as described by Gerber et al (2006). Fluorinated surfactant F₈H₁₁PC was mixed with Pluronic F-68 at a molar ratio of 10:1

in ISOTON II at a final concentration of 20 mM. Homogeneous dispersions were obtained after magnetic stirring for 12 hours at room temperature. The dispersions were sonicated using a Vibracell sonicator operating at 20 kHz with a total output power of 600 W. The dispersion was pre-sonicated for 30 seconds, at 30% power whilst keeping the tube immersed in a cooling bath to maintain the sample at room temperature. The dispersion was then sonicated for 15 seconds at 50 % power whilst keeping the headspace above the dispersion filled with N₂ saturated with perfluorohexane (C₆F₁₄). Following sonication, the gas flow was stopped and 14 ml of ISOTON II diluent was added to the bubble dispersion before turning the tube upside down three times. Microbubbles were formed with a fluorinated lipid constituting the shell component and perfluorocarbonated gas as the internal compartment (Figure 2.4).

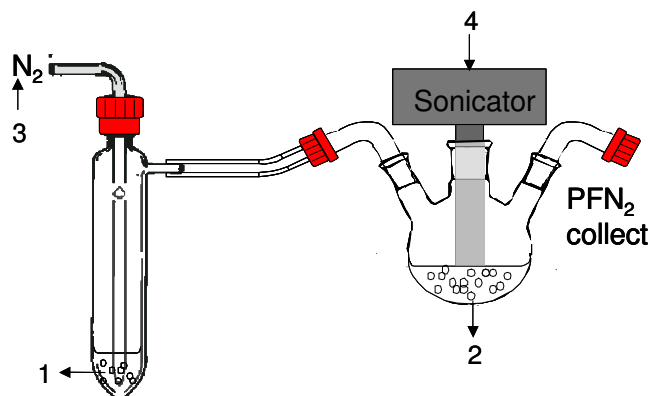


Figure 2.4 Schematic representation of microbubble formation by the sonication process. 1. The lipid is produced by adding perfluoroalkyl chains to a lipid molecule. 2. Powdered lipid is hydrated in isotonic diluent in a three neck round bottom flask. 3. N₂ gas is bubbled through perfluorohexane and into the headspace above the lipid suspension. 4. The third neck provides access for a probe type sonicator, which is used for 45 seconds at 20 kHz to generate PFC gas microbubbles, coated with a PFC lipid membrane.

2.3.2.9 Preparation of bubble liposomes

Formulations were prepared at specific ratios in chloroform:methanol (9:1 v/v) as shown in Table 2.3. MLV were prepared by the lipid-hydration method (as discussed previously in section 2.3.2.5). Following this, MLV were sonicated to produce SUV (as discussed previously in section 2.3.2.6). Bubble liposomes were prepared from liposomes and

perfluoropropane gas. The 6 ml sterilised vials containing 2 ml of liposome suspension were filled with perfluoropropane gas, capped and then pressurised with perfluoropropane gas. The vial was placed in a bath type sonicator for 10 - 15 minutes to form bubble liposomes (Suzuki et al 2007).

2.3.2.10 Determination of size and zeta potential

The size of MLV was determined using laser diffraction particle size analyser Sympatec Helos, equipped with an R2 lens allowing measurements in the range of 0.25 - 87.5 μm (Sympatec Limited, UK). Particle sizes were measured three times and the average expressed as the volume mean diameter (v_{md}) in micrometres (μm). For SUV, sizes were determined using a ZetaPlus (Brookhaven Instrument Corporation, NY) using the photon correlation spectroscopy (PCS) technique. PCS is based on the theory that the observed time dependency of the fluctuations in intensity of scattered light from a colloidal dispersion, is a function of the rate of diffusion, or Brownian motion of the scattering particles and hence their size in suspension (Tscharnuter 2000; Gun'ko et al 2003). For analysis, the liposome suspension was diluted as appropriate using ddH₂O or in citric acid for microbubbles prepared by the gas-releasing chemical reaction and the measurements recorded at 25 °C. The size reported for each sample was the average of three readings and each reading was a mean of measurements recorded for 3 minutes.

Surface charge was measured indirectly as zeta potential. The measurements were performed at 25 °C using a ZetaPlus instrument (Brookhaven Instrument Corporation, NY) using 50 μl

of the sample diluted to 2 ml in 0.1 M phosphate-buffered saline. The reported measurements are the mean of three samples, each of which is the average values of 10 readings.

2.3.2.11 Colloidal stability and Polyelectrolyte theory

Colloidal systems have been defined as dispersions of a finely divided phase in a dispersion medium (Skarba 2008). Dispersion medium, also identified as the continuous phase, is a liquid in most colloidal systems (Gurumoorthy & Khan 2011). The subdivided phase can be a solid, known as sol, or liquid, known as emulsion. Colloidal particles in colloidal systems can range in size from 1 nm to 1 μm (Hiemenz & Rajagopalan 1997). Since the particles exhibit Brownian motion they collide frequently with each other resulting in adherence and floc formation (flocculation). This destabilises the colloidal system. However, a dispersed state is maintained if the particles repel each other that stabilises the system. The attraction between colloidal particles results from van der Waals forces that range between 5 – 10 nm in many colloidal systems (Skarba 2008). Long-range repulsion (~ 10 nm) is therefore required between the particles to impart stability that should be at least as strong as the attractive force and comparable in the range of the attractive interaction (Gurumoorthy & Khan 2011). Colloidal particles surrounded with an electrical double layer (electrostatic or charge stabilisation) contribute to the stability. The theory by Derjaguin, Landau, Verwey and Overbeek (DLVO) (Skarba 2008) provides a very useful tool to understand colloid stability that is based on balance of forces between electrical double layers. For charged particles of similar nature such forces are repulsive and the long-range van der Waals forces are attractive. Thus, the sum of these two contributions dictates the potential energy of the particles. The colloidal system stability can be assessed against aggregation from the plot of potential energy

as a function of separation between the surfaces of charged colloidal particles (Figure 2.5). The presence of an electrolyte in colloidal systems facilitates the screening of the repulsive forces between electrical double layers. In the latter case, the potential energy curve has deep attractive minimum at small separations, the system will be unstable and aggregation will occur (Skarba 2008).

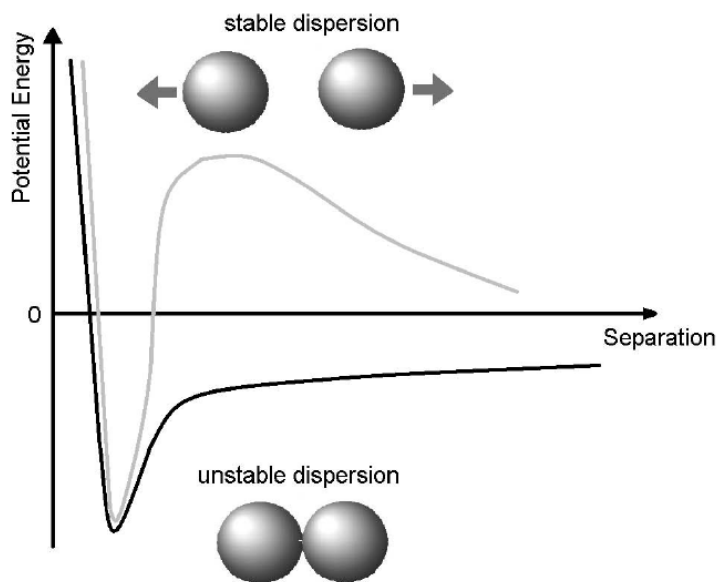


Figure 2.5 Potential energy as a function of separation between the surfaces of charged colloidal particles. Dispersion is stable with no salt added (grey line), but at high salt concentration (black line) aggregation occurs.

Polyelectrolytes have been defined as polymers carrying charged ionisable groups and depending on the charge, polyelectrolytes can be anionic or cationic (Skarba 2008). Synthetic polyelectrolytes have a wide range of industrial applications in oil recovery, paper making, mineral processing, etc. DNA and proteins are examples of natural polyelectrolytes (Skarba 2008). Properties of colloidal particles can be substantially modified by attaching polyelectrolyte to the particle surface (Adamson 1997).

2.3.2.12 MRI studies - preparation of microbubbles as pressure probes for MRI

To prevent buoyant advection of lipid coated microbubbles through the suspending medium, the gas-filled microbubbles were stabilised by a polysaccharide gel, gellan gum. The dry powder was dissolved in distilled water to a concentration of 2 % w/v whilst stirring vigorously for 8 hours under vacuum (450 torr) until a gas free homogeneous preparation was achieved. Lipid coated microbubbles were then blended with an equal concentration of glycerol before mixing with the gellan gum to a concentration of 1.25 % v/v. Having achieved a homogeneous preparation, the fluid can be used directly as an MRI contrast agent to pressure. The MRI experiments were performed using a 2.35 T Biospec small animal scanner (Bruker, Germany). The samples were placed in the holder, which is placed in the bore of the magnet. As the fluid is static, ultra fast imaging can be used without concern for flow artefacts. The fluid pressure was varied using a remotely connected syringe pump whilst the RARE sequence is run, monitored and recorded using a traditional piezoelectric pressure sensor (Figure 2.6). The average signal over the sample volume was plotted alongside the recorded pressure to test for correlation between external pressure and the signal intensity. A control sample, containing just gellan gum, was also tested to ensure that sensitivity is indeed coming from the presence of lipid coated microbubbles and not from trapped gas or other unintentional contrast mechanisms.



Figure 2.6 Schematic representation of the MRI experiment. The MRI experiments are performed using a 2.35 T Biospec small animal scanner (Bruker, Germany). The samples and a control are placed in the holder, which is placed in the bore of the magnet. The fluid pressure is varied using a remotely connected syringe pump whilst the RARE sequence is run and monitored, recorded using a traditional piezoelectric pressure sensor.

2.3.2.13 Statistical analysis

For all experiments, means and standard deviations were calculated. To determine statistical significance the one way analysis of variance (ANOVA) was performed on all data, with the statistical significance determined to 0.05 confidence intervals ($p < 0.05$). Tukey's post hoc test was conducted to determine which conditions differ significantly from each other.

2.4 Results and discussion

2.4.1 Particle size analysis of lipid-coated microbubbles

Particle size measurements are used to monitor a number of industrial processes (Etzler & Deanne 1997). The most appropriate representation for the particle size distribution measured using a given technique will depend on the sensitivity of the technique. There are a range of methods employed in particle size analysis including laser diffraction, which measures the volume of material of a given size, since the light energy reported by the detector system is proportional to the volume of material present. This contrasts with counting-based techniques such as image analysis, which measure and report the number of particles of a given size (Malvern Instruments Ltd 2009).

In this work, microbubble size distributions were compared and collected using two laser diffraction instruments: Sympatec Helos (UK) and Malvern Mastersizer (Model-S) (UK), to those distributions determined by microscopic imaging analysis. To investigate and develop protocols for sizing of microbubbles, DSPC microbubble formulations were prepared in the presence or absence of cholesterol and/or PEG-distearate and sizes determined.

From Table 2.4, it can be seen that there is a good consistency between the size of microbubbles measured by the Sympatec Helos and those recorded by image analysis, with the measured sizes not being significantly different ($p>0.05$), whereas a large difference is seen with the sizes measured by Malvern Mastersizer. Comparison between the two laser diffraction instruments show that although they employ the same principle of laser diffraction, they produced significantly different particle size distributions ($p<0.05$). This difference

suggests that each manufacturer's choice of numerical algorithms used to analyse the diffraction data are critical to the calculation of the particle size distribution. Sympatec Helos has a size measuring range of 1 μm to 87.5 μm , whereas Malvern Mastersizer measures materials from 0.02 μm to 2000 μm . The objective of this study was to identify a fast and reliable method to size the microbubble formulations; sizes obtained from image analysis were used as a benchmark of accuracy and the sizes obtained from Sympatec Helos have been shown to closely reflect these sizes. Therefore the Sympatec set-up was subsequently used to analyse microbubble particle diameters. The difference in size for the various formulations is discussed later in section 2.4.2.1.

Table 2.4 Comparison of sizes produced by laser diffraction and by microscopic imaging analysis.

Formulation	Volume mean distribution (VMD) (μm)		
	Sympatec Helos	Malvern Mastersizer	Microscopy
DSPC	$30.9 \pm 1.2 \mu\text{m}$	$139.1 \pm 7.25 \mu\text{m}^*$	$32.4 \pm 5.81 \mu\text{m}$
DSPC:Chol	$31.6 \pm 1.2 \mu\text{m}$	$119.9 \pm 16.34 \mu\text{m}^*$	$31.3 \pm 3.78 \mu\text{m}$
DSPC:Chol:PEG-distearate 5 %	$40.4 \pm 1.1 \mu\text{m}$	$74.95 \pm 42.72 \mu\text{m}^*$	$32.5 \pm 3.09 \mu\text{m}$

Results represent mean \pm SD of triplicate experiments. (Significance, measured by one-way ANOVA is shown by $*p < 0.05$).

2.4.2 Preparation of microbubbles by homogenisation

The formation of microbubbles by homogenisation is critically dependent on the phase transition temperature (T_c) of the lipid, with microbubbles being formed only at temperatures below this. The T_c is the temperature required to induce a change in the physical state of the lipid from the ordered gel phase, where the hydrocarbon chains are fully extended and closely packed, to the disordered liquid crystal phase, where the hydrocarbon chains are randomly oriented and fluid (Figure 2.7) (Lees 2008).

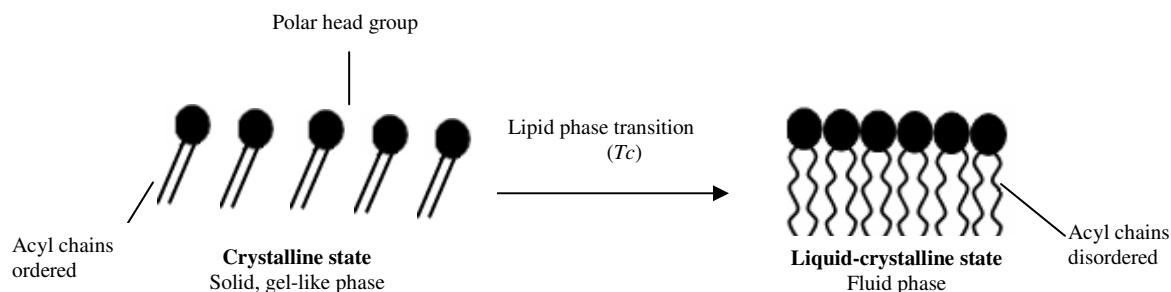


Figure 2.7 Schematic representation of phase transition temperature of lipids. The T_c is the temperature required to induce a change in the physical state of the lipid from the ordered gel phase, where the hydrocarbon chains are fully extended and closely packed, to the disordered liquid crystal phase, where the hydrocarbon chains are randomly oriented and fluid.

The lipids are in their lowest energy state when their hydrophobic chains are together and away from hydrophilic regions, and their hydrophilic head groups are in the surrounding medium. When the lipids are subjected to high shear mixing in the presence of gas and liquid, the lipid molecules orient themselves to form a monolayer at the gas liquid interface of the microbubbles. Since DSPC has a T_c of 55 °C (Frezard 1999), it was possible to form microbubbles at room temperature ~ 25 °C. However, when the T_c of the lipid was below room temperature, the formation of microbubbles was not possible (results not shown). This was further supported with an attempt to produce microbubbles containing the cationic lipid 3 β -[N-(N',N'-(dimethylaminoethane)-carbonyl) cholesterol (DC-Chol) and/or 1,2-dioleoyl-*sn*-glycero-3-phosphoethanolamine (DOPE), which was unsuccessful due to the low T_c (i.e. below 4 °C in some instances) of both lipids, which when used the outlined methods resulted in the formation of liposomes with an aqueous core rather than lipid-coated microbubbles (results not shown).

Typical air-filled DSPC microbubbles prepared using the homogenisation method described in section 2.3.2.1 are shown in Figure 2.8. Four different formulations were tested to see:

1. The effect of cholesterol: cholesterol has been shown to improve the stability of aqueous liposomes bilayer (Gregoriadis 1979); therefore the potential of cholesterol to similarly influence microbubbles would be of value.
2. The effect of PEGylation: liposomes with hydrophilic coatings are subject to less aggregation due to the highly solvated PEG groups on their surface. Close overlap of these liposomes is limited by steric hindrance, where on overlap the PEG chains would have to lose their conformational freedom and their water of hydration, thus increasing the free energy of the system (ΔH) (Florence & Attwood 2005).

Figure 2.8A shows microbubbles prepared by DSPC only. The microbubbles are shown to be heterogeneous in nature and range from 2 - 3 microns up to over 30 microns in diameter. The inclusion of cholesterol into the formulation (Figure 2.8B) results in a slightly more homogenous distribution. The addition of 5 % or 10 % PEG to this DSPC:Chol formulation (Figure 2.8C and D respectively) results in size distributions similar to that of DSPC only formulation (Figure 2.8A). Previous work investigating microbubbles prepared by the method (Vangala et al 2007a) also used microscopic analysis and found DSPC based systems to be more heterogeneous in size compared to 1,2-dipalmitoyl-*sn*-glycero-3-phosphocholine (DPPC) formulations.

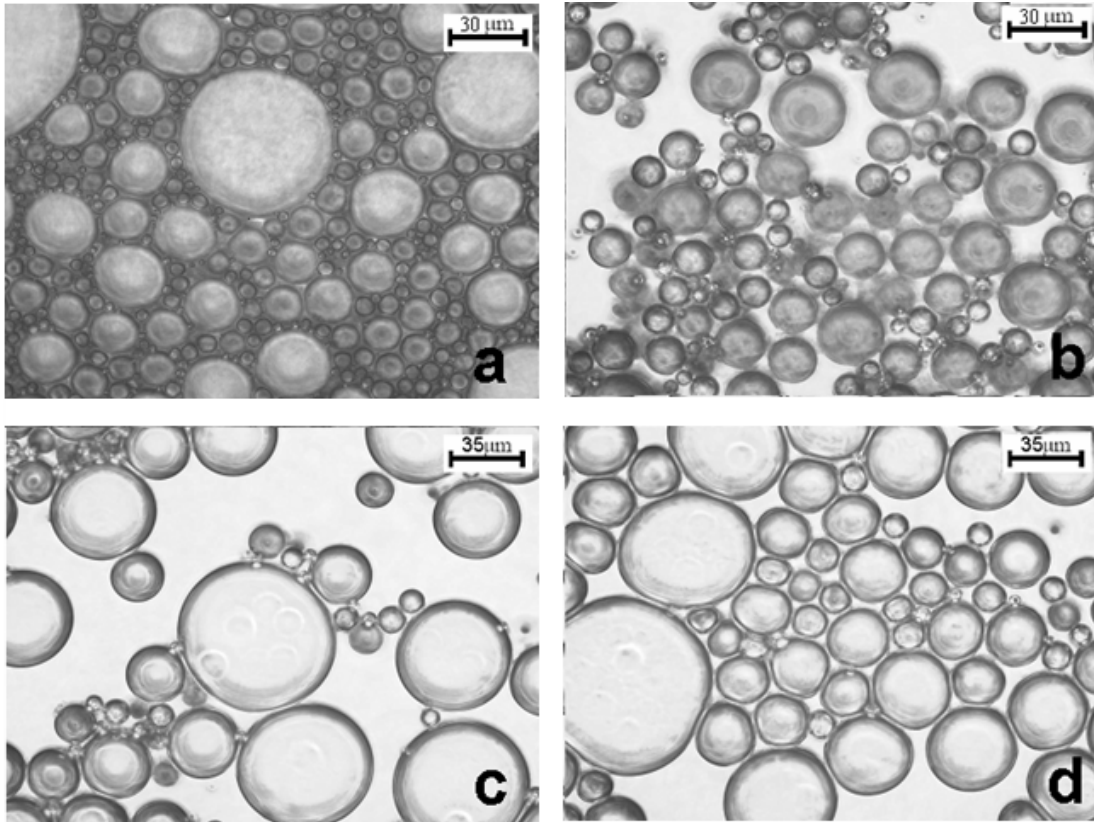


Figure 2.8 Microscopic images of microbubbles. (A) air-filled DSPC microbubbles (B) DSPC:Chol (C) DSPC:Chol 5 % PEG-distearate (D) DSPC:Chol 10 % PEG-distearate on day 0. For all four formulations microbubbles were observed to be polydisperse.

To confirm the liquid and gas phases within the lipid-based microbubbles, air-filled DSPC microbubbles were also prepared with fluorescein sodium in the aqueous phase and visualised under the light microscope with a fluorescent filter (Figures 2.9A and B, respectively). Microbubble structures can be seen with the aqueous background dyed fluorescent green, with the gas core of the microbubble showing no colour. Figures 2.9C and D show microbubbles prepared with the inclusion of the lipophilic dye 1,2-dipalmitoyl-*sn*-glycero-phosphoethanolamine-N-(Lissamine Rhodamine B Sulfonyl). Again, microbubble structures can be seen under the light microscope and the rhodamine filter (Figure 2.9C) with the lipid layers being stained red by rhodamine (Figure 2.9D). Excess rhodamine-lipid is seen as precipitate in the aqueous phase.

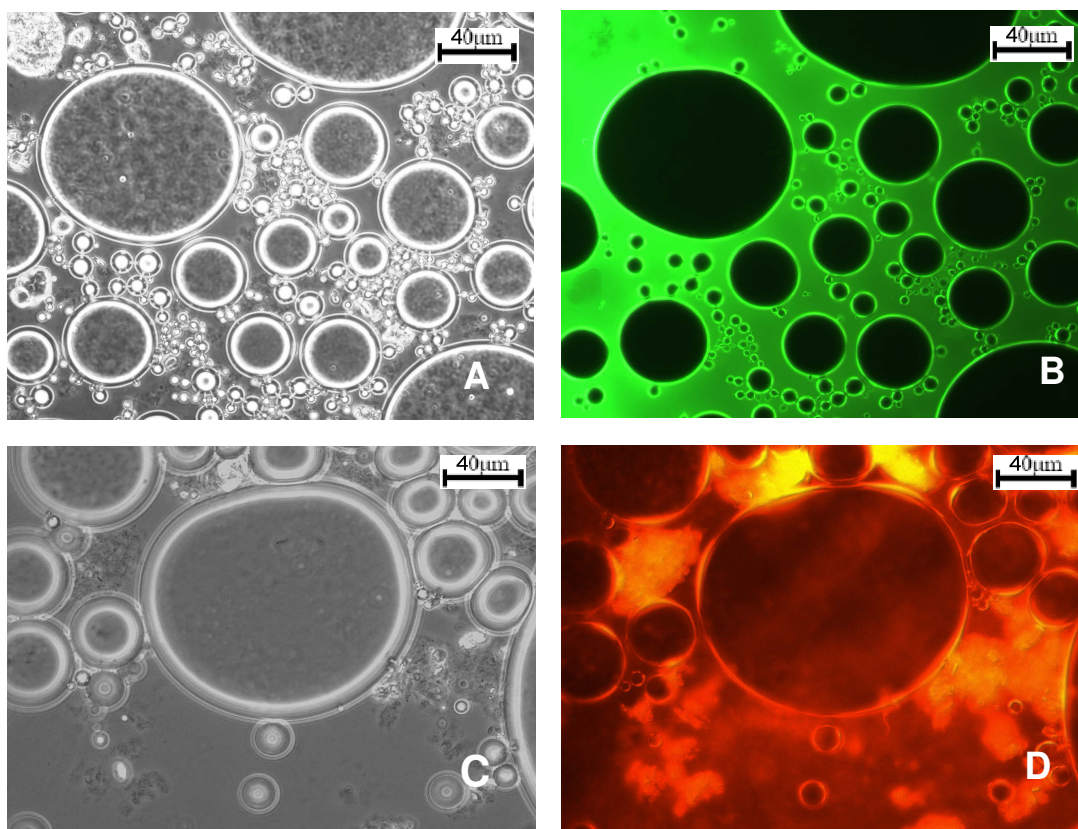


Figure 2.9 Fluorescent staining of microbubbles. DSPC-based microbubbles with the inclusion of fluorescein sodium (A) light microscope and (B) fluorescent filter. The inclusion of 1,2-dipalmitoyl-*sn*-glycerophosphoethanolamine-N-(Lissamine Rhodamine B Sulfonyl) (C) light microscope and (D) rhodamine filter.

2.4.2.1 Stability of microbubbles prepared by homogenisation

To investigate the stability of various lipid-coated microbubble formulations over time, the four formulations described in section 2.4.2 were prepared and stored at room temperature (25 °C) for up to 28 days. After initial preparation, the microbubble size distribution, as measured by the laser diffraction technique, of air-filled DSPC microbubbles was $30.9 \pm 1.2 \mu\text{m}$. By day 7 this had increased to $44.5 \pm 8.3 \mu\text{m}$, a 14 % increase (Figure 2.10), suggesting possible aggregation and/or coalescence of the microbubbles. Thereafter no significant change in size was noted. Given that cholesterol is an important component in lipid vesicles for improving the mechanical stability of the lipid bilayers (Zhang et al 2002; Gregoriadis 1979), studies were conducted to investigate the effect of its inclusion on microbubble characteristics. After

initial preparation, formulations containing DSPC supplemented with cholesterol (1:1 molar ratio) were not significantly different in size from the microbubble formulation containing only DSPC. However, unlike the DSPC formulation, microbubbles formulated from DSPC:Chol (1:1) remained stable in terms of microbubble size over the 28 days ($28.6 \pm 4.1 \mu\text{m}$ value with no significant change in size; $p > 0.05$; Figure 2.10), suggesting that cholesterol has a stabilising effect on these microbubbles in a similar nature to aqueous-filled liposomes, which display reduced vesicle aggregation/coalescence (Liu et al 2000).

The effect of PEG-distearate on microbubble size was also determined. The addition of coatings such as polyethylene-glycol onto the surface of liposomes is believed to act by forming a hydrophilic coat and causing steric hindrance at the membrane surface (Kenworthy et al 1995). PEG-distearate is the most widely used polymer to impart steric stabilisation, as it is quite soluble in organic solvents and water, and it is a very flexible polymer due to high anisotropy of its monomer i.e. high length:thickness ratio (Lasic & Papahadjopoulos 1995). The addition of PEG-distearate to DSPC and cholesterol microbubble formulations at 5 % and 10 % was therefore investigated as a potential mechanism to stabilise the liposomes. For both formulations, initial microbubble sizes were significantly larger ($p < 0.05$) than the DSPC:Chol formulations ($40.4 \pm 1.1 \mu\text{m}$ and $40.9 \pm 3.8 \mu\text{m}$ respectively; Figure 2.10). However comparing the two PEG formulations, the 5 % PEG-distearate formulation remained stable over 28 days with no significant change in size ($p > 0.05$), whilst the 10 % PEG-distearate microbubbles decreased in size over 28 days to $26.6 \pm 7.4 \mu\text{m}$ ($p < 0.05$) (Figure 2.10).

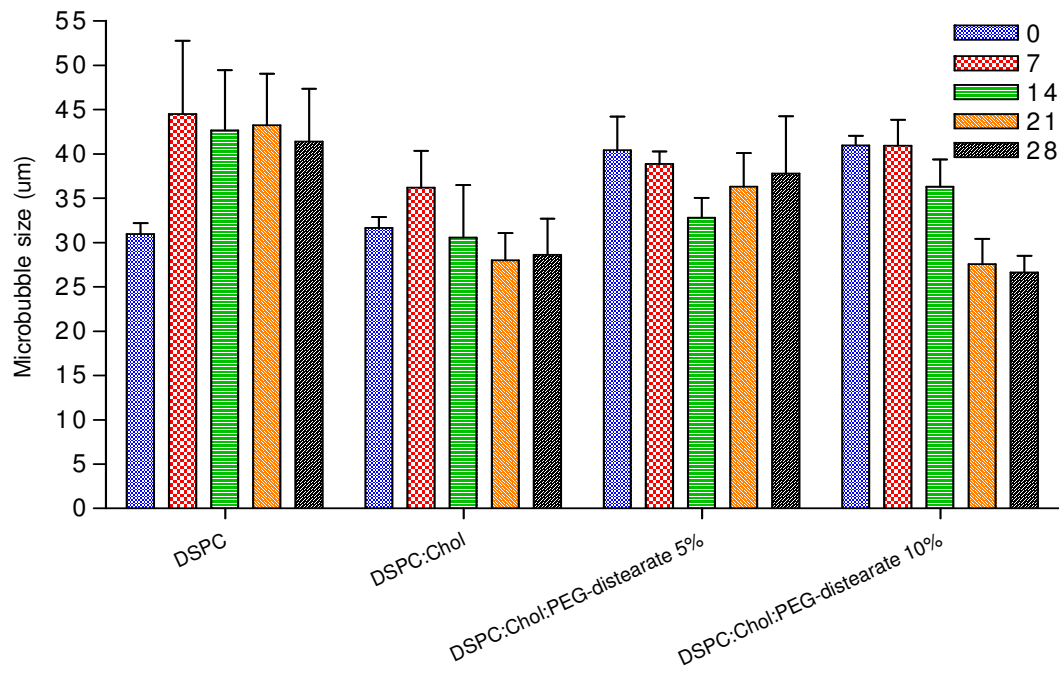


Figure 2.10 Size (μm) of air-filled DSPC supplemented with cholesterol and/or PEG-distearate at 5 % and 10 %. Microbubbles were prepared by homogenisation, determined by dynamic light scattering technique on a Sympatec Helos (Sympatec Limited, UK) in ddH₂O at 25 °C over 28 days. Results represent mean \pm SD of triplicate experiments.

As a thick foam was produced over the aqueous medium comprising of air-filled microbubbles, stability was also assessed in terms of foam volume over time (Figure 2.11). In general, foam consists of a non-equilibrium dispersion of gas in a relatively small quantity of solution usually containing surface-active materials. Surfactants such as phospholipids, proteins, or polymers, whose molecules cover the air-liquid interfaces to prevent collapse of the foam, are generally effective in increasing the foam stability (Shrestha et al 2006). From Figure 2.11, it can be seen that the foam volume of DSPC microbubbles on day 0 was 6.3 ± 1.2 ml and did not significantly change ($p > 0.05$) over the 28 day period. Whilst the microbubbles containing cholesterol in the formulation were stable in terms of microbubble size, the overall foam was shown to be unstable; on day 0 the foam volume was 3.7 ± 0.3 ml, however, this volume decreased over time to 1.1 ± 1.3 ml ($p < 0.05$; Figure 2.11) by day 28. This suggests that the foam was less stable following the addition of cholesterol to DSPC formulations and

the decrease in volume may be due to the collapse of the foam and the destruction of bubbles over time (Figure 2.11). It has been noted previously that when DSPC is intercalated with cholesterol this results in a lowering of the transition temperature with respect to the DSPC (Dopico 2007). Therefore, it is possible that by decreasing the transition temperature of the lipid mixture, cholesterol may have decreased the stability of the microbubbles and this is reflected by the decrease in foam volume.

Similar to the microbubbles prepared with cholesterol, a decrease in foam volume was observed for both the 5 % PEG-distearate formulation (4.2 ± 0.3 ml on day 0 to 0.5 ± 0.1 ml by day 28) and 10 % PEG-distearate formulation (3.8 ± 1.5 ml on day 0, to 0.7 ± 0.0 ml by day 28) (Figures 2.12C and D). This suggests that the addition of PEG-distearate did not stabilise the microbubble monolayers against foam collapse ($p < 0.05$). Visual images of these foams over time are shown in Figure 2.12.

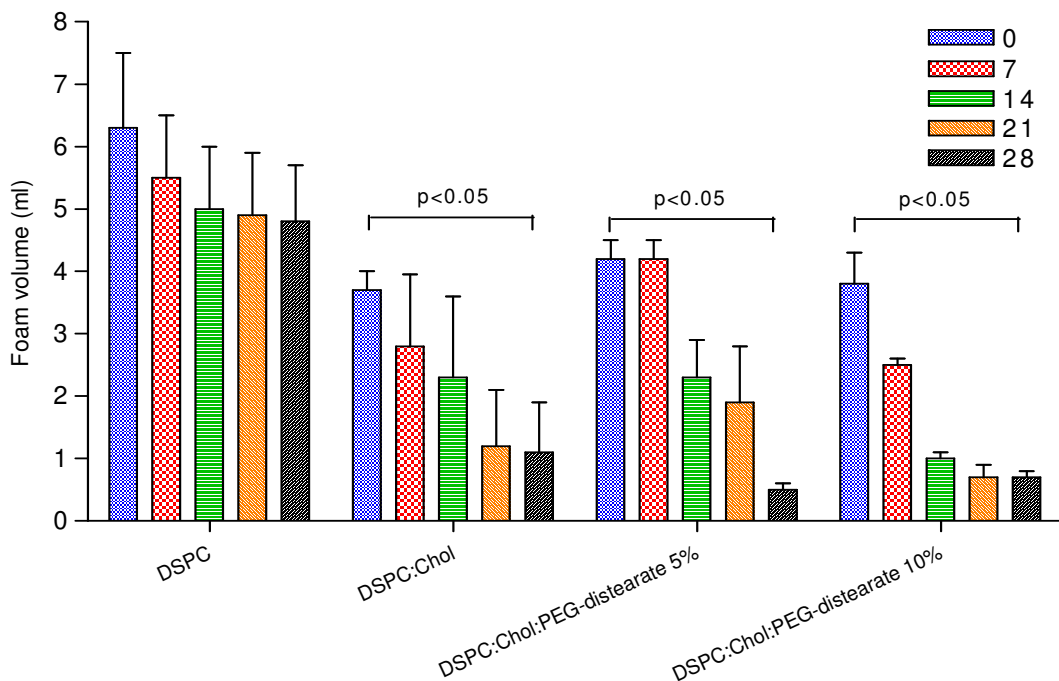


Figure 2.11 Foam volume (ml) of air-filled DSPC supplemented with cholesterol and/or PEG-distearate at 5 % and 10 %. Results represent mean \pm SD of triplicate experiments.

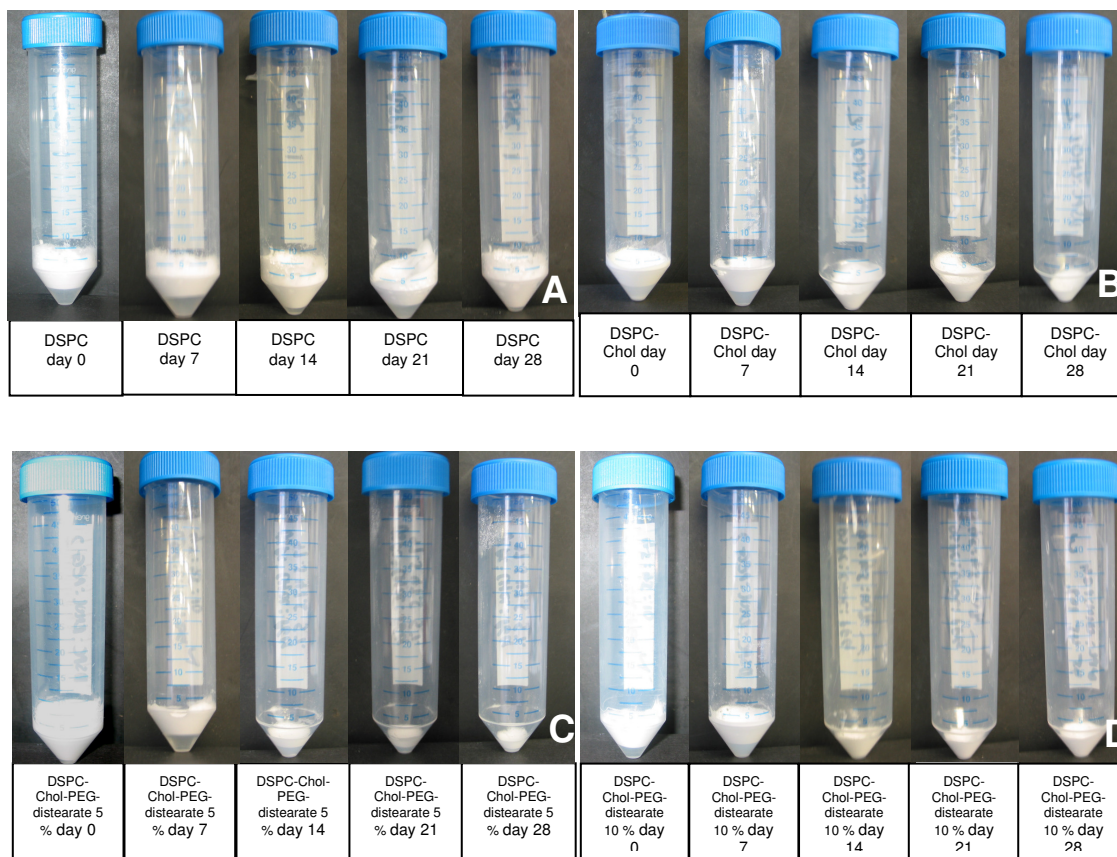


Figure 2.12 Observation of foam volume (ml). (A) air-filled DSPC microbubbles supplemented with either (B) cholesterol and/or PEG-distearate at (C) 5 % or (D) 10 %. The thick foam comprises of air-filled microbubbles which was produced over the aqueous medium i.e. water.

2.4.3 Preparation of microbubbles by a gas-releasing chemical reaction

As shown in the previous sections, using the homogenisation method it was possible to prepare a range of gas filled microbubbles from high transition temperature lipids. However, it was also noted that microbubbles containing cationic lipids could not be prepared using this method. Therefore a second method, based on the work of Liu et al (2005), was also investigated to prepare lipid-coated microbubbles. This method is based on the application of citric acid being added to an aqueous suspension containing liposomes, which have sodium bicarbonate (base) entrapped within them. Hydrogen ions from the acidic external solution can diffuse through the membrane phase of the lipid particles to initiate CO₂ formation within

the liposomes. As citric acid is a triprotic acid, it can donate three protons when reacting with a base. Therefore in addition to the gas three salts can be produced, monosodium citrate, disodium citrate and trisodium citrate. H_2O will also be produced in the reaction. As shown in Figure 2.13, after the addition of citric acid, CO_2 gas bubbles started to form. These bubbles were previously shown to be entrapped within the intravesicular space of the liposomes (Liu et al 2005). Previous work by Quaia (2005) has also shown that such CO_2 microbubbles can be employed to detect hepatocellular carcinomas and to characterise focal liver lesions after injection through a catheter placed within the hepatic artery, as for selective hepatic angiography.

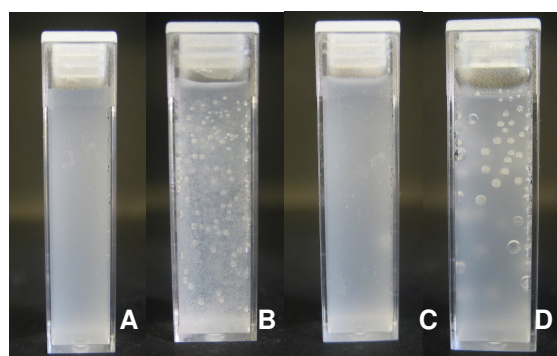


Figure 2.13 Images of microbubbles before and after pressurisation. DSPC:Chol (A) before and (B) after addition of citric acid and DSPC:DOPE:DC-Chol formulation (C) before and (D) after addition of citric acid. By adding an acid solvent into the liposome suspension, hydrogen ions diffuse through the membrane phase of the lipid particles to initiate CO_2 formation.

This method was therefore used to prepare microbubbles of the same lipid composition as those previously prepared by the homogenisation technique (i.e., DSPC, DSPC:Chol, DSPC:Chol:PEG 5 % and 10 %). Furthermore, two cationic formulations were prepared, DSPC:Chol:DC-Chol (33:33:33 % molar ratio) and DSPC:DOPE:DC-Chol (33:33:33 % molar ratio). These systems were prepared to investigate the possibility of formulating cationic microbubbles and to look at the effect of cholesterol and DOPE as helper lipids.

The sizes of microbubbles were determined using photon correlation spectroscopy. Whilst the measurement of these microbubbles was difficult to validate by this method (the buoyancy of the vesicles could interfere with the accuracy, or remaining aqueous-filled vesicles may also be present and therefore sized), the sizes determined were consistent with those of Liu et al (2005) and so were employed to further investigate the systems. From Table 2.5, it can be seen that in all cases the average sizes of the CO₂ microbubbles formed were significantly smaller than those previously prepared by the homogenisation method (Figure 2.10 vs Table 2.5 respectively) with microbubbles sizes of 2 microns or less. In addition, cationic microbubbles were able to be prepared by the CO₂ microbubble method unlike the homogenisation method.

Table 2.5 Size (nm) and zeta potential (mV) of microbubbles formed by gas-releasing chemical reaction.

Formulation	Size (nm)	Zeta Potential (mV)
DSPC	843.5 ± 176.4	1.6 ± 3.9
DSPC:Chol	983.3 ± 427.2	4.7 ± 2.7
DSPC:Chol:PEG-distearate 5 %	1768.0 ± 786.6	4.9 ± 3.8
DSPC:Chol:PEG-distearate 10 %	1439.0 ± 564.0	5.5 ± 3.7
DSPC:Chol:DC-Chol	270.8 ± 37.84	41.7 ± 1.6
DSPC:DOPE:DC-Chol	301.0 ± 29.2	45.2 ± 1.9

The size of the microbubble was measured in ddH₂O and zeta potential was determined in 0.001M phosphate buffered saline (PBS) at 25 °C using a zeta potential analyser. Results represent mean ± SD of triplicate experiments.

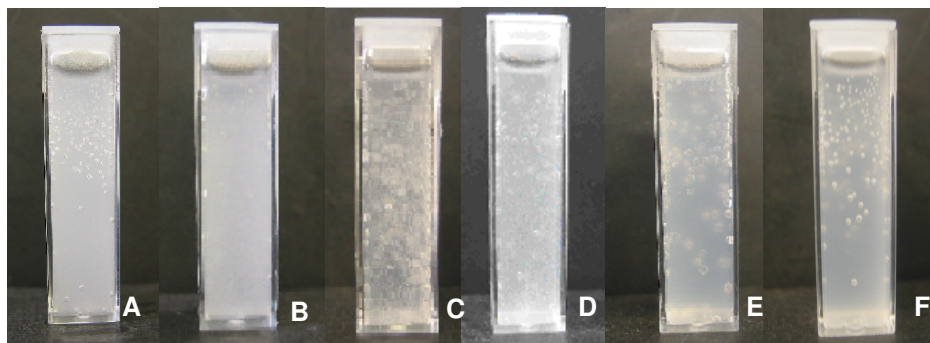


Figure 2.14 Images of CO₂ microbubbles of various liposome formulations. (A) DSPC, (B) DSPC:Chol, (C) DSPC:Chol:PEG-distearate 5 %, (D) DSPC:Chol:PEG-distearate 10 %, (E) DSPC:Chol:DC-Chol, (F) DSPC:DOPE:DC-Chol liposome suspensions containing gas bubbles. After adding citric acid, CO₂ gas bubbles started to form in the intravesicular space of the liposomes.

Comparison between the six different formulations prepared by the gas-release method of Liu et al (2005) show that liposomes prepared from DSPC were 843.5 ± 176.4 nm, with the addition of cholesterol to DSPC formulations resulting in a slight increase in microbubble size, 983.3 ± 427.2 nm (Table 2.5). A similar observation with aqueous-filled liposomes has been reported by Szoka and Papahadjopoulos (1980) where it was found that the inclusion of cholesterol at a 1:1 molar ratio increased both the mean size and the size heterogeneity of the liposomes, as measured by negative-stain electron microscopy. The addition of PEG-distearate to the DSPC-cholesterol microbubble formulations at 5 % and 10 % resulted in an increase in microbubble size to 1768.0 ± 786.6 nm and 1439.0 ± 564.0 nm respectively (Table 2.5). It can be seen that as the concentration of PEG-distearate increased from 5 % to 10 %, there was a decrease in microbubble size. It is generally expected that the particle size of a liposome becomes larger by addition of PEG-lipid because the curvature of liposomal particle decreases as the component of lipid bilayer increases (Yoshida et al 1999). The particle size of liposomes was, however, seen to decrease with increasing amount of PEG-lipid added. This correlates with previous studies of aqueous-filled liposomes. For example, Garbuzenko et al

(2005) reported a decrease in liposome size and specific turbidity when PEG-DSPE mol% was increased in liposomes composed of hydrogenated soy phosphatidylcholine (HSPC). Similarly, Yoshida and co-workers (1999) found that the particle size of liposomes prepared from DPPC decreased with increasing mole fraction of PEG-lipid. The authors suggest that this is due to a steric repulsion among the PEG chains exposed from the outer leaflet of liposomal bilayer membranes, thereby increasing the curvature of liposomal particle.

With regard to the zeta potential, from Table 2.5 it can be seen that the DSPC formulation had a charge of 1.6 ± 3.9 mV indicating a near neutral zeta potential. The addition of cholesterol to the DSPC formulation had no significant effect on the zeta potential (4.7 ± 2.7 mV; Table 2.5). A similar result was found for the formulations containing PEG-distearate, where as the percentage of PEG increased to 10 %, there was only a slight change in zeta potential to 5.5 ± 3.7 mV. This is supported by previous work (Malvern Instruments Ltd 2008), where it was found that with increasing concentration of PEG derivatised phospholipid, the zeta potential decreased. This decrease in zeta potential is caused by the presence of the PEG chains on the liposome surface reducing the mobility of the liposomes and hence the zeta potential. The zeta potential is defined as the difference in potential between the surface of the Stern layer (Stern (or shear) plane) and the distant electroneutral region of the bulk solution, and is measured by means of electrophoretic mobility in response to an electrical field (Shaw 1992).

Microbubble formulations were also prepared containing the cationic DC-Chol lipid within the DSPC:Chol formulations. In comparison to DSPC:Chol, there was a decrease in measured size (983.3 ± 427.2 nm for DSPC:Chol compared with 270.8 ± 37.8 nm for those containing

DC-Chol), and the zeta-potential increased to 41.7 ± 1.6 mV as would be expected with the DC-Chol systems (Table 2.5). Replacement of cholesterol with DOPE in these formulations resulted in no difference in the size and zeta-potential, with DSPC:DOPE:DC-Chol microbubbles being 301.0 ± 29.2 nm in size with a positive zeta potential of 45.2 ± 1.9 mV (Table 2.5). Both cholesterol and DOPE have been suggested to have a stabilising effect on aqueous liposomes (Malcharek et al 2005), and this stabilising effect is reflected by the similarity in size and surface charge for both formulations indicating that both cholesterol and DOPE are serving a similar role. DOPE has been used as a neutral complement lipid in cationic reagent mixtures; it is believed to facilitate transfection due to its tendency to form hexagonal phase structures at temperatures above 10°C (www.avantilipids.com).

The method used above is based on a previous study reported by Liu et al (2005). The authors developed stable CO_2 encapsulated echogenic liposome formulations and characterised the acoustic properties by ultrasound imaging and intensity analysis. In the present study, it can be concluded that this method has allowed the development of *in situ* CO_2 gas bubble formation inside liposomes using a range of formulations including cationic lipids, which was a drawback with the microbubbles prepared by homogenisation. Whilst the systems were characterised and compared based on photon correlation spectroscopy methods, it cannot at this stage be confirmed if the characterised systems were lipid-coated microbubbles or remaining aqueous-filled systems. However using facilities available, the characterisation of the system gave some indication of the properties of the various systems. Studies to further investigate these systems were not undertaken as the microbubbles developed by this

technique had poor stability (being stable for only 45 minutes) and their use was subsequently discontinued, with no further analysis or development undertaken.

2.4.4 Preparation of microbubbles by sonication

A further method to prepare lipid-coated microbubbles was based on the use of fluorinated-lipid perfluoroalkylated glycerol-phosphatidylcholine. Fluorinated-lipid based microbubbles (*F*-GPC) were produced according to the method of Gerber et al (2006) who previously compared air-filled microbubbles with a standard phospholipid dimyristoylphosphatidylcholine (DMPC) membrane against microbubbles filled with perfluorocarbonated-nitrogen gas and a fluorinated phospholipid *F*-GPC membrane. The authors found a synergistic stabilisation effect between the fluorinated lipid and fluorocarbon gas that allows long-lived microbubbles to be produced. This synergy led to microbubbles that have a half-life in an ultrasound field that can reach 70 minutes. PFCs, when used as part of the filling gas, retard bubble dissolution very effectively due to very low water solubility (Gerber et al 2006). Due to high biological inertness, high oxygen solubility and extremely low solubility in water, PFCs are being investigated for a range of biomedical uses, including intravascular oxygen transport, (Riess 2001) diagnosis and drug delivery.

Following the protocol of Gerber et al (2006), microbubbles were prepared and were around 500 nm in diameter and spherical in nature based on microscopic analysis (Figure 2.15). The sizes were also measured by photon correlation spectroscopy (PCS), and were measured to be 357.0 ± 95.5 nm (Table 2.6).

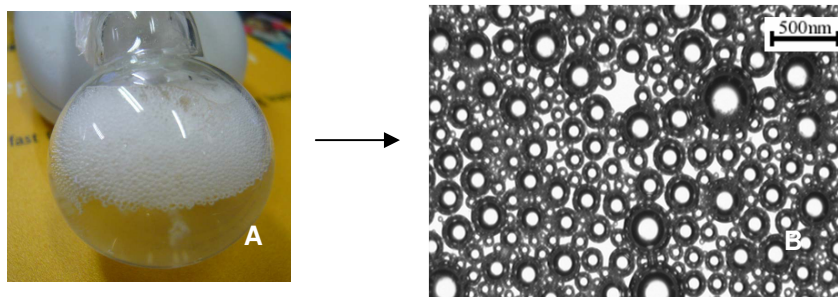


Figure 2.15 Optical image of *F*-GPC (PFC) based microbubbles (A) optical image (B) microscopic image of *F*-GPC based microbubbles. Following sonication, microbubbles with a fluorinated lipid constituted the shell component and internal fluorocarbon gas component were produced.

Table 2.6 Size (nm) of *F*-GPC based microbubbles.

Formulation	Size (nm)	Polydispersity (PI)
<i>F</i> -GPC microbubbles	357.0 ± 95.5	0.347 ± 0.04

The size of the microbubbles was measured in ddH₂O at 25 °C using PCS. Results represent mean ± SD of triplicate experiments.

From Table 2.6, it can be concluded that using this method microbubbles of less than 500 nm can be prepared when fluorinated lipid constituted the shell component and internal fluorocarbon gas component is used. However, these microbubbles were also found to be unstable and break down over a short period (30 minutes) similar to microbubbles prepared by the gas-releasing chemical reaction (section 2.4.3).

2.4.5 Preparation of ‘bubble liposomes’

The fourth method looked at the preparation of so-called ‘bubble liposomes’ (Suzuki et al 2007). Bubble liposomes have a monolayer-covered air bubble similar to lipid-coated microbubbles, however, when prepared by the method of Suzuki et al (2007) they are commonly referred to as bubble liposomes. Previous studies have investigated liposomal bubbles for gene delivery (Suzuki et al 2007); the authors found that the combination of bubble liposomes and ultrasound exposure could be an effective and novel gene delivery

method *in vitro* and *in vivo*. In the present work, bubble liposomes were produced by placing SUV liposomes in vials, supercharging with perfluoropropane gas and then placing the vial in a bath sonicator (Figure 2.16). Formulations were prepared with lipid compositions similar to those previously outlined in Table 2.7.



Figure 2.16 Preparation of bubble liposomes. Bubble liposomes were produced by placing SUV liposomes in vials, supercharging with perfluoropropane gas and then placing the vial in a bath sonicator.

Table 2.7 Size (nm) and zeta potential (mV) before and after pressurisation with perfluoropropane.

Formulation	Size (nm) and zeta potential (mV)			
	Before pressurisation		After pressurisation	
	Size (nm)	Zeta potential (mV)	Size (nm)	Zeta potential (mV)
1. DSPC	181.7 ± 82.2	-0.34 ± 1.0	148.2 ± 85.4	-0.04 ± 0.4
2. DSPC:Chol	120.6 ± 5.7	-1.24 ± 1.8	125.0 ± 2.3	-0.60 ± 0.4
3. DSPC:Chol:PEG-distearate 5 %	140.1 ± 16.3	-0.87 ± 1.7	132.6 ± 11.8	0.28 ± 0.7
4. DSPC:Chol:PEG-distearate 10 %	250.1 ± 23.5	0.27 ± 1.0	413.0 ± 41.8	-0.27 ± 0.5
5. DSPC:Chol:DC-Chol	107.1 ± 6.0	9.0 ± 5.3	107.2 ± 3.3	0.60 ± 1.0
6. DSPC:DOPE:DC-Chol	101.5 ± 5.0	8.5 ± 2.3	106.3 ± 3.5	1.2 ± 1.5

The size (nm) of the microbubbles was measured in ddH₂O and zeta potential (mV) was determined in 0.001M PBS at 25 °C using a zeta potential analyser. Results represent mean ± SD of triplicate experiments.

Sonication has long been used as a convenient method for producing SUV, with the smallest size possible. Following three minutes of sonication of MLV, the sizes of the liposomes ranged from 100 to 250 nm (Table 2.7). However, it can be seen that the size of the liposomes produced depended on lipid concentration and composition. After three minutes of sonication, the 10 % PEG formulation was found to have a size of around 250 nm compared to the cationic formulations, which were around 100 nm in size. Given the hydrated PEG on the surface of liposomes is reported to extend around 3 - 5 nm (depending on the PEG molar mass) (Medscape 2010) from the surface of the vesicles, this would not be responsible for the increased measured size however it may be due to the presence of 10 % PEG causing a reduced curvature of the vesicle construct and a subsequent larger vesicle size (Schiffelers et al 2006). Alternatively it has been suggested, that the vesicle size may start to increase after a minimum size has been achieved, due to vesicle fusion resulting from colliding of vesicles in the process (Zhang et al 2002).

Following pressurisation, the sizes of the microbubbles formed were again measured. The DSPC systems were measured at 148.2 ± 85.4 nm with a zeta potential of -0.04 ± 0.4 mV. The addition of cholesterol to the DSPC formulations resulted in slightly smaller microbubble size of 125.0 ± 2.3 nm with a surface charge of -0.60 ± 0.4 mV. The addition of PEG-distearate at 5 % to DSPC and cholesterol formulations resulted in microbubble sizes of 132.6 ± 11.8 nm. However at 10 %, an increase in microbubble size was found 413.0 ± 41.8 nm. As previously reported, the addition of PEG-distearate to the phosphate head group of the lipid may have improved the longevity and stability of the liposomes. The addition of PEG to lipids is useful in that the liposomes are significantly stabilised, their size distribution becomes more narrow,

and a mobile non-rigid surface is created on the outside of the liposome (Heldt et al 2001). The addition of a cationic lipid, DC-Chol, to DSPC and cholesterol formulations resulted in microbubble sizes of 107.2 ± 3.3 nm and a surface charge of 0.60 ± 1.0 mV. The addition of DOPE to DSPC and DC-Chol formulations resulted in microbubble size of 106.3 ± 3.5 nm and a surface charge of 1.2 ± 1.5 mV. Interestingly the zeta potentials of the cationic liposomes were significantly lower than previously measured prior to pressurisation (Table 2.7).

However from Table 2.7, it can be seen that there is very little difference in the sizes of all formulations and zeta-potentials of the non-cationic formulations of the samples before and after pressurisation. It is therefore difficult to justify if indeed gas is incorporated within these systems. Figure 2.17A-L shows each of the formulations before and after pressurisation and in some cases a change in visual turbidity is noted. However again this does not support a conclusion that gas was incorporated within lipid constructs. Previous work (Suzuki et al 2007) used ultrasound imaging to confirm that the perfluoropropane gas was trapped within the bubble liposomes and echo signals were apparently enhanced when compared with conventional PEG-liposomes. However, Pitt & Hussein (2009) have suggested that there is no experimental or theoretical evidence to substantiate the claim that perfluoropropane gas is trapped within the bubble liposomes. Pitt & Hussein (2009) have argued that the authors have not presented any physical studies or theoretical arguments that prove that the resulting product consists of the gas trapped within the liposomes. Since liposomes are vesicles with one or more bilayers of amphiphilic surfactant surrounding an aqueous interior, it has been suggested that there is no thermodynamic driving force that would induce the hydrophobic

PFP gas to form bubbles inside the aqueous interior of the liposome (Pitt & Hussein 2009). It is likely that the pressurised gas would dissolve into the liposomal suspension and remove surfactant from the liposomes to form gas bubbles that are stabilised by a surfactant monolayer on their exterior surface (Pitt & Hussein 2009). Furthermore, it is well known that insonation in an ultrasonic cleaning bath redistributes the size of liposomes, most likely by shearing existing liposomes into smaller ones. The sheared and broken liposomes would provide the surfactant required to nucleate and grow the dissolved PFP into surfactant-stabilised gas bubbles (Pitt & Hussein 2009). The authors suggest that the bubble liposomes produced may have been similar to Definity[®], a gas bubble contrast agent made from PFP gas stabilised by a lipid shell that is similar in chemistry to what these authors used for their liposomes (Pitt & Hussein 2009). In Definity[®], a single phospholipid monolayer forms the interface between the PFP gas and the aqueous environment. On the basis of the size distribution data and on the assumptions made above, we undertook no further validation or optimisation of the procedure.

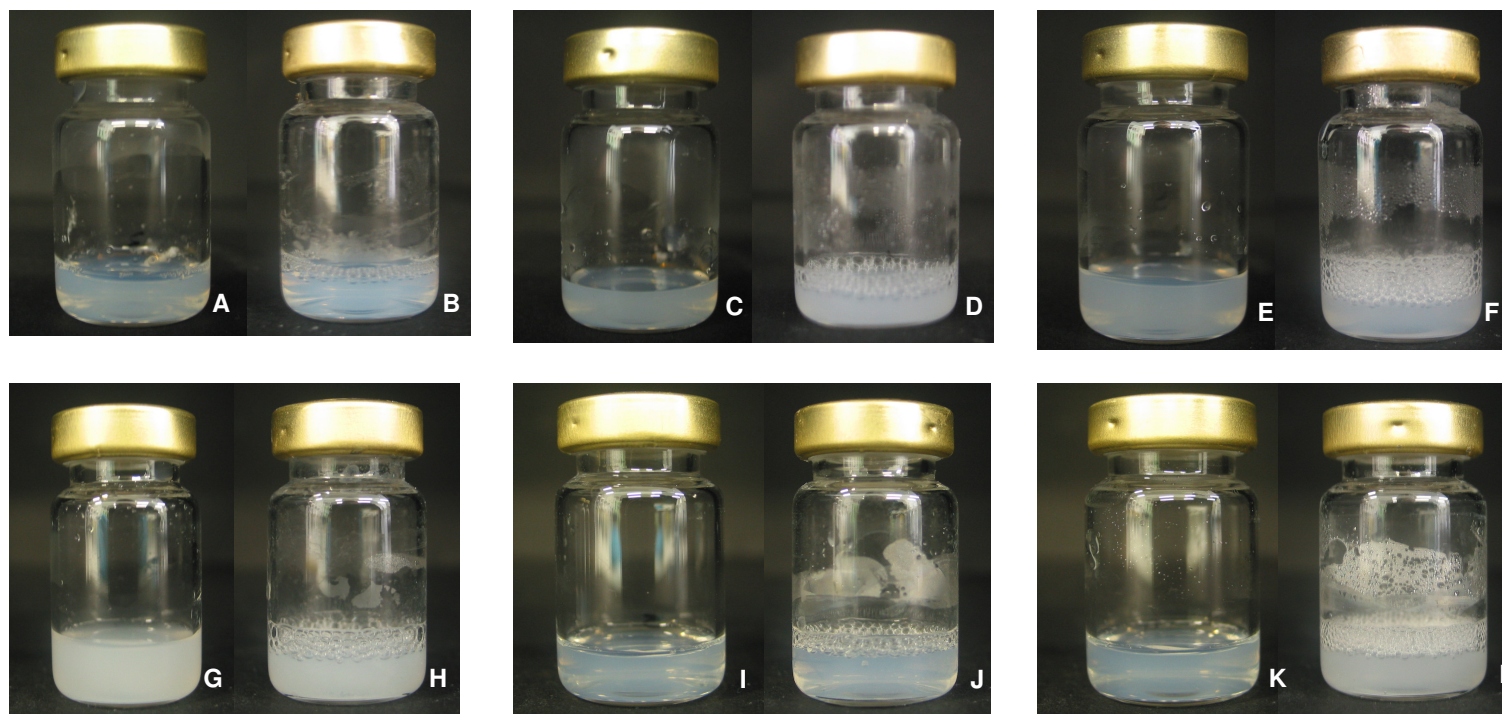


Figure 2.17 Images of various bubble liposome formulations. DSPC (A) before pressurisation (B) after pressurisation became bubble liposomes in the vial. DSPC:Chol (C) before pressurisation (D) after pressurisation. DSPC:Chol:PEG-distearate 5 % (E) before pressurisation (F) after pressurisation. DSPC:Chol:PEG-distearate 10 % (G) before pressurisation (H) after pressurisation. DSPC:Chol:DC-Chol (I) before pressurisation (J) after pressurisation. DSPC:DOPE:Chol (K) before pressurisation (L) after pressurisation.

2.4.6 Formulations to proceed forward into subsequent studies

Summarising from the above studies, microbubbles were produced using four different methods, by homogenisation, gas-releasing chemical reaction, sonication and pressurisation/agitation and the results are summarised in Table 2.8.

Table 2.8 Summary of the characterisation data.

Parameter	Preparation method			
	Homogenisation	Gas release	Sonication	Pressurisation
Vesicle size range	2-35 microns	300nm – 2µm	400nm	100-420nm
Able to prepare cationic systems	×	✓	×	✓
Stability	28 days	45 minutes	30 minutes	2 days

All four methods showed differences in characterisation for each of the different formulations tested. DSPC microbubbles prepared by homogenisation were found to produce microbubbles in the size range of 30 µm, and were found to be the most stable over time (28 days). This formulation has previously been reported to remain stable under high pressures exerted in MRI (Vangala et al 2007a), and therefore was chosen for further MRI studies. Microbubbles produced by gas-releasing chemical reaction, sonication and pressurisation/agitation were all found to be unstable within a few hours. Of these three methods, sonication produced microbubble sizes of less than 500 nm, which would be a useful comparison along with the DSPC microbubbles. Therefore this method was also chosen for further investigation. As discussed previously (Gerber et al 2006), a strong synergy between a fluorinated lipid and a fluorocarbon gas component has been suggested; this formulation was therefore compared to a standard phospholipid DSPC to determine the potential of these formulations as pressure probes in MRI.

2.4.7 MRI studies - stability of the microbubbles as pressure probes

Whilst lipid-coated microbubbles were reported to be more stable than free gas microbubbles, they were still noted to be damaged as a result of the application of pressure. This was proposed to be due to the fragile properties of their membranes and the propensity of the gas to dissolve into the surrounding fluid causing drifts in the NMR signal (Morris et al 2008). This effect, coupled with their intrinsic buoyancy, limits their application as contrast agents in MRI. To circumvent this problem, polysaccharide gels have been used to increase the viscosity of the surrounding medium and have been shown to allow lengthy and stable imaging of microbubbles using MRI, whilst retaining high diffusion of water (Morris et al 2008). As the *F*-GPC based microbubbles were unstable in water and to ensure fair characterisation, both of the *F*-GPC based microbubbles and the DSPC microbubble formulation were combined with gellan gum (2 %) to a concentration of 3 % gas v/v. Preliminary trials of this showed an increase in the stability of the *F*-GPC based microbubbles such that they could be used for the duration of the MRI experiment (results not shown). Work described in here was done in collaboration with Dr Martin Bencsik at the School of Science and Technology, Nottingham Trent University.

2.4.7.1 Comparison of stability of air-filled DSPC and F-GPC microbubbles

To investigate the stability of microbubbles under various pressures, and hence their applicability as MRI contrast agents, both formulations were subjected to cycling pressure fluctuations and the MRI signal intensity measured. By comparing the signal intensity before and after cycling the system pressure, the drift in NMR sensitivity due to microbubble damage can be measured. The preparations (and a control gellan gum sample containing no microbubbles) were synchronously subjected to time varying

pressure using an in-house manufactured acrylic cell containing three independent chambers connected to a PC controlled syringe pump with Swagelok[®] (Solon, OH) connectors. The MRI experiments were performed using a 2.35 T Biospec (Bruker, Germany) small animal scanner. The samples were driven into the holder, which is placed in the bore of the magnet. The fluid pressure is varied whilst the RARE (Hennig et al 1986) MRI sequence is run, during which the pressure is monitored using a traditional piezoelectric pressure sensor. The control sample permits confirmation that the sensitivity is due to the presence of lipid-coated microbubbles and not trapped gas or other unintentional contrast mechanisms.

Whilst the DSPC microbubbles were found to drift by 20 % signal change per bar, the *F*-GPC microbubbles were considerably more stable at 5 % signal change per bar (Figure 2.18). By increasing the pressure to which the system is cycled, it is possible to assess the value, at which the microbubbles begin to become damaged, which is the point at this drift is measurable. Using this method, the *F*-GPC microbubbles were found to withstand pressures up to 2.6 bar with minimal damage as opposed to the DSPC microbubbles, which were damaged at above 1.3 bar (Figure 2.18).

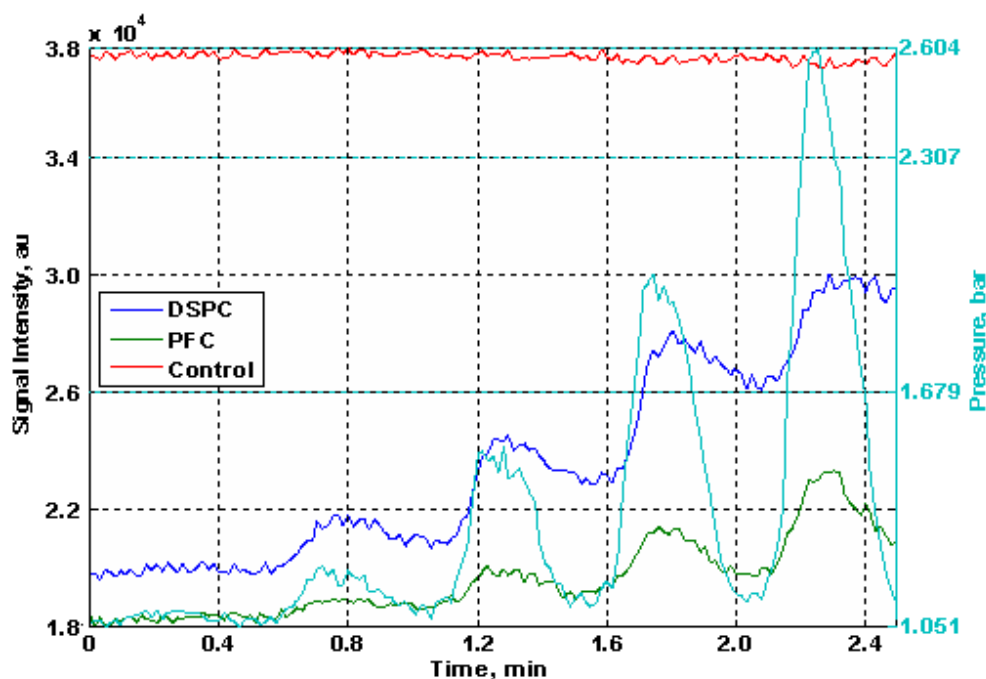


Figure 2.18 Comparison of stability of air-filled DSPC and *F*-GPC microbubbles. The two preparations were combined with an aqueous preparation of gellan gum (2 % w/v) to a concentration of 3 % gas v/v to prevent migration and improve stability. The preparations and a control gellan gum sample containing no microbubbles were synchronously subjected to time varying pressure using an in-house manufactured acrylic cell. The averaged signal found in each well (axis on the left hand side), in addition to the measured pressure (axis on the right hand side) are plotted against time. Experiment conducted at the School of Science and Technology, Nottingham Trent University.

2.4.7.2 Comparison of air-filled and N₂-filled DSPC microbubbles as pressure probes

In parallel to these studies, DSPC microbubbles were also formulated containing N₂ gas rather than air. In terms of the size of the microbubbles, the N₂ filled microbubbles were found to be slightly larger in size ($35.9 \pm 1.2 \mu\text{m}$) compared to air-filled DSPC microbubbles which were $30.9 \pm 0.5 \mu\text{m}$ after initial preparation. In contrast to the air-filled microbubbles, the N₂ gas filled microbubble formulation was found to remain stable over 28 days with microbubble sizes showing no significant change ($p > 0.05$) over the 28 day period of the study (Figure 2.19A). In terms of foam volume (Figure 2.19B), a small decrease from $19.3 \pm 1.2 \text{ ml}$ on day 0 to $15.0 \pm 0.5 \text{ ml}$ on day 28 was found ($p < 0.05$) (Figure 2.20).

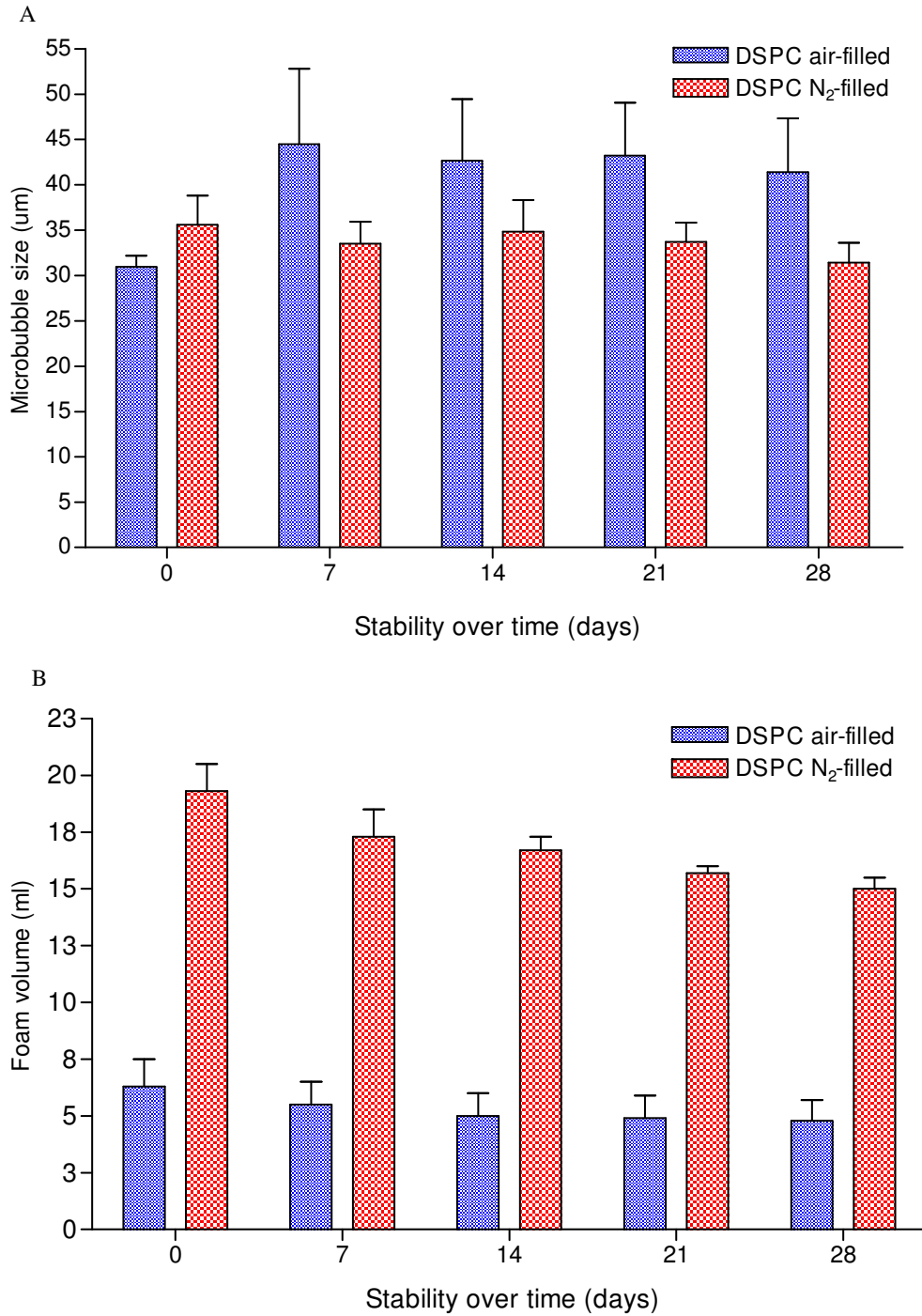


Figure 2.19 (A) Size (µm) and (B) foam volume (ml) of air-filled and N₂-filled DSPC microbubbles over 28 days. N₂ gas filled microbubble formulation was found to remain stable over 28 day period of the study and a small decrease in foam volume was found. Results represent mean ± SD of triplicate experiments.

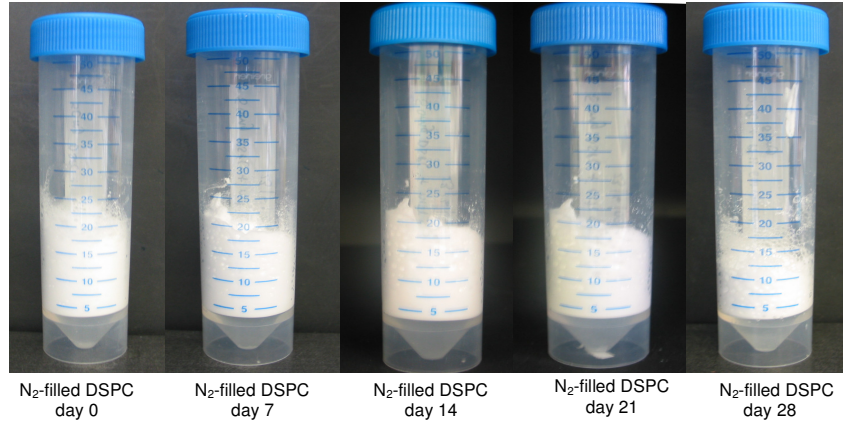


Figure 2.20 Observation of foam volume (ml) of N_2 -filled DSPC microbubbles over 28 days.

From the MRI studies, it was also found that the N_2 -filled microbubbles exhibited a sensitivity of 36 % signal change per bar and the air-filled microbubbles exhibited a sensitivity of 20 % signal change per bar at the start of the experiment (Figure 2.21). At the end of the experiment, the N_2 -filled microbubbles exhibited a sensitivity of 30% signal change per bar (a loss of 16 % of sensitivity), whilst the air-filled microbubbles exhibited a sensitivity of 9 % signal change per bar (a loss of 55 % of sensitivity) (Figure 2.21). After the first cycle of pressure change, the sensitivity exhibited by the N_2 -filled microbubbles remained fairly constant whilst that of the air-filled microbubbles demonstrates a continuous drop due to continuous bubble damage. This is a good indicator that the microbubbles containing N_2 gas are considerably more stable than their air filled counterparts and may allow for significantly more stable measurements of pressure using MRI.

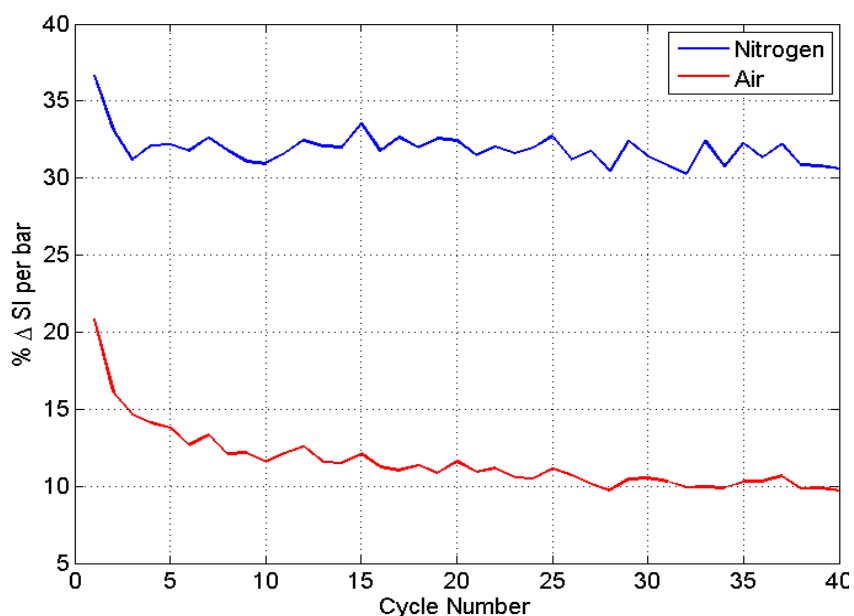


Figure 2.21 A comparison of the time course of the signal sensitivity for air and N₂-filled DSPC microbubbles. The two preparations were combined with an aqueous preparation of gellan gum (2 % w/v) to a concentration of 3 % gas v/v to prevent migration and improve stability. The signal sensitivity is determined for each cycle of pressure and plotted against time. Experiment conducted at the School of Science and Technology, Nottingham Trent University.

2.5 Conclusion

A novel contrast agent, which allows stable MRI measurements of fluid pressure over time, has been produced using lipid-coated microbubbles. Both the formulation of the microbubble shell and the gas incorporated were shown to influence stability and sensitivity: the addition of 5 % PEG and/or cholesterol was shown to stabilise the structures in terms of microbubble size. However, an overall decrease in foam volume was noted with such formulations and therefore microbubbles formulated from DSPC alone were adopted for further studies. The sensitivity of these systems could be improved using nitrogen rather than air within the microbubbles and the inclusion into polysaccharide gel counteracted their intrinsic buoyancy without reducing NMR sensitivity. However, their large size limits their medical application to non-parenteral routes. Biomedical applications of these systems may still include their application as novel contrast agents for imaging of sites accessible via non-parenteral routes such as

in bladder cancer or in the imaging of various pressure regions within joints and chronic joint disorders. Smaller *F*-GPC microbubbles were also prepared which can withstand higher pressures than the DSPC microbubbles and further refinement to improve their stability will allow their biomedical application to include echocardiography and other diagnostic ultrasound techniques, whilst the large microbubble systems may also be suitable for petrochemical applications.

Chapter 3

Cellular responses of macrophages to liposomes and lipid-coated microbubbles: *in vitro* studies

Graphical Abstract:



A diagram of phagocytosis of particulate carriers by macrophages. Macrophages take up the carriers by the process of endocytosis. Drugs are released from the carriers following intralysosomal degradation of the carriers.

3.1 Introduction

Liposomes are of considerable interest as carriers for the controlled delivery of drugs because many substances can be encapsulated in aqueous and lipid phases. One of the most well known observations in the field of liposome research is that intravenously (IV) injected liposomes are rapidly taken up by macrophages in the mononuclear phagocyte system (MPS), such as the liver and spleen (Gregoriadis 1988). More recent studies have shown that after intramuscular (IM) injection of cationic liposomes, an infiltration of macrophages was noted (Henriksen-Lacey et al 2010). Since this characteristic may be advantageous for directing antigens or immunomodulating agents to macrophages, many investigators have used liposomes as adjuvants, depots for slow release of antigens, and targeting agents for delivery of antigens to macrophages, which are one of the antigen-presenting cells (APCs) (Gregoriadis 1990; Alving 1991). However, the changes liposomes exert in these cells with which they interact remain unresolved.

3.1.1 Mononuclear phagocyte system (MPS)

The mononuclear phagocyte system consists of a number of different cells. These include bone marrow monoblasts and promonoblasts, peripheral monocytes, and tissue macrophages (Ahsan et al 2002). Of these different cells, the major differentiating cells of the mononuclear phagocyte system are the macrophages. There are three types of macrophage precursors: monocytes, promonocytes, and monoblasts. These cells all come from a common progenitor termed the colony-forming unit granulocytes-macrophages. The least mature cell of the mononuclear phagocyte system, the monoblasts, differentiate into monocytes. For 24 hours they remain in the bone marrow before they enter the peripheral blood. The monocytes then migrate

from the peripheral blood to extravascular tissue where they differentiate into macrophages (Ahsan et al 2002). Macrophages colonise the liver (kupffer cells), lungs (alveolar-interstitial macrophages), spleen, lymph nodes, thymus, gut, and marrow (Ahsan et al 2002). Macrophages have a crucial role in host defence against a number of infectious agents, including viruses, parasites, bacteria, and protozoa. A variety of substances attract the macrophages to an infected area, which include bacterial components and endotoxins, complement components, immune complexes, and collagen fragments (Ahsan et al 2002). Once the macrophages reach the infected area, they use a variety of mechanisms to phagocytose and kill infectious agents. Macrophages take protein antigens from infectious agents and generate immunogenic fragments, which facilitate their important role in the induction and regulation of the immune response (Ahsan et al 2002). Liposomes have been evaluated as carriers to deliver encapsulated molecules to mammalian cells *in vitro* and *in vivo*. Once administered in the body, liposomes of conventional formulations are avidly removed from the circulation by the macrophages of the MPS (Katragadda et al 2000).

3.1.2 Uptake of liposomes by macrophages

A number of steps can describe the complex interaction of liposomes with phagocytic cells; cell surface adsorption, cellular intact vesicle uptake by an energy dependent mechanism and lysosomal degradation of the liposomes and their content (Figure 3.1). Liposome adsorption to the cell surface seems to be the rate limiting step, since it can be assumed that stably adsorbed vesicles are more susceptible to subsequent uptake than vesicles that are only loosely interacting with the cell surface (Ahsan et al 2002).



Figure 3.1 A diagram of phagocytosis of particulate carriers by macrophages. Macrophages take up the carriers by the process of endocytosis. ● Drugs are released from the carriers following intralysosomal degradation of the carriers (Ahsan et al 2002).

In order for the liposomes to deliver biologically active agents to mononuclear phagocytes, several conditions must be met i.e. macrophages *in situ*: liposomes must readily bind to and be phagocytosed by free and fixed phagocytes, they must prevent degradation of entrapped drug, they must retain the encapsulated agent for delivery to the intracellular compartment of the MPS cells and they must localise to macrophages in organs where metastases or macrophage-associated disorders occur (Fidler 1992). A number of factors of the intended liposomes determine the extent of liposome binding and ingestion by the macrophage. These include composition, type, size and surface properties of liposomes (Ahsan et al 2002).

3.2 Aims and objectives

The aim of the work presented in this chapter was to examine the effect of liposome formulations on macrophage cells, so as to assess their potential activation of macrophages using *in vitro* models.

Factors considered were:

- Liposome composition
- Liposome concentration
- Incubation time of liposomes with macrophages *in vitro*.

To achieve this, a murine macrophage J774 was used as the model cell line, which has been widely used *in vitro* because of its similar response to stimulation as naïve macrophages (Chen et al 1999; Stumpo et al 2003). To investigate macrophage responses *in vitro*, a range of markers were measured:

1. Cell proliferation: using the 3-(4,5-dimethylthiazol-2-yl)-5-(3-carboxymethoxyphenyl)-2-(4-sulfophenyl)-2H-tetrazolium (MTS) assay (Figure 3.2). The tetrazolium compound, MTS, in the presence of phenazine methosulfate (PMS), is converted to its formazan product by the dehydrogenase coenzymes, nicotinamide adenine dinucleotide phosphate (NADPH) or nicotinamide adenine dinucleotide (NADH), which only exists in metabolically active cells. The formazan product is water-soluble and can be quantitatively measured by absorbance at 490 - 500 nm (Cory et al 1991).

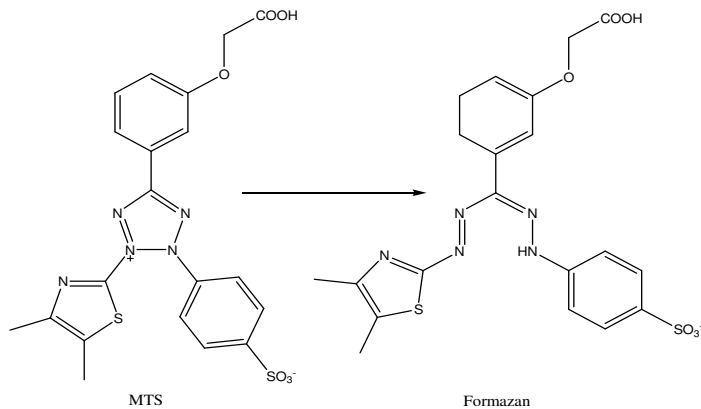


Figure 3.2 Structure of MTS tetrazolium and its formazan product.

2. Phagocytic activity: β -N-Acetylglucosaminidase (NAG, also known as N-acetyl- β -D-glucosaminidase), a lysosomal enzyme, is secreted by mammalian cells when phagocytosis takes place, and is a useful marker of phagocytic activity levels (Pettis et al 2000). Assay of NAG content can be undertaken using a colorimetric method based on the hydrolysis of 4-Nitrophenyl N-acetyl- β -D-glucosaminide (NP-GlcNAc) by NAG (Figure 3.3), and the consequent product o-Nitrophenol can be measured at 405 nm (Product information of N-acetyl- β -D-glucosaminidase assay kit).

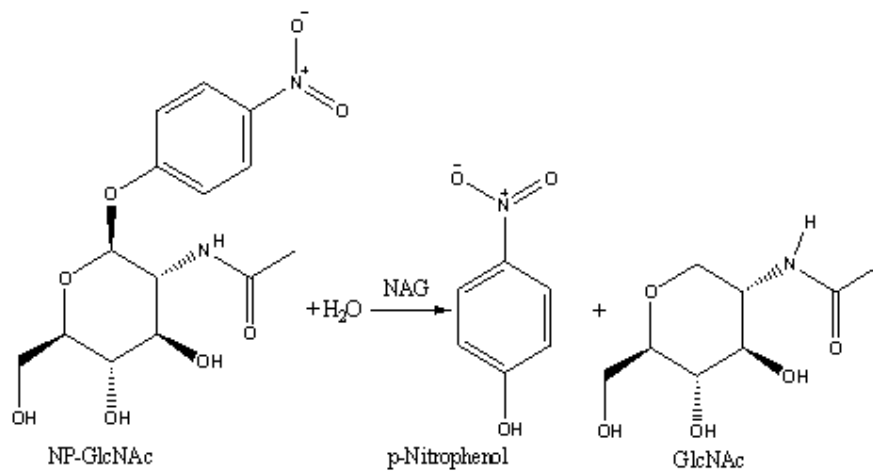


Figure 3.3 Reaction of NAG assay and relative compounds.

Other cellular markers are available, including cytotoxicity and alkaline phosphatase, but initial studies focused on the cell proliferation and phagocytic activity markers.

3.3 Materials and methods

3.3.1 Materials

Chemicals	Supplier
β -N-Acetylglucosaminidase (NAG)	Sigma-Aldrich, Poole, Dorset, UK
CellTiter 96 [®] AQueous One Solution Cell Proliferation Assay	Promega, Southampton, UK
Chloroform	Thermo Fisher Scientific, Loughborough
Dulbecco's modified eagle medium (DMEM)	Invitrogen, Paisley, UK
ELISA plates (flat bottomed)	Grenier Bio-One Ltd, UK
Foetal bovine serum (Heat-Inactivated)	Invitrogen, Paisley, UK
Penicillin-streptomycin-glutamine (100X)	Invitrogen, Paisley, UK
Polyethylene-glycol distearate	Sigma-Aldrich, Poole, Dorset, UK
Methanol	Thermo Fisher Scientific, Loughborough
Lipids	Supplier
Cholesterol (Chol)	Sigma-Aldrich, Poole, Dorset, UK
3 β -[N-(N',N'-(dimethylaminoethane)- carbamoyl] cholesterol (DC-Chol)	Avanti lipids, Alabaster, AL, USA
Dioleoylphosphatidylethanolamine (DOPE)	Avanti lipids, Alabaster, AL, USA
1,2-distearoyl- <i>sn</i> -glycero-3-phosphocholine (DSPC)	Avanti lipids, Alabaster, AL, USA

3.3.2 Methods

3.3.2.1 Resuscitation of frozen BALB/c cell line

An ampoule containing BALB/c cells (murine macrophage-like cell line) was removed from liquid nitrogen storage and half submerged in a 37 °C water bath for approximately 2 minutes, until the cells had thawed. The outside of the ampoule was wiped with a tissue moistened with 70 % isopropanol, before placing into a sterile microbiological safety cabinet in order to maintain sterile conditions. Under sterile conditions, the ampoule lid was removed, and the cell solution was slowly pipetted into a 75 cm² cell culture flask containing 20 ml of Dulbecco's Modified Eagle Medium (DMEM) supplemented with 10 % foetal bovine serum (FBS) and 1 % penicillin / streptomycin / L-glutamine, in order to dilute the toxic effects of dimethyl sulfoxide (DMSO). The cells were incubated at 37 °C under sterile conditions in a humid 5 % CO₂ conditions.

3.3.2.2 Cell quantification

Adherent BALB/c cells were brought into solution. From this cell suspension, 100 µl was removed and mixed with Trypan Blue. 10 µl of the Trypan Blue cell suspension was loaded onto a haemocytometer and viewed microscopically. The bright cells (i.e. viable cells) were counted and from this the cell concentration was calculated (including dilutions). The cells that stained blue indicated non-viable cells.

3.3.2.3 Optimisation of cell number

The concentration of macrophages was optimised using MTS assay by CellTiter 96[®] AQueous One Solution reagent, which is widely used for determining the number of viable cells in proliferation: Suzuki et al (2003) evaluated the effect of oxytocin on

proliferation of human endometrial endometrioid adenocarcinoma cell lines; O'Hare et al (2005) measured the cell viability of Ba/F3 cells transfected with Bcr-Abl kinase; Garcia-Pedrero et al (2007) measured the cell proliferation of BT549 breast cancer cells.

To establish working cell concentrations, macrophages were plated at serial concentrations of 0.01, 0.05, 0.1, 0.3, 0.5, 0.7 and 1×10^6 cells/well into a 96-well plate in 100 μ l medium in triplicate, and 100 μ l medium was also added into the plate in triplicate as blank. The plate was then incubated for 24 hours at 37 °C in a humid 5 % CO₂ under sterile conditions to let macrophages adhere to the bottom of wells. 20 μ l CellTiter 96[®] AQueous One Solution reagent was added into each well followed by a 4 hour incubation. The absorbance was read at 490 nm hourly to optimise the incubation time. The initial number of cells that produced an assay signal near the low end of the linear range of the assay (Product information of CellTiter 96[®] AQueous One Solution reagent) was selected.

3.3.2.4 Optimisation of liposome concentration

Macrophages were plated into 96-well plates at the cell number optimised in section 3.3.2.3. To optimise the liposome concentration, the cationic liposome formulation DSPC:DOPE:DC-Chol was tested at concentrations of 0.05, 0.5, 5, 50 and 500 μ g/ml.

3.3.2.5 Preparation for assays

Macrophages were plated into 96-well plates at the cell number optimised in section 3.3.2.3, and the liposome concentration optimised in section 3.3.2.4. 100 μ l of cells were loaded per well and subsequently incubated at 37 °C in a humid 5 % CO₂ under sterile conditions for 24 hours. The liposome formulations (prepared as described in

chapter 2) were re-suspended in culture medium at 5 µg/ml concentration and added to the wells to replace the supernatant in each well (Table 3.1); the supernatant of the untreated macrophage wells was replaced by fresh culture medium as control; 100 µl of culture medium in triplicate was used as background. The plate was ready for use in assays after 24 hour incubation.

Table 3.1 Summary table of the formulations tested. Liposomes were prepared in a range of compositions and in some cases as either MLV or SUV (to compare the effect of vesicle size) and in the format of lipid-coated microbubbles, to compare gas versus aqueous-filled vesicles.

Formulation	Aqueous-filled liposomes		Lipid-coated liposomes	
	MLV	SUV	Gas - Air	Gas – Nitrogen
DSPC	√	√	√	√
DSPC:Chol	√			
DSPC:Chol:PEG-distearate 5 %	√			
DSPC:Chol:DC-Chol	√	√		
DSPC:DOPE:DC-Chol	√			

3.3.2.6 Cell proliferation

Cell proliferation was measured using the MTS assay with CellTiter 96[®] AQueous One Solution. Macrophages were plated and treated with liposome samples as described in section 3.3.2.5. 20 µl CellTiter 96[®] AQueous One Solution reagent was added into each well followed by a further incubation in a period which was also optimised in section 3.3.2.3. The absorbance was measured at 490 nm. The reading of the background well was as used as a negative control; the reading of the untreated cell well was used as a positive control.

3.3.2.7 Phagocytic activities

Phagocytic activities were determined using a NAG assay with β-N-Acetylglucosaminidase assay kit, following the product information. Macrophages were plated and treated with liposome samples as described in section 3.3.2.5. 10 µl

of supernatant in each well was mixed with 90 μl of substrate solution as test sample; 2 μl of NAG control enzyme and 98 μl of substrate solution were mixed as positive control; 100 μl of substrate solution was used as the background; 300 μl of standard solution was used as the standard. The reaction components above were added into a 96-well plate in triplicate. After incubation at 37 °C for 10 minutes, the absorbance was measured at 405 nm. The concentration of NAG was calculated using the following equation:

$$\text{Units/ml} = \frac{(A_{405\text{sample}} - A_{405\text{blank}}) \times 0.05 \times 0.3 \times \text{DF}}{A_{405\text{standard}} \times \text{time} \times V_{\text{enz}}}$$

- Unit denotes that 1 unit will hydrolyse 1.0 μmole of 4-Nitrophenyl N-acetyl- β -D-glucosaminide to p-nitrophenol and N-acetyl- β -D-glucosaminide per 1 minute at pH 4.7 at 37 °C.
- $A_{405\text{sample}}$ denotes the absorbance of the sample at 405 nm.
- $A_{405\text{blank}}$ denotes the absorbance of the blank at 405 nm.
- 0.05 denotes the concentration ($\mu\text{mole/ml}$) of 4-nitrophenol in the standard solution.
- 0.3 denotes the final volume (ml) of the reaction components after the addition of the stop solution.
- DF denotes enzyme dilution factor, the value in this case is 100.
- $A_{405\text{standard}}$ denotes the absorbance of the standard solution at 405 nm.
- Time denotes the incubation time (minutes).
- V_{enz} denotes the volume (ml) of the sample.

3.3.2.8 *Statistical analysis*

For all experiments, means and standard deviations were calculated. To determine statistical significance the one way analysis of variance (ANOVA) was performed on all data, with the statistical significance determined to 0.05 confidence intervals ($p < 0.05$). Tukey's post hoc test was conducted to determine which conditions differ significantly from each other.

3.4 Results and discussion

3.4.1 Optimisation of cell number

Varying concentrations of macrophages were investigated using the CellTiter 96 AQueous One Solution Cell Proliferation Assay in order to optimise the cell number for the assays. The initial number of cells per well that produced an assay signal near the low end of the linear range of the assay would be selected as the optimised cell number to be employed in further studies. The incubation time after the addition of CellTiter 96 AQueous One Solution reagent was also investigated in order to optimise the assay condition.

The assay signals were determined hourly (up to 4 hours) (Figure 3.4). A general trend of increasing absorbance values with increasing cell numbers was noted. A comparison between the results showed that a longer incubation leads to higher absorbance levels which remained in the reading range of the micro-plate reader (Figure 3.4). However, the results of 2, 3 and 4 hour incubation, after the addition of the CellTiter 96 AQueous One Solution reagent, showed a larger and better signal range than that obtained after a 1 hour incubation. Therefore, a 2 hour incubation was chosen as the incubation time for all subsequent experiments, due to it offering the strongest linear correlation ($r^2 = 0.928$) compared with that of 3 hours ($r^2 = 0.894$) and 4 hours ($r^2 = 0.924$). Overall, a cell count of 3×10^5 cells/well was chosen as the standard cell count number, due to it being near the low end of the linear range, therefore offering a range of responses to be measured.

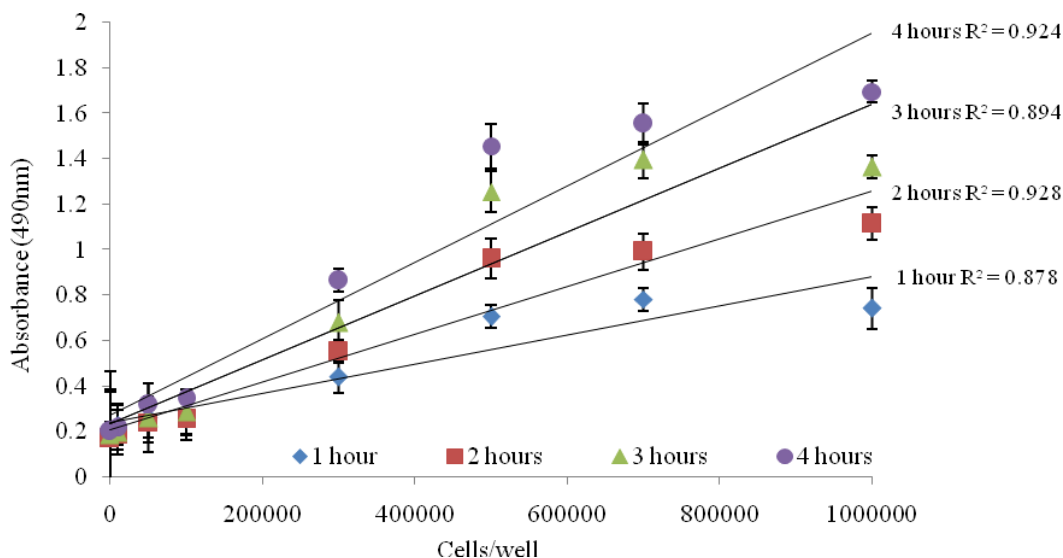


Figure 3.4 Effect of cell number of macrophages on absorbance at 490 nm measured using the CellTiter 96[®] AQueous One Solution Cell Proliferation Assay. Cells were incubated for 1 to 4 hours after the addition of the CellTiter 96[®] AQueous One Solution reagent. Results represent mean \pm SD of triplicate experiments.

3.4.2 Optimisation of liposome concentration

As it is well known, cationic liposomes are reported to show cytotoxic effects (McNeil & Perrie 2006). To optimise the liposome concentration, the cationic formulation DSPC:DOPE:DC-Chol was tested at a concentration of 0.05, 0.5, 5, 50 and 500 $\mu\text{g/ml}$ for further assays. It can be seen from Figure 3.5, that as the concentration of liposome increased, there was a reduction in the percentage of viable cells. At a liposome concentration of 500 $\mu\text{g/ml}$, the cell viability was around 60 %, in comparison to the least concentrated (0.05 $\mu\text{g/ml}$) having more than 95 % viable cells. 5 and 0.5 $\mu\text{g/ml}$ concentrations appear to be the optimum i.e. produced greater cell viability. Since the 5 $\mu\text{g/ml}$ concentration has previously been reported for liposomes in cell culture studies (Majumdar et al 1992), this concentration was selected to be used for the rest of the formulations.

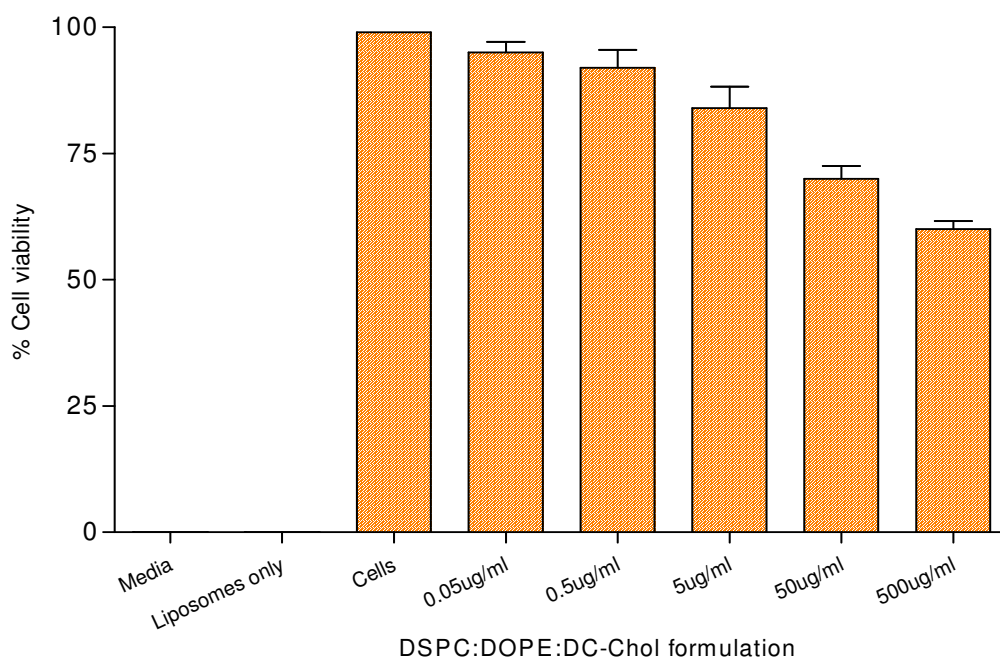


Figure 3.5 Effect of liposome concentration on cell viability. Cells were plated in triplicate at 3×10^5 cells/well and the % cell viability of DSPEC:DOPE:DC-Chol formulation added at liposome concentrations of 0.05, 0.5, 5, 50 and 500 $\mu\text{g/ml}$ was determined. Results represent mean \pm SD of triplicate experiments.

3.4.3 Characterisation of liposomes

The uptake of liposomes by resident, as well as cultured macrophages has been studied previously (e.g. Wassef et al 1984; Schwendener et al 1984; Ivanov et al 1985). From these previous studies it is generally believed that cellular uptake of liposomes is mediated by adsorption of liposomes onto the cell surface and subsequent endocytosis. Early studies indicated that liposomes, which bind to the surface of some cells, are internalised through a coated pit-mediated pathway (Straubinger et al 1983; Chin et al 1989). However, the extent of liposome binding and subsequent ingestion by macrophages depends on a number of factors. These include composition, type, size and surface properties of liposomes. To investigate the interaction of liposome composition with macrophages a range of liposome formulations were prepared. Table 3.2 shows the size and the surface charge properties of the liposomes investigated.

MLV formulated from DSPC or DSPC:Chol showed no significant difference in their size (both 18 to 20 microns in size) or zeta potential (both near neutral) (Table 3.2). Sonication of the DSPC liposomes for 3 minutes produced small vesicles (126.9 ± 12.6 nm), however, the zeta potential was not significantly different (Table 3.2). The inclusion of 5 % PEG-distearate to the DSPC:Chol formulation again caused no significant change in vesicle sizes of the MLV (18.2 ± 1.05 μ m; Table 3.2). However the zeta potential for these formulations was significantly lower ($p < 0.05$), which may reflect the highly hydrated PEG coating of the liposomes. Finally, two cationic liposome formulations containing DSPC in combination with the cationic lipid DC-Chol and either DOPE or cholesterol were investigated. Interestingly, the MLV formed with these cationic formulations were significantly smaller in size (600 - 700 nm) and cationic in nature compared to their neutral counterpart (Table 3.2). This may be a result of the reduced laminarity of the vesicles when cationic lipids are used: strong electrostatic repulsion on hydration may result in reduced bilayers and ultimately smaller vesicles (Perrie & Gregoriadis 2000a). The addition of cholesterol in replacement of the DOPE had no significant effect on the size, around 600 nm and the zeta-potential of 32 to 34 mV (Table 3.2). Previous reports have shown that sonication of cationic liposomes reduces their size but has no significant effect on their zeta potential (Perrie & Gregoriadis 2000a). Sonication of the cationic formulation DSPC:Chol:DC-Chol for 3 minutes were able to produce small vesicles (108.5 ± 22.5 nm), however, the zeta potential remained unchanged.

Table 3.2 Characterisation data for the various formulations.

Formulation	Moles (μ moles)	Composition	Size (nm)	Zeta Potential (mV)
DSPC	16	MLV	18510.0 \pm 8.4	-3.25 \pm 4.4
DSPC	16	SUV	126.9 \pm 12.6	-0.66 \pm 1.9
DSPC:Chol	8:8	MLV	19340.0 \pm 0.4	-5.19 \pm 11.0
DSPC:Chol:PEG-distearate 5 %	7.6:7.6:0.8	MLV	18160 \pm 1.0	-19.5 \pm 7.9
DSPC:Chol:DC-Chol	5.28:5.28:5.28	MLV	689.8 \pm 56.8	34.7 \pm 5.9
DSPC:Chol:DC-Chol	5.28:5.28:5.28	SUV	108.5 \pm 22.5	26.4 \pm 3.0
DSPC:DOPE:DC-Chol	5.28:5.28:5.28	MLV	589.5 \pm 20.2	32.2 \pm 6.8

The size (nm) of the liposomes was measured in ddH₂O and zeta potential (mV) was determined in 0.001M phosphate buffered saline (PBS) at 25 °C using a zeta potential analyser. Results represent mean \pm SD of triplicate experiments.

3.4.4 Effect of liposome composition on cell viability

Synthetically prepared phospholipids have well-defined fatty acid compositions and can be obtained with different or identical saturated or unsaturated chains (New 1990). DSPC is a synthetic, 18-carbon, fully saturated, phospholipid and is often used as bulk lipid for the preparation of liposomes in order to stabilise and rigidify the lipid bilayer (Gregoriadis 1990). From Figure 3.6, it was found that the aqueous-filled DSPC neutral liposomes exhibited no measured influence on cell proliferation, with the cell viability being around 93 % and not significantly different from the control. This absence of significant impact on cell viability between neutral particles and cells *in vitro* is in line with previous studies. In the early work of Leserman et al (1981) no biological effect was detected with untargeted liposomes made of neutral lipids composed of dipalmitoylphosphatidylcholine, cholesterol, and dipalmitoylphosphatidyl-ethanolamine modified with N-hydroxysuccinimidyl-3-(2-pyridyldithio)-propionate (SPDP). A study by Hsu and Juliano (1982) also found that neutral liposomes associate less effectively and are therefore less likely to be taken up

by the cells than negatively charged liposomes. This finding is also consistent with the study by Fidler (1988) who found that the binding of neutral MLV by macrophages composed exclusively of phosphatidylcholine (PC) is less efficient compared with MLV formulations composed of negatively charged phospholipids such as phosphatidylserine (PS) and phosphatidylglycerol (PG) (Ahsan et al 2002). Furthermore, a study by Ratner et al (1986) has suggested that liposomes composed of phosphatidylcholine (PC) are poorly internalised by the J774 macrophage cell line. However, other authors have also found low, but measurable, interactions between cells and neutral particles (Miller et al 1998; Lee et al 1993). The study by Miller et al (1998) examined the effect of liposome surface charge on liposomal binding and endocytosis in two different cell lines: a human ovarian carcinoma cell line (HeLa) and the J774 mononuclear macrophage cell line. The large unilamellar liposomes were composed of DOPE with and without the addition of either a positively charged lipid, 1,2-dioleoyl-3-dimethylammonium propanediol (DODAP), or a negatively charged lipid, 1,2-dioleoyl-*sn*-glycero-3-phosphatidylserine (DOPS). In some experiments 5 mol % of the anionic PEG2000-PE or a neutral PEG lipid of the same molecular weight was added. The authors found that the incorporation of a neutral PEG lipid into liposomes permits the independent variation of liposome steric and electrostatic effects in a manner that may allow interactions with cells of the reticuloendothelial system to be minimised, yet permit strong interactions between liposomes and proliferating cells. In this present work, since the cell viability was found to be above 90 %, the results are in good agreement with the general concept that cytotoxicity of liposomes depends on lipid composition and liposome concentration.

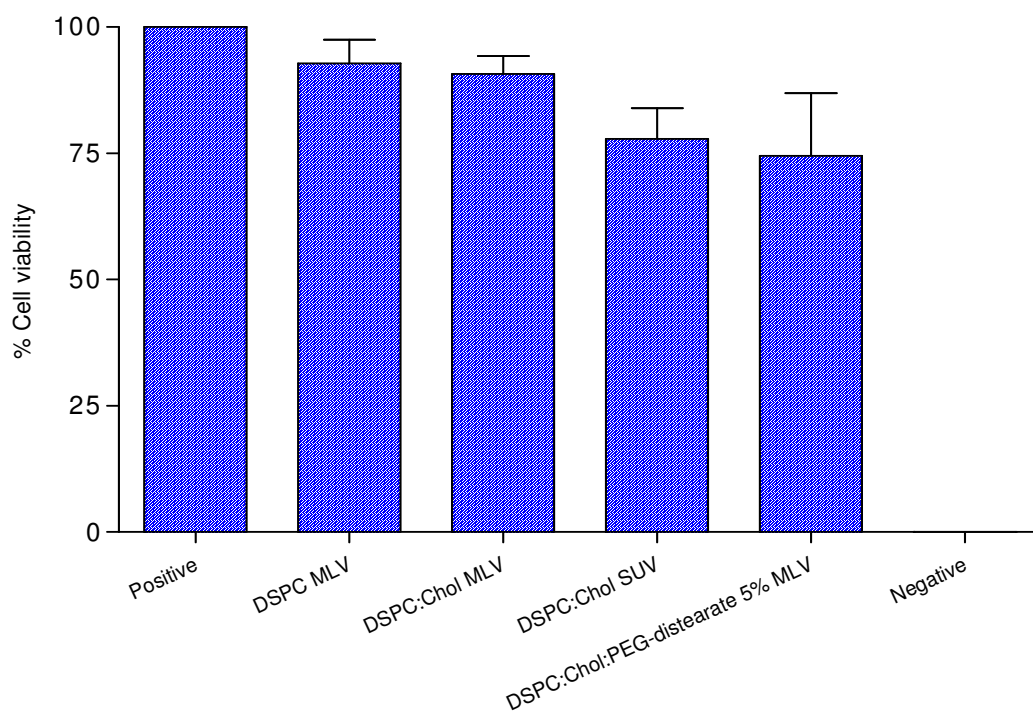


Figure 3.6 The effect of liposome composition on cell viability. Cell viability for DSPC in the presence and absence of cholesterol and PEG-distearate at 5 $\mu\text{g/ml}$ concentration. Cells were plated in triplicate at 3×10^5 cells/well. Results represent mean \pm SD of triplicate experiments.

When cholesterol was added to DSPC-based liposomes, the effect of liposomes on cell viability was essentially the same ($90.7 \pm 3.6\%$ versus $92.8 \pm 6.7\%$) (Figure 3.6). Conversely, for the small unilamellar vesicles a difference in viability was seen of around 78%. This decrease in cell viability may be due to the small particle size of the liposomes. Previous work (Gamon et al 1989; Crommelin 1984) has found that the smaller DSPC:Chol vesicles are unattractive for therapeutic applications because of several limitations including, low aqueous entrapped volume, particle instability due to lack of charge stabilisation and a strong dependence of circulation on particle size, length of the saturated acyl chains and lipid dose.

The impact of PEG binding to cholesterol on *in vitro* behaviour of liposomes in terms of cell viability was also investigated. From Figure 3.6, it was found that following

addition of inert hydrophilic polymer PEG-distearate, there was a significant difference ($p < 0.05$) in cell viability compared to the neutral DSPC formulation ($74.4 \pm 12.5\%$ versus $92.8 \pm 6.7\%$ respectively; Figure 3.6). Compared with the DSPC:Chol MLV, again a significant difference was found ($74.4 \pm 12.5\%$ versus $90.7 \pm 3.6\%$ respectively). The polyethylene-glycol (PEG) chain of liposome surfaces has a steric hindrance effect on the liposomes with various molecules. This effect is also considered to reduce the interaction of liposomes with cells (Kuhl et al 1994). This stabilising effect has also been reported to be responsible for the prolonged circulation time within the systemic circulation after intravenous injection (Vertut-Doi et al 1996), as the liposomes are thought to be masked from uptake by macrophages of the MPS.

Cationic liposomes are taken up by a variety of cells through electrostatic interactions between the cationic charge of the liposomes and the anionic charge of the cells (Aramaki et al 1999). From the results in Figure 3.7, it can be seen that the cell viability for both of the multilamellar formulations, including both helper lipids cholesterol and DOPE, was around 60 %, whereas for the small unilamellar vesicles a cell viability of 65 % was found. This is a significant reduction in cell viability compared to the neutrally charged formulations. Previous work has found that cationic liposomes display some disadvantages such as cytolytic and cytotoxic activities. Liang & Chou (2009) have found that cationic vesicles with more positive zeta potentials are associated with a significant poor survival of HaCaT and SCC25 cells in mixed HSPC/DXDAB or EPC/DXDAB vesicular systems. However, no effect on particle size of cationic vesicles on the corresponding cytotoxicity of HaCaT and SCC25 was evident in this study, although some researchers have proposed that

smaller vesicles can be taken up by cells more easily (Win & Feng 2005). This absence of any difference between the MLV and SUV may be explained by the suggestion of Jubeh et al (2004) that the variation in the adhesion intensity of vesicles with particle size may drop as contact time increases. Notably, the zeta potential of cationic vesicles and not the particle size seems to dominate the cell viability. Cell membranes have large negatively charged domains, which should attract positively charged vesicles. A high affinity of cationic vesicles for cell membranes is expected, primarily because of the electrostatic interactions. After cationic liposomes are bound to cellular membranes, uptake may proceed by means of several mechanisms, such as endocytosis, pinocytosis or phagocytosis (Weinstein 1981; Lorenz et al 2006). Other studies of the interaction of cationic liposomes with cells have also established that the behaviour of liposomes on cells depends primarily on the charge density of cationic charge (Barbour & Hopwood 1983; Miller et al 1998). Pure DODAB cationic vesicles have also been demonstrated to generate a positive charge on the bacterial cell surfaces and induce bacterial death (Campanha et al 1999; Vieira & Carmona-Ribeiro 2006). This fact may explain why cytotoxicity is a function of the zeta potential of cationic vesicles.

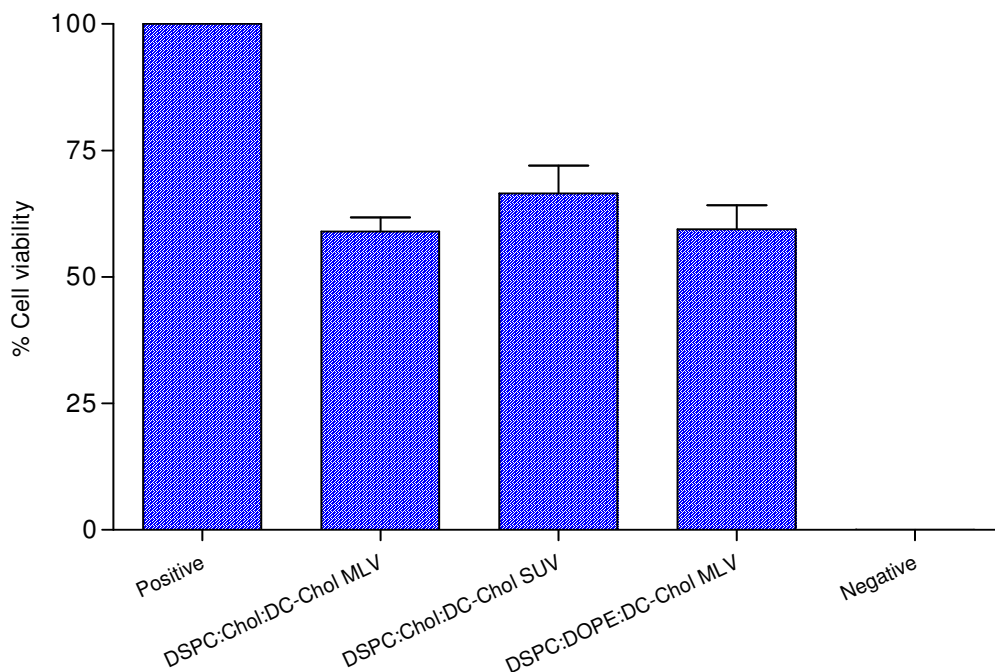


Figure 3.7 The effect of cationic liposomes on cell viability. Cell viability for cationic formulations at 5 µg/ml concentration. Cells were plated in triplicate at 3×10^5 cells/well. Results represent mean \pm SD of triplicate experiments.

3.4.5 Effect of microbubbles on cell viability

As discussed previously in chapter 2, microbubbles were formulated by the homogenisation method composed of the neutral lipid, DSPC, filled with either air or N₂. To investigate the potential of these systems for potential therapeutic and/or diagnostic applications, these microbubbles were investigated in terms of their effect on cell proliferation. The microbubbles were compared to aqueous-filled DSPC liposomes. From Figure 3.8, a similar result was found to that of aqueous-filled liposomes where 93 % cell viability was found for all three formulations with no significant difference. This suggests that incorporation of either air or nitrogen within the microbubbles had no significant impact on cell proliferation, and the microbubbles are not toxic to the cells. Previous work (Tran et al 2007) investigated the effect of ultrasound and microbubbles on cell viability. The authors found that using ultrasound

alone, Sonovue microbubbles alone, or a combination of both did not show any effect on cell viability using acoustic pressures up to 300 kPa, with no significant difference compared to the control (Tran et al 2007).

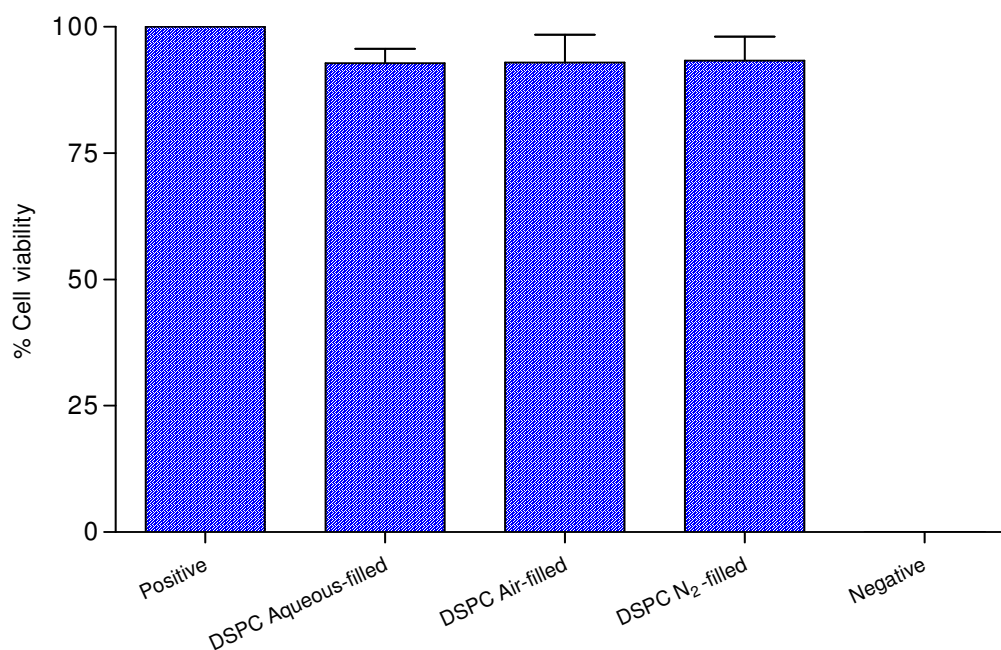


Figure 3.8 The effect of microbubbles on cell viability. Cell viability for aqueous-filled and lipid-coated microbubbles formulations at 5 $\mu\text{g/ml}$ concentration. Cells were plated in triplicate at 3×10^5 cells/well. Results represent mean \pm SD of triplicate experiments.

3.4.6 Phagocytic activities

It is well known that macrophages internalise particulate carriers, such as those formulated in the above studies, by the process of endocytosis (Silverstein et al 1977; Van Oss 1978). However, there is no acceptable explanation about how the extent of phagocytosis by macrophages is related to physicochemical characteristic properties of particulate carriers. In particular, the influence of surface charge and size of particulate carrier on phagocytosis is not fully understood. Effects that have been noted include:

- Surface charge: It is believed that charged carriers are better phagocytosed by macrophages because of the non-specific electrostatic interactions between cells

and carriers (Raz et al 1981; Van Oss, 1978). Some authors (Allen et al 1991a) also argue that macrophages may have receptors that help carriers adsorb by electrostatic attraction on the surface of the macrophages. Thus, a stable adsorption may lead to enhanced uptake of the carriers by macrophages.

- Particle size: It has been postulated that the size of liposomes might influence their availability to interact with the microenvironment of the cell surface as well as the degree and strength of interaction necessary for adsorption (Schwendener et al 1984).

Therefore to investigate the uptake of the various formulations tested NAG release, as an indicator of phagocytic activity, in the culture supernatant of macrophages exposed for 24 hours to liposomes and microbubble formulations was determined. From Figure 3.9, it can be seen that in comparison to the positive control, all of the aqueous liposome formulations did not stimulate measurable phagocytic activity in the macrophages tested. According to the research of Horisawa et al (2002), large particles are likely to attach to the surface of the macrophage rather than to be uptaken, with the upper size limit for macrophage phagocytosis being 5 μm . This may be true for the multilamellar liposomes, however, not for the small unilamellar liposomes since they were around 150 - 200 nm in size. A study by Magee et al found that the initial interaction of the liposomes with cells seemed to rely only on the charge attraction between the positively charged particles and the negatively charged cells. Therefore, the cationic liposomes formulations (Table 3.2) were also tested. However similar to the neutral formulations, these formulations did not result in measurable release of NAG, suggesting that these formulations were effectively 'inert' at the concentrations tested, i.e. low impact on phagocytosis.

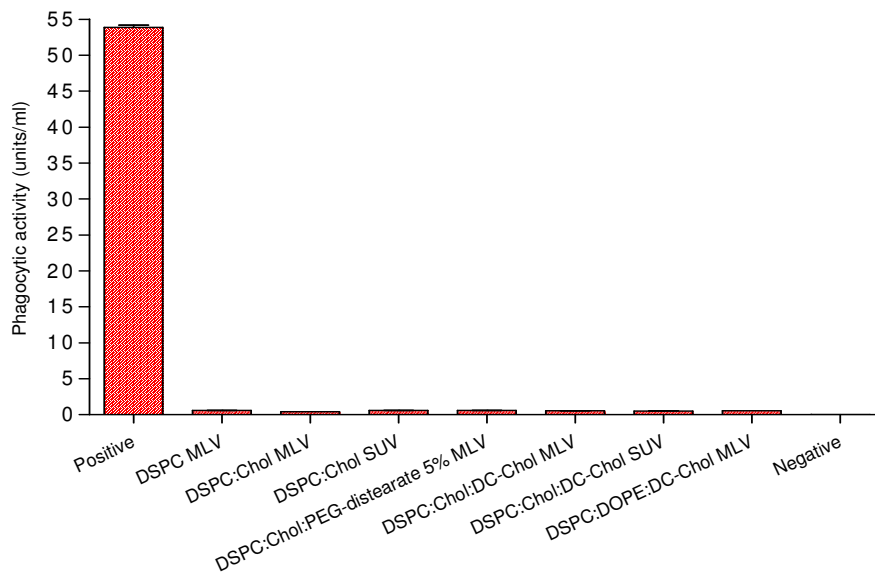


Figure 3.9 Phagocytic activity (units/ml) measured for aqueous-filled liposomes. Cells were plated in triplicate at 3×10^5 cells/well and the phagocytosis of the various formulations at liposome concentration of $5 \mu\text{g/ml}$ was determined. The reading of background well was as used as a negative control; the reading of untreated cell well was used as a positive control. Results represent mean \pm SD of triplicate experiments.

For the microbubble formulations, again no phagocytic activity was found (Figure 3.10) suggesting these formulations would not stimulate macrophage uptake with an aqueous or gas core making no difference.

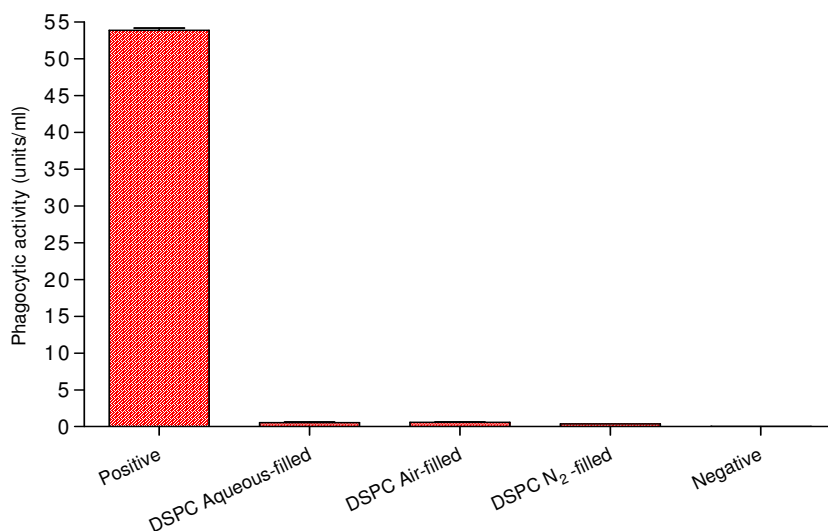


Figure 3.10 Phagocytic activity (units/ml) measured for microbubbles. Cells were plated in triplicate at 3×10^5 cells/well and the phagocytosis of the various formulations at liposome and microbubble concentration of $5 \mu\text{g/ml}$ was determined. The reading of background well was as used as a negative control; the reading of untreated cell well was used as a positive control. Results represent mean \pm SD of triplicate experiments.

3.5 Conclusion

Both the aqueous-filled liposomes and gas-filled liposomes were tested for their effect on cell proliferation and phagocytic activity in a macrophage cell line. None of the formulations within the concentrations selected influenced either of the activities measured however this will be concentration dependent particularly in the case of the cationic formulations. In terms of the application of the lipid-coated microbubbles, this demonstrates their further potential in diagnostic imaging given that these lipid-coated microbubbles were demonstrated in the previous chapter to act as potential contrast agents that allow stable MRI measurements of fluid pressure over time. Whilst their large size prohibits their delivery intravenously, given their low measured toxicity and contrast agent application, there remains a potential for these systems to be used for example as low cost imaging tools e.g. in bladder cancers.

In addition to the application of microbubbles as contrast agents (Bauer & Solbiati 2003; Ohlerth & O'Brien 2007), publications have suggested their potential as vaccine adjuvants due to their ability to enhance the targeting of antigens into dendritic cells (DCs) in cancer immunotherapy (Suzuki et al 2009). However the preliminary studies included in this chapter with regard to uptake within macrophages was not suitably encouraging to support further investigations into their application in this respect. Therefore, further studies into the development of vaccine adjuvants then focused on aqueous-filled liposome systems.

Chapter 4

Investigating the use of liposomes as vaccine adjuvants

Graphical Abstract:



DDA:TDB:2 μ g Ag85B-ESAT-6 MLV DDA:TDB:2 μ g Ag85B-ESAT-6 SUV DDA:TDB:2 μ g Ag85B-ESAT-6 DRV



25% PEG:2 μ g Ag85B-ESAT-6 MLV 25% PEG:2 μ g Ag85B-ESAT-6 SUV 25% PEG:2 μ g Ag85B-ESAT-6 DRV

Freeze-fracture images of liposomes prepared from dimethyldioctadecylammonium (DDA) and α' , α' -trehalose 6,6'-dibehenate (TDB) liposomes with and without polyethylene glycol (PEG), prepared with 2 μ g of Ag85B-ESAT-6 and produced in three formats: multilamellar (MLV), small unilamellar (SUV) and as dehydration-rehydration vesicles (DRV). The method of production influenced size and location of the antigen. The DDA:TDB MLV liposomes presented a concentric lamellar structure in which the fracture faces were smooth, whereas the corresponding 25 % PEGylated formulation showed a phase change and/or disruption of the lamellae. The SUV were predominantly unilamellar vesicles but these small vesicles were clustered together. The corresponding DRV liposomes had a more regular morphology compared to MLV liposomes.

4.1 Introduction

The use of liposomes as vaccine adjuvants has been investigated extensively over the last few decades and based on the studies reported in chapter 3 further investigations into the development of vaccine adjuvants focused on aqueous-filled liposome systems. In particular, cationic liposomal adjuvants have been investigated. In the literature the cationic lipid dimethyldioctadecylammonium (DDA) has been shown to enhance immune responses to a range of antigens including antigens for tuberculosis (TB) (Ag85B-ESAT 6) (Agger et al 2008a), malaria (Vangala et al 2006) and hepatitis B (Vangala et al 2007b). However, cationic liposomes are, in general, not sufficiently immunostimulatory, and therefore a range of immunostimulatory agents have been added to these formulations. One such combination consists of liposomes formed of DDA stabilised with the synthetic mycobacterial immunomodulator α,α' -trehalose 6, 6'-dibehenate (TDB) inserted into the lipid bilayers at a molar ratio of 5:1. This cationic liposome system was developed to mediate protection against TB but, in addition, has shown promising protective efficacy against other infectious diseases requiring different immunological profiles (Christensen et al 2009).

4.1.1 Dimethyldioctadecylammonium (DDA) and α,α' -trehalose 6, 6'-dibehenate (TDB)

DDA was discovered as an adjuvant by Gall in the mid 1960s (Gall 1966) and is a synthetic amphiphile, which contains a quaternary ammonium group with two 18-carbon-long alkyl chains forming the hydrophobic moiety and two methyl groups, which together with the ammonium group form the polar head group (Figure 4.1). The positively charged head group carries a monovalent counterion, typically bromide or chloride. Due to its amphiphilic character DDA can form liposomal structures when dispersed in aqueous media at temperatures above its gel-to-liquid phase transition

temperature (~ 47 °C) (Davidson et al 2005). DDA is known to induce cell-mediated immunity and delayed-type hypersensitivity (Snippe et al 1982), and along with its cationic nature and surfactant properties, has been shown to be an effective adjuvant in numerous applications, including mucosal immunisation (Klinguer et al 2001), gene delivery (Esposito et al 1999) and subunit vaccine delivery (Lindblad et al 1997; Brandt et al 2000; Holten-Andersen et al 2004; Rosenkrands et al 2005).

The mechanism of action behind the adjuvant effect of DDA has been attributed to its positive surface charge and its ability to associate antigens (Hilgers et al 1985). This was recently confirmed and further elaborated by using ovalbumin (OVA) as a model antigen (Korsholm et al 2007). Stimulation of immature bone marrow-derived dendritic cells (BMDCs) with fluorescently labelled OVA showed that adsorption of OVA onto DDA enhanced the cellular acquisition of the antigen. Further inhibition of active cellular processes by OVA stimulation at 4 °C or by the addition of cytochalasin D reduced the cellular uptake, suggesting that active actin-dependent endocytosis is the predominant uptake mechanism (Korsholm et al 2007). DDA-mediated OVA uptake was further associated with a functional enhancement of the APCs. This was shown by measuring the increase in IFN- γ production and cellular proliferation of purified autologous DO11.10 T-cells transgenic for a T-cell receptor recognising a major histocompatibility complex (MHC) class II-restricted OVA-epitope (OVA323-339). Both proliferation and IFN- γ production was increased upon interaction with either murine BMDCs or purified B-cells, stimulated with OVA adsorbed to DDA (Korsholm et al 2007, Christensen et al 2009). Recent studies replacing DDA with a neutral lipid, DSPC, further demonstrate the role of the cationic lipid in the liposomal adjuvant by showing that neutralisation of the surface charge of

the liposomes changes the biodistribution profile and diminishes their immunogenicity (Henriksen-Lacey et al 2010).

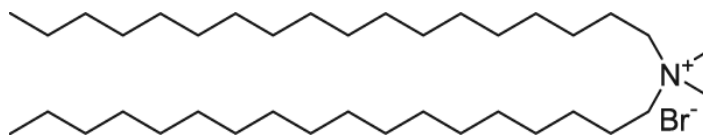


Figure 4.1 Structure of dimethyldioctadecylammonium (DDA)

The second component of the liposome adjuvant system, α,α' -trehalose 6,6'-dibehenate (TDB) (Figure 4.2), is a synthetic analog of trehalose 6,6'-dimycolate (TDM) with two saturated fatty-acid chains of 22 carbons (behenyl), each replacing the branched mycobacterial mycolic acids of >70 carbons. These two behenyl chains are linked by ester bonds to carbon number 6 of each of the two glucopyranose rings making up the trehalose head group (Figure 4.2). TDB has been shown to retain much of the bioactivity of the native form, whilst showing less toxicity as a result of the shorter fatty acid chains (Pimm et al 1979; Olds et al 1980). The combination of the DDA with TDB has been previously shown to be an efficient adjuvant for TB subunit vaccines (Holten-Andersen et al 2004), inducing a strong gamma interferon (IFN- γ) response, considered to be the key cytokine for induction of a Th₁ immune response, essential for effective anti-mycobacterial immunity (Flynn et al 1993; Cooper et al 1993).

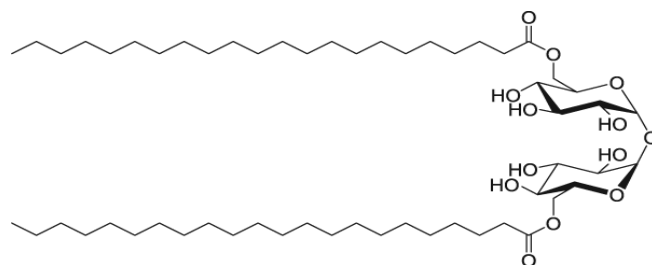


Figure 4.2 Structure of α,α' -trehalose 6,6'-dibehenate (TDB)

4.1.2 Antigen delivery system and immunostimulator

DDA:TDB was first studied by Holten-Andersen et al (2004). Using ESAT-6 as a possible TB antigen they investigated the ability of seven different immunostimulators to increase the protective efficacy of DDA, which included four mycobacteria-derived immunostimulators. DDA combined with monophosphoryl lipid A (MPL) and/or TDB induced an effective IFN- γ response and protection in mice was equivalent to that provided by BCG vaccination (Christensen et al 2009). The adjuvant activity of DDA:TDB when combined with Ag85B-ESAT-6 was recently compared to aluminium hydroxide, an adjuvant approved for human use (Davidsen et al 2005). CD4⁺ T cells in mice secreted high levels of IFN- γ and low levels of interleukin-5 (IL-5) in response to DDA:TDB whereas the opposite pattern was observed for aluminium hydroxide (Davidsen et al 2005; Christensen et al 2009). Although high levels of IgG1 antibody titres were seen with both DDA:TDB-adjuvated vaccine and aluminium hydroxide-adjuvated vaccine, higher levels of IgG2 antibody titres were seen with DDA:TDB (Davidsen et al 2005; Agger et al 2008b). Recent studies have identified DDA:TDB to induce a multi-functional CD4⁺ T-cell populations expressing several cytokines, mainly tumour necrosis factor-alpha (TNF- α)⁺, IL-2⁺, and IFN- γ ⁺, TNF- α ⁺, IL-2⁺. In mice such a population is maintained for at least 1 year and thus are long-lived (Lindenstrom et al 2009). Additionally, a depot

formed at the site of injection by DDA:TDB has been shown to retain antigen in recent biodistribution studies (Henriksen-Lacey et al 2009). This could be a possible function of strong repulsive charges.

4.1.3 Improving immunogenicity through modification of the liposomes composition

Modifying the liposome composition in delivery systems has been attempted so as to improve immunogenicity (Christensen et al 2009). Delivery systems combined with non-ionic lipids and cholesterol, such as Ag85B-ESAT-6, was shown to decrease IFN- γ and IgG2 levels (Vangala et al 2006). However IgG1 titers remained relatively unchanged in the presence or absence of non-ionic lipids and cholesterol (Vangala et al 2006). A similar pattern emerged when DDA and TDB were incorporated into poly(D,L-lactic-co-glycolic acid) microspheres (PLGA), a decrease in IFN- γ and IgG2 levels and no difference in IgG1 levels, when compared to DDA:TDB (Kirby et al 2008a). DDA:TDB was also consistently better at initiating a diverse immune response encompassing both cell mediated immunity (CMI) and humoral immune responses, when compared to other types of microspheres than PLGA (Kirby et al 2008b; Christensen et al 2009).

Yet despite a range of studies, the mechanism behind the immunostimulatory effect obtained with the cationic liposomal vaccine adjuvant DDA:TDB remains unclear. One of the proposed hypotheses is the 'depot effect' in which the liposomal carrier helps to retain the antigen at the injection site thereby increasing the time of vaccine exposure to the immune cells (Henriksen-Lacey et al 2010). The depot effect has been suggested to be primarily due to electrostatic forces between the net negatively charged protein and the positively charged liposomes i.e. aggregation between the

cationic liposomes and serum proteins, thereby causing a liposomal net which retains the antigen (Henriksen-Lacey et al 2010). The aim of this current study was to further test this hypothesis by investigating whether sterically stabilising the DDA:TDB system with polyethylene glycol (PEG) reduces aggregation, and subsequently influences the formation of a depot at the site of injection and the immune response.

4.1.4 Steric stabilisation using polyethylene glycol (PEG)

Poly (ethylene glycol) (PEG) is the most widely used hydrophilic polymer for the steric stabilisation of liposome drug delivery systems. PEG is a linear polyether diol with many useful properties, such as biocompatibility, solubility in aqueous and organic media (Powell 1980), very low toxicity, immunogenicity and antigenicity (Dreborg & Akerblom 1990), and good excretion kinetics (Yamaoka et al 1994). These properties allow its use in a variety of applications (Harris 1992), including its application in therapeutic products such as Caelyx, which is a PEGylated liposomal delivery system for doxorubicin. PEG can be incorporated on the liposomal surface in different ways, but the most widely used method at present is to anchor the polymer in the liposomal membrane via a cross-linked lipid (i.e. PEG-distearoylphosphatidylethanolamine (DSPE) as schematised in Figure 4.3) (Allen et al 1991b, 2002). PEG has been used to derivatise therapeutic proteins and peptides, increasing drug stability and solubility, lowering toxicity, increasing half-life (Caliceti & Veronese 2003), decreasing clearance and immunogenicity.

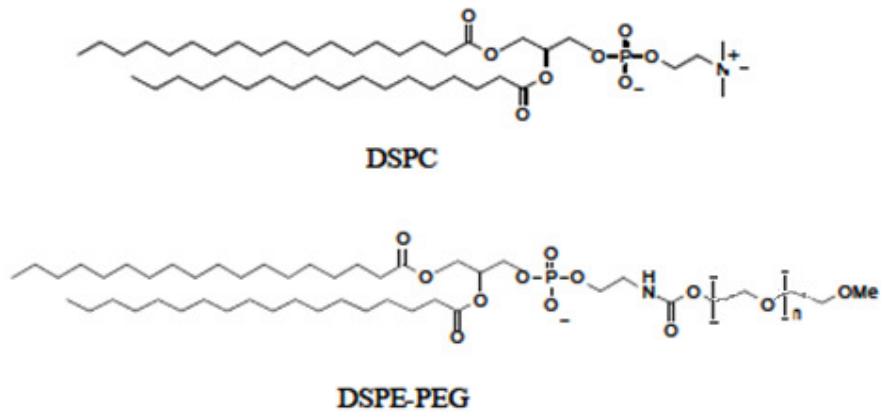


Figure 4.3 Chemical structures of distearoylphosphatidylcholine (DSPC), distearoylphosphatidyl-ethanolamine after conjugation with poly (ethylene glycol) (PEG) (DSPE-PEG).

PEG provides a strong interbilayer repulsion on the surface of liposomes (Needham et al 1992; Immordino et al 2006). These act to stabilise liposome preparations by overcoming the attractive van der Waals forces and thus avoid aggregation. When bilayers that are combined with PEG1900-lipid are analysed by x-ray, from the lipid surface it is revealed the grafted polymer extends around 50 angstroms and produces strong inter-membrane repulsive forces (Needham et al 1992; Immordino et al 2006). The conformational flexibility together with molecular mass of the bound polymer and its uniformity (molecular cloud) enables the hydrophilic shell of PEG to avoid liposomal particle aggregation and decreases the particle-protein interaction (Torchilin et al 1994). By contrast liposome-protein interactions are not decreased when dextran, a more rigid polymer, is grafted to liposomes even when it is used at comparable quantities (Needham et al 1992). Many studies have focused on elucidating the optimal concentration of PEG that should be incorporated in the liposomal membrane. For example, Levchenko et al (2002) demonstrated that PEG concentrations of more than 6 mol% shield the electric surface potential of cationic liposomes, while higher concentrations (more than 15 mol%) were found to cause

unfavourable structural changes in the liposomal bilayer, and thus enhance the rapid clearance of liposomes from circulation, whilst other studies (Carstens et al 2007) suggested higher levels are required to mask cationic surfaces. For this reason, in this study lower concentrations i.e. 5, 10 mol% and higher concentration i.e. 25 mol% were included in the preparation of PEG-coated cationic liposomes.

4.2 Aims and objectives

The aim of this work was to see whether sterically stabilising DDA:TDB with PEG reduces aggregation in the presence of proteins and serum and whether it has an influence on the biodistribution, adjuvant properties and the formation of a depot at the site of injection. To do this the objectives were:

1. To look at the effect of PEG on the DDA:TDB system, i.e. characterisation of the systems in terms of size, charge, loading, release and aggregation in the presence and absence of serum.
2. To look at the effect of entrapping antigens within the liposomes rather than surface adsorption i.e. characterisation of the systems in terms of size, charge, loading and release.
3. To look at the effect of PEGylation on biodistribution i.e. investigating whether different methods of antigen entrapment can alter the biodistribution of the antigen and liposomes.
4. Finally, to look at the effect of adsorbing and entrapping antigens on vaccine efficacy using the subunit Ag85B-ESAT-6 antigen.

4.3 Materials and methods

4.3.1 Materials

Chemicals	Supplier
[³ H] thymidine	Perkin Elmer (Waltham, MA)
2,2'-azino-bis (3-ethylbenzthiazoline-6-sulfonic acid)	Sigma-Aldrich, Poole, Dorset, UK
Acetic acid	Fisher Scientific (Leicestershire, UK)
Bicinchoninic acid (BCA)	Sigma-Aldrich, Poole, Dorset, UK
Citric acid	Sigma-Aldrich, Poole, Dorset, UK
Chloroform (HPLC grade)	Fisher Scientific (Leicestershire, UK)
Concanavalin A	Sigma-Aldrich, Poole, Dorset, UK
Coomasie (Brilliant Blue)	Sigma-Aldrich, Poole, Dorset, UK
Dimethyl sulphoxide (DMSO)	Sigma-Aldrich, Poole, Dorset, UK
DuoSet [®] capture ELISA	R&D systems, UK
ELISA plates (flat bottom, high binding)	Greiner Bio-One Ltd, UK
Foetal bovine serum (Heat-Inactivated)	Invitrogen, Paisley, UK
Glycine	Sigma-Aldrich, Poole, Dorset, UK
Heparin	Sigma-Aldrich, Poole, Dorset, UK
Horseradish peroxidase-conjugated goat anti-mouse immunoglobulin IgG, IgG1 & IgG2b subclasses	AbD serotec, Oxford, UK
Hydrogen peroxide	Sigma-Aldrich, Poole, Dorset, UK
I ¹²⁵ (NaI in NaOH solution)	Perkin Elmer (Waltham, MA)
iodo-GEN [®] pre-coated iodination tubes	Pierce Biotechnology (Rockford, IL)

Incomplete Freund's adjuvant	Sigma-Aldrich, Poole, Dorset, UK
Marvel	Premier Int. Foods Ltd, Lincs, UK
Methanol (HPLC grade)	Fisher Scientific (Leicestershire, UK
Ovalbumin (OVA)	Sigma-Aldrich, Poole, Dorset, UK
Penicillin-streptomycin-glutamine (100X)	Invitrogen, Paisley, UK
Phosphate buffer saline tablets (PBS)	Sigma-Aldrich, Poole, Dorset, UK
Plain filter mats	Molecular Devices Ltd., Wokingham, UK
Potassium chloride	Sigma-Aldrich, Poole, Dorset, UK
Potassium phosphate	Sigma-Aldrich, Poole, Dorset, UK
Protein molecular weight standard	Invitrogen, Paisley, UK
RPMI 1640 cell culture medium	Biosera Ltd, UK
SDS-PAGE 12% Tris-Glycine gels	Invitrogen, Paisley, UK
Sephadex G-75	Sigma-Aldrich, Poole, Dorset, UK
Sodium chloride	Sigma-Aldrich, Poole, Dorset, UK
Sodium dodecyl sulphate	Sigma-Aldrich, Poole, Dorset, UK
Sodium phosphate dibasic	Sigma-Aldrich, Poole, Dorset, UK
Solvable	Perkin Elmer (Waltham, MA).
Tetramethylbenzidine	Sigma-Aldrich, Poole, Dorset, UK
Tris-base	IDN Biomedical, Inc (Aurora, Ohio)
Trypan blue	Sigma-Aldrich, Poole, Dorset, UK
Tween-20	Sigma-Aldrich, Poole, Dorset, UK
Ultima Gold scintillation fluid	Perkin Elmer (Waltham, MA)

Lipids	Supplier
1,2-dipalmitoyl (³ H-DPPC)	Perkin Elmer (Waltham, MA)
1,2-distearoyl-sn-glycero-3-phosphoethanolamine-N-methoxy-poly(ethylene glycol) 2000 (DSPEPEG2000)	Avanti Polar Lipids, Inc. (Alabaster, AL)
Dimethyldioctadecylammonium bromide (DDA)	Avanti Polar Lipids, Inc. (Alabaster, AL)
Trehalose 6,6'-dibehenate (TDB)	Avanti Polar Lipids, Inc. (Alabaster, AL)

Non-His-tagged protein Ag85B-ESAT-6 was produced as described previously (Olsen et al 2001) and were provided by Statens Serum Institute, Denmark. Tris-base, obtained from IDN Biomedical, Inc (Aurora, Ohio) was used to make Tris buffer and adjusted to pH 7.4 using HCl; unless stated otherwise Tris buffer was used at 10 mM, pH 7.4. Double distilled water was used in the preparation of all solutions.

4.3.2 Method

4.3.2.1 Lipid-hydration method

MLV were prepared using the previously described lipid-film hydration method (Bangham et al 1965) (Figure 4.4). Briefly, weighed amounts of DDA, TDB and PEG (Table 4.1) were dissolved in chloroform/methanol (9:1, by volume) and the organic solvent was removed by rotary evaporation followed by flushing with N₂ to form a thin lipid film on the bottom of a round-bottom flask. The lipid film was hydrated in 10 mM Tris-buffer at pH 7.4, to a final concentration of 1.98 mM DDA with 0.25 mM TDB added in the case of DDA:TDB, by heating for 20 min at 60 °C. The Ag85B-ESAT-6 antigen was added post-hydration of the lipid film.

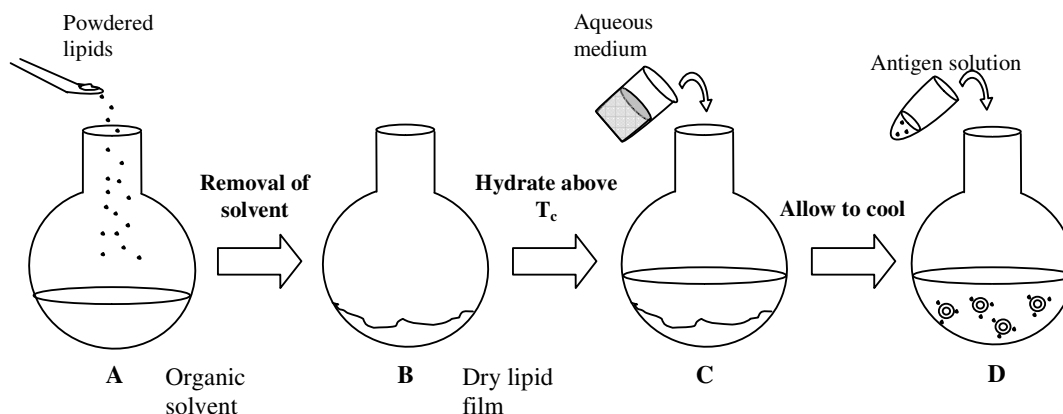


Figure 4.4 Schematic representation of the lipid-hydration method. (A) Weighed amounts of lipids were first dissolved in chloroform/methanol (9:1, by volume), (B) followed by removal of the solvent under vacuum to leave a thin lipid film, which was then purged with a gentle stream of N_2 to remove any residual solvent. (C) Vesicles were subsequently formed by simply hydrating the lipid film with an aqueous phase for 20 minutes, at a temperature $10^\circ C$ above the main phase transition of DDA ($T_c \approx 47^\circ C$), with the final concentrations of DDA and TDB corresponding to 1.25 mg/mL and 0.25 mg/mL respectively. (D) Finally, the solution was allowed to cool before addition of Ag85B-ESAT-6, followed by vortex mixing.

4.3.2.2 Small unilamellar vesicles (SUV)

To generate SUV, the MLV produced in section 4.3.2.1 were disrupted using sonic energy to fracture large liposomes into smaller structures (< 100 nm). In this instance, a probe sonicator (Soniprep 150) was used to produce SUV. The tip of the sonicator probe was placed onto the liposome surface of the MLV mixture. The milky MLV suspension transforms into a clear SUV suspension.

4.3.2.3 Dehydration-rehydration method

The dehydration-rehydration method (Kirby & Gregoriadis 1984a) was used for incorporation of Ag85B-ESAT-6 into liposome vesicles (Figure 4.5). In brief, MLV prepared according to the lipid hydration method outlined above was sonicated to produce SUV. These SUV composed of 1.98 mM DDA with 0.25 mM TDB in the presence or absence of PEG (0.112, 0.223, 0.558 mM) were mixed with Ag85B-ESAT-6, frozen at $-70^\circ C$ and freeze dried overnight ($-40^\circ C$, vacuum to 40 mbar).

Controlled rehydration of the dried powder led to the formation of antigen containing DRV. Controlled rehydration was achieved by addition of 10 % of the final volume, which was standardised at 1 ml. Therefore 100 μ l was added initially to these formulations, which were vortexed and left at room temperature for 30 minutes. A further 100 μ l was added and formulations again were incubated for 30 minutes at room temperature and subsequently made up to 1 ml. DRV preparations were then centrifuged twice at 125,000 \times g for 20 minutes to remove non-entrapped antigen and resuspended in distilled water, to the appropriate volume.

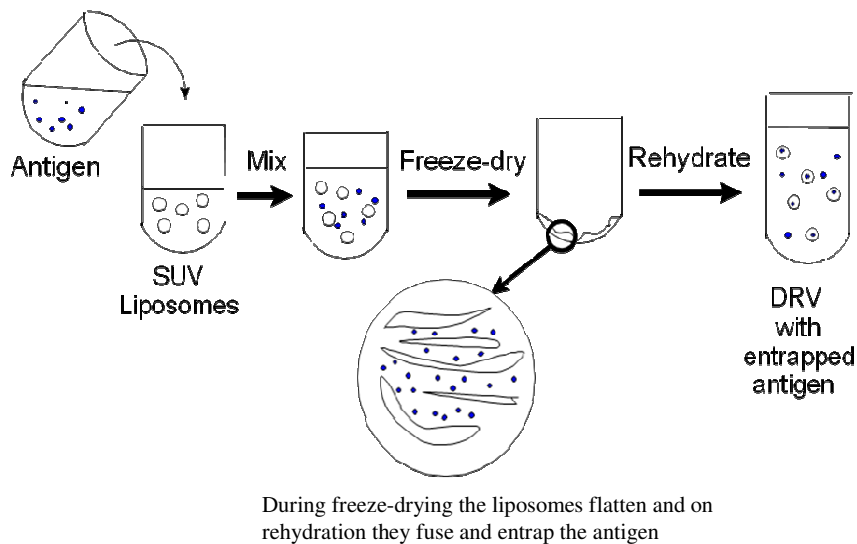


Figure 4.5 Schematic representation of the dehydration-rehydration method. In brief, MLV prepared according to the lipid hydration method outlined above was sonicated to produce SUV. These SUV were mixed with Ag85B-ESAT-6, frozen at -70 $^{\circ}$ C and freeze dried overnight (-40 $^{\circ}$ C, vacuum to 40 mbar). Controlled rehydration of the dried powder led to the formation of antigen containing DRV vesicles.

Table 4.1 Weight (mg) and moles of DDA:TDB and 5 %, 10 % and 25 % PEG.

DDA:TDB	DDA	TDB	PEG
Formulation	Weight (mg)/Moles	Weight (mg)/Moles	Weight (mg)/Moles
DDA:TDB only	1.25 / 1.98×10^{-6}	0.25 / 2.53×10^{-7}	0 / 0
+ 5 % PEG	1.19 / 1.94×10^{-6}	0.24 / 2.40×10^{-7}	0.314 / 1.12×10^{-7}
+ 10 % PEG	1.125 / 1.78×10^{-6}	0.22 / 2.28×10^{-7}	0.63 / 2.23×10^{-7}
+ 25 % PEG	0.94 / 1.49×10^{-6}	0.19 / 1.90×10^{-7}	1.57 / 5.58×10^{-7}

4.3.2.4 Determination of vesicle size and zeta potential

The vesicle size and zeta-potential was determined using the photon correlation spectroscopy (PCS) technique. The measurements were performed at 25 °C using a ZetaPlus (Brookhaven Instrument Corporation, USA). Polystyrene size standard 220 ± 6 nm (Duke scientific corp, Duke, NC) was used as a control. The samples were diluted with 10 mM Tris-buffer at pH 7.4 to achieve the optimal vesicle concentration.

4.3.2.5 Sodium dodecyl sulphate polyacrylamide gel-electrophoresis (SDS page)

Cationic formulations were mixed with OVA (either 100 µg/ml or 1 mg/ml) and ultra-centrifuged twice at 125,000 ×g, for 60 minutes at room temperature in order to pellet the liposomes. Supernatant was then removed and pellets were re-suspended back into their original volume, using the corresponding buffer solution. Upon heating at 90 °C for 3 minutes, 10 µl samples of pellet and supernatant from each of the formulations were analysed via SDS-PAGE for semi-quantification of the protein concentrations present.

4.3.2.6 Quantification of non-adsorbed antigen via the BCA Assay

The BCA assay has a working range of 5 to 25 µg of protein. To test non-adsorbed concentrations of OVA, triplicate 25 µl supernatant samples were tested. OVA protein concentrations present within the supernatants were quantified by the BCA Protein Assay in accordance with the associated protocol (Sigma-Aldrich Co. Ltd. Dorset, UK). The principle of the assay is that it relies on the formation of Cu²⁺ protein complex under alkaline conditions followed by the reduction of the Cu²⁺ to Cu¹⁺. The amount of reduction is proportional to the protein present. An OVA standard curve was formed at concentrations of 0 - 1 mg/ml with 25 µl of sample and 225 µl of reagent added per well of a 96 well plate.

4.3.2.7 Radiolabeling of Ag85B-ESAT-6 antigen

Known volumes of Ag85B-ESAT-6 (0.8 mg/ml) and I¹²⁵ were added to the IODO-GEN® tube and left for 1 hour with intermittent swirling. Typical volumes for the production of 1 ml radiolabelled Ag85B-ESAT-6 would require the mixing of 100 µl Ag85B-ESAT-6 (0.8 mg/ml) with 6 MBq I¹²⁵. A gel filtration column containing Sephadex-G75 was prepared using double distilled water and equilibrated using Tris buffer. The I¹²⁵-Ag85B-ESAT-6 solution was added to the column and elucidated using Tris buffer, maintaining a steady flow through the column. Aliquots (0.25 ml) were collected and analysed for I¹²⁵ content using a Cobra™ CPM Auto-Gamma® counter (Packard Instruments Company inc, IL, USA). Verification of Ag85B-ESAT-6 presence was undertaken using the BCA assay in which protein presence resulted in a visual colour change from green to purple. The samples with the highest protein content and highest γ-counts were then collected and pooled for subsequent use as radiolabelled protein. The final sample was diluted accordingly with Tris buffer.

4.3.2.8 Ag85B-ESAT-6 antigen adsorption / entrapment to cationic liposomes

To assess the degree of antigen adsorption, I¹²⁵-labeled Ag85B-ESAT-6 was added to the liposomes and left for 1 hour with intermittent shaking. For antigen entrapment I¹²⁵-labeled Ag85B-ESAT-6 was added to the SUV liposomes, frozen at -70 °C and freeze dried overnight (-40 °C, vacuum to 40 mbar). Controlled rehydration of the dried powder led to the formation of Ag85B-ESAT-6 containing DRV. Due to their relatively small size and highly cationic nature, DDA-based liposomes do not pellet efficiently during centrifugation, even at high speeds. Therefore to aid sedimentation during centrifugation, liposomes were subsequently placed in a solution of OVA (1 mg/ml) and centrifuged (125,000 ×g, 4 °C, 1 hour), resuspended in Tris buffer and centrifuged again to ensure removal of all non-bound Ag85B-ESAT-6. The I¹²⁵ recovery in the pooled supernatant after two washes (unbound antigen) and the pellet (bound antigen) was measured. The percentage of Ag85B-ESAT-6 adsorbed and entrapped was calculated as a percentage of the total radioactivity recovered from both supernatant and pellet.

$$\frac{\text{Radioactivity of washed sample}}{\text{Radioactivity of unwashed sample}} \times 100\%$$

To ensure reliability of entrapment values, the total recovery of protein antigen was also calculated using the following equation (including any dilutions)

$$\frac{\text{Radioactivity of washed sample} + \text{Radioactivity of supernatant}}{\text{Radioactivity of unwashed sample}} \times 100\%$$

4.3.2.9 Ag85B-ESAT-6 antigen retention in simulated *in vivo* conditions

Antigen release from liposomes stored in simulated *in vivo* conditions was determined using liposomes adsorbing and entrapping I¹²⁵-labelled Ag85B-ESAT-6. Aliquots of each formulation were diluted (1:5) using 50 % FCS in Tris buffer and incubated in a shaking water bath at 37 °C for 96 h. At time intervals, samples were centrifuged twice and Ag85B-ESAT-6 release was calculated as a percentage of the recovered radioactivity.

4.3.2.10 Biodistribution of cationic liposomes adsorbing and entrapping Ag85B-ESAT-6 antigen

Inbred female Balb/C (6-10 weeks of age) mice were housed in cages within a laminar flow safety enclosure and provided with irradiated food and filtered drinking water. Experimentation strictly adhered to the 1986 Scientific Procedures Act (UK). All protocols have been subject to stringent ethical review and were carried out in a designated establishment. Four to six days prior to injection, mice were injected subcutaneously (s.c.) with 200 µl pontamine blue (0.5 % w/v). Liposomes containing the tracer molecule H³-DPPC were produced as described in sections 4.3.2.1-2. To obtain isotonicity, trehalose was added to the hydrating buffer to a final concentration of 10 % w/v. Each immunisation dose contained 2 µg Ag85B-ESAT-6 with 25 ng ³H-DPPC, 250 µg DDA and 50 µg TDB ± 12.6 µg/31.5 µg PEG. Mice were injected intramuscularly (i.m; 50 µl) into the left quadriceps. At time-points 1 day, 4 days and 14 days post injection (p.i) (Figure 4.6) mice were terminated by cervical dislocation. Spleen, injected muscle site and popliteal lymph nodes were removed and weighed into plastic γ-vials to which 1.5 ml SOLVABLE™ was added. Samples were assessed for I¹²⁵ content using a Cobra™ CPM Auto-Gamma® counter. Fully digested tissue samples were bleached using hydrogen peroxide (200 µl) and transferred to glass

scintillation vials followed by the addition of Ultima Gold (10 ml) for H³ quantification.

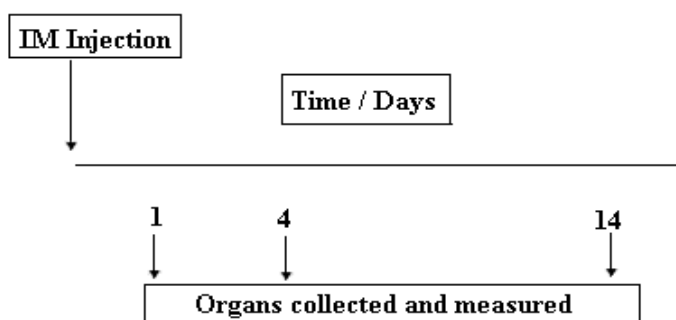


Figure 4.6 Time-points for the biodistribution study, days 1, 4 and 14 post injection (p.i)

4.3.2.11 Immunological analysis of liposome formulations

Nine groups of five female C57BL/6 mice (6 - 10 weeks of age), received doses of liposome vaccine formulations containing 2 µg of Ag85B-ESAT-6 in a 50 µl volume. A second group received 2 µg of Ag85B-ESAT-6 in a 50 µl volume. Naïve groups received the appropriate volume of PBS. Vaccine formulations were administered intramuscularly, and each mouse received three doses at intervals of two weeks. Serum samples were taken at 12 days after the first administration and at two week intervals thereafter.

4.3.2.12 Analysis of Ag85B-ESAT-6 specific antibody isotypes

Sera samples obtained at different time intervals after immunisation were analysed for the presence of anti-Ag85B-ESAT-6 IgG, IgG1 and IgG2b antibodies by enzyme-linked immunosorbent assay (ELISA) (Figure 4.7). ELISA plates (flat bottom, high binding) were coated with 50 µl of Ag85B-ESAT-6 per well (3 µg/well) in PBS and incubated at 4 °C overnight. Unbound antigen was aspirated and residual washings were removed by blotting firmly onto paper towel. Plates were blocked with 100 µl per well of 4 % w/v Marvel (dried skimmed milk powder) in PBS. Serum samples

were serially diluted to washed plates and incubated for 1 hour at 37 °C. Anti-Ag85B-ESAT-6 antibodies were detected by addition of horseradish peroxidase conjugated anti-mouse isotype specific immunoglobulin (goat anti-mouse IgG, IgG1, or IgG2a), and subsequent addition of substrate solution, 2,2'-azino-bis (3-ethylbenzthiazoline-6-sulfonic acid) (ABTS) in citrate buffer incorporating 5 µl of 30 % H₂O₂/50 ml following repeated incubation and washing steps. Absorbance was measured at 405 nm (Bio-Rad, Herts, UK).

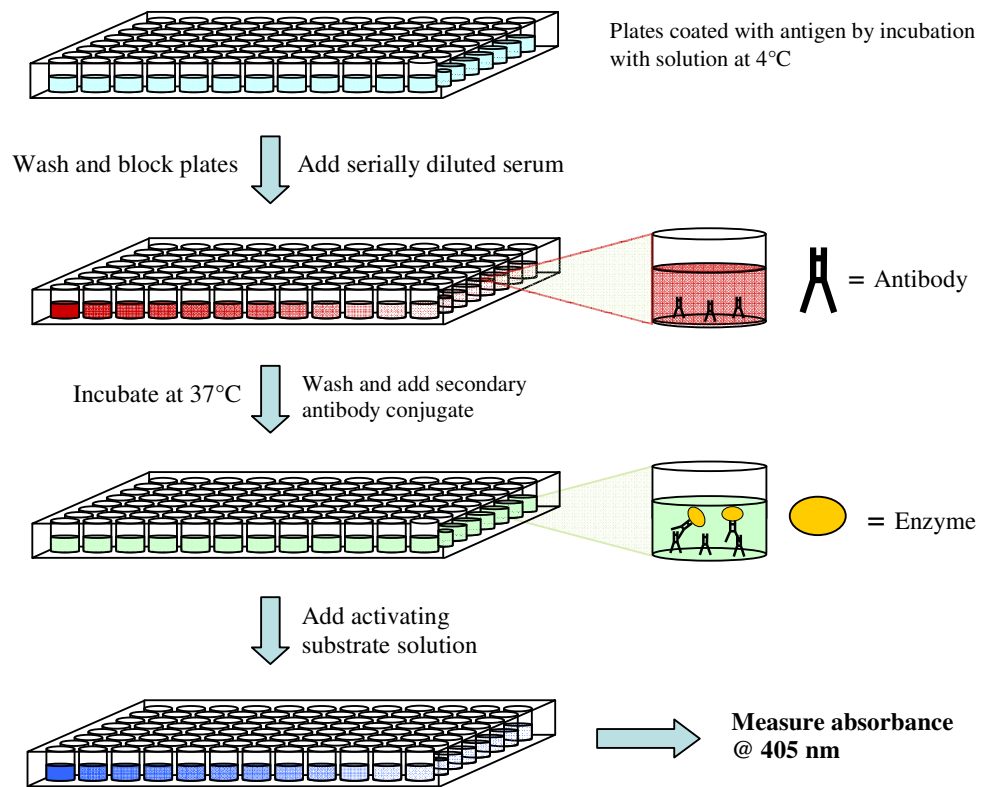


Figure 4.7 Schematic representation of analysis of antibody production by enzyme-linked immunosorbent assay (ELISA). Serially diluted serum samples are added to 96-well microplates coated with antigen and blocked with Marvel (4 % (w/v)) in PBS. Serum antibodies recognise antigen adsorbed to wells. Antibodies are then detected using secondary antibody conjugate, which recognises antibody bound to antigen adsorbed to wells, following repeated incubation and washing steps.

4.3.2.13 Spleen cell culture preparation

Upon termination of experiments, mice were humanely culled and their spleens aseptically removed and placed into ice-cold sterile PBS. Spleens were treated as follows: a crude suspension of spleen cells in 10 ml working media (RPMI 1640 cell culture medium supplemented with 10 % (v/v) foetal bovine serum, 2 mM L-glutamine, penicillin (100 U/ml) and streptomycin (100 µg/ml)) was prepared by gently grinding the spleen on a fine wire screen. After allowing the cell suspension to settle for approximately 5 minutes the liquid was transferred to sterile 20 ml 'Falcon' tubes, without disturbing the cellular debris at the bottom. The cell suspension was centrifuged at 1200 rpm for 10 minutes at 15 °C. After centrifugation the supernatant was removed, the cell pellet resuspended in 10 ml fresh working media and the centrifugation procedure was repeated.

4.3.2.14 Analysis of spleen cell proliferation

For study of antigen specific proliferative responses, aliquots of 100 µl volumes of sterile media or antigen in sterile media (at the concentrations stated (0.05, 0.5, 5 and 25 µg/ml)) were seeded onto 96 well suspension culture plates and 100 µl volumes of viable splenocytes (approximately 8×10^6 cells/ml) added to each well (Figure 4.8). As a positive control, cells were co-cultured with concanavalin A at a concentration of 3 µg/ml. Covered plates were incubated in a humid, 5 % CO₂ environment at 37 °C for 72 hours. After 72 hours incubation, half a microcurie of [³H] thymidine in 40 µl volumes of freshly prepared sterile working media was added to each well, and the incubation continued for a further 24 hours. The well contents were harvested onto plain filter mats using a cell harvester (Titertek). After drying, the discs representing each well were punched from the filter mats into 5 ml volumes of scintillation fluid

and the incorporation of [^3H] thymidine into the cultured cells was measured using standard counting procedures (Figure 4.8).

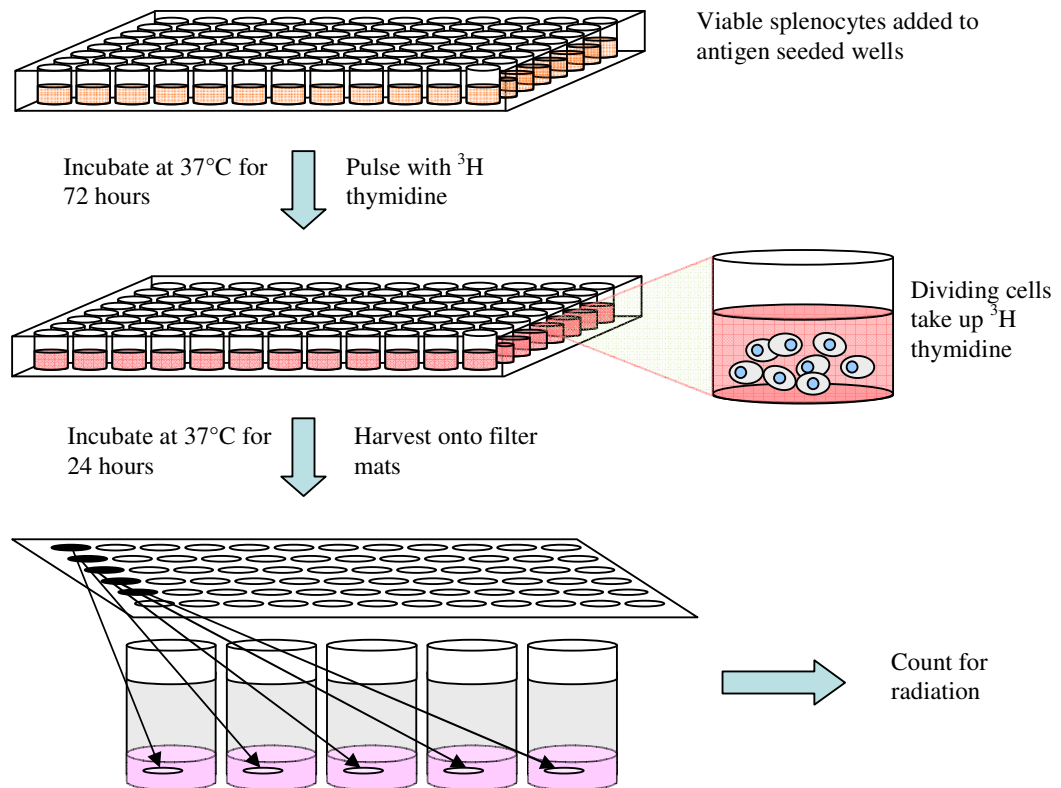


Figure 4.8 Schematic representation spleen cell proliferation analysis. Antigen is seeded onto 96 well suspension culture plates and incubated with viable splenocytes at 37 °C (5 % CO_2) for 72 hours. Cells are then pulsed with ^3H thymidine, incubated, and harvested onto filter mats, which are counted for ^3H using standard counting procedures.

4.3.2.15 Analysis of cytokine production

Splenocytes were isolated and cells were plated onto 96-well plates. Cells were incubated for 40 hours at 37 °C, in a humid (5 % CO_2) environment, after which supernatants were removed and stored at -70 °C for later analysis. Cytokine levels of IL-2, IL-5, IL-6, IL-10 and IFN- γ in the cell culture supernatants were quantified using the DuoSet® capture ELISA kits according to the manufacturer's instructions (Figure 4.9). Briefly, ELISA plates were first coated with capture antibody, followed

by washing and blocking. Samples of cell culture supernatants were then added and cytokines detected by addition of a detection antibody, enzyme marker (Streptavidin-HRP) and substrate solution following repeated incubation and washing steps. Absorbance was measured at 405 nm (Bio-Rad, Herts, UK) (Figure 4.9).

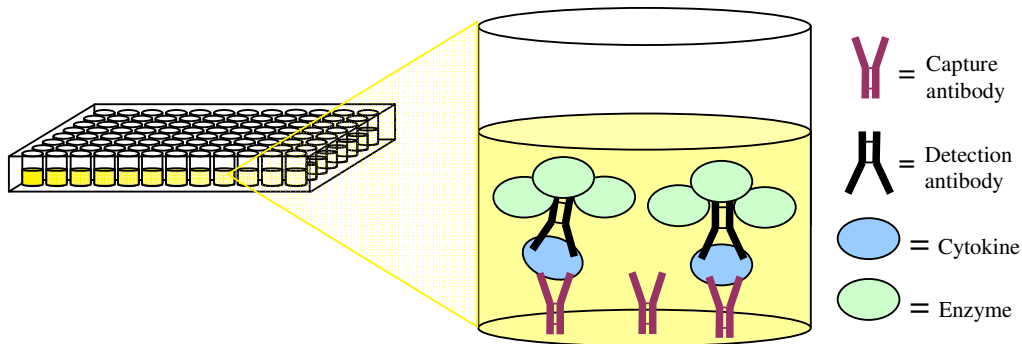


Figure 4.9 Schematic representation of cytokine detection using DuoSet® capture ELISA kits. Spleen cell culture supernatants are added to 96 well microplates coated with capture antibody. Addition of detection antibody and enzyme marker, followed by activation with substrate solution, allows determination of cytokine secretion by optical density measurements.

4.3.2.16 Freeze-fracture microscopy

A drop of each incubation mixture (approximately 5 μ l) was placed on a ridged, gold specimen support or was sandwiched between two copper plates for fracture in a double replica device. Samples were frozen by rapid plunging into a constantly stirred mixture of propane:isopentane (3:1) cooled by liquid nitrogen. Fracture was performed on a Balzers BAF 400D apparatus at a temperature of -110°C . Replicas were floated free on distilled water and cleaned in 40 % chromic acid. Images were viewed using a transmission microscope.

4.3.2.17 Statistical analyses

For all experiments, means and standard deviations were calculated. To determine statistical significance the one way analysis of variance (ANOVA) was performed on all data, with the statistical significance determined to 0.05 confidence intervals ($p < 0.05$). Tukey's post hoc test was conducted to determine which conditions differ significantly from each other.

4.4 Results and discussion

4.4.1 The effect of PEGylation DDA:TDB MLV characteristics

DSPEPEG₂₀₀₀ (PEG) is an amphiphilic molecule composed of a hydrophobic phospholipid and hydrophilic PEG chain. Here the PEGylated lipid was incorporated into 'empty' (i.e. no antigen present) DDA:TDB systems at 5, 10 and 25 mol%. The size and zeta-potentials were measured (Figures 4.10A and B).

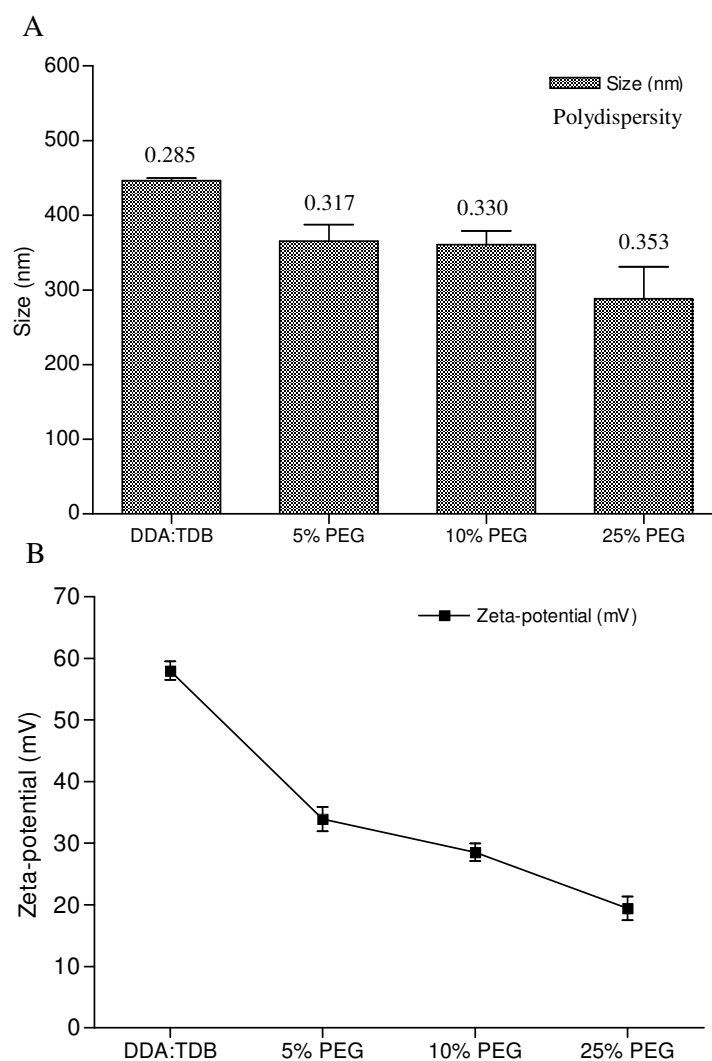


Figure 4.10 (A) Vesicle size (nm) (bars) and polydispersity (values) and (B) zeta-potential (mV) of DDA:TDB 5, 10, 25 % PEG liposomes. Size and zeta-potential measured in Tris buffer (1 mM) using a Brookhaven ZetaPlus instrument. Results represent mean \pm SD of triplicate experiments.

From Figure 4.10, it can be seen that the incorporation of PEG to the DDA:TDB MLV influenced the size, polydispersity and zeta-potential of the liposomes. As the amount of PEG increased there is a decrease in vesicle size, with liposomes prepared from DDA:TDB alone being around 446.3 ± 3.3 nm, whilst formulations containing 5, 10 and 25 % PEG being 365.1 ± 22.2 nm ($p < 0.01$) for 5 %, 360.5 ± 18.6 nm ($p < 0.01$) for 10 % and 287.7 ± 43.3 nm ($p < 0.001$) for 25 % PEG formulation respectively (Figure 4.10). This may be due to PEG in the formulation influencing the lipid packaging within the systems and/or reducing the number of bilayers within the MLV system which would subsequently reduce the vesicle size. Since the attachment of PEG molecules to the surface of liposomes both strongly reduces the attractive forces (van der Waals), and increases the repulsive forces (steric, electrostatic, and hydration) (Kenworthy et al 1995; Lasic & Martin 1995), increasing PEG concentration causes disaggregation of liposome assemblies and a gradual reduction of liposome size. It is important to note that replacement of similar amounts of DDA with a zwitterionic lipid (DSPE) did not have the same effect (unpublished data from our lab).

The zeta potential, which is related to the charge on the surface of the particle and is important for interactions of liposomes with biological systems *in vivo* (Scherphof et al 1997; Scherphof & Kamps 1998), was also measured for these systems. From the results (Figure 4.10B), it can be seen that as the amount of PEGylation increased there was a drop in zeta potential from 58 ± 1.5 mV when no PEG is present to around 19.4 ± 1.9 mV when the bilayer contains 25 % PEG ($p < 0.001$) (Figure 4.10B). This gradual reduction in zeta potential is possibly due to the hydrophilic chains of the

PEG grafted onto the DSPE extending out from the surface of the liposomes masking the cationic charge of the DDA.

4.4.2 The effect of antigen adsorption onto MLV DDA:TDB

A range of procedures for the preparation of the liposomes can be employed. However, preparation of liposomes by addition of aqueous solution of antigens to dried lipid films, resulting in multilamellar vesicles (MLV), is generally the most convenient method of liposome preparation for vaccine formulations. Yet, the addition of an anionic antigen to cationic MLV will result in electrostatic interactions, influencing the physico-chemical properties of the vesicles. To investigate and initially characterise the interaction of anionic subunit antigens with the various MLV systems, ovalbumin (OVA) was used as the model protein. However, for later loading and release studies Ag85B-ESAT-6, a novel tuberculosis subunit antigen, was used. Ovalbumin (OVA), a glycoprotein consisting of 385 amino acids, has a molecular mass of 43 kDa (Nisbet et al 1981; Huntington & Stein 2001) and has a negative charge at neutral pH so will adsorb to DDA:TDB similar to Ag85B-ESAT-6. Due to its low cost and characteristics which generally map to common subunit antigens, it is often used as a model antigen of low immunogenicity in assessment of novel adjuvants (Stewart-Tull 1991).

The effect of OVA adsorption at various ratios (10 µg/ml, 100 µg/ml and 1000 µg/ml) with various PEGylated DDA:TDB MLV (5 %, 10 % and 25 % PEG) was determined on the size and zeta-potential (Figure 4.11). The size and the zeta-potential of 'empty' systems (where no OVA is present) were initially measured and compared to formulations containing OVA (Figure 4.11). For all four formulations,

the addition of 10 μg of OVA had no measurable effect on the size and the zeta-potential of the liposomes (Figure 4.11). On the addition of 100 μg of OVA to DDA:TDB, 5 % and 10 % PEG formulation a significant ($p < 0.05$) increase in size was found compared to their OVA free counterparts with the size being 755.6 ± 77.8 nm for DDA:TDB, 542.8 ± 55.9 nm for 5 % and 515.4 ± 5.5 nm for 10 % PEG respectively compared to 446.3 ± 3.3 nm, 365.1 ± 22.3 nm and 360.5 ± 18.6 nm for the OVA free formulations respectively (Figure 4.11A). For the 25 % PEG formulation there was no significant increase in size ($p > 0.05$) (403.2 ± 33.7 nm compared to 401.7 ± 43.3 nm with OVA free formulations). In terms of zeta-potential, the addition of 100 μg of OVA resulted in a reduction in measured potential with the DDA:TDB formulation. However, for the remaining three pegylated formulations, no significant change in zeta potential was found (Figure 4.11B). Following the addition of 1000 μg of OVA, all four formulations were found to aggregate with sizes between 1-2 microns; this increase in size was also associated with a drop in zeta-potential with all formulations having a neutral charge after the addition of OVA (Figure 4.11B).

These results suggest that at low OVA concentrations, the liposomes are able to adsorb the antigen without notable influence to the physico-chemical characteristics measured. As the concentration of OVA increases, surface neutralisation and aggregation of the vesicles is promoted due to electrostatic interactions between the anionic protein and the cationic liposomes, as is commonly reported with anionic nucleic acids and cationic liposomes (e.g. McNeil & Perrie 2006). Similarly the aggregation of protein to cationic liposomes has been previously reported by Brgles et al (2008) where by using 2.5 mg OVA or greater, the systems aggregated (and

sedimented) due to saturation of the liposomes. The concentration at which this occurs will be due to the binding capacity of the liposomes at a higher concentration (1000 µg) of OVA the liposomes will become saturated and a large fraction of antigen will not be bound to the vesicles, and therefore will remain free in solution (Korsholm et al 2007). However liposomes with higher concentrations of PEGylated surface coating, already display a reduced cationic zeta potential due to the hydrophilic PEG coating prior to the addition of OVA (Figure 4.11B). Therefore this will limit the interaction of the OVA with the liposomes due to both the reduced cationic nature of the system, and due to steric hindrance which will prohibit the OVA interacting with the liposome surfaces. Steric hindrance is where the tightly bound water molecules form a hydrated film around the particle and repel the protein interactions (van Vlerken et al 2007). In turn, this will limit the changes in liposome size and zeta potential (Figure 4.11) as vesicle-OVA interactions are blocked.

4.4.3 Adsorption of antigen to MLV DDA:TDB

4.4.3.1 Adsorption of OVA

To confirm if PEGylation was limiting protein-binding, the degree of adsorption of various concentrations of OVA to the various DDA liposome formulations was investigated. Adsorption was evaluated by sodium dodecyl sulfate-polyacrylamide gel electrophoresis (SDS-PAGE) and BCA assay following ultra-centrifugation.

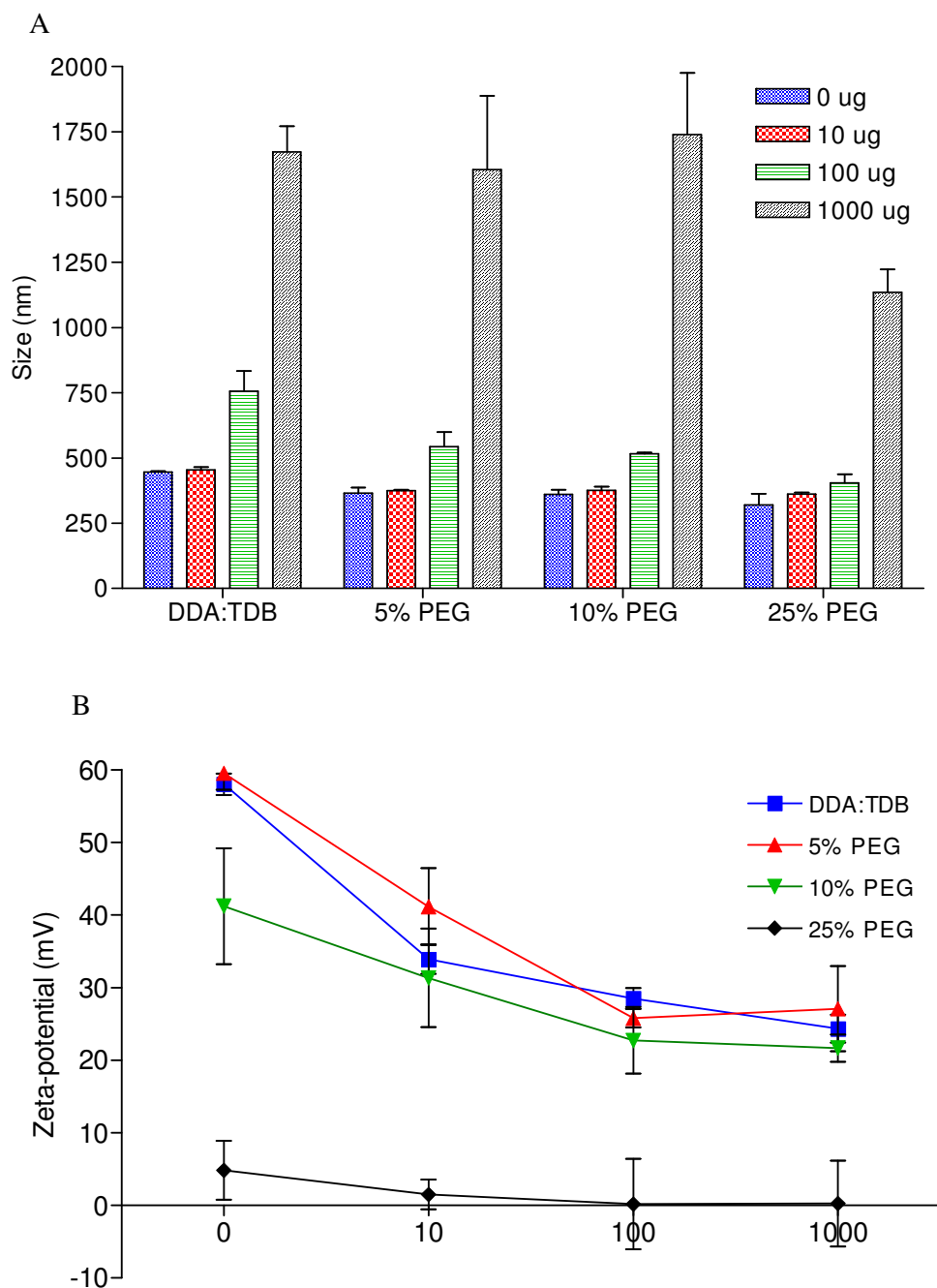


Figure 4.11 (A) Vesicle size (nm) and (B) zeta-potential (mV) of DDA:TDB, 5, 10, 25 % PEG liposomes following the addition of OVA at 10 µg/ml, 100 µg/ml and 1000 µg/ml. Size and zeta-potential measured in Tris buffer (1 mM) using a Brookhaven ZetaPlus instrument. Results represent mean ± SD of triplicate experiments.

SDS is an anionic detergent that binds quantitatively to proteins, giving them linearity and uniform charge, so that they can be separated solely on the basis of their size (Caprette 2010). The SDS has a high negative charge that overwhelms any charge the protein may have, imparting all proteins with a relatively equal negative charge. The SDS has a hydrophobic tail that interacts strongly with protein (polypeptide) chains. The polyacrylamide gel electrophoresis separates protein molecules according to their size. An electric current is used to move the protein molecules across a polyacrylamide gel. The negatively charged protein molecules are pulled to the positive end by the current. The smaller molecules are able to navigate faster than larger ones, so they make it further down the gel allowing SDS-PAGE to separate different protein molecules according to their size (Caprette 2010).

The BCA assay was used to measure free protein present in the supernatants as lipids present in the resuspended pellet interfered with the assay components. However, one of the limitations of the BCA assay is that for protein samples it has a linear range of 100 - 1000 $\mu\text{g/ml}$. Therefore, samples containing 10 $\mu\text{g/ml}$ of protein were not tested as the concentration would be out of the linear range, whereas 100 $\mu\text{g/ml}$, although being below the linear range, and 1000 $\mu\text{g/ml}$ concentrations were tested (Figure 4.12A). From Figure 4.12A, it can be seen that for the 0, 5 and 10 % PEG formulations no free OVA was detected in the supernatants when 100 $\mu\text{g/ml}$ was added, whereas for the 25 % PEG formulation 4.9 % (4.9 μg) of free OVA was found. With the addition of 1000 μg of OVA, the levels of non-adsorbed OVA increased for all four of the formulations, and the amount of non-adsorbed protein increased with increasing PEG concentrations, from ~25 % with DDA:TDB formulations up to ~80 % when 25 % PEG was present in the formulation (Figure 4.12A). These results were

confirmed using SDS page. From Figure 4.12B, it can be seen that no protein bands were detected in the supernatants of all formulations incubated with 100 $\mu\text{g/ml}$, whereas protein bands were present for the pelleted samples confirming antigen adsorption to the liposomes. Figure 4.12C shows the SDS page analysis of formulations prepared with 1000 $\mu\text{g/ml}$. Again in line with the results in 4.12A, higher levels of protein are detected in the supernatant with formulations containing increasing PEG concentrations. This coincides with decreasing levels of protein associated with the pelleted liposomes. These findings are summarised in Table 4.2. In line with these studies, Korsholm et al (2007) also found that the majority of the protein was found to be associated with liposomes at concentrations of OVA less than 1 mg/ml. Therefore taken together these findings (Figures 4.11 and 4.12) demonstrate that cationic liposomes are able to bind anionic proteins such as OVA, and the binding of OVA to these liposomes results in decreased zeta potential and increased vesicle size, presumably due to the electrostatic interactions promoting vesicle aggregation. With increasing concentration of PEG on the surface of the liposomes, the protein binding capacity of the liposomes is reduced due to the hydrophilic coating produced by the PEG. Therefore the steric coating of the DDA:TDB liposome reduces electrostatic interactions of the liposomes with proteins thereby limiting their ability to carry sub-unit antigens on their surface.

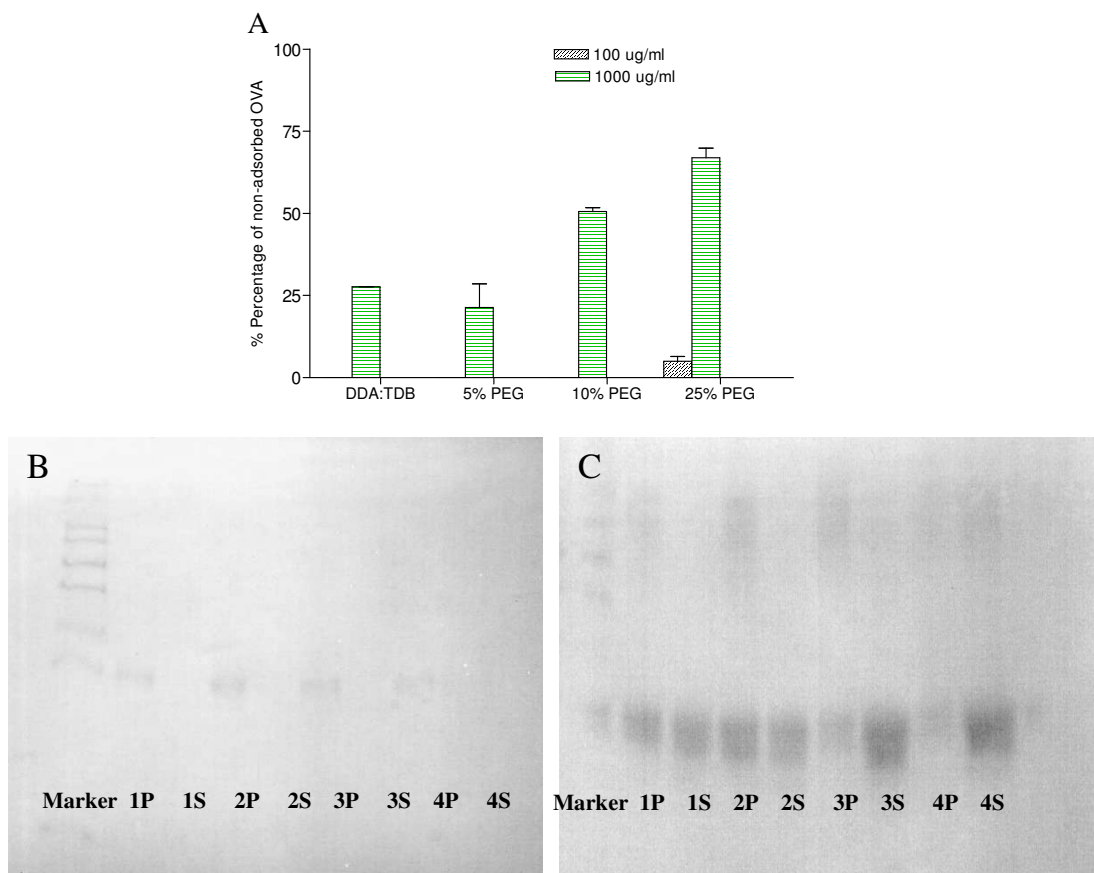


Figure 4.12 Adsorption of OVA. (A) Percentage (%) of non-adsorbed OVA (100 µg/ml and 1000 µg/ml) present within the supernatants of DDA:TDB 5, 10 and 25 % PEG formulations were quantified by the BCA protein assay. These results of the BCA protein assay were confirmed by SDS page (B) 100 µg/ml and (C) 1000 µg/ml of OVA. Lane 1 = DDA:TDB, lane 2 = 5 % PEG, lane 3 = 10 % PEG, lane 4 = 25 % PEG. P = pelleted liposomes; S = supernatant. Results represent mean ± SD of triplicate experiments.

Table 4.2 Description table of the bands and corresponding formulations including the result of the BCA assay for the % protein non-adsorbed.

Lane P = pellet S = supernatant	Formulation	% Protein non-adsorbed 100 µg/ml	% Protein non-adsorbed 1000 µg/ml
1P	DDA:TDB		
1S	DDA:TDB	None detected	27.6 ± 0.03%
2P	5 % PEG		
2S	5 % PEG	None detected	21.3 ± 7.2%
3P	10 % PEG		
3S	10 % PEG	None detected	50.6 ± 1.1%
4P	25 % PEG		
4S	25 % PEG	4.9 ± 1.5%	66.9 ± 2.9%

4.4.3.2 Adsorption of Ag85B-ESAT-6 antigen

To further confirm the binding efficiency of antigens to DDA based liposomes, the adsorption capacity of the systems for the mycobacterial Ag85B-ESAT-6 fusion protein was investigated. This protein has been identified as a promising vaccine antigen against TB in several studies (e.g. Olsen et al 2001; Langermans et al 2005); a disease for which a Th₁ type immune response is required for protection. The degree of adsorption of antigen (% of total used; 0.01 mg) to DDA:TDB liposomes in the presence and absence of PEG was determined using ¹²⁵I-labelled Ag85B-ESAT-6 to both validate previous studies and allow lower antigen concentrations to be tested. Again the addition of PEG was found to have an effect on protein adsorption, with DDA:TDB adsorbing around 97 % of Ag85B-ESAT-6 (Figure 4.13), in line with previous studies (Davidsen et al 2005), whilst the loading was reduced to ~ 80 % for the 25 % PEG formulation. The ability of tracking radio-labelled protein allows adsorption studies to be conducted with higher sensitivity than is the case with BCA and SDS page assays. As can be seen from Figure 4.13, that even at low subunit antigen concentrations, the presence of PEG on the surface of the cationic liposomes influences the electrostatic binding of the antigen to the MLV surface. However, to a much lesser extent than that seen when higher protein concentrations are used (Figure 4.12).

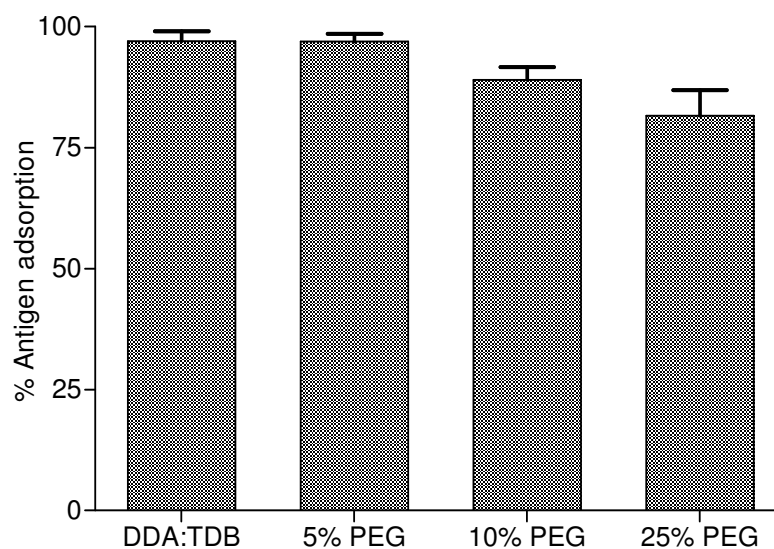


Figure 4.13 Quantification of antigen adsorption of DDA:TDB, 5, 10, 25 % PEG liposomes using ¹²⁵I-labelled Ag85B-ESAT-6. MLVs were prepared by the lipid-hydration method. Non-adsorbed antigen was removed via centrifugation. Results represent mean ± SD of triplicate experiments.

4.4.4 Interactions of MLV liposomes with serum proteins

4.4.4.1 Particle size and zeta potential

Due to their surface charge, cationic liposomes are known to interact with biological media and aggregate into larger constructs (McNeil & Perrie 2006). To investigate possible electrostatic interactions of the DDA with biological media and the effect pegylation of these liposomes has on these interactions, the various DDA:TDB liposomes were placed into a solution containing 50 % FCS (aiming to mimic the protein environment found *in vivo* that the liposomes may encounter upon injection).

Upon exposure to 50 % FCS, an immediate visible aggregation of DDA:TDB cationic liposomes occurred, with particles sizes increasing from 482 nm to over 700 nm after exposure for 60 minutes (Figure 4.14A). Similarly formulations containing 5 % PEG also showed a significant ($p < 0.05$) increase in size post-exposure to 50 % FCS. In contrast, with the 10 % or 25 % PEG formulation (Figure 4.14A), no significant difference in size and zeta potential was observed (Figure 4.14B).

For cationic liposomes, interactions with serum proteins *in vivo* results in aggregation and quick clearance from the circulation. For example, Opanasopit et al (2002) found that cationic particles are particularly susceptible to forming aggregates after binding of negatively charged plasma proteins, which are then either entrapped in the pulmonary capillary bed or taken up by the MPS. However, it is also well documented that pegylated liposomes have excellent stability in body fluid environments (Moghimi & Szebeni 2003). The use of PEG to provide a hydrophilic shield over the surface of the particle is the most usual means of minimising these interactions with plasma proteins (Fattal & Barratt 2009). For cationic liposomes, although the high zeta potential value of 48.0mV should generate enough electrostatic repulsion to keep the particles stable in colloidal systems, the highly cationic surface will promote interaction with serum proteins or opsonins in the body fluid leading to aggregation. However, the pegylated formulations (in particular those containing 10 % and 25 % PEG) were stabilised against such aggregation due to the presence of the flexible polymer preventing protein-liposome interactions (both the loading of antigens and serum proteins). A neutral zeta potential and steric outer layer appears to create a physical barrier between protein and liposome carrier. A study by Huang et al (2008) also showed that PEG stabilised cationic niosomes in serum condition. The authors found that turbidity of cationic niosomal suspensions increased to relatively high levels, indicating an increase in particle size induced by aggregation or protein absorption on the particle surface. Meanwhile, the turbidity of pegylated niosomes changed little in 6 hours and showed only a slight increase in 20 hours (Huang et al 2008).

Overall, this work suggests that DDA:TDB liposomes can be prepared by the addition of PEG to be resistant to aggregation in the presence of biological media whilst still being able to carry significant levels of adsorbed antigen. This offers the potential to investigate a cationic liposome formulation which may not aggregate after intramuscular injection, and offer a different pharmacokinetic profile where a depot may not be formed, thus allowing the role of vaccine delivery systems biodistribution to be further investigated.

4.4.4.2 Antigen retention in the presence of biological moieties

It has been previously reported that association of antigen with the adjuvant delivery system can improve vaccine efficacy (Holten & Andersen 2004). To look at the potential of these systems to retain their antigen after injection, antigen release from liposomes incubated in either Tris buffer or simulated *in vivo* conditions (50 % FCS as previous) and antigen retention measured using I¹²⁵-labelled Ag85B-ESAT-6. Each formulation was diluted (1:5) using 50 % FCS in Tris buffer and incubated in a shaking water bath at 37 °C for 96 hours. Over the 96 h period of the study a high degree of I¹²⁵-Ag85B-ESAT-6 adsorbed to DDA:TDB liposomes was maintained (Figure 4.15) with only 2 % loss in the initial 24 hour period and no significant loss following in the next 24 h (Figure 4.15).

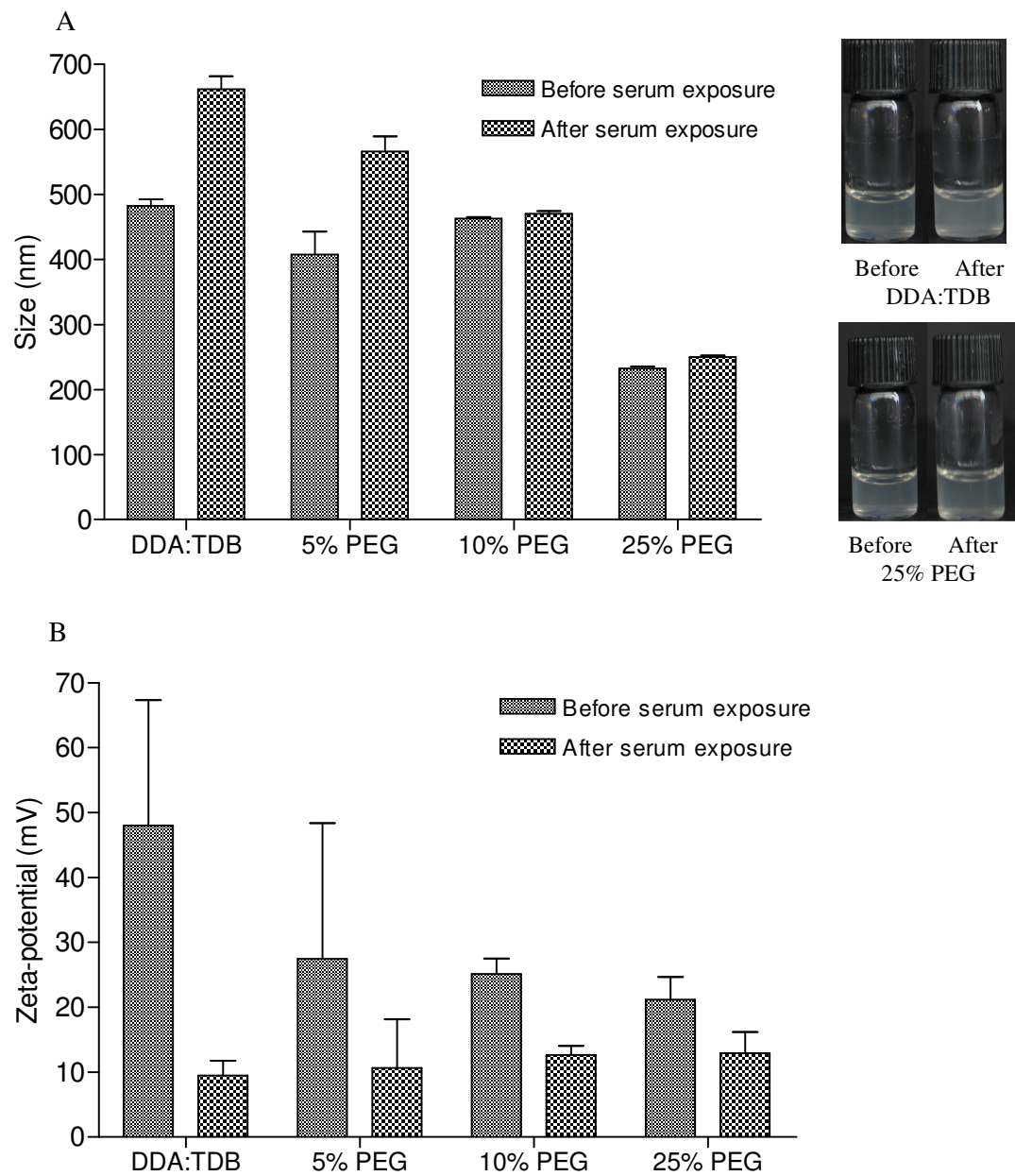


Figure 4.14 (A) Vesicle size (nm) and (B) zeta-potential (mV) of DDA:TDB, 5, 10, 25 % PEG liposomes upon exposure to stimulated *in vivo* conditions (represented by storage at 37 °C in 50 % FCS). Results represent mean \pm SD of triplicate experiments.

A similar result was found for the 5 % PEG formulation. However, over time antigen loss was noted for both of these formulations and at 96 hours around 83 - 88 % antigen remained with the liposome formulation suggesting these formulations offer a sustained and prolonged release (Figure 4.15). However, whilst the presence of PEG on the surface of liposomes had been shown to inhibit liposome aggregation in simulated *in vivo* conditions, these systems were less able to retain antigen under such conditions with increasing levels of PEG resulting in a higher release of antigen from the system. For the 10 % PEG formulation, the initial antigen adsorption was 89 % respectively and a steady release was seen over time to around 69 % after 96 hours of incubation. For the formulation containing 25 % PEG, the release rate was significantly ($p < 0.05$) greater again with only 31% of the antigen remaining adsorbed after 96 hours (Figure 4.15). From these results, it is apparent that with increasing amount of PEG there was a greater release of antigen from the liposome systems over time, in particular with the 10 % and 25 % PEG formulations.

These results suggest that the addition of PEG to the liposomes is limiting electrostatic interactions therefore reducing binding and resulting in increased loss of adsorbed antigen over time. A similar result has been reported by Huang et al (2008). The authors used bovine serum albumin to evaluate the protein/gene carrier binding efficiency of serum albumin with PEG niosomes and found that it was significantly lower than that of cationic niosomes. In particular the authors noted that a neutral zeta-potential and steric outer layer, due to PEG modification, appeared to create a physical barrier between protein and gene carrier. Control studies in which fetal calf serum (FCS) was mixed with I^{125} -Ag85B-ESAT-6 without liposomes did not result in aggregates which could be pelleted by the same centrifugation method, therefore

dismissing the possibility that dissociated antigen may have given false positives due to an association with serum proteins. Overall this suggests that protein from the FCS adds cumulatively to the vaccine antigen rather than competitively displacing the vaccine antigen from the surface of the liposomes.

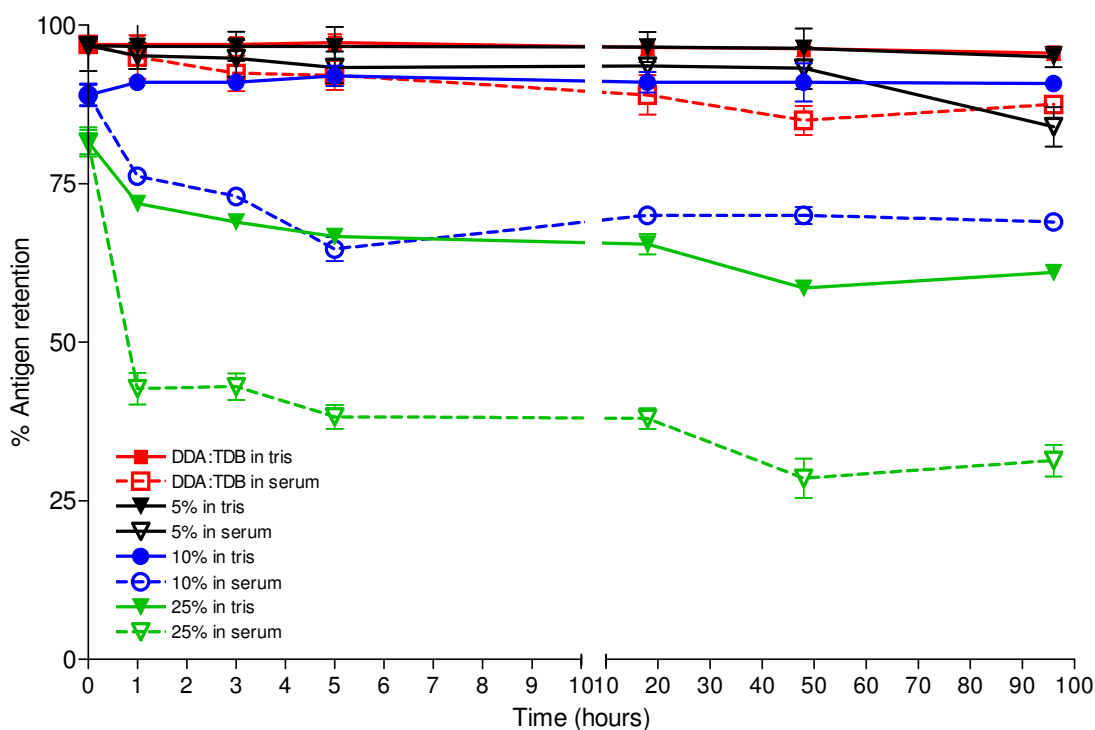


Figure 4.15 Adsorbed Ag85B-ESAT-6 antigen retention profile. DDA:TDB 5, 10, 25 % PEG MLV liposomes stored under simulated *in vivo* conditions with antigen (represented by storage at 37 °C in 50 % FCS). Results represent mean \pm SD of triplicate experiments.

4.4.5 Entrapment of antigen within DRV cationic liposomes

Given the advantages of PEGylation in inhibiting liposome aggregation in the presence of biological moieties but the disadvantage that its presence reduces antigen surface-loading, a method to entrap the antigen within liposomes were considered. The preparation of dehydration-rehydration vesicles (DRV) was first established by Kirby and Gregoriadis (1984a) and was developed to promote higher entrapment within vesicles than could be achieved with other methods such as the lipid hydration

method or the reverse-phase evaporation method. With the DRV method, a process of dehydration followed by rehydration has been employed to entrap material inside the liposomes. The starting point is the preparation of 'empty' aqueous filled SUV. To this SUV suspension the solute to be entrapped within the liposomes is added, such that the solute is outside the liposomes in the external medium. Lyophilisation of the mixture, followed by subsequent rehydration with an initial low volume of water brings about a reorganisation of the lipid membranes such that after fusion they reform liposomes in which a considerable proportion of the aqueous solute is now located within the vesicles. The liposomes obtained are larger than the original SUV and oligolamellar in nature. The advantages of employing this method include (Gregoriadis et al 1999):

- High entrapment of a range of solutes including small drugs, DNA, peptides and proteins.
- Large scale production of SUV can be undertaken in a range of ways prior to addition of the solute to be entrapped.
- No exposure of the drug to be entrapped to solvents.
- Prior to rehydration the product is in a freeze-dried state offering longer term stability.

4.4.5.1 Comparison of size and zeta potential of pegylated DRV

The DRV method has shown to promote greater humoral and cell-mediated immune responses against the encoded antigen in immunised mice in contrast to naked DNA or DNA complexed to preformed liposomes (Gregoriadis et al 1997; Perrie et al 2001). Previously in section 4.4.2, the effect of OVA (0 µg, 10 µg, 100 µg and 1000 µg) on the size and zeta-potential of MLV prepared from DDA:TDB with (5, 10 and 25 %) and without PEG was investigated. To consider the potential of entrapping antigen within the liposomes, similar formulations were also prepared by the DRV method.

The sizes of the various DRV constructs are shown in Figure 4.16. It can be seen that the incorporation of PEG to 'empty' DDA:TDB, 5 %, 10 % and 25 % DRV formulations resulted in vesicle sizes of around 450 nm for DDA:TDB, 370 nm for 5 %, 365 nm for 10 %, which were similar in size to their MLV counterparts, however the 25 % PEG formulation was somewhat smaller in size compared to the MLV counterparts (120.9 nm versus 287.7 nm respectively).

As with MLV based systems (Figure 4.11) following the addition of 10 µg of OVA, there was no significant increase in size for the DRV DDA:TDB, 5 %, 10 % and 25 % PEG formulation (Figure 4.16A). The addition of 100 µg/ml of OVA did have a significant effect on the size of the DDA:TDB ($p < 0.05$) and the 5 % PEG formulations ($p < 0.01$), where an increase in size was found due to the incorporation of the protein within the DRV vesicles. However, this was not the case for the 10 % and 25 % PEG formulations where no significant change in size was measured compared to their equivalent 'empty' DRV. On further increases in antigen

concentration to 1000 μg , all 4 of the DRV formulations show major increases in vesicle size suggesting at high protein/cationic lipid concentrations larger vesicle constructs are formed in all cases. This is supported by the zeta-potential studies (Figure 4.16B), which assist to evaluate the extent of cationic lipid and anionic antigen interactions. In the instance of no protein and 10 μg and 100 μg (with the exception of 25 % PEG at the latter concentration) the zeta-potential does not change, suggesting that a considerable amount of antigen is not interacting with the vesicle surface and is either not surface bound or located within the liposomes presumably bound to the cationic charges of the inner bilayers. However, as the concentration of antigen is increased to 1000 μg a significant ($p < 0.05$) reduction in cationic charge was found for all formulations compared to their empty liposomal counterparts. Again this suggests a high protein/lipid ratios may result in the inner vesicle core of the DRV become full with more protein being complexed on the vesicle surface, thus causing neutralisation of the vesicles cationic charge.

It has previously been reported that by employing the DRV procedure, consistently high entrapment values for a range of antigens and solutes can be achieved, depending on the liposome composition and the moiety being entrapped (Gregoriadis et al 1996). The 25 % PEG formulation did not form DRV vesicles and remained as SUV. It could be that due to the high PEG content, which is known to have unfavourable structural changes in the liposomal bilayer and the neutral charge, may have resulted in the formulation remaining as SUV.

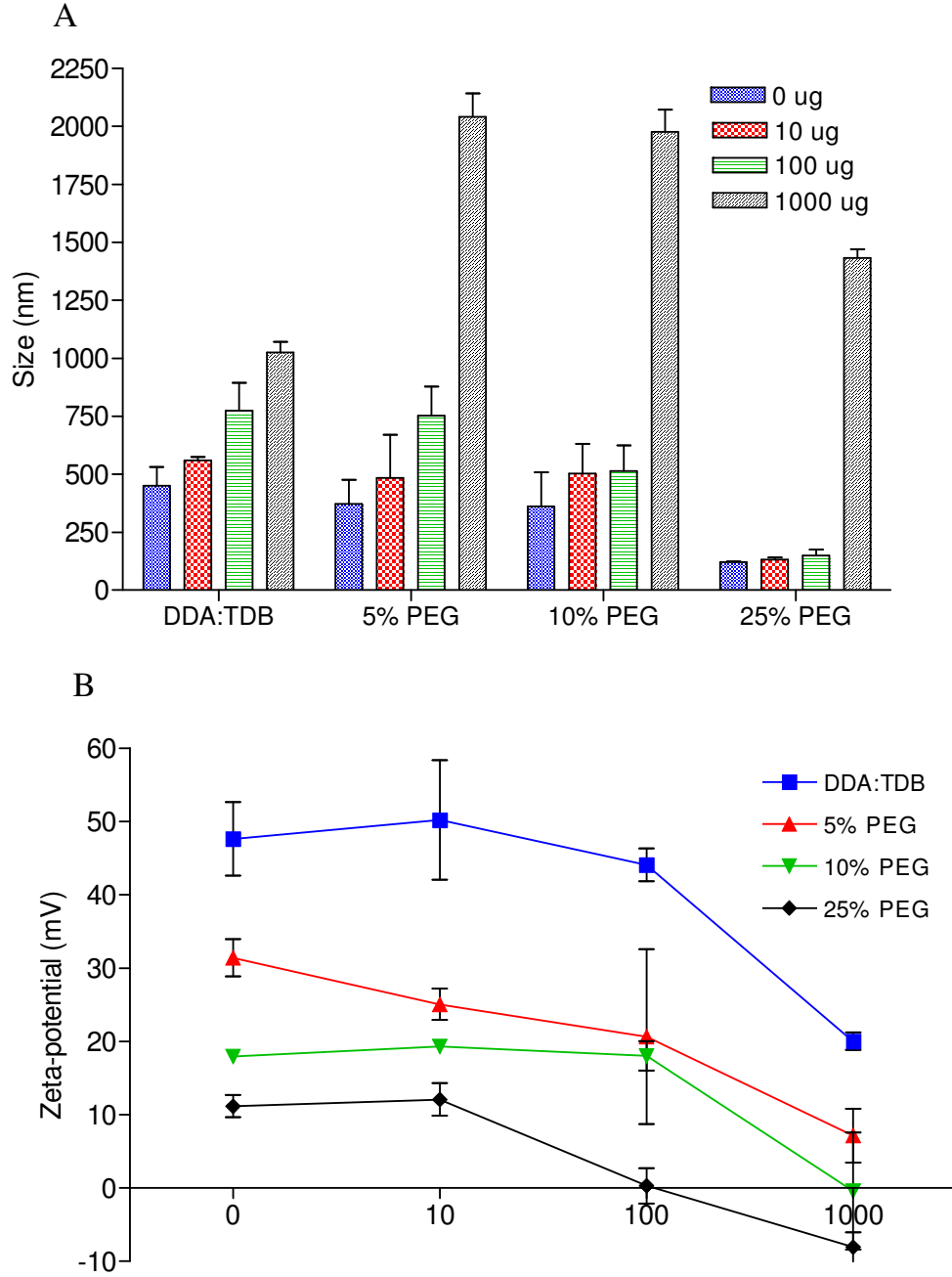


Figure 4.16 (A) Vesicle size (nm) and (B) zeta-potential (mV) of DDA:TDB, 5, 10, 25 % PEG liposomes following the entrapment of OVA at 10 µg/ml, 100 µg/ml and 1000 µg/ml. Size and zeta-potential measured in Tris buffer (1 mM) using a Brookhaven ZetaPlus instrument. Results represent mean ± SD of triplicate experiments.

4.4.5.2 The effect of PEGylation DDA:TDB SUV characteristics

In order to investigate if vesicle size had an effect, smaller vesicles were prepared by sonicating the MLV to produce SUV prior to the addition of antigen. The liposomes produced were in the range of 100 - 250 nm in size (Table 4.3).

Table 4.3 Characterisation data for the SUV based liposomes with 2 µg of Ag85B-ESAT-6.

Formulation	Size (nm)	Polydispersity (PI)	Zeta-potential (mV)
DDA:TDB	250.2 ± 43.3	0.384 ± 0.05	45.6 ± 1.8
10 % PEG	144.1 ± 9.3	0.279 ± 0.05	20.8 ± 1.0
25 % PEG	120.0 ± 12.2	0.255 ± 0.04	2.9 ± 1.0

Results represent mean ± SD of triplicate experiments.

From Table 4.3, it can be seen that the incorporation of PEG to the DDA:TDB SUV influenced the size, polydispersity and zeta-potential of the liposomes. As the amount of PEG increased there is a decrease in vesicle size, with liposomes prepared from DDA:TDB alone being around 250.2 ± 43.3 nm whilst formulations containing 10 %, and 25 % PEG being 144.1 ± 9.3 nm ($p < 0.001$) for 10 %, and 120.0 ± 12.2 nm ($p < 0.001$) for 25 % PEG formulation respectively (Figure 4.3). In terms of the zeta-potential, it can be seen that as the amount of PEGylation increased there was a drop in zeta potential from 45.6 ± 1.8 mV when no PEG is present to around 2.9 ± 1.0 mV when the bilayer contains 25 % PEG ($p < 0.001$). These results showed a similar trend to that found with the MLV based liposomes (section 4.4.1)

4.4.5.3 Comparison of MLV, SUV and DRV antigen loading and retentions

From the results obtained above from sections 4.4.1 - 4.4.5.2 on the basis of adsorption, release, and serum stability data for the MLV systems and the initial characterisation data for the SUV and DRV systems, it was decided that in addition to the DDA:TDB formulation, the 10 % and 25 % PEG formulations would be taken forward for the biodistribution studies based on:

1. The MLV 10% PEG formulation having an initial antigen adsorption of 89 % and a steady release to around 69 % after 96 hours. The results obtained for the 5 % PEG were similar to that of DDA:TDB and for the 25 % PEG a less initial antigen adsorption and greater release was found.
2. The 10 % and the 25 % formulations were found to be stable in the presence of serum proteins compared to the 5 % and DDA:TDB formulations which were found to aggregate.

Further characterisation work involving quantifying and determining release of entrapped (DRV) and adsorbed antigen (SUV) was carried out on the DDA:TDB, 10 %, and the 25 % PEG formulations.

To quantify the amount of associated antigen with the different liposome types (MLV, SUV and DRV), ¹²⁵I-labelled Ag85B-ESAT-6 was used (Figure 4.17). The DDA:TDB DRV based formulation had 98 % of the antigen associated with the pellet, a similar result to that of MLV and SUV based formulations (Figure 4.17). However compared to the MLV and SUV systems, the entrapment for the 10 % PEG DRV formulation was higher at ~98 % (similar to that of the DDA:TDB DRV) compared with 89 % for the MLV and 88 % for SUV systems of the same

composition (Figure 4.17). When the PEG content was increased to 25 % in the systems there was no significant difference between the MLV, DRV and SUV formulations with all three showing antigen association of 80-82 % (Figure 4.17).

The DRV method is reported to promote entrapment of solutes (Kirby & Gregoriadis 1984a) however in the case of systems where there is electrostatic interactions between the solute and the liposomal membrane, as is the case with anionic protein and cationic liposomes, it is not always clear where the antigen is located (adsorbed on the surface versus entrapped within the liposomes). From the data in Figure 4.17, there is no evidence of differences between the three types of formulations that the antigen is entrapped within the DRV compared with surface adsorbed. However, to confirm that the antigen is entrapped and not surface adsorbed further experiments were carried out as described in detail in section 5.3.1.

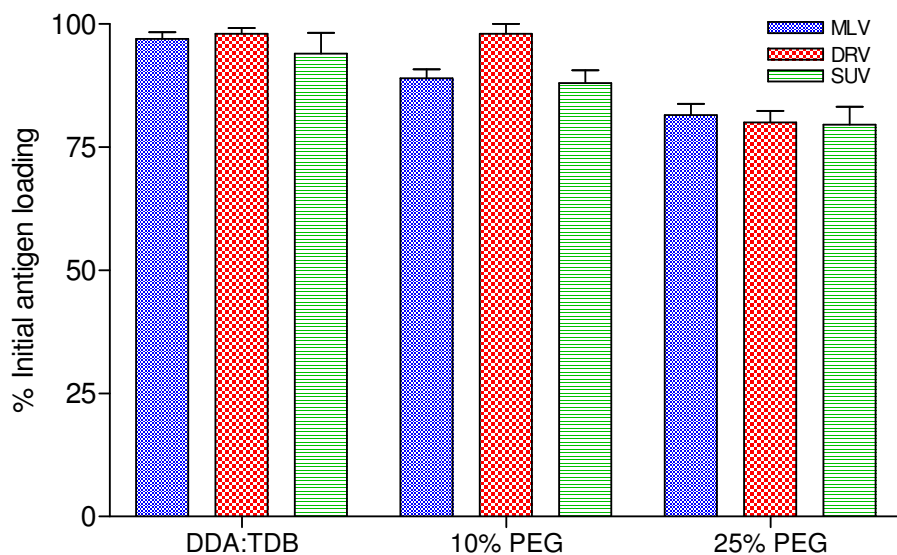


Figure 4.17 Quantification of antigen entrapment of DDA:TDB, 5, 10, 25 % PEG liposomes using ¹²⁵I-labelled Ag85B-ESAT-6. DRVs were prepared by the dehydration-rehydration method. Non-adsorbed antigen was removed via centrifugation. Results represent mean \pm SD of triplicate experiments.

The ability of these systems to retain the associated antigen when incubated in either Tris buffer or simulated *in vivo* conditions (50 % FCS as previous) was also tested (Figure 4.18). In terms of antigen retention profiles of the various formulations (Figure 4.18), after 24 hours significant differences in the level of antigen retention was measured. For the MLV based formulations DDA:TDB had an antigen retention of 89 %, whereas for 10% and 25 % PEG a retention of 70 % and 38 % was found. A similar pattern of antigen retention was found for the SUV based liposomes (Figure 4.18A). Thereafter, all six formulations investigated showed no further significant release. For the DRV based liposomes, the DDA:TDB DRV formulation had a slightly higher retention profile compared to the MLV formulation with antigen entrapment of 93 % compared with 89 % after four days of incubation for the DRV and MLV respectively (Figure 4.18A). A similar higher retention over time was found for the 10 % PEG DRV formulation around 80 % entrapment compared to 69 % antigen adsorption for the equivalent MLV after 96 hours (Figure 4.18B). For the 25

% formulations, again a better release profile was found when the antigen was entrapped with 54 % antigen retention compared to 31 % and 35 % for MLV and SUV formulations after 96 hours (Figure 4.18C). These results suggest generally the DRV systems were able to retain their associated antigen compared to their equivalent MLV and SUV counterparts. This finding is supported by Perrie and Gregoriadis (2000b). The authors found that interaction of DNA with preformed cationic SUV or with cationic SUV made of DOPE and DOTAP (1:1 molar ratio) leads to the formation of large complexes with externally bound DNA. However, dehydration of the DNA-SUV complexes and subsequent rehydration generates submicron liposomes incorporating most of the DNA in a fashion that prevents DNA displacement.

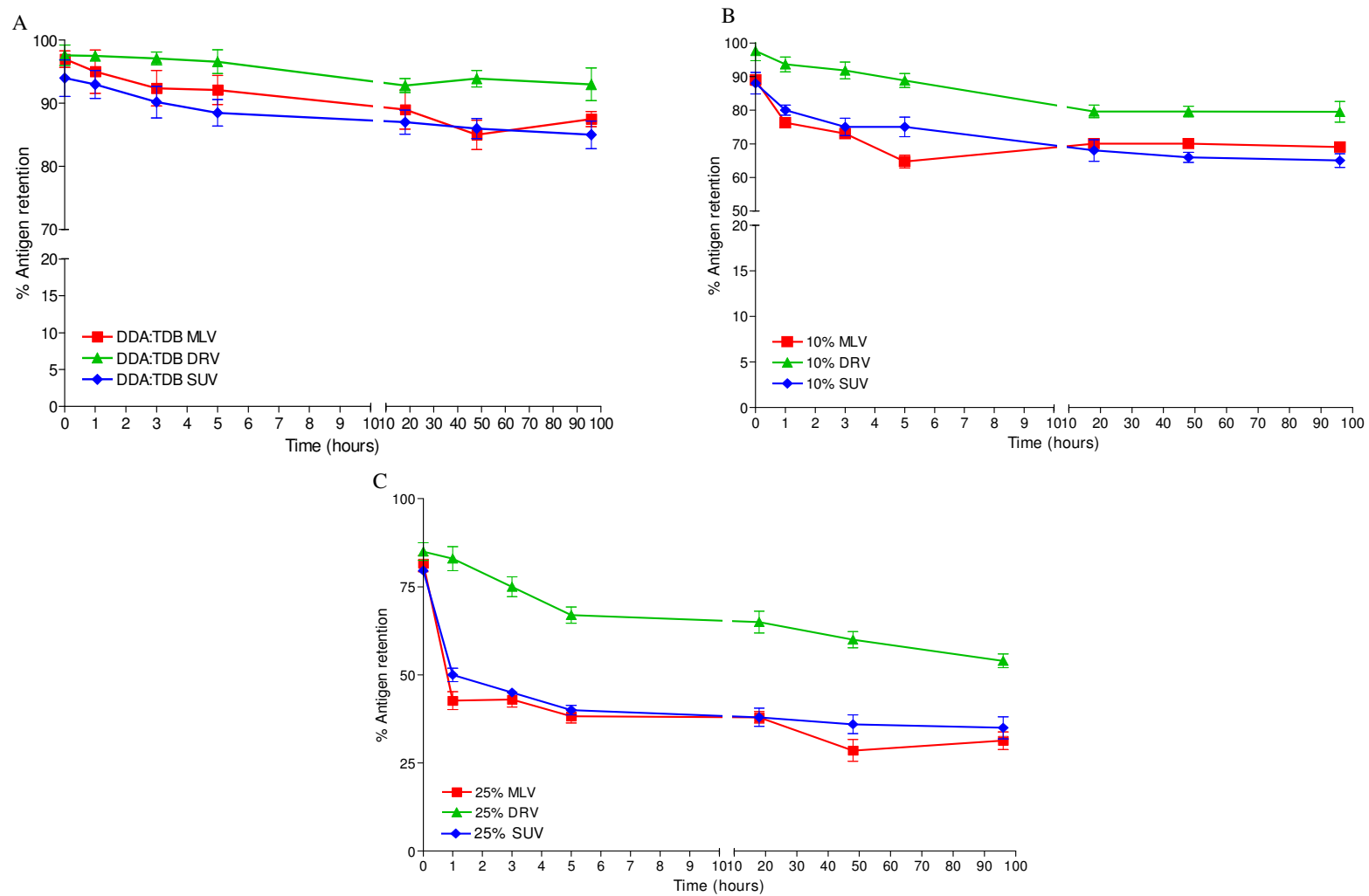


Figure 4.18 Ag85B-ESAT-6 antigen release profile. (A) DDA:TDB, (B) 10 % PEG and (C) 25 % PEG MLV, DRV and SUV (to allow comparison) liposomes when stored under simulated *in vivo* conditions (50 % FCS, 37 °C). Results represent mean \pm SD of triplicate experiments.

4.4.5.4 Addition of cryoprotectant: a modified DRV procedure for the formation of small liposomes

Liposomes entrapped antigen vesicles prepared by the DRV procedure (Gregoriadis et al 1999) produce liposomes of relatively large size (> 200 nm) and subsequently Zadi and Gregoriadis (2000) developed a novel and non-destructive method of producing small liposomal vesicles, which are still able to retain a high percentage of entrapped solutes. It is a modification of the DRV procedure, where a disaccharide is utilised as a cryoprotectant during freeze-drying. The method is an extension of Crowe and Clegg's (1973) suggestion that disaccharides added to vesicles could replace water that normally surrounds the polar groups of the lipids.

When liposomes are subjected to the DRV procedure, the freeze-drying process removes the water content of the vesicles. With water removal, the vesicles fuse due to the physical changes in the bilayers structure, with a transition from the gel to liquid phase, creating larger liposomes than those prior to the process (i.e. SUV). The disaccharides interact with the polar groups of the phospholipids by hydrogen bonds and as a consequence stabilise the vesicles during freeze-drying (Crowe et al 1988).

To utilise this method to produce smaller DDA:TDB with entrapped antigen, sucrose was used as the cryoprotectant added during the freeze-drying stage at a sucrose to lipid mass ratio of 1:1, based on previous studies, reporting this as the optimal sucrose/lipid mass ratio (Zadi & Gregoriadis 2000).

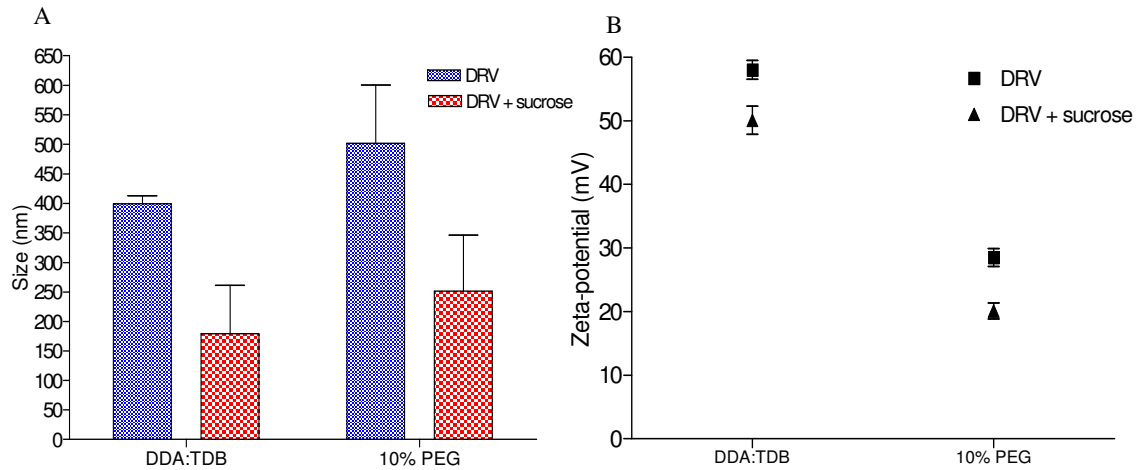


Figure 4.19 Effect of sucrose on (A) vesicle size (nm) (B) zeta potential (mV) within DRV liposomes. Results represent mean \pm SD of triplicate experiments.

From Figure 4.19A, it can be seen that vesicle sizes reduced considerably when sucrose was added to the liposome suspension, in the case of DDA:TDB from 400 nm to 179 nm, and for the 10 % PEG from 500 nm to 251 nm. The zeta-potential for DDA:TDB, 58.0 mV versus 50.1 mV with sucrose and for 10 % PEG, 28.5 mV versus 20.1 mV, was unaffected by the addition of sucrose (Figure 4.19B). The initial antigen loading was not affected by the addition of the cryoprotectant with the percentage of antigen entrapment being around 95 - 97 % for DDA:TDB and 85 - 90 % for the 10 % PEG formulation (Figure 4.20). During the DRV procedure, the liposomes endure two distinct stresses, freezing and drying (Allison et al 2000). Upon rehydration, the liposomal bilayer membranes lose functionality and become disrupted, causing the membrane to fuse and aggregate and resulting in the production of large vesicles in which the antigen becomes entrapped. However, in the presence of sugars this disruption does not occur (Crowe et al 1985).

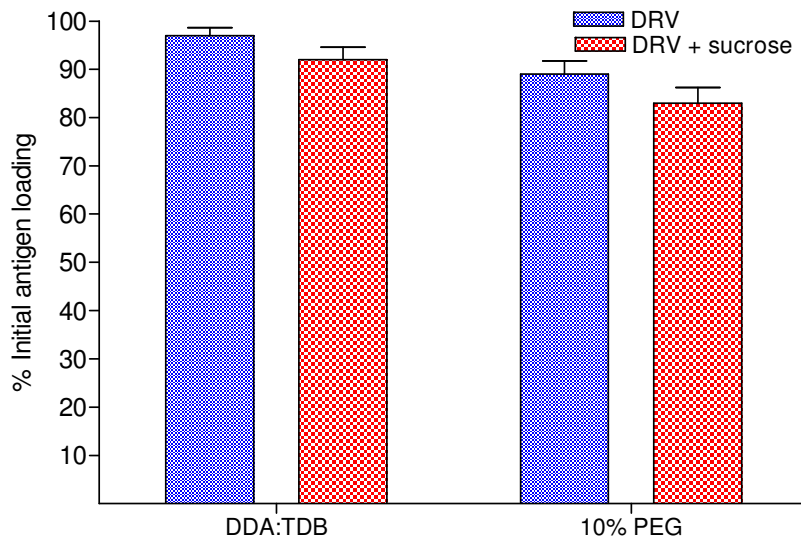


Figure 4.20 Quantification of antigen entrapment of DDA:TDB and 10 % PEG liposomes with addition of sucrose using ^{125}I -labelled Ag85B-ESAT-6. DRVs were prepared by the dehydration-rehydration method. Non-adsorbed antigen was removed via centrifugation. Results represent mean \pm SD of triplicate experiments.

4.4.6 Biodistribution studies of liposomes and their associated antigens

The biodistribution of liposomes depends on the physicochemical properties of the liposomes such as liposome size, surface charge and composition as well as on other factors such as dose and route of administration. Previous biodistribution studies (Henriksen-Lacey 2010) have found that DDA:TDB forms an efficient depot of antigen at the injection site. The ‘depot effect’ is when the antigen is retained at the injection site, thereby increasing the time of vaccine exposure to the immune cells. With the DDA:TDB formulation this has been suggested to be due to the strong electrostatic charges i.e. aggregation between the cationic liposomes and serum proteins, thereby causing a liposomal depot to form which retains the antigen. Therefore, the PEGylated formulations were prepared to address whether the aggregation between the liposomes and serum proteins is responsible for the depot effect. Since pegylated liposomes have excellent stability in the presence of serum proteins due to the hydrophilic shield over the surface (Immordino et al 2006), this

will offer the potential to investigate cationic liposome formulations which may not aggregate after intramuscular injection of the particle. In addition the ability to entrap antigen within the liposomes, rather than surface adsorb, may promote enhanced retention of the antigen with the liposomes. Therefore within biodistribution studies the effect of PEGylation on various liposome systems (MLV, SUV and DRV) was considered.

To follow the fate of the liposomes and the antigen, mice were vaccinated i.m. with I¹²⁵-labelled Ag85B-ESAT-6 with H³-labelled liposomes in order to analyse the fate of injected antigen in the presence and absence of a pegylated liposomal carrier. On days 1, 4 and 14 post vaccination, major organs/tissues (spleen, non-injected and injected muscle site and popliteal lymph node (PLN)) were isolated and I¹²⁵ and H³ content was determined. No other organs were tested based on previous studies (Henriksen-Lacey et al 2010) which demonstrated these to be the major site of interest after i.m. immunisation.

4.4.6.1 The effect of PEGylation on MLV retention at the site of injection

From Figure 4.21, it can be seen that for the DDA:TDB formulation the levels of liposomes retained at the injection site after four days had not decreased significantly compared to day 1, and more than 40 % of the original dose was still present even after 14 days (Figure 4.21A; Table 4.4). Considering the effect of PEG, on days 1 and 4 there was no significant difference between the DDA:TDB and the 10 % PEG formulation, with the percentage liposome retention being similar for both formulations but by day 14 there was significantly more ($p < 0.01$) DDA:TDB liposomes present compared to the 10 % PEG formulation. In contrast, the 25 % PEG

liposomes were removed faster than the DDA:TDB with significantly lower levels found at the injection site on day 1 ($p<0.05$) and day 14 ($p<0.001$). Simultaneously, Ag85B-ESAT-6 detection showed that more than 70 % of the initially co-administered antigen dose was found at the SOI 1 day p.i. when administered with DDA:TDB liposomes, and the presence of 10 % PEG in the formulation made no significant difference (Figure 4.21B Table 4.4), whereas only 7 % of the initial antigen dose was detected when administered together with 25 % PEG formulation at the same time-point (Figure 4.21B). By day 4, DDA:TDB retained significantly higher levels at the injection site compared to both PEGylated formulations but by day 14 there was no significant difference.

These results suggest that higher levels of PEG are able to significantly inhibit the formation of a liposome depot at the injection site and also severely limit the retention of antigen at the site. This suggests that the presence of PEG on the surface of the liposomes may allow the faster drainage of the liposomes from the site of injection. Previous biodistribution studies (Henriksen-Lacey et al 2010) demonstrated the requirement of a cationic vesicle for the formation of a depot at the site of injection which promoted antigen retention. The authors compared neutral DSPC liposomes with DDA:TDB liposomes and found that the level of both liposomes and antigen at the SOI were significantly lower in the case of the DSPC formulation at all time points and by day 14 p.i. is undetectable. It was hypothesised that the decrease in antigen retention at the SOI for DSPC liposomes when compared to DDA based liposomes, is due to the non-aggregating nature of DSPC liposomes in the presence of biological components. However, in this case the opposite was true for the 10 % PEG formulation as it was found from the characterisation work that although the 10 %

PEG formulation did not aggregate in the presence of serum proteins, the formulation still formed a depot of antigen at the site of injection.

4.4.6.2 The effect of PEGylation on SUV retention at the site of injection

In order to investigate if vesicle size had an effect on the liposome depot effect, smaller vesicles were prepared by sonicating the MLV to produce SUV prior to the addition of antigen. From Figure 4.21C, 61 % of DDA:TDB SUV liposomes remained at the site of injection after day 1, which dropped to 52 % on day 4, and 15 % by day 14. The addition of 10 % PEG had no significant effect on day 1 with the percentage of liposomes at the site of injection being around 50 % compared to 61 % found with the DDA:TDB liposomes. However, a significant difference was found compared to DDA:TDB on day 4, and 14 with only 14 % versus 55.9 % on day 4, and 1.8 % versus 15.0 % liposomes on day 14. Following the addition of 25 % PEG, similar to the MLV based formulation the liposomes were removed faster than the DDA:TDB with significantly lower levels found at the injection site on day 1 ($p<0.05$) and day 14 ($p<0.001$).

Simultaneously, Ag85B-ESAT-6 detection showed that more than 78 % of the initially co-administered antigen dose was found at the SOI 1 day p.i. when administered with DDA:TDB liposomes. Furthermore, the presence of 10 % PEG made a significant difference to the amount of antigen present ($p<0.05$) which was around 43.4 % (Figure 4.21D Table 4.4), whereas only 5 % of the initial antigen dose was detected when administered together with 25 % PEG formulation at the same time-point (Figure 4.21D). By day 4 and 14, DDA:TDB retained significantly higher levels at the injection site compared to both PEGylated formulations.

When comparing the MLV and the corresponding SUV liposomes (summarised in Table 4.4), there was no significant difference in the liposome retention for DDA:TDB at the site of injection on days 1 and 4. However on day 14, a significantly higher ($p<0.05$) percentage of liposome retention was found for the MLV liposomes compared to the SUV liposomes (~30 % versus ~15 % respectively). For the 10 % PEG formulation, there was no significant difference in the liposome retention at the site of injection on days 1 and 14. However, a significant difference in the liposome retention was found at the site of injection on day 4, with a significantly higher ($p<0.05$) percentage of liposome retention found for the MLV liposomes compared to the SUV liposomes (48 % versus ~14 % respectively). For the 25 % PEG formulation, there was no significant difference in the percentage of liposome retention at the site of injection between the MLV and the SUV formulations at all time-points (Table 4.4).

In terms of antigen retention for the DDA:TDB formulation, no significant difference was found between the MLV and SUV formulations on day 1 and 14 (Table 4.4). However, a higher % of antigen retention was found on day 4 (47 % compared to the MLV formulation around 24 %).

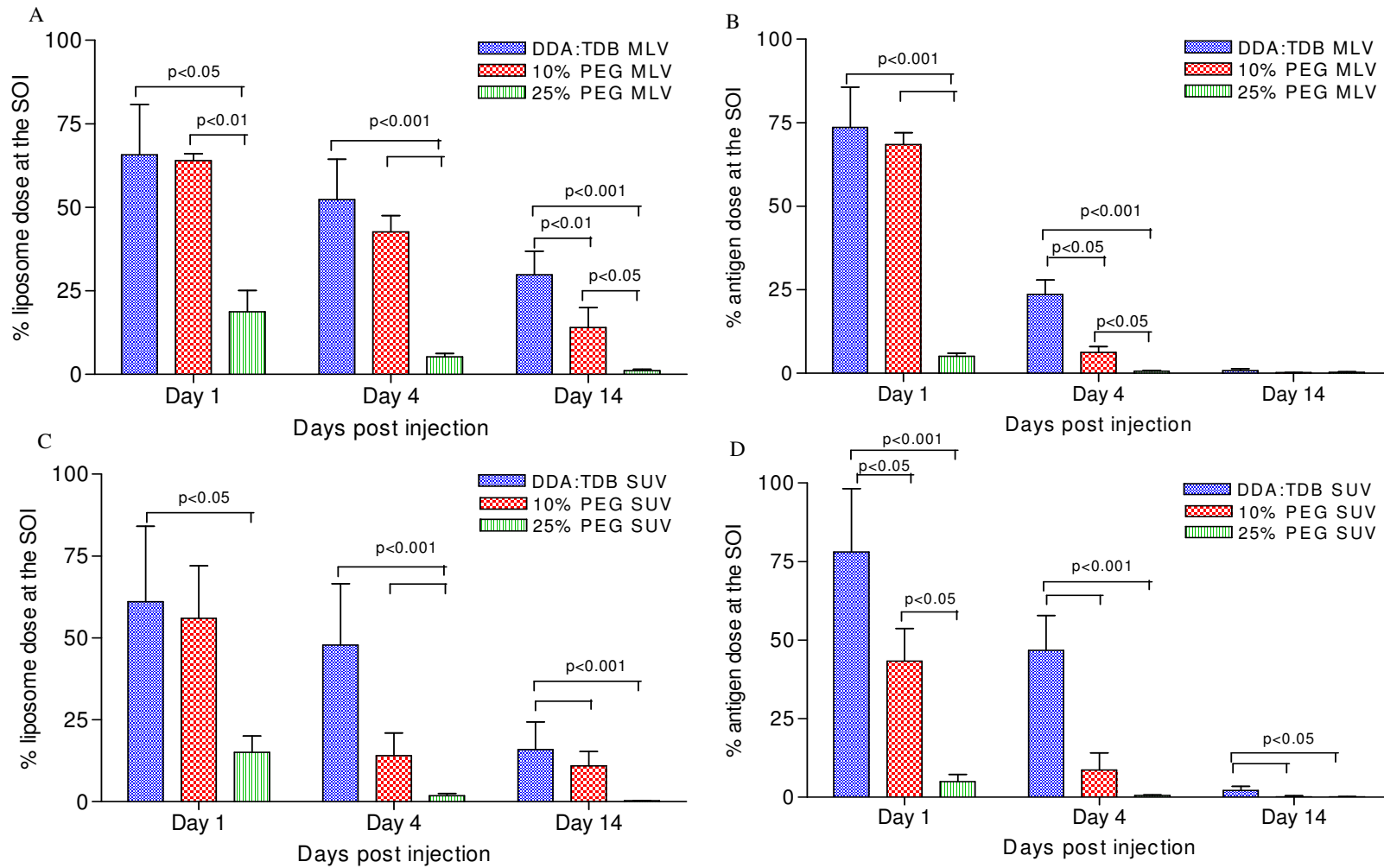


Figure 4.21 Pharmacokinetic profile of (A) liposome and (B) antigen for MLV and (C) liposome and (D) antigen for SUV following i.m. injection. Liposomes and Ag85B-ESAT-6, radiolabelled with H^3 and I^{125} respectively, were detected at the site of injection using γ -counting and scintillation counting techniques. The proportion of each radionuclide as a % of the initial dose was calculated. Results represent mean \pm SD of five mice.

This higher level of antigen retention suggests that perhaps the SUV based liposomes, due to their small size, aggregate more extensively with serum proteins thereby causing the antigen to retain at the site of injection longer. For the 10 % PEG, a significant difference ($p < 0.05$) was found on day 1 with a higher percentage of antigen retention found with the MLV formulation, however by day 4 and 14 there was no significant difference. Furthermore, the percentage of antigen retention for the 25 % PEG formulation MLV and SUV was similar at all time-points with no significant difference ($p > 0.05$).

From these results, it was found that higher levels of PEG in both the MLV and SUV liposomes is able to significantly inhibit the formation of a liposome depot at the injection site. In spite of this when comparing the MLV and SUV liposomes a higher percentage of liposome retention was found with the MLV based liposomes. Although a higher level of PEG severely limits the retention of antigen at the site of injection, from this data it was found that size has an effect as well, with a faster drainage of the antigen from the site of injection found with the smaller 10 % pegylated liposomes on day 1 compared to the MLV counterpart. At higher PEG concentrations, there was no difference, however since the 25 % PEG MLV liposomes are considerably smaller than the other MLV systems (362 nm versus 454 nm with the DDA:TDB formulation) size may again be playing a role. On the other hand, in the absence of PEG, liposome size had no effect on the liposome retention at the SOI at all time points and had little effect on the depot effect at early time points. However a significantly higher percentage of antigen was found with the SUV based formulation at the SOI on day 4, and slightly more on day 14. Thus a larger group size would be required to elucidate if this small difference is indeed significant.

Table 4.4 Summary of the percentage (%) of liposome and antigen retention at the SOI for the MLV and SUV formulations on days 1, 4 and 14.

Formulation	MLV			SUV		
	Size (nm)	Liposomes	Antigen	Size (nm)	Liposomes	Antigen
DDA:TDB Day 1		65.7 ± 29.6%	73.5 ± 12.0%		61.1 ± 23.0%	78.0 ± 20.2%
Day 4	454.3 ± 11.0 nm	52.3 ± 12.0%	23.5 ± 4.4%	250 ± 43.3 nm	55.9 ± 16.0%	46.8 ± 11.1%
Day 14		29.8 ± 7.0%	0.80 ± 0.6%		15.0 ± 4.9%	2.1 ± 1.3%
10 % PEG Day 1		63.9 ± 2.2%	68.4 ± 3.6%		47.8 ± 18.8%	43.4 ± 10.4%
Day 4	375.0 ± 4.2 nm	42.6 ± 4.9%	6.2 ± 1.8%	144.1 ± 9.3 nm	14.0 ± 6.9%	8.6 ± 5.5%
Day 14		13.9 ± 6.0%	0.16 ± 0.05%		1.8 ± 0.8%	0.14 ± 0.3%
25 % PEG Day 1		18.7 ± 6.3%	5.1 ± 0.92%		15.9 ± 8.4%	4.97 ± 2.3%
Day 4	362.0 ± 6.4 nm	5.3 ± 0.95%	0.65 ± 0.2%	120.2 ± 12.2 nm	10.9 ± 4.3%	0.56 ± 0.1%
Day 14		1.06 ± 0.44%	0.32 ± 0.13%		0.27 ± 0.07%	0.13 ± 0.03%

Results represent mean ± SD of five mice.

Previous studies (Henriksen-Lacey et al 2010) have compared the biodistribution profile of sonicated and non-sonicated DSPC:TDB liposomes and found no significant difference in the amount of antigen and liposome present at the site of injection. Although these were neutral based liposomes, in this work a similar result was found with the cationic DDA:TDB liposomes suggesting that cationic interactions with serum proteins can promote a depot effect with both small and large cationic systems.

4.4.6.3 The effect of entrapping antigen within the liposomal systems on their biodistribution

In order to investigate whether depot formation of antigen could be further improved, Ag85B-ESAT-6 was entrapped within DRV liposomes rather than surface adsorbed to MLV. Previous studies have found that the development of DRV made possible high-yield entrapment of macromolecules in liposomal formulations and was initially applied to proteins (Factor VIII) (Kirby & Gregoriadis 1984b). In subsequent studies, DRV liposomes were shown to be immunogenic for entrapped tetanus toxoid. This was comparable with tetanus toxoid covalently linked to multilamellar vesicles (Davis & Gregoriadis 1987).

The clearance of the DDA:TDB DRV and modified DRV (mDRV) (both with and without PEG) was also investigated using radio-label to track them as previously described for MLV and SUV. From the results (Figure 4.22A), around 64 % of DDA:TDB DRV liposomes remained at the site of injection after 24 hours, which dropped to 47 % on day 4, and 29 % by day 14. The addition of 10 % PEG had a significant ($p<0.05$) effect on liposome retention initially (52 % liposome retention compared to 64 % found with the DDA:TDB formulation). However, longer term no significant effect on clearance was noted with the presence of 10 % PEGylation of the DRV (Figure 4.22A). Further increases in the PEG content to 25 % further increased liposome clearance rates, with significantly lower liposome levels found at the injection site on day 1 ($p<0.01$) and day 14 ($p<0.01$) (Figure 4.22A).

For the smaller modified DRV formulations, formulated as DDA:TDB and DDA:TDB:10% PEG, there was no significant difference between the two formulations at each of the time points measured (Figure 4.22A). On comparing the DRV and mDRV for DDA:TDB, there was no significant difference at day 1 and 4, however by day 14 significantly higher ($p<0.05$) levels of the smaller vesicles had been cleared from the injection site (29 % for the DRV compared to 15 % found with the mDRV formulation; Figure 4.22A). For the 10 % PEG formulations, no significant difference was found at any of the time points.

In terms of antigen retention, a significant ($p<0.05$) higher percentage of antigen was found with the DDA:TDB DRV compared with the 10 % PEG formulation on day 1 (67 vs 54 % respectively) and day 4 (24 % compared to 10 %), however by day 14 there was no significant difference (Figure 4.22B). With the 25 % PEG formulation, antigen was cleared from the site of injection faster than DDA:TDB with significantly

lower levels of antigen at the injection site on day 1 ($p<0.01$) and day 14 ($p<0.01$) (Figure 4.22B). A similar pattern of antigen retention was found with the corresponding mDRV formulations and comparing DRV and mDRV of the same formulation showed no significant difference in antigen retention. These studies suggest that reducing the size of DRV liposomes with or without 10 % surface PEG had no effect on the retention of liposomes and antigen at the SOI (Table 4.5).

Table 4.5 Summary of the percentage (%) of liposome and antigen retention at the SOI for the DRV and mDRV formulations on days 1, 4 and 14.

Formulation	DRV			mDRV		
	Size (nm)	Liposomes	Antigen	Size (nm)	Liposomes	Antigen
DDA:TDB Day 1		64.5 ± 3.7%	67.1 ± 8.3%		52.0 ± 25.3%	54.4 ± 26.1%
Day 4	560.1 ± 13.3 nm	47.0 ± 3.7%	24.2 ± 4.8%	179.0 ± 82 nm	45.8 ± 25.3%	26.0 ± 5.9%
Day 14		28.6 ± 6.0%	2.4 ± 2.1%		14.6 ± 3.9%	1.2 ± 0.7%
10 % PEG Day 1		51.6 ± 10.6%	54.1 ± 7.6%		65.9 ± 15.9%	62.6 ± 17.6%
Day 4	502.2 ± 128.0 nm	42.0 ± 10.2%	9.98 ± 6.2%	251.0 ± 95.1 nm	30.2 ± 14.9%	7.5 ± 6.0%
Day 14		26.3 ± 14.9%	3.7 ± 3.4%		19.1 ± 8.7%	2.12 ± 1.43%
25 % PEG Day 1		24.5 ± 7.9%	6.6 ± 2.2%			
Day 4	132.45 ± 8.9 nm	5.9 ± 7.8%	1.05 ± 0.22%			
Day 14		2.1 ± 0.1%	0.62 ± 0.12%			

Results represent mean ± SD of five mice.

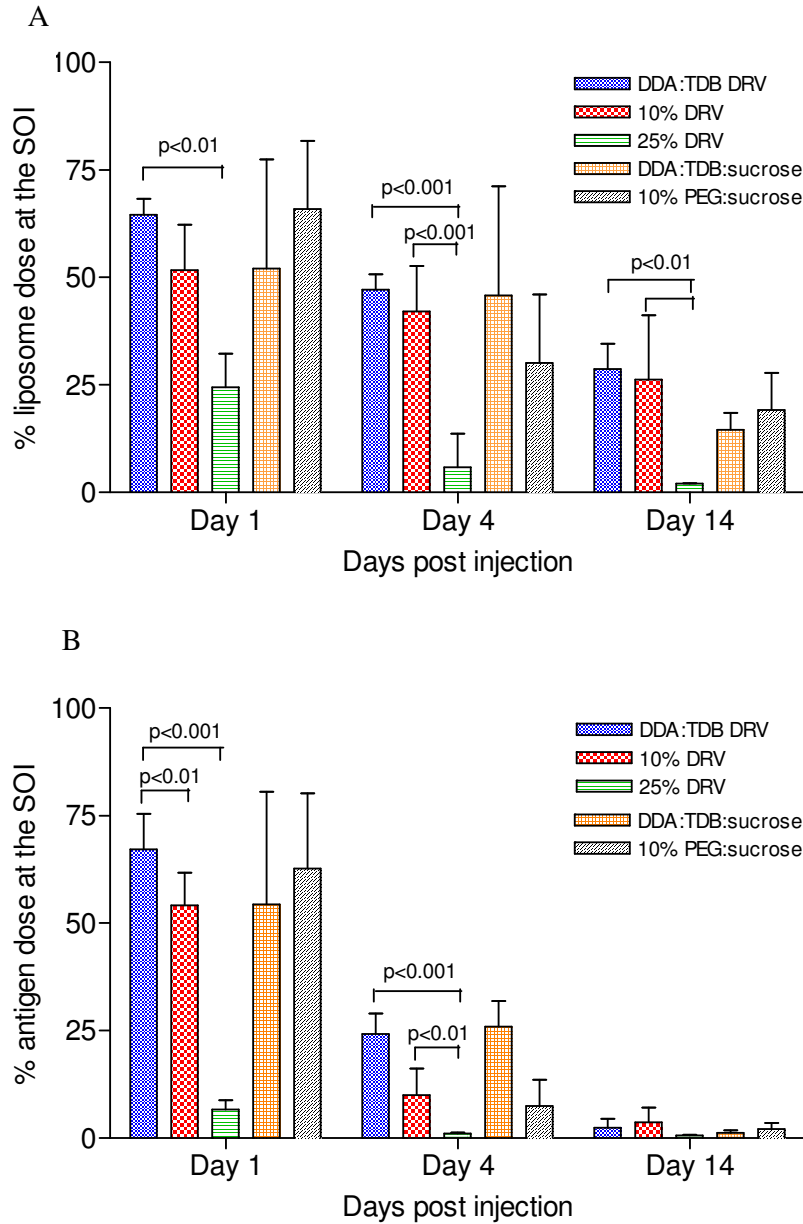


Figure 4.22 Pharmacokinetic profile of (A) liposome and (B) antigen for DRV and mDRV following i.m. injection. Liposomes and Ag85B-ESAT-6, radiolabelled with H^3 and I^{125} respectively, were detected at the site of injection using γ -counting and scintillation counting techniques. The proportion of each radionuclide as a % of the initial dose was calculated. Results represent mean \pm SD of five mice.

When comparing the MLV with DRV formulations (Table 4.4 and 4.5 respectively), it was found that comparable liposome compositions had a similar percentage of liposome retention at the site of injection at all three time-points, irrespective of their preparation method. More importantly, in terms of antigen retention, again there was no significant difference between the two preparations methods, with a similar percentage of antigen retention at the site of injection, for DDA:TDB, 10 % and 25 % PEG compositions at each of the three time points (Table 4.4 and 4.5). Similarly, comparison of SUV with mDRV shows no significant difference in antigen retention for both compositions. This suggests that regardless of whether the antigen is entrapped within the vesicle or adsorbed onto the outer surface, it has no effect on the retention of antigen and liposomes.

The aim of the biodistribution study was to see whether the aggregation between the liposomes and serum proteins is responsible for the depot effect. Pegylated liposomes were employed to provide the hydrophilic shield over the surface (Immordino et al 2006), to investigate cationic liposome formulations which may not aggregate after intramuscular injection of the particle. From the results, it was found for the various liposome systems, MLV, SUV and DRV, higher levels of PEG, i.e. 25 % PEG, were able to significantly inhibit the formation of a liposome depot at the injection site. The inclusion of 25 % of PEG also severely limited the retention of antigen at the site of injection. With the 10 % PEG formulations, although from the characterisation studies it was found that this formulation did not aggregate in the presence of serum proteins, it was found that this formulation formed a depot of liposomes and antigen at the site of injection. The 10 % PEG has a zeta-potential of around 20 mV as opposed to 50 - 60 mV usually found with the DDA:TDB formulation. This suggests that it is not

entirely the cationic charge responsible for the depot formation. In addition, there was no significant difference on whether the antigen is entrapped (DRV) or adsorbed (MLV) on the surface on the retention of the antigen and the liposomes.

4.4.7 Detection of vaccine components in the popliteal lymph nodes

The left popliteal lymph node (PLN) is the local lymph node to which the lymph from the SOI (the left quadriceps) drains. Therefore, it will be the primary site at which the antigen will be presented to the T cells. The presence of both liposome and antigen vaccine components to the PLN was therefore analysed. The distribution of vaccine components to the draining PLN is shown in Figure 4.23. With the pegylated formulations, in particular, the 25 % PEG MLV and DRV liposomes although not significant, a marked increase in liposomes was found compared to the DDA:TDB liposomes suggesting that the liposomes drain quickly to the PLN when depot is not obtained. This was significant ($p < 0.05$) in the case of 25 % PEG SUV liposomes on day 4 (Figure 4.23D).

In terms of antigen retention, all three MLV formulations had a similar percentage of antigen retention on days 1 and 4, however, on day 14 the 25 % PEG formulation had a slightly higher level of antigen draining to the lymph nodes (0.02 % compared to 0.01 % found with the DDA:TDB formulation; Figure 4.23B). A similar result was found for the 25 % PEG SUV (Figure 4.23D). For the DRV based formulation again a higher percentage of antigen drainage was found with the 25 % PEG DRV formulation 0.16 % compared to 0.009 % found with the DDA:TDB formulation (Figure 4.23B and F). From the initial biodistribution results, it was found that 25 % PEG formulation cleared from the site of injection significantly faster compared to the

DDA:TDB formulation which formed a depot of antigen. From this data, it appears that the 25 % PEG formulation drained quickly to the PLN with significantly higher levels found with the SUV formulation. It has previously been suggested (Mann et al 2009) that a formulation that is able to get around the body would be able to stimulate a strong antibody mediated response, whereas one that forms a depot could likely aid a cell mediated response. DDA:TDB forms a depot at the site of injection and has been previously found to stimulate a Th₁ type immune response (Davidsen et al 2005).

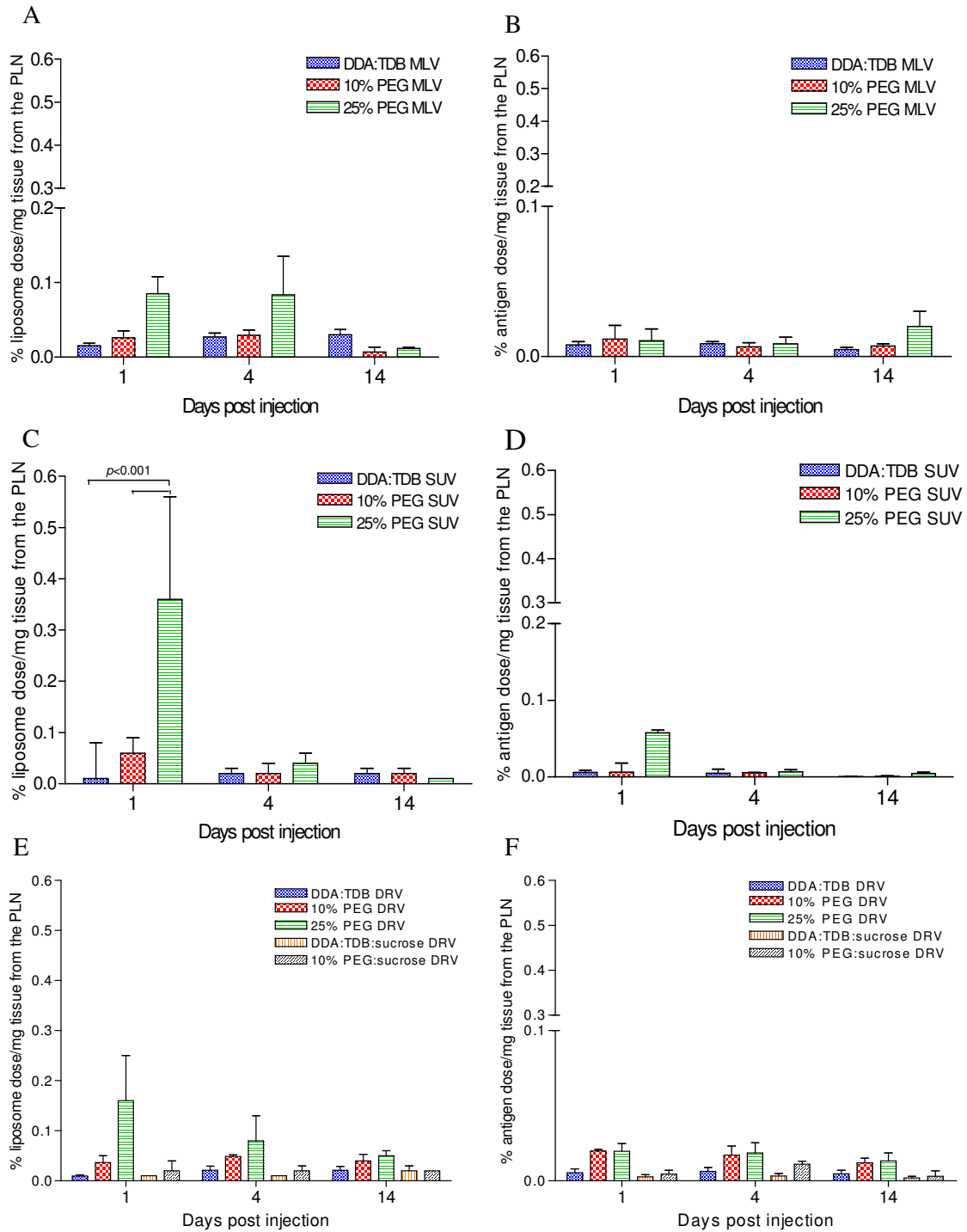


Figure 4.23 Draining of liposomes and Ag85B-ESAT-6 to the PLN after i.m injection. DDA:TDB, 10% PEG and 25% PEG (A) liposomes (B) antigen of MLV, (C) liposomes (D) antigen of SUV and (E) liposomes (F) antigen of DRV and mDRV. The proportion of each radionucleotide as a percentage of the initial dose and divided by the mass of the tissue (mg) was calculated. Results represent mean \pm SD of 5 mice.

4.4.7.1 Monocyte influx to the SOI as determined by pontamine blue staining

In accordance with previous studies (Henriksen-Lacey et al 2010), pontamine blue dye was used as a marker for infiltrating monocytes to the SOI. Using this method, it was found that mice injected with antigen alone showed little/no blue staining at the site of injection whereas mice injected with cationic liposomes showed localised blue staining at the injection site (Henriksen-Lacey et al 2010). Furthermore, the authors found a noticeable increase in the intensity of blue staining at the site of injection in mice injected with DDA:TDB liposomes as compared to DDA liposomes suggesting a role for TDB in the activation of the innate immune system, notably in the recruitment of circulating monocytes to the site of injection (Henriksen-Lacey et al 2010).

Considering the different PEGylated and non-PEGylated formulations all of the liposome formulations tested induced monocyte infiltration, however the kinetics and intensities were varied (Figure 4.24): at day 14, higher level of monocyte infiltration can be seen with the DDA:TDB and 10 % PEG formulations compared with the 25 % PEG formulations (Figure 4.24). It is interesting that on day 14 p.i, the presence of DDA:TDB MLV liposomes at the SOI was equal to that of 10 % PEG liposomes and this was comparable with the DRV based formulations. Korsholm et al (2010) found that intraperitoneal injection of DDA based liposomes resulted in a significant recruitment of neutrophils, monocytes, mature macrophages and activated natural killer cells (Korsholm et al 2010) correlating nicely with the large monocyte infiltration observed in this and previous studies (Henriksen-Lacey et al 2010). However, with the SUV based liposomes all three liposome formulations induced a slower monocyte influx to the SOI suggesting that perhaps size of the liposome influences the recruitment of circulating monocytes to the site of injection.

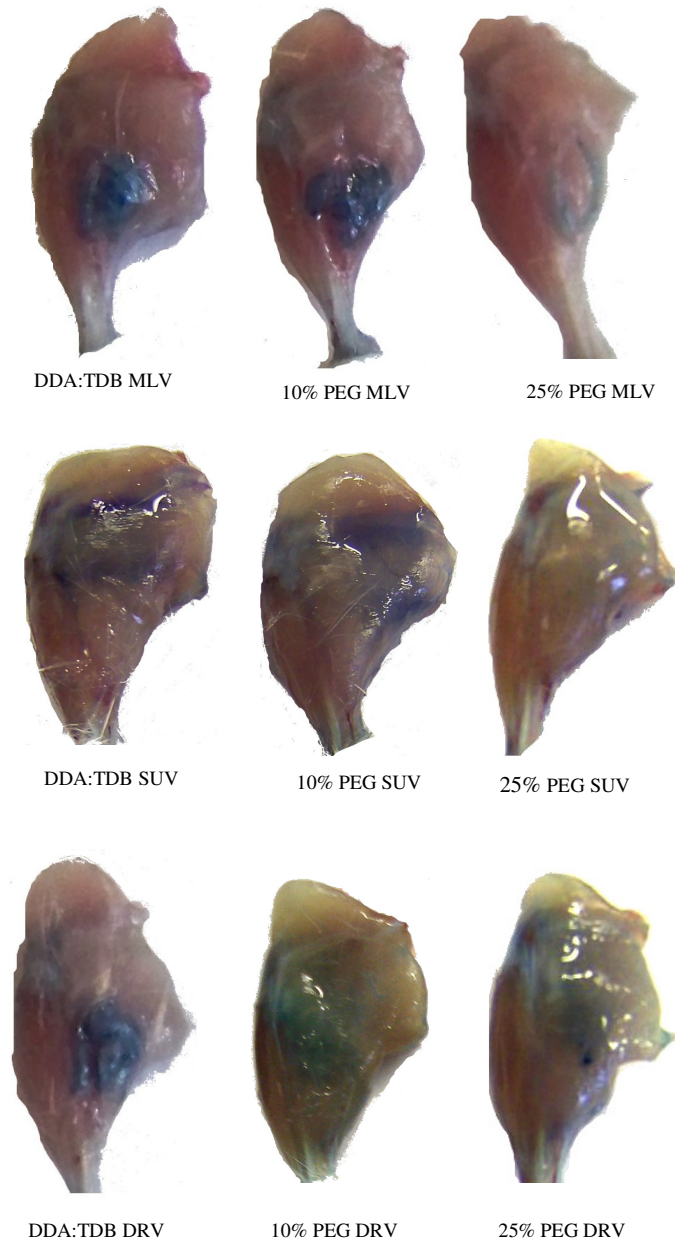


Figure 4.24 Pontamine blue staining at the site of injection (quadriceps) after 14 days injection. DDA:TDB, 10 %, 25 % PEG liposomes MLV, SUV and DRV. A higher level of monocyte infiltration can be seen with the DDA:TDB and 10 % PEG formulations compared with the 25 % PEG formulations for all three MLV, SUV and DRV based liposomes.

4.4.8 Synopsis of the biodistribution data

Previous biodistribution studies (Henriksen-Lacey 2010) have found that DDA:TDB forms an efficient depot of antigen at the injection site. With the DDA:TDB formulation this has been suggested to be due to the strong electrostatic charges i.e. aggregation between the cationic liposomes and serum proteins, thereby causing a liposomal depot to form which retains the antigen. Therefore, the PEGylated formulations were prepared to address whether the aggregation between the liposomes and serum proteins is responsible for the depot effect. It has been demonstrated that higher levels of PEG i.e. 25 % was able to significantly inhibit the formation of a liposome depot at the injection site and also severely limit the retention of antigen at the site therefore resulting in a faster drainage of the liposomes from the site of injection.

4.4.9 Testing the potential of the various formulations as vaccine adjuvants

To test the potential of the various formulations as vaccine adjuvants, immunological analysis was carried out in order to determine the efficacy of the liposome formulations in achieving the desired immune response, encompassed quantification of Ag85B-ESAT-6 specific IgG antibody production, cytokine secretion and spleen cell proliferation (the ability of spleen cells to respond to re-stimulation with antigen). In terms of antibody responses, IgG is the most obvious choice for detection from blood samples. It can activate both the complement system and mediate opsonisation, thus leading to enhanced phagocytosis (Goldsby et al 2003). Further, the analyses will encompass the measuring of both the IgG1 and IgG2a subsets. Production of IgG1 generally follows activation of Th₂ type cells, whereas IgG2a is produced following secretion of Th₁ type cytokines such as IFN- γ (Zhu et al 2007). Therefore, these

investigations will give an indication of both the level and type of humoral response initiated by the formulations tested. Cell proliferation analysis will provide an indication of both B cell and T cell activation in response to the antigen, giving further insight into the type and level of immune response achieved by each formulation. Cytokine ELISAs can be used as assay markers of both Th₁ (IFN- γ and IL-2) and Th₂ (IL-5 and IL-6) responses, providing further elucidation into the method of action of each formulation. IFN- γ is considered the key cytokine marker for anti-mycobacterial immunity (Agger & Andersen 2001), being the major macrophage activator element, indicative of CD4⁺ recruitment, whilst also playing a role in B cell differentiation (Playfair & Bancroft 2004), therefore vital for cell mediated immunity (Mosmann & Sad 1996). IL-2 is a growth factor secreted by T-cells, thus indicative of T-cell activation, which in turn can lead to B-cell proliferation and differentiation. IL-2 is therefore another essential signal in directing cell mediated immunity (Playfair & Bancroft 2004), whilst also playing a role in the humoral response. In terms of the Th₂ cytokine markers, IL-5 promotes B-cell proliferation and differentiation, and also leads to eosinophil production and activation, whereas IL-6 is key in differentiation to plasma cells (Playfair & Bancroft 2004), an important facet in memory responses and innate immunity, and therefore useful in vaccines.

4.4.9.1 Antibody production

Antibody ELISAs were performed at regular intervals (see section 4.3.2.12) to determine the antigen specific antibody production initiated by each formulation (Figure 4.25). In terms of IgG, Figure 4.25A shows there was no significant difference at all time-points. Ag85B-ESAT-6 alone did not give detectable levels of IgG at the first time point, whereas all liposome formulations were able to induce measurable

levels of IgG. A comparison between the formulations at the first time point show a trend of increasing IgG levels with higher levels of PEG, but no notable differences between MLV, SUV and DRV. At the subsequent time-points, free antigen was able to induce IgG levels of log end point serial dilutions of around 3.0 (Figure 4.25A). In comparison, all liposome formulations were able to induce significantly ($p<0.05$) higher levels of IgG relative to free antigen, however there was no significant difference between the various liposome formulations. At the next two time-points a similar story in terms of IgG levels was noted.

Considering the IgG1 and IgG2b (Figures 4.25B and C respectively) antibody isotype immune responses, the responses were similar to those of IgG with the exception of 25 % PEG MLV and DRV formulation where Ag85B-ESAT-6-specific IgG2b levels were comparable to the free Ag85B-ESAT-6, even at the later time point. In contrast, the DDA:TDB MLV and DRV formulations appeared to show the highest and most enhanced IgG2b responses compared to the free Ag85B-ESAT-6 from 35 days onwards (Figure 4.25C). Interestingly there were no significant differences ($p<0.05$) in antibody responses from mice immunised with 10 % PEG DRV formulations with entrapped antigen compared with the group which received antigen adsorbed to 10 % PEG SUV. However, from the data it can be seen that the DDA:TDB MLV and DRV are able to elicit high titres of all three antibody isotypes, and also show strong Ag85B-ESAT-6-specific IgG2b mediated immune responses.

Previous studies (Vangala et al 2007b) have shown that DDA:TDB was superior in inducing a cell mediated immune response as well as an IgG2 antibody response, compared to other cationic liposome systems in a hepatitis B study using hepatitis B

surface antigen (HBsAg). As discussed previously, there have been a number of attempts to optimise the DDA:TDB immune response by modification of the composition of the delivery system. Vangala et al (2006) incorporated non-ionic lipids and cholesterol, which resulted in a significant reduction of Ag85B-ESAT-6-specific IFN- γ and IgG2 levels, while the induction of IgG1 titers was comparable between the formulations with and without non-ionic lipids and cholesterol (Vangala et al 2006). Incorporation of the two lipid components, DDA and TDB, into poly(D,L-lactic-co-glycolic acid) microspheres (PLGA) also resulted in a decrease in IFN- γ and IgG2 levels and no difference in IgG1 levels, when compared to DDA:TDB (Kirby et al 2008a). The results presented here suggest that following the addition of PEG, whilst the IgG1 titer was comparable between the formulations, a reduction of Ag85B-ESAT-6-specific IgG2 levels was found.

4.4.9.2 Cytokine production

Following on from the antibody ELISA, the next immunological investigation of this study was determining cytokine production induced by each formulation. The cytokines assayed encompassed indicators for both Th₁ and Th₂ immune responses. For Th₁, IFN- γ (considered the key cytokine marker for tuberculosis immunity) and IL-2 were measured, and for Th₂, IL-5 and IL-6 were measured (Figure 4.26). In terms of IFN- γ (Figure 4.26A), PEGylation of the formulations was seen to reduce responses for MLV, SUV and DRV formulations, with DDA:TDB systems being significantly ($p < 0.05$) higher than their 25 % PEG formulation equivalents. Comparison between all the formulations shows that DDA:TDB MLV gave the highest levels. The results for the IL-2 cytokine were similar to those of IFN- γ (Figures 4.26A and B), with the presence of PEG in the formulations reducing IL-2

levels. IL-5 which is an indicator of a Th₂ type immune response was significantly higher ($p < 0.05$) for the 10 % PEG MLV compared to the DDA:TDB. Although not significant, a higher level of IL-5 was produced for the corresponding 10% PEG SUV formulation (Figure 4.26C). IL-6 is a pro-inflammatory cytokine and a significant higher level of this cytokine was produced for the DDA:TDB MLV ($p < 0.05$) and DRV ($p < 0.001$) formulations compared to the pegylated liposomes (Figure 4.26D).

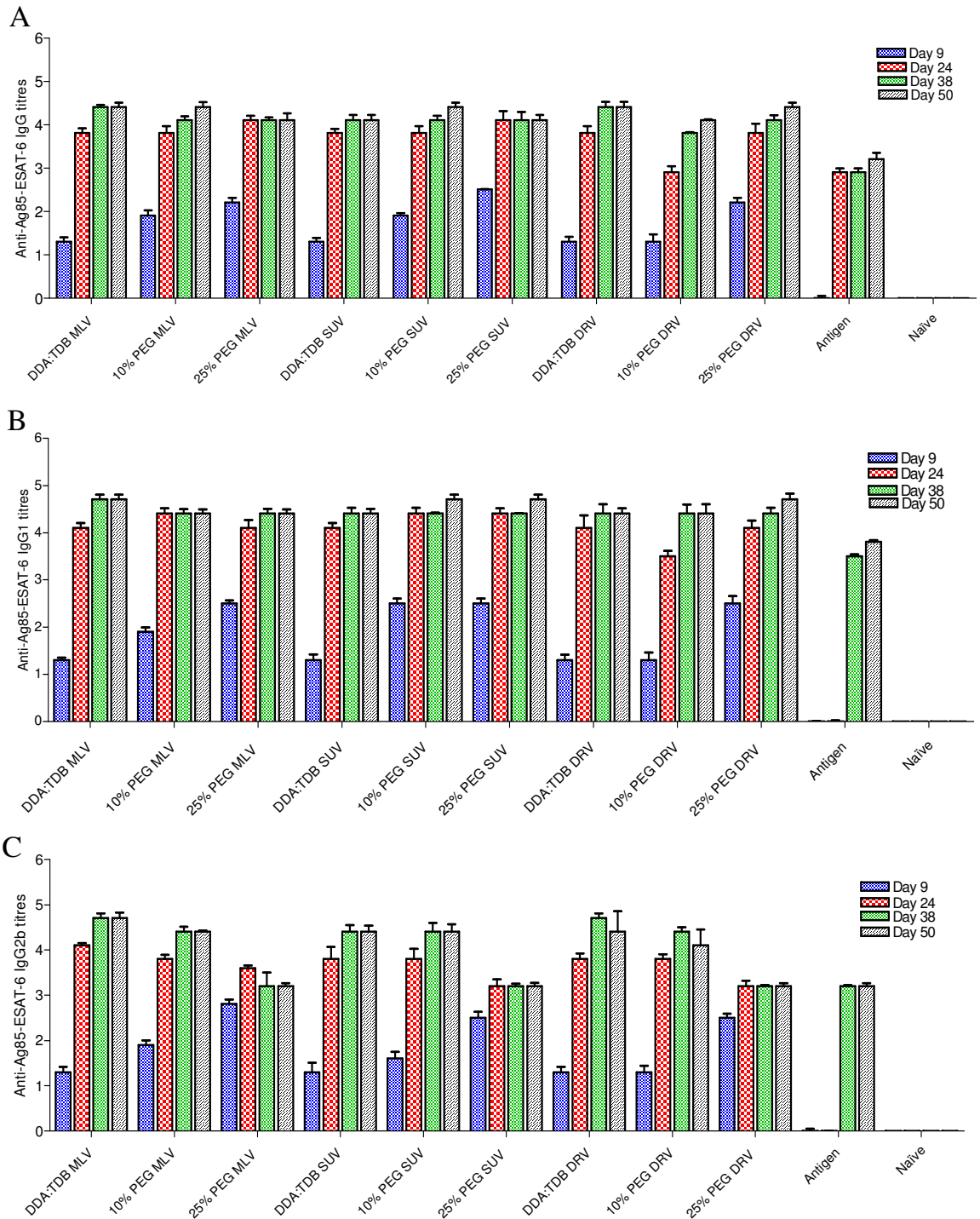


Figure 4.25 Ag85B-ESAT-6 specific antibody titres. Groups of five female BALB/c mice, approximately six weeks old, received doses of vaccine formulations containing 2 µg of Ag85B-ESAT-6 in a 50 µl volume. Vaccine formulations were administered intramuscularly, and each mouse received three doses at intervals of two weeks. Serum samples were taken at 12 days after the first administration and at two week intervals thereafter. Sera samples obtained at different time intervals after immunisation were analysed for the presence of anti-Ag85B-ESAT-6 IgG (A), IgG1 (B) and (C) IgG2b antibodies by enzyme-linked immunosorbent assay (ELISA).

It has been reported that an important mechanism of the ability of DDA (present in all formulations) to act as an adjuvant in the delivery of antigen is the immediate electrostatic interaction with the cell surface, followed by induction of active uptake (Smith Korsholm et al 2007). This observation implicates the loss of DDA molecules from the 25 % PEG formulation, thus leading to inefficient antigen uptake and lack of immunological effect. For the DRV based formulation, significantly higher levels of IFN- γ were found and this is comparable to the MLV based formulation demonstrating high levels of cell-mediated immunity with the addition of PEG having no effect. With the DDA:TDB DRV based formulation, a significantly higher level of IL-2 was produced compared to the pegylated formulations suggesting that the formulations containing PEG perhaps stimulate a Th₂ type immune response. This was confirmed from the IL-5 cytokine results, where a significantly higher level of this cytokine was produced for the 10 % and 25 % PEG formulations. For the SUV based formulations, a similar trend was found with the pegylated formulations having a higher level of IL-5.

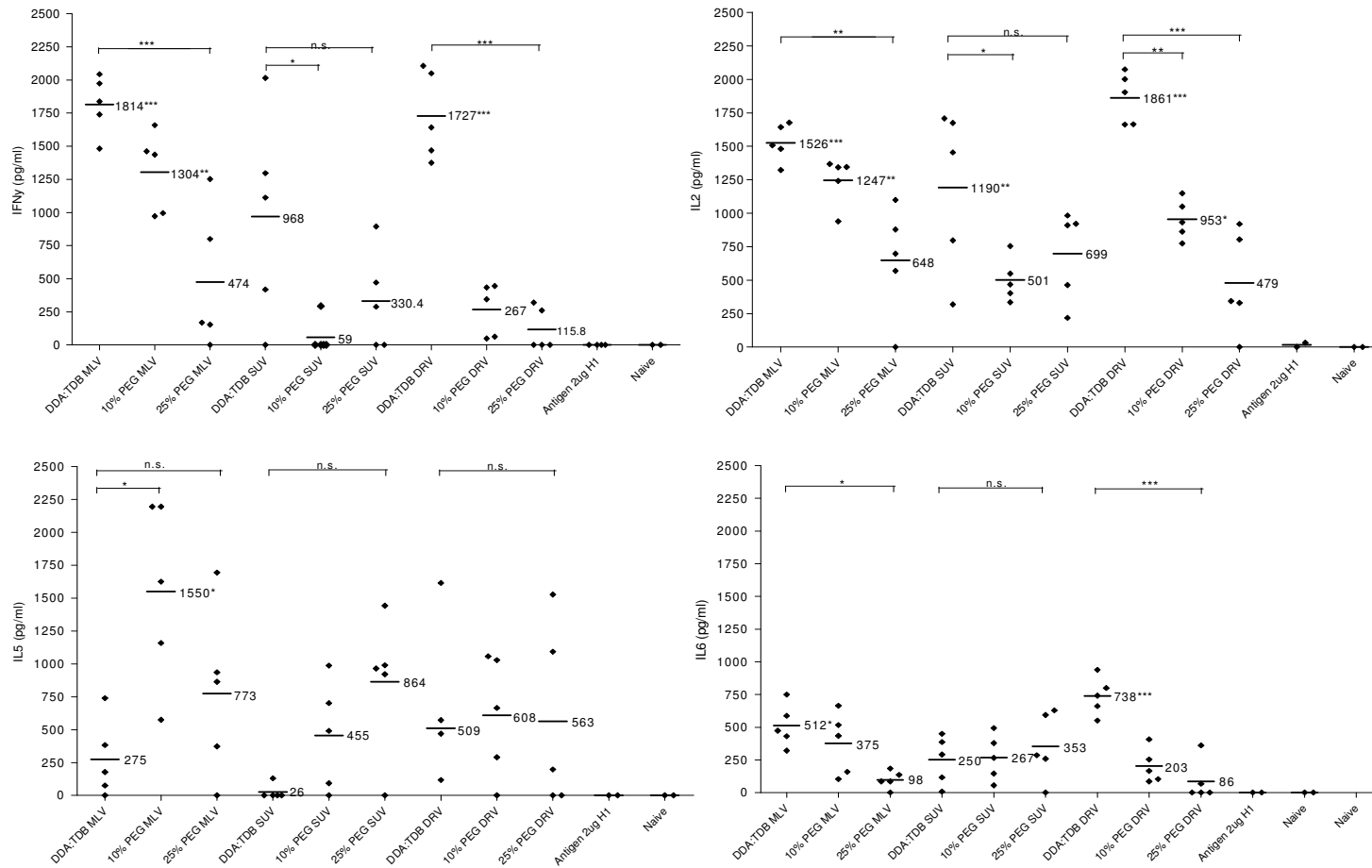


Figure 4.26 Ag85B-ESAT-6 specific cytokine production. Cytokines were detected using DuoSet[®] capture ELISA kits (mouse IFN-γ (A), IL-2 (B), IL-5 (C), IL-6 (D)) purchased from R&D systems, Abingdon, UK, according to the manufacturers instructions. Filled diamonds represent the mean of three measurements for each individual spleen. Horizontal lines represent average group values (n = 5) and are shown numerically on the chart. ** denotes significantly increased levels in comparison to naïve controls (n=5, $p < 0.01$) *** denotes significantly increased levels in comparison to naïve controls (n=5, $p < 0.001$) n.s. denotes no statistical difference between groups (n=5, $p > 0.05$).

4.4.9.3 Cell proliferation

Following on from the cytokine work, each formulation was also investigated for its ability to initiate antigen specific spleen cell proliferation (Figure 4.27) In comparison to the DDA:TDB MLV formulation (the previously studied system; Davidsen et al 2005), a significant ($p < 0.01$) increase in cell proliferation was found with the 10 % PEG formulation. The 25 % PEG MLV, SUV and DRV reduced cell proliferation compared to their non-pegylated counterparts, however this was not significant ($p > 0.05$). The cytokine results taken in conjunction with the cell proliferation results seem to indicate that the increased cell proliferation for the 10 % PEG formulation may be due to B cell proliferation, since IFN- γ was increased for DDA:TDB, and IL-5 was increased for 10 % PEG. It is likely that PEG formulations stimulate a Th₂ type immune response and this increase in cell proliferation is due to B cell proliferation since an antibody mediated immune response is mediated by B-cells. From the biodistribution studies (Figures 4.21 and 4.22), it was found that 25 % PEG formulations, regardless of the method of preparation, did not form a depot at the site of injection.

It is likely that a vaccine formulation that is able to get circulate around the body would be able to stimulate a strong antibody mediated response such as the pegylated formulation, whereas one that forms a depot could likely aid a cell mediated response such as the DDA:TDB formulation. In an antibody mediated response, antibody is produced primarily in order to neutralise disease threats such as tetanus and diphtheria toxins, or free virus likely to infect host cells. Conversely, the cell mediated side acts against infected cells that are (generally) restricted in their ability to migrate, that are

present within tissues, and dealt with more effectively by a cell mediated type response that will isolate and destroy infected cells. Any adjuvants / co-adjuvants will also have an input on the type of response. This therefore might not be as straightforward, and the antibody and cell mediated responses will have significant overlap in any case. Furthermore, there have been studies that have found that hydrophilic surfaces, such as those of pluronic-coated nanoparticles, activate the alternative pathway rather than the classical pathway of the complement cascade (Reddy et al 2007). The authors have suggested that the activation of the alternative pathway may be due to the OH groups on the polyhydroxylated nanoparticles binding to the exposed thioester of C3b to activate complement by the alternative pathway.

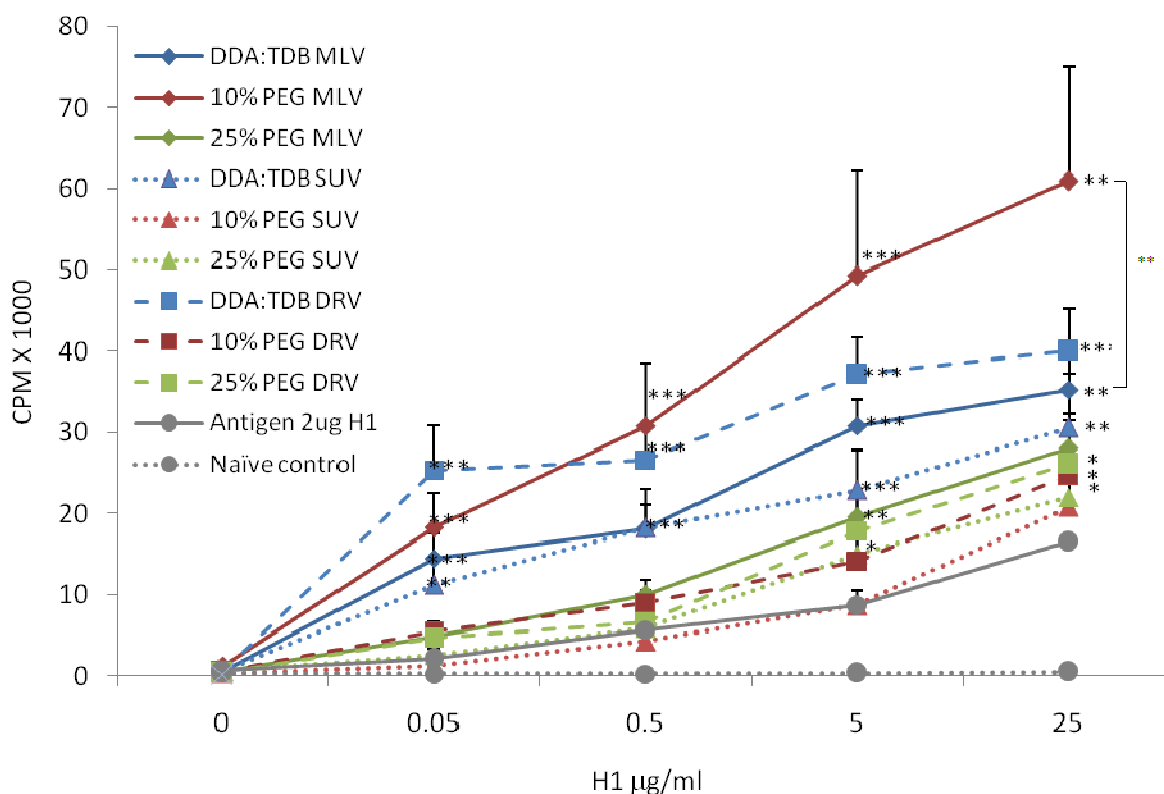


Figure 4.27 Spleen cell proliferation in response to stimulation/re-stimulation with Ag85B-ESAT-6 antigen. Cell proliferation was measured by incorporation of ^3H into cultured splenocytes. * denotes significantly increased levels in comparison to naïve controls ($n=5$, $p<0.05$), ** denotes significantly increased proliferation in comparison to naïve controls ($n=5$, $p<0.01$). *** denotes significantly increased proliferation in comparison to naïve controls ($n=5$ $p<0.001$).

4.5 Conclusion

PEG is the most widely used hydrophilic polymer for the steric stabilisation of liposome drug delivery systems. The aim of this study was to see whether by sterically stabilising DDA:TDB with PEG reduces aggregation and whether it has an influence on the biodistribution, adjuvant properties and the formation of a depot at the site of injection. Table 4.6 summarises the results of this chapter. From the initial characterisation studies, it was found that incorporating increasing amount of PEG 5 %, 10 % and 25 % resulted in a decrease in vesicle size due to PEG in the formulation influencing the lipid packaging within the systems and/or reducing the number of bilayers which would subsequently reduce the vesicle size. A reduction in zeta potential was found due to the hydrophilic chains of the PEG extending out from the surface of the liposomes therefore masking the cationic charge of the DDA. In terms of antigen loading, the addition of PEG to the liposomes was found to limit electrostatic interactions, thereby reducing binding and resulting in increased loss of antigen over time. From the biodistribution studies, it was found that higher levels of PEG i.e. 25 %, was able to significantly inhibit the formation of a liposome depot at the injection site. PEG also severely limited the retention of antigen at the site, thus resulting in a faster drainage of the liposomes from the site of injection. This was reflected by the immunisation study where lower levels of IgG2b antibody, IFN- γ and IL-2 was found compared to the DDA:TDB formulation and a higher level of IL-5 cytokine suggested that the pegylated formulations stimulate a Th₂ type immune response.

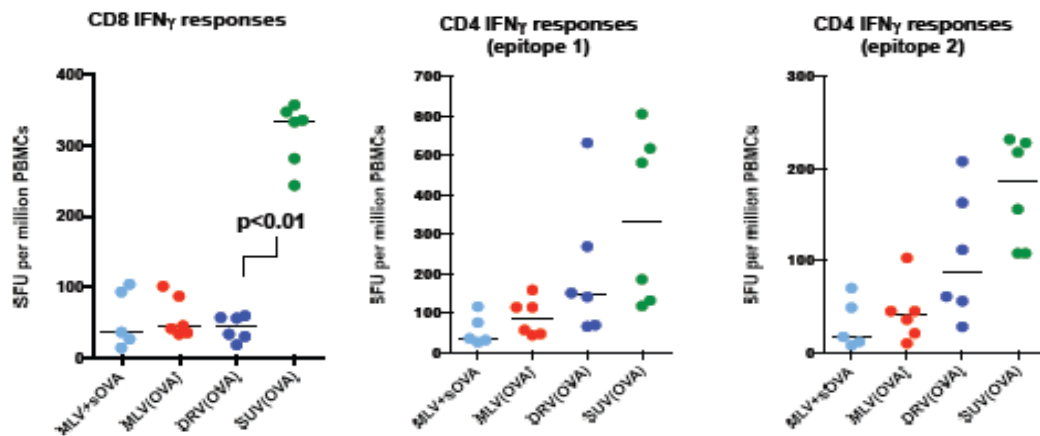
Table 4.6 Summary table of the effect of PEG, on a number of characteristics.

Characteristics	Effect of PEGylation	Effect of vesicle size	Effect of antigen entrapment within DRV
Particle size	Increasing PEG, reduced vesicle size	MLV \approx DRV \approx SUV	Particle size increased with increasing amount of antigen entrapment
Particle zeta potential	Increasing PEG, reduced vesicle zeta-potential	MLV \approx DRV \approx SUV	Zeta-potential reduced with increasing amount of antigen entrapment
Antigen Loading	Increasing PEG, reduced antigen loading	MLV \approx DRV $>$ SUV	Increasing antigen loading reduced antigen entrapment
Biodistribution	High PEG concentration reduced antigen and liposome retention at the SOI	MLV \approx DRV $>$ SUV	Similar biodistribution profile found to that of MLV liposomes
Antibody responses	Increasing PEG resulted in higher levels of IgG and IgG1 and lower levels of IgG2b	MLV \approx DRV \approx SUV	No effect
Cytokine responses	Increasing PEG reduced IFN- γ and IL-2 but increased IL-5 levels	MLV \approx DRV $>$ SUV	No effect
Cell proliferation	Increasing PEG resulted in a B-cell proliferation	MLV \approx DRV \approx SUV	No effect

Chapter 5

Incorporation of immunostimulatory components to the DDA:TDB adjuvant delivery system

Graphical Abstract:



Small unilamellar vesicles (SUVs) are more potent at inducing anti-OVA T-cell responses than multilamellar vesicles (MLVs) whereas incorporating OVA within the liposomal vesicle has no effect on CD8⁺ T-cell IFN- γ spleen responses and a small non-significant effect on CD4⁺ IFN- γ responses.

5.1 Introduction

The immune system is divided into two parts, innate immunity and adaptive immunity. B and T lymphocytes are the key players of the adaptive immune system and recognise pathogens through high affinity receptors. Activation of the adaptive immune system is delayed, and thus in order to eradicate microorganisms the rapidly responding innate immune system plays a major role in host defense during the early stages of infection (Werling & Jungi 2003). To initiate an innate immune response, pathogens exhibit conserved molecular patterns that are recognised by germline-encoded receptors, namely the toll-like receptor (TLR) family (Werling & Jungi 2003; Kaisho & Akira 2002).

5.1.1 Toll-like receptors (TLR)

TLRs are pattern recognition receptors present on diverse cell types that recognise specific molecular patterns present in pathogens like bacteria, virus or fungi (Takeda et al 2003). There are currently 10 TLRs in the human gene database which are mainly transmembrane proteins with an extracellular domain having leucine rich repeats (LRR) and a cytosolic domain called the Toll/IL-1 receptor (TIR) domain (Lahiria et al 2008). The ligands for these receptors are highly conserved microbial molecule like lipopolysaccharides (LPS) (recognised by TLR 4), lipopeptides (recognised by TLR 2 in combination with TLR 1 or TLR 6), flagellin (by TLR 5), single or double stranded (ds) RNA (by TLR 7 with TLR 8 and by TLR 3 respectively), and CpG motif containing DNA (recognised by TLR 9) (Lahiria et al 2008). The activation of TLRs by their cognate ligands leads to production of inflammatory cytokines, up-regulation of MHC molecules and co-stimulatory signals. This links innate recognition with adaptive immune responses namely T and B cell activation and memory response after the host encounters any

pathogen (Akira & Takeda 2004). Thus, this profound property of TLRs to link innate and adaptive immunity can be used extensively by adding microbial components in experimental vaccines to evoke robust and durable immune response (Iwasaki & Medzhitov 2004; van Duin et al 2006). The various TLR agonists that are being used as adjuvants are listed in Table 5.1. However, a weakness of many vaccine adjuvants is the limited induction of CD8⁺ T-cell responses against protein antigens. Using CD8-inducing Toll-like receptor 3 and 9 agonists in vaccine adjuvants might overcome this limitation. Here we are interested in the versatility of cationic liposomes based on DDA:TDB in combination with different immunostimulatory ligands, including polyinosinic-polycytidylic acid (poly(I:C), TLR 3 ligand), and CpG (TLR 9 ligand) in combination with DDA:TDB using ovalbumin (OVA) protein as a model antigen.

5.1.1.1 Poly(I:C) - TLR 3 agonist

TLR 3 recognises viral double-stranded RNA and thus is important in antiviral responses. Poly(I:C) is the synthetic analogue of dsRNA and although this was used in a phase I and II trial in the treatment of leukemia patients, its toxicity resulted in withdrawal from the market (Robinson et al 1976). The TLR 3 signaling pathway has therefore been studied extensively to make a better adjuvant in order to control the toxicity exerted by poly(I:C) (Salem et al 2006; Asahi-Ozaki et al 2006; Lahiria et al 2008). A study by Asahi-Ozaki et al (2006) reported that that co-administration of vaccine prepared from recombinant a virulent avian influenza virus with both poly(I:C) and chitin microparticles (CMP) as mucosal adjuvants elicits protective immunity against highly pathogenic influenza virus H5N1 infection. Unfortunately, the use of poly(I:C) has been associated with side effects as a result of the induction of pro-inflammatory cytokines (Lahiria et al 2008).

Table 5.1 Adjuvants and their corresponding TLR receptors.

TLR	Adjuvants
TLR 1 + TLR 2	Pam3Cys MALP2
TLR 2 + TLR 6	Pam3Cys
TLR 2	BCG peptidoglycan
TLR 3	Poly(I:C) Poly (I):poly (C ₁₂ U)
TLR 4	MPL A E6020 BCG peptidoglycan LPS analogues Aminoalkyl glucosaminide phosphates
TLR 5	Flagellin
TLR 7/8	Resiquimod Imiquimod 3M-019 R-848 3M compound 008
TLR 9	CpG

5.1.1.2 Unmethylated CpG DNA - TLR 9 agonist

TLR 9 is located on the inner endosomal membrane and recognises CpG DNA (Wagner 2004; Lahiria et al 2008). Synthetic CpG DNA has shown promising therapeutic potential in a range of pathophysiological conditions (Kreig 2006) and was further shown by Waag et al (2006) to mediate protection against lung infection or death in BALB/c mice challenged with *Burkholderia mallei*. In an experimental model of murine toxoplasmosis (a parasitic disease caused by the protozoan *Toxoplasma gondii*), CpG DNA improved the immune response resulting in increased survival and a decrease in parasite burden in the central nervous system (CNS) of mice after weeks (Zimmermann et a 2008). A number of studies however argue the conjugation of CpG to plasmid protein antigens or

formulations with delivery systems maximises the adjuvant effect of CpG (Singh et al 2001).

5.2 Aims and objectives

The aim of the study was to evaluate the adjuvanting capacity of cationic liposomes based on DDA:TDB in combination with immunostimulatory ligands, including TLR ligands. Polyinosinic-polycytidylic acid, poly(I:C) TLR 3 ligand), and CpG (TLR 9 ligand) were evaluated in combination with DDA:TDB.

The objectives of the study were:

- To evaluate how incorporation of immunostimulatory components affect the physico-chemical properties of the liposomes. Several modification of the DDA:TDB liposomes, including size either as multilamellar vesicles (MLV), small unilamellar vesicles (SUV), antigen association and addition of TLR agonist either entrapped within the vesicles or adsorbed onto the liposome surface was investigated for immunogenic capacity as vaccine adjuvants.
- To identify a formulation with the ability to induce cell-mediated responses, characterised by IFN- γ cytokine production by CD8⁺ T-cells.

5.3 Materials and Methods

5.3.1 Materials

Chemicals	Supplier
Acetic acid	Fisher Scientific (Leicestershire, UK)
Bicinchoninic acid (BCA)	Sigma-Aldrich, Poole, Dorset, UK
Chloroform (HPLC grade)	Fisher Scientific (Leicestershire, UK)
Coomasie (Brilliant Blue)	Sigma-Aldrich, Poole, Dorset, UK
CpG-ODN type C	Invivogen, San Diego, USA
DuoSet [®] capture ELISA	R&D systems, UK
ELISA plates (flat bottom, high binding)	Greiner Bio-One Ltd, UK
Foetal bovine serum (Heat-Inactivated)	Invitrogen, Paisley, UK
Horseradish peroxidase-conjugated goat anti-mouse immunoglobulin IgG, subclasses	AbD serotec, Oxford, UK
I ¹²⁵ (NaI in NaOH solution)	Perkin Elmer (Waltham, MA)
ODO-GEN [®] pre-coated iodination tubes	Pierce Biotechnology (Rockford, IL)
Methanol (HPLC grade)	Fisher Scientific (Leicestershire, UK)
OliGreen quantification reagent	Molecular Probes-Invitrogen, UK
Ovalbumin (OVA)	Sigma-Aldrich, Poole, Dorset, UK
Poly(I:C) synthetic analog of dsRNA	Invivogen, San Diego, USA
Protein molecular weight standard	Sigma-Aldrich, Poole, Dorset, UK
SDS-PAGE 12 % Tris-Glycine gels	Sigma-Aldrich, Poole, Dorset, UK
Sephadex G-75	Sigma-Aldrich, Poole, Dorset, UK
Tris-base	IDN Biomedical, Inc (Aurora, Ohio)

Trypsin	Sigma-Aldrich, Poole, Dorset, UK
Lipids	Supplier
Trehalose 6,6'-dibehenate (TDB)	Avanti Polar Lipids, Inc. (Alabaster, AL)
Dimethyldioctadecylammonium bromide (DDA)	Avanti Polar Lipids, Inc. (Alabaster, AL)

5.3.2 Methods

5.3.2.1 Lipid hydration method

MLV were prepared using the previously described lipid-film hydration method (Bangham et al 1965) (Figure 4.4). Briefly, weighed amounts of DDA and TDB were dissolved in chloroform/methanol (9:1 by volume) and the organic solvent was removed by rotary evaporation followed by flushing with N₂ to form a thin lipid film on the bottom of a round-bottom flask. The lipid film was hydrated in 10 mM Tris-buffer at pH 7.4 by heating for 20 minutes at 60 °C. In all formulations the final OVA concentration in a 50 µl dose was 20 µg, and the final concentration of DDA and TDB was 250 µg and 50 µg, CpG was at 20 µg/dose and poly(I:C) at 50 µg/dose.

5.3.2.2 Small unilamellar vesicles

To generate SUV, the MLV produced in section 5.3.2.1 were disrupted using sonic energy to fracture large liposomes into smaller structures (< 100 nm). In this instance, a probe sonicator (Soniprep 150) was used to produce SUV. The tip of the sonicator probe

was placed onto the liposome surface of the MLV mixture. The milky MLV suspension transforms into a clear SUV suspension.

5.3.2.3 Dehydration-rehydration method

For the preparation of DRV, the MLV prepared according to the lipid hydration method outlined above was sonicated to produce SUV were mixed in the presence and absence of OVA, CpG and poly(I:C), frozen at -70 °C and freeze dried overnight (-40 °C, vacuum to 40 mbar). Controlled rehydration of the dried powder led to the formation of antigen containing DRV. Controlled rehydration was achieved by addition of 10 % of the final volume, which was standardised at 1 ml. Therefore 100 µl was added initially to these formulations, which were vortexed and left at room temperature for 30 minutes. A further 100 µl was added and formulations again incubated for 30 minutes at room temperature and subsequently made up to 1 ml. DRV preparations were then centrifuged twice at 125,000 ×g for 20 minutes to remove non-entrapped antigen and/or components and resuspended in distilled water, to the appropriate volume.

5.3.2.4 Determination of vesicle size and zeta potential

The vesicle size and zeta-potential was determined using the photon correlation spectroscopy (PCS) technique. The measurements were performed at 25 °C using a ZetaPlus (Brookhaven Instrument Corporation, USA). Polystyrene size standards 220 ± 6 nm (Duke scientific corp, Duke, NC) was used as a control. The samples were diluted with 10 mM Tris-buffer at pH 7.4 to achieve the optimal vesicle concentration.

5.3.2.5 Trypsination experiment

Cationic formulations were mixed with OVA (100 µg/ml) and ultra-centrifuged twice at 125,000 ×g, for sixty minutes at room temperature in order to pellet the liposomes. Supernatant was then removed and pellets were re-suspended back into their original volume, using the corresponding buffer solution. The protein and liposome were incubated in trypsin at 0 µg/ml, 100 µg/ml, 200 µg/ml and 400 µg/ml for 2 hours at 37 °C (this would remove any adsorbed protein) and then after this treatment, the formulations were ultra-centrifuged at 125,000 ×g, for 60 minutes at room temperature. Supernatant was then removed and pellets were re-suspended back. Upon heating at 90 °C for 3 minutes, 10 µl samples of pellet and supernatant from each of the formulations were analysed via SDS-PAGE for semi-quantification of the protein concentrations present. For the radiolabelled experiments, OVA was radiolabelled with I¹²⁵ and the procedure above was repeated but rather than carrying out SDS page, I¹²⁵ activity was measured.

5.3.2.6 OVA antigen adsorption / entrapment to cationic liposomes

To assess the degree of antigen adsorption, I¹²⁵-labeled OVA was added to the liposomes and left for 1 hour with intermittent shaking. For antigen entrapment, I¹²⁵-labeled OVA was added to the SUV liposomes, frozen at -70 °C and freeze dried overnight (-40 °C, vacuum to 40 mbar). Controlled rehydration of the dried powder led to the formation of OVA containing dehydration-rehydration vesicles (DRV). Formulations were centrifuged (125,000 ×g, 4 °C, 1 hour), resuspended in Tris buffer and centrifuged again to ensure removal of all non-bound OVA. The I¹²⁵ recovery in the pooled supernatant after two washes (unbound antigen) and the pellet (bound antigen) was measured. The percentage

of OVA adsorbed and entrapped was calculated as a percentage of the total radioactivity recovered from both supernatant and pellet.

$$\frac{\text{Radioactivity of washed sample}}{\text{Radioactivity of unwashed sample}} \times 100\%$$

To ensure reliability of entrapment values, the total recovery of protein antigen was also calculated using the following equation (including any dilutions)

$$\frac{\text{Radioactivity of washed sample} + \text{Radioactivity of supernatant}}{\text{Radioactivity of unwashed sample}} \times 100\%$$

5.3.2.7 OVA antigen retention in simulated *in vivo* conditions

Antigen release from liposomes stored in simulated *in vivo* conditions was determined using liposomes adsorbing and entrapping I^{125} -labelled OVA. Aliquots of each formulation were diluted (1:5) using 50 % FCS in Tris buffer and incubated in a shaking water bath at 37 °C for 96 hours. At time intervals, samples were centrifuged twice and OVA release was calculated as a percentage of the recovered radioactivity.

5.3.2.8 Oligreen assay

Quantification of the CpG content was determined according to the manufacturer's instructions. Briefly, aliquots of encapsulated oligonucleotide were diluted in TE assay buffer (10 mM Tris-HCl, 1 mM EDTA, pH 7.5). A 10 µl aliquot of the diluted sample was added to 100 µL of a 1:200 dilution of Oligreen™ reagent. An oligonucleotide standard curve was prepared using the 2 µg/ml oligonucleotide stock solution. Fluorescence of the OLIGREEN™-antisense complex was measured using excitation and

emission wavelengths of 485 nm and 520 nm, respectively. Surface associated antisense was determined by comparing the fluorescence measurements in the absence and presence of detergent.

5.3.2.9 Immunisation studies

C57BL/6 mice (6 mice per group) were injected with the liposomal formulations into the tibial muscle (25 μ l per leg) in a triple homologous vaccination regimen, with 2 week intervals between immunisations. Tail bleeds for serum samples were performed at indicated time-points (days 14, 28, 42, 70 and 128). Spleens were removed at the sacrifice time-point and used for measuring IFN- γ production by ELISpot.

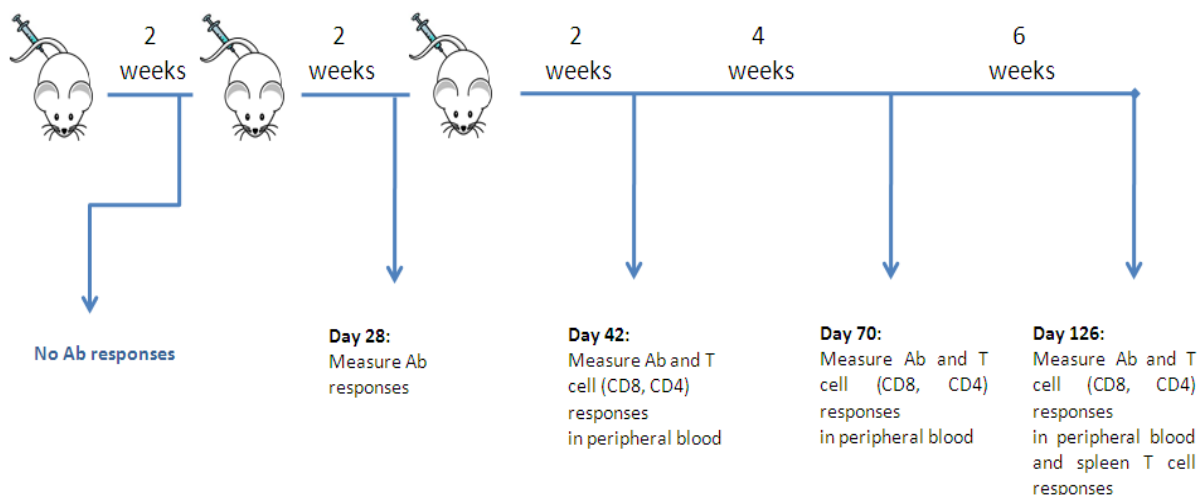


Figure 5.1 Immunisation study timeline. C57BL/6 mice (6 mice per group) were injected with the liposomal formulations into the tibial muscle (25 μ l per leg) in a triple homologous vaccination regimen, with 2 week intervals between immunisations. Tail bleeds for serum samples were performed at indicated time-points (days 14, 28, 42, 70 and 128). Spleens were removed at the sacrifice time-point and used for measuring IFN- γ production by ELISpot.

5.3.2.10 Analysis of anti-OVA antibody production following vaccination with the liposomal formulations

Total IgG antibodies against whole OVA protein were measured in a standard end-point titre ELISA. Briefly, immunosorbent plates were coated with OVA protein 2 µg/ml in PBS. Mouse sera were diluted to 1:100, added in duplicate wells, and serially diluted in threefold steps. Absorbance at 405 nm was measured using a microplate reader (BioTek, UK). The endpoint titers were taken as the x axis intercept of the dilution curve at an absorbance value three standard deviations greater than the optical density at 405 nm for naïve mouse sera.

5.3.2.11 Spleen ELISpot assay

IFN- γ production in total mouse splenocytes was measured using *ex vivo* IFN- γ ELISpot, using coating and detecting antibodies from Mabtech. Splenocytes were isolated from immunised C57/BL6 mice and restimulated overnight with peptides corresponding to two CD4⁺ and one CD8⁺ OVA epitopes at 1 µM final concentration. Plates were developed and analysed using AID ELISpot (AID Diagnostika GmbH) reader system and software.

5.3.2.12 Statistical analyses

For all experiments, means and standard deviations were calculated. To determine statistical significance the one way analysis of variance (ANOVA) was performed on all data, with the statistical significance determined to 0.05 confidence intervals ($p < 0.05$). Tukey's post hoc test was conducted to determine which conditions differ significantly from each other.

5.4 Results and discussion

5.4.1 Quantification of entrapped protein

To determine the fraction of liposome-bound OVA exposed on the outer liposomal membrane, the DDA:TDB with OVA both surface adsorbed and entrapped was incubated in a solution of the proteolytic enzyme trypsin. Trypsin does not pass through the liposomal bilayer and, therefore, the encapsulated protein is protected from enzymatic digestion. Briefly, the liposomal OVA formulation was incubated in 0, 100, 200 and 400 $\mu\text{g/ml}$ trypsin. After 2 hours of incubation at 37 $^{\circ}\text{C}$, samples were centrifuged to remove adsorbed protein. The fraction of remaining entrapped OVA, protected from enzymatic digestion, was determined by SDS page and confirmed by radiolabelled work. The results of the SDS page are shown in Figure 5.2.

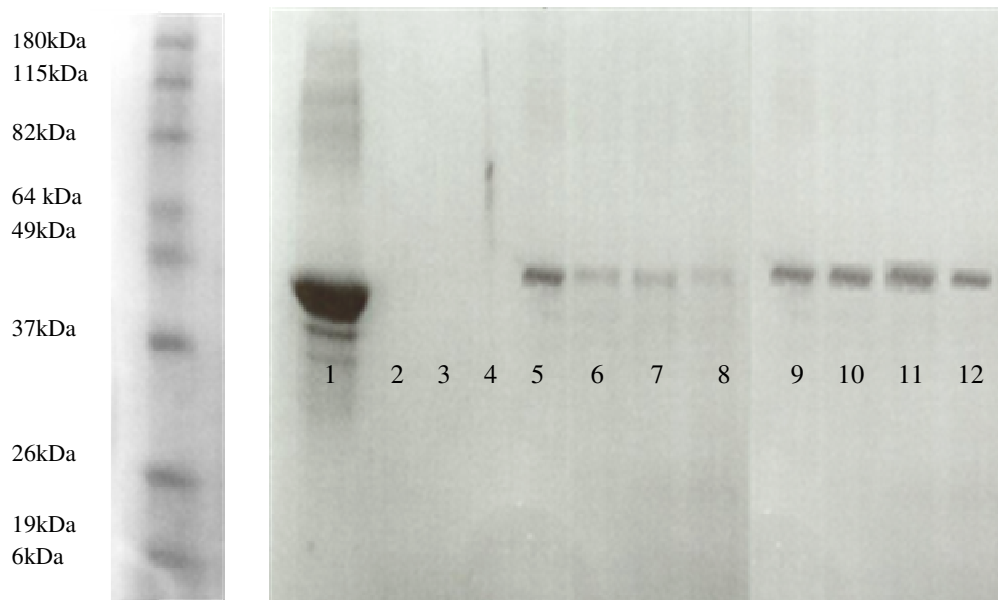


Figure 5.2 SDS page of DDA:TDB MLV and DRV liposomes exposed to trypsin at (0, 100, 200 and 400 $\mu\text{g/ml}$). Lane 1 - OVA no trypsin, lane 2 - OVA 100 $\mu\text{g/ml}$ trypsin, lane 3 - OVA 200 $\mu\text{g/ml}$ trypsin, lane 4 - OVA 400 $\mu\text{g/ml}$ trypsin, lane 5 - DDA:TDB MLV no trypsin, lane 6 - DDA:TDB MLV 100 $\mu\text{g/ml}$ trypsin, lane 7 - DDA:TDB MLV 200 $\mu\text{g/ml}$ trypsin, lane 8 - DDA:TDB MLV 400 $\mu\text{g/ml}$ trypsin, lane 9 - DDA:TDB DRV no trypsin, lane 10 - DDA:TDB DRV 100 $\mu\text{g/ml}$ trypsin, lane 11 - DDA:TDB DRV 200 $\mu\text{g/ml}$ trypsin, lane 12 - DDA:TDB DRV 400 $\mu\text{g/ml}$ trypsin.

From the SDS page results in lane 1, which is the non-trypsin exposed OVA control, a very strong band could be seen, whereas lanes 2, 3 and 4 which are trypsin exposed samples no bands suggesting that trypsin has digested the protein. Whereas for the liposomal formulations, firstly the DDA:TDB MLV formulation so this is where the protein is adsorbed to the surface of the liposome it can be seen that lane 5 the non-trypsin exposed sample strong band whereas with increasing concentration of trypsin in lanes 6, 7 and 8 the bands become lighter suggesting trypsin digestion with increasing concentration. Trypsin degrades proteins by cleaving lysyl and arginyl bonds. Lanes 9, 10, 11 and 12 are the DRV based formulations, so this is where the protein is entrapped and it is found that at all concentrations of trypsin the bands are the same. This suggests that the protein is in fact entrapped within the lipid bilayer and not surface adsorbed. A study by van Slooten et al (2001) investigated the fraction of surface-exposed human interferon gamma (hIFN- γ) present on the external surface of the liposomes. The authors used a similar trypsination experiment. The authors found that liposome-entrapped hIFN- γ molecules, which are not exposed on the liposome surface, were protected from enzymatic degradation, as the enzyme is unable to cross bilayers.

To confirm the results of the SDS page, the above experiment was repeated with I^{125} OVA and the activity of OVA adsorbed to the liposomes or entrapped within the lipid bilayers was measured. Figure 5.3A shows DDA:TDB MLV liposomes with OVA adsorbed to the surface. It can be seen that the non trypsin exposed sample had an initial adsorption of OVA around 65%, but with increasing concentration of trypsin there is less protein adsorbed to the surface. Figure 5.3B, shows DDA:TDB DRV liposomes with OVA entrapped within the lipid bilayers. Similar to the results of the SDS page, at all

concentrations of trypsin, the percentage of OVA entrapped is the same around 65 to 70% suggesting protein is entrapped within the liposomes and not surface adsorbed.

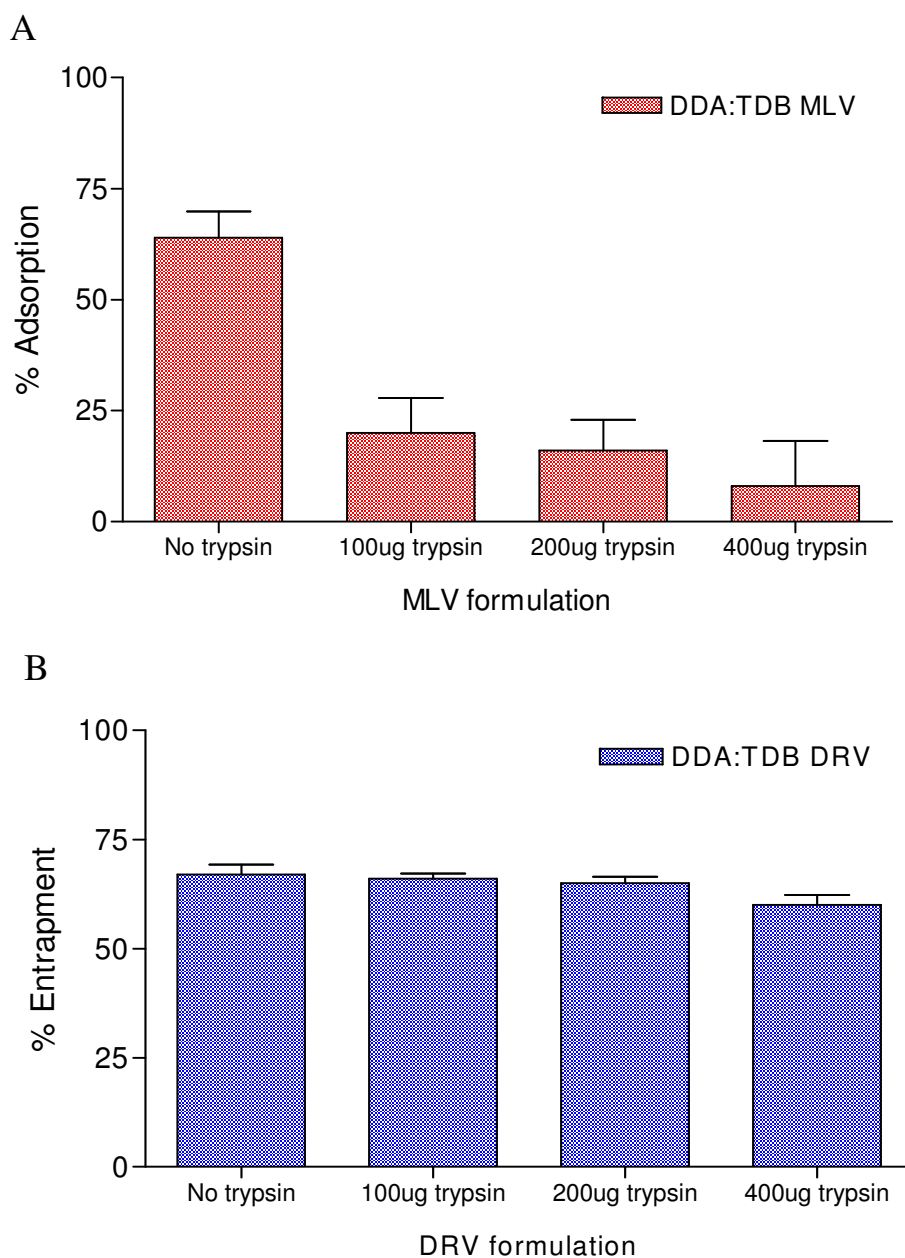


Figure 5.3 Percentage (%) of OVA (A) adsorption and (B) entrapment following exposure to trypsin. Results represent mean \pm SD of triplicate experiments.

5.4.2 Incorporation of immunostimulating compounds

5.4.2.1 Multilamellar vesicles (MLV)

Incorporation of certain immunostimulating compounds into DDA:TDB liposomes may affect the immunological properties, as well as the physico-chemical properties, of the adjuvant formulation. We have looked at the characterisation of the physico-chemical properties since this is important for issues such as formulation with antigen and stability. Incorporation of immunostimulatory components was found to affect the particle size and surface charge of MLV based liposomes (Figure 5.4A). Empty DDA:TDB liposomes were found to be 572.6 ± 50.4 nm in size with a positive surface of 59.9 ± 10.5 mV. The adsorption of OVA resulted in an increase in size to 1047.1 ± 135.8 nm, whereas with the addition of CpG and poly(I:C) to the DDA:TDB OVA liposomes made no further significant difference in the size (1116.9 ± 176.0 nm). However, a significant difference ($p < 0.05$) in the zeta potential was found after the addition of the immunostimulatory components (Figure 5.4B). This drop in surface charge may be due to poly I:C being negatively charged resulting in strong electrostatic interactions between the opposite charged components and hence increase in size.

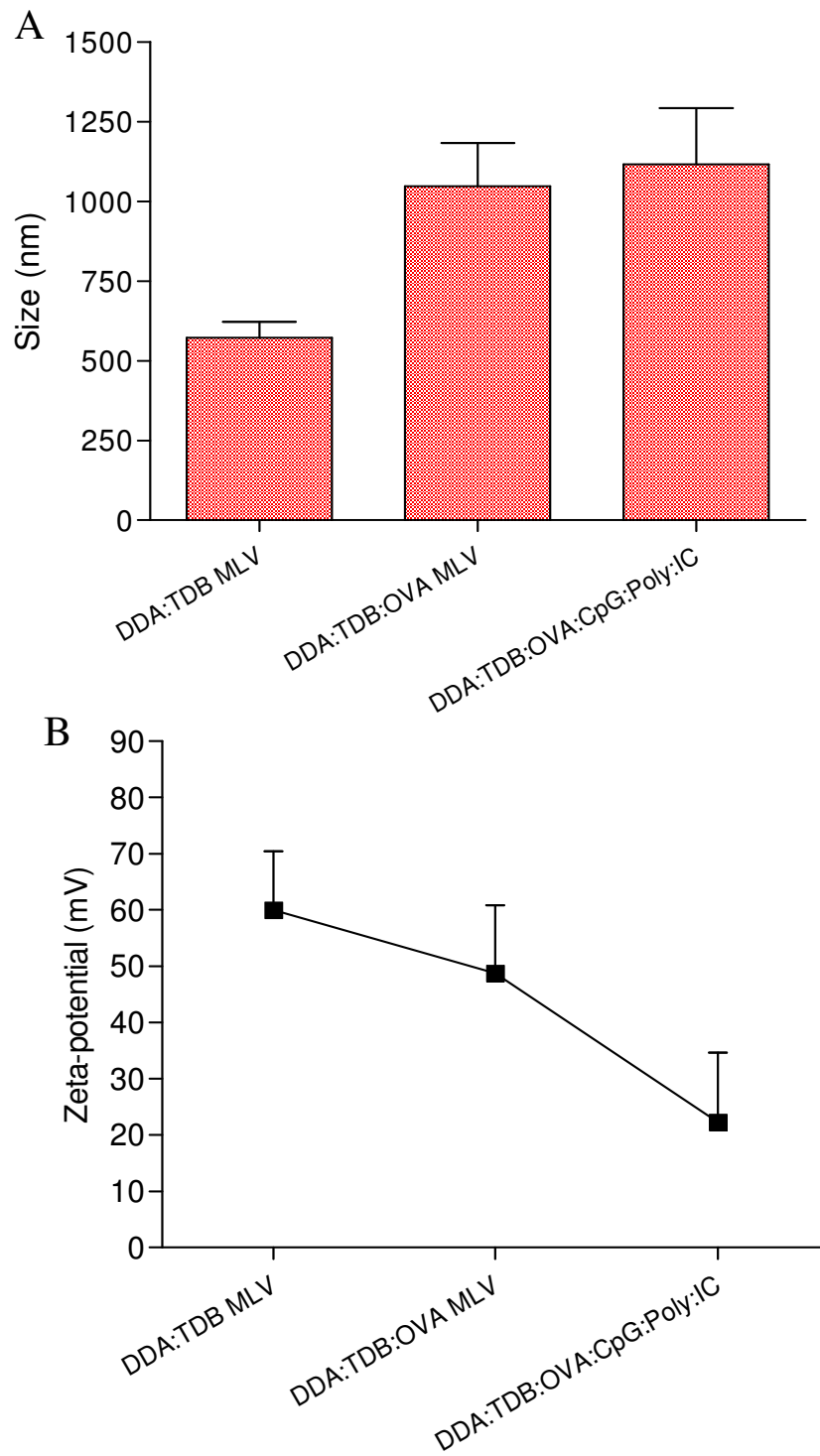


Figure 5.4 (A) Vesicle size (nm) and (B) zeta-potential (mV) of DDA:TDB MLV liposomes prepared by the lipid-hydration method with OVA and immunostimulatory components CpG and poly(I:C). Results represent mean \pm SD of triplicate experiments.

5.4.2.2 Dehydration-rehydration vesicles (DRV)

When the dehydration-rehydration method was used to incorporate the OVA within the liposomes (Figure 5.5A), the size of the liposomes was 546 ± 23.7 nm that was significantly smaller than vesicles prepared with surface complexed OVA. In contrast, with the entrapment of only CpG within the DDA:TDB DRV the size of the liposomes significantly increased to 1010 ± 235 nm and zeta potential significantly reduced to near neutral (3.4 ± 1.3 mV). This suggests a reconfiguration of the system compared to the DDA:TDB entrapping OVA. However, the addition of poly(I:C) in combination with CpG resulted in vesicles of a similar size (1101.9 ± 55.8 nm) but with a negative zeta potential (-39.9 ± 11.1 mV) (Figure 5.5B). Finally the addition of the three components OVA, CpG and poly:IC resulted in a no further significant change in zeta potential but a slight increase in size to 1399.2 ± 172.5 nm. The reversal in measured zeta potential suggests a neutralization of the cationic nature of the liposomes in the presence of the various anionic components such that they are present on the outer surfaces of the vesicles and not fully incorporated within the DRV vesicles.

5.4.2.3 Small unilamellar vesicles (SUV)

Following the sonication of MLV liposomes the addition of OVA to the SUV based liposomes resulted in an increase in size from 150 nm to 591.9 nm (Figure 5.6A) and a drop in zeta-potential from 50.1 mV to 33.9 mV (Figure 5.6B). The addition of immunostimulatory components to the DDA:TDB SUV liposomes, firstly the TLR 9 CpG and secondly CpG and poly(I:C), also resulted in an increase in size of the liposomes, to around 785.8 nm and 978.6 nm, with a drop in surface charge to around -43.9 and -50.1 mV.

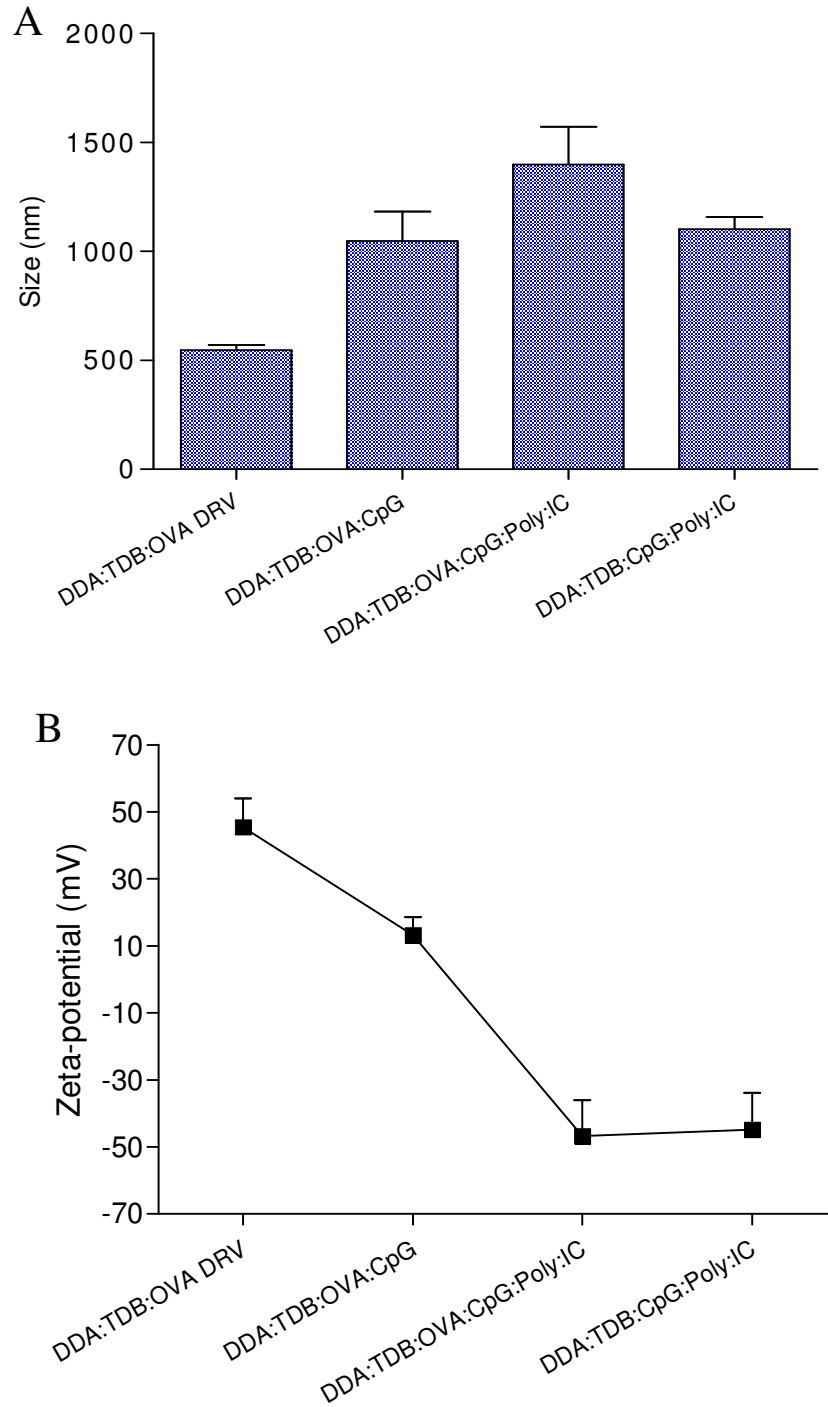


Figure 5.5 (A) Vesicle size (nm) and (B) zeta-potential (mV) of DDA:TDB DRV liposomes prepared by the dehydration-rehydration method with OVA and immunostimulatory components CpG and poly(I:C). Results represent mean \pm SD of triplicate experiments.

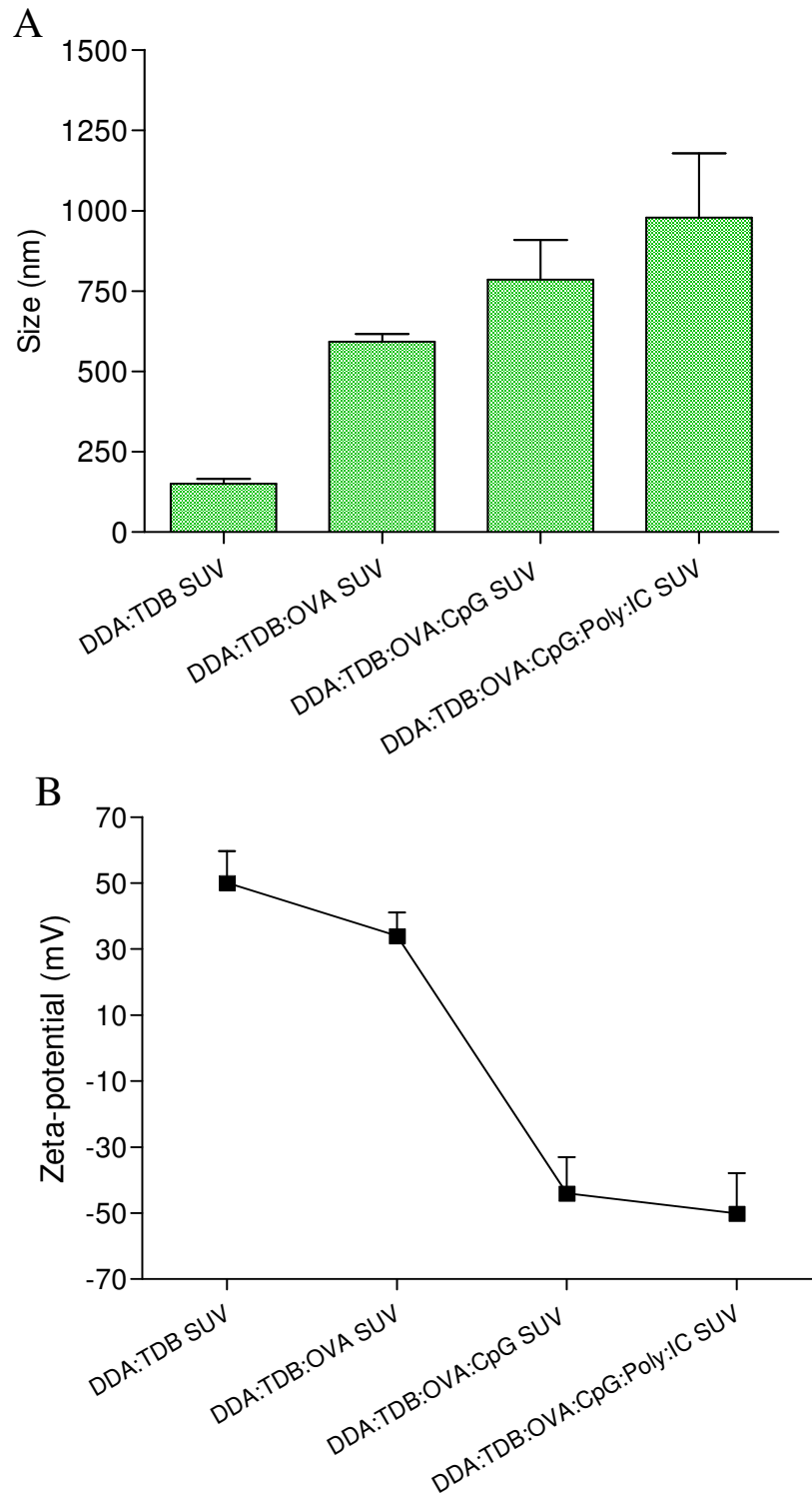


Figure 5.6 (A) Vesicle size (nm) and (B) zeta-potential (mV) of DDA:TDB SUV liposomes prepared by the lipid-hydration method with OVA and immunostimulatory components CpG and poly(I:C). Results represent mean \pm SD of triplicate experiments.

5.4.2.4 Quantification of OVA adsorption and entrapment

Figures 5.7A, B and C show OVA retention measured in simulated *in vivo* conditions i.e. in 50 % FCS in Tris buffer and compared to formulations in Tris buffer. The percentage of OVA incorporation was calculated as a percentage of the total radioactivity recovered from both supernatant and pellet in both conditions. For the MLV liposomes (Figure 5.7A), although in the tris condition a difference in release was found between the two formulations, with a greater release with the formulation containing the immunostimulatory components, in a serum condition a similar sustained release profile was found. For the SUV liposomes (Figure 5.7B), an initial burst release was found with the formulation containing poly(I:C) to around 45 % OVA retention after 96 hours of incubation, whereas DDA:TDB and DDA:TDB with CpG had similar release profiles, around 60 % antigen retention after 96 hours. Previous studies (Henriksen-Lacey et al 2010) have found that the strong repulsive charges between positively charged liposomes and negatively charged serum proteins are responsible for the slow release of antigen. However, the greater release with this formulation maybe due to the positively charged quaternary ammonium head groups of the DDA molecule binding to the negatively charged phosphate groups in the backbone of the nucleic acid structure. This results in an overall negative charge as found with the characterisation studies and the greater release compared to the other formulations. For the formulation containing the TLR 3 agonist poly(I:C), a similar result is found with the DRV based formulations (Figure 5.7C) suggesting that regardless of the nature of the liposome-antigen association, the release of 46 - 50 % after 96 hours is equal between the liposomal preparations. However, the rate of release over time varies to some extent. Protein release from the DRV (protein) liposome

formulations was slow and controlled over time. With sustained release, the DRV based formulations may act as an effective depot (Storm & Crommelin 1998) from which the protein antigen can slowly leak from the liposome and maintain therapeutic levels of antigen for presentation to APC.

5.4.2.5 Quantification of CpG using the OliGreen assay

Synthetic oligonucleotides are used in a number of different molecular biology techniques, including DNA amplification (PCR), DNA sequencing, site directed mutagenesis, and *in situ* hybridisation. These techniques require that precise concentrations of ssDNA oligonucleotide are present in the reactions. OliGreen is an intercalating cyanine dye that selectively binds to oligonucleotides within a linear detection range extending over more than four orders of magnitude with a single dye concentration. There are very low variations between signals (Singer et al 1997) and it is considered as a sensitive practical alternative to other methods such as detecting oligonucleotides on electrophoretic gels stained with ethidium bromide (Ahn et al 1996). In this case, OliGreen ssDNA quantitation reagent was used to quantify CpG adsorption and entrapment. The results are shown in Table 5.2.

Table 5.2 Quantification of CpG using the OliGreen assay.

Formulation	Incorporation of CpG		
	MLV	SUV	DRV
DDA:TDB:CpG	N/A	69 ± 9.2%	66 ± 2.9%
DDA:TDB:CpG:poly(I:C)	55 ± 6.5%	51 ± 3.0%	59 ± 6.2%

Results represent mean ± SD of triplicate experiments.

From the OliGreen results, it can be seen that the incorporation of CpG for the MLV, SUV and the DRV based liposomes was between 51 - 69 %. When CpG alone was added to DDA:TDB liposomes, a higher adsorption and entrapment was found for SUV liposomes around 69 % and for DRV liposomes around 55 %. However, following the addition of poly(I:C) less incorporation of CpG was found. It may be that poly(I:C) displaces the surface bound or entrapped CpG and therefore reduces CpG content within the liposomes. Studies by Beaudette et al (2009) also looked at the co-encapsulation of CpG DNA and antigen in acid-degradable microparticles. The authors also used an OliGreen assay as a method of quantification and found an incorporation of CpG into the particles with efficiencies of up to 60 - 70 %.

Following these initial characterisation studies, the effect of entrapping the OVA antigen within the liposomes, as opposed to adsorbing it to the liposome surface, on protein immunogenicity was evaluated.

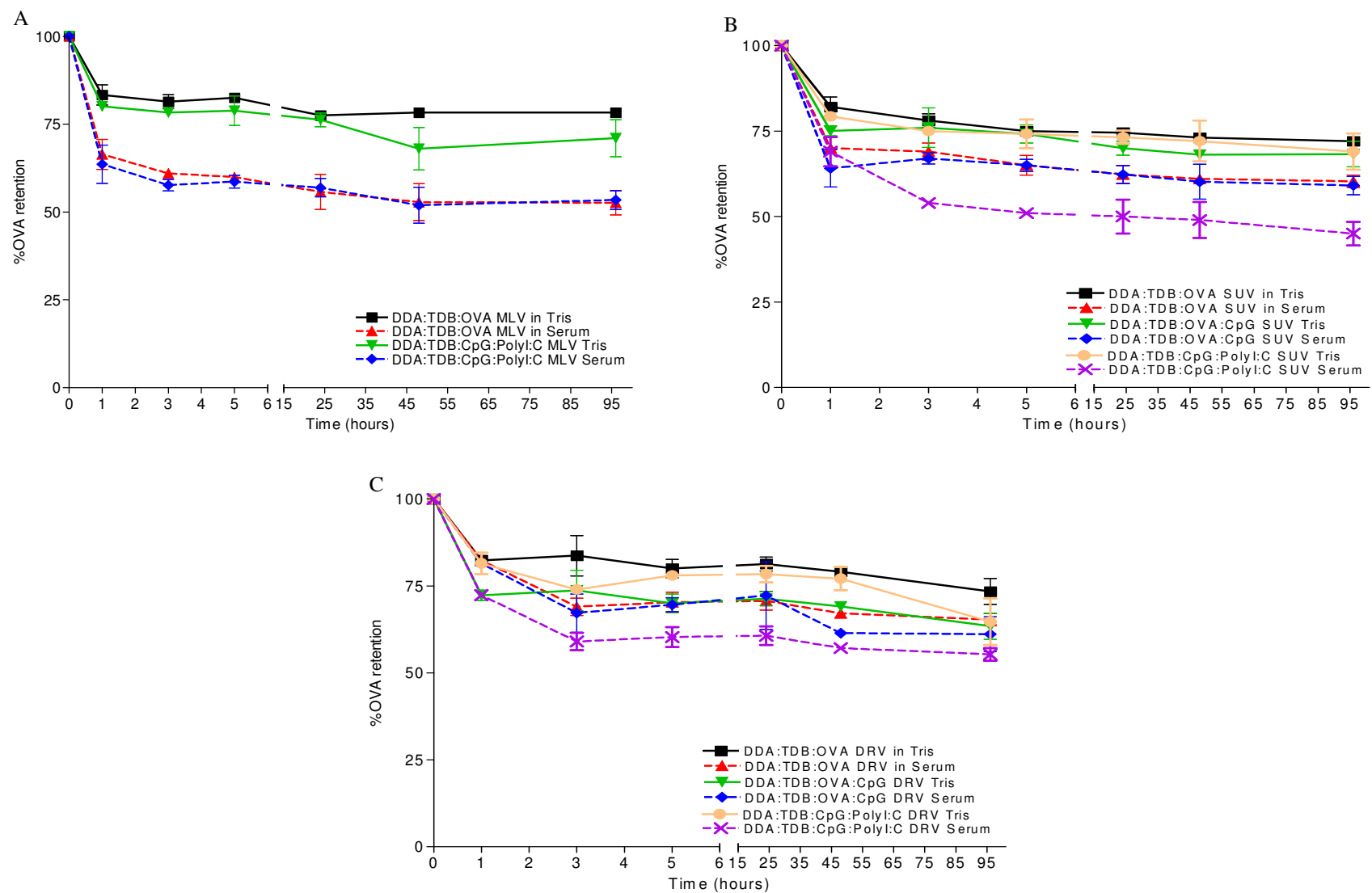


Figure 5.7 OVA retention profile. (A) MLV (B) SUV (C) and DRV liposomes which were stored in tris and under simulated *in vivo* conditions (50% FCS, 37 °C). Results represent mean \pm SD of triplicate experiments.

5.4.3 Immunisation studies

As described above, cationic DDA:TDB liposomes, prepared as either MLV, SUV and DRV were combined with OVA protein with and without the TLR agonists CpG oligonucleotide (TLR 9 ligand) and poly(I:C) (TLR 3 ligand). The aim was to identify a formulation with the ability to induce cell-mediated responses, characterised by IFN- γ cytokine production by CD8⁺ T-cells. Work described in here was done in collaboration with Dr. Anita Milicic and Professor Adrian Hill at the Jenner Institute, University of Oxford.

5.4.3.1 Antigen-specific CD8⁺ T cells in the spleen and peripheral blood

CD8⁺ T-cell responses are initiated during infection when peptide antigens are presented by dendritic cells in the lymph nodes or in the spleen if the infection is blood-borne. Following their activation, antigen-specific CD8⁺ T-cell clones undergo a process of rapid proliferation in the secondary lymphoid tissue to give rise to effector cells that migrate to the periphery to resolve the infection. Thus, the progeny of the stimulated naive CD8⁺ T cell may be engaged either in clonal expansion or in the killing of infected target cells (Bannard et al 2009). In the present work, splenocytes were isolated from immunised C57BL/6 mice and restimulated overnight with peptides corresponding to two CD4⁺ and one CD8⁺ OVA epitope at a 1 μ M final concentration. IFN- γ secretion in the spleen and peripheral blood by CD4⁺ and CD8⁺ T cells was measured using *ex vivo* IFN- γ ELISpot. As shown in Figure 5.8A, in the spleen it was found that SUV based liposomes were more potent at inducing anti-OVA CD8⁺ T-cell responses ($p < 0.01$) than MLVs, since 350 spot forming units (SFU) per million peripheral blood mononuclear cells (PBMC) were found with SUV based liposomes compared to 50 SFU per million PBMCs for the MLV

liposomes. In terms of CD4⁺ a higher level of IFN- γ was produced with the SUV based formulations, with a SFU per million PBMCs of around 200 compared to 50 and 90 with the MLV and DRV based formulations although this was not significant (Figure 5.8B and C). In terms of IFN- γ secretion in the peripheral blood (Figure 5.9), again a statistically significant increase in CD8⁺ response was found with the DDA:TDB SUV together with the TLR 9 ligand CpG ($p < 0.01$).

The results presented here suggest that liposome uptake by DCs is dependent on the size of the vesicles, with the SUV based liposomes inducing higher anti-OVA CD8⁺ T-cell responses therefore stimulating a Th₁ immune response. A study by Mann et al (2009) found that smaller vesicles (~ 250 nm) enhanced Th₂ responses whilst larger liposomes (~ 980 nm) induced high levels of IFN- γ and IgG2 antibodies characteristic of a Th₁ response. In addition, the larger liposomes also gave better protection in an influenza challenge model in ferrets (Mann et al 2009). Thus, particle size has also been shown to have a significant effect on vesicle trafficking to lymph nodes (Oussoren et al 1997), antigen uptake (Foged et al 2005) and processing by APCs (Brewer et al 2004). Furthermore, in the present work it was also found that the incorporation of OVA within the liposomal vesicle had no effect on CD8 T-cell IFN- γ spleen and peripheral blood responses as no significant difference ($p > 0.05$) was found between the MLV and DRV formulations (Figure 5.9).

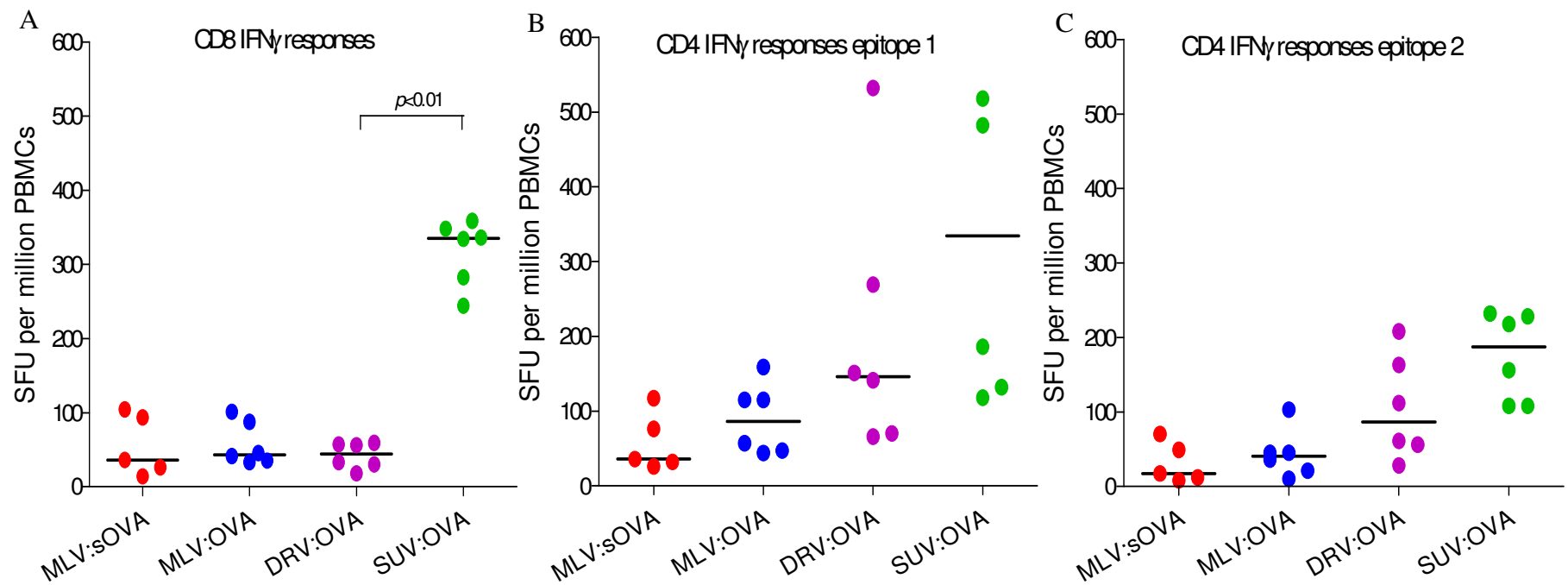


Figure 5.8 Spleen T-cell responses. (A) CD8⁺ IFN- γ responses (B) CD4⁺ epitope 1 IFN- γ responses (C) CD4⁺ epitope 2 IFN- γ responses. Splenocytes from C57BL/6 mice (n=6 per group) vaccinated with 3 homologous injections were analysed for IFN- γ production 14 weeks after the last injection. Experiment conducted at the Jenner Institute, University of Oxford.

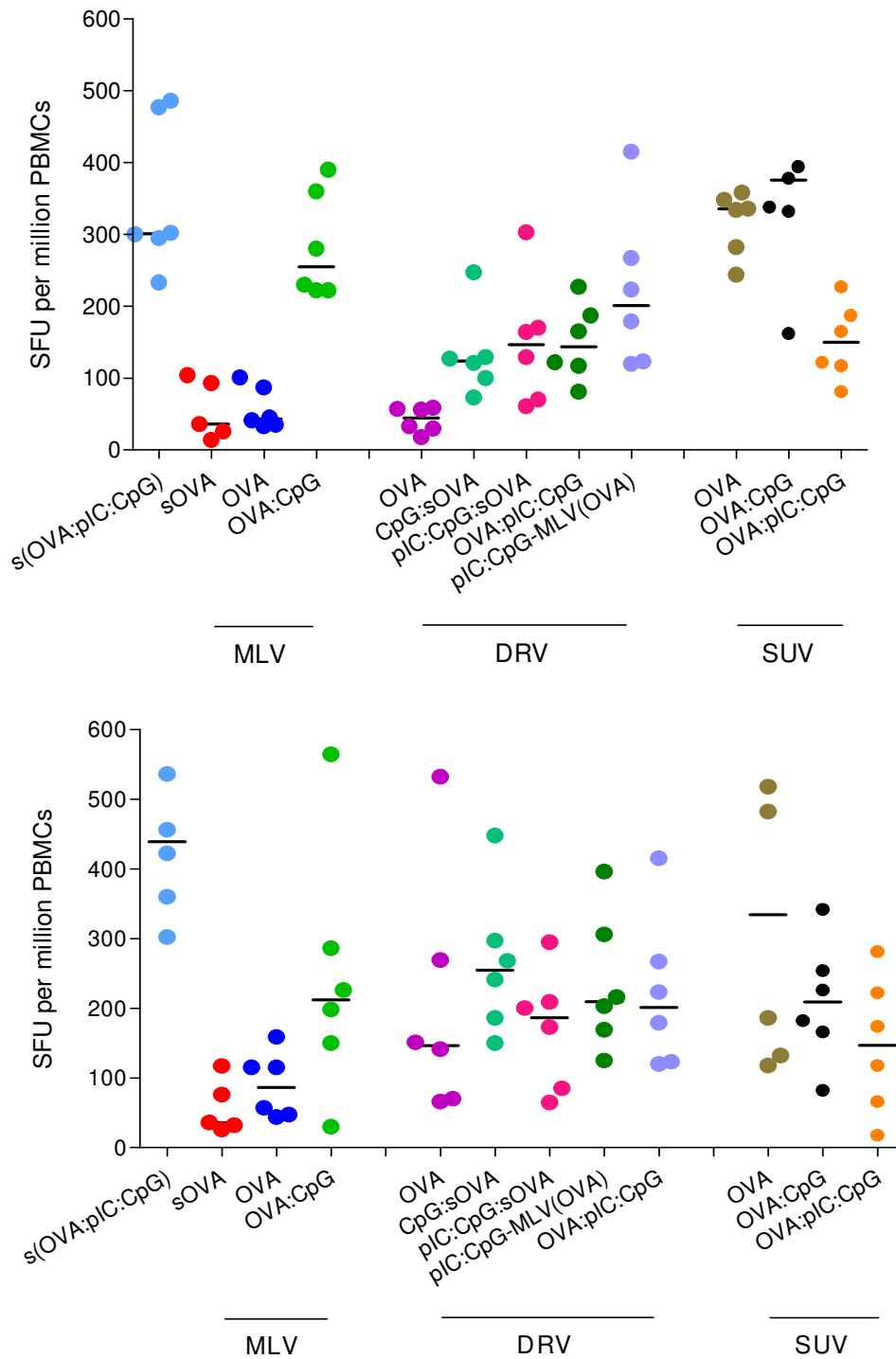


Figure 5.9 Peripheral blood T-cell responses. (A) CD8⁺ IFN- γ responses (B) CD4⁺ epitope 1 IFN- γ responses. Experiment conducted at the Jenner Institute, University of Oxford.

5.4.3.2 Antibody responses

To test the potential of the various formulations as vaccine adjuvants, immunological analysis was carried out in order to determine the efficacy of the liposome formulations in achieving the desired immune response, encompassed quantification of OVA specific IgG antibody production. In terms of antibody responses, IgG is the most obvious choice for detection from blood samples. It can activate both the complement system and mediate opsonisation, thus leading to enhanced phagocytosis (Goldsby et al 2003). Antibody ELISAs were performed at regular intervals (days 14, 28, 42, 70 and 128) to determine the antigen specific antibody production initiated by each formulation. From the results it was found that the highest IgG titres were obtained after vaccination with SUVs with adsorbed OVA, as well as SUVs and MLVs associated with OVA and CpG ($p < 0.05 - 0.001$ at day 42 (Figure 5.10A) and $p < 0.05 - 0.01$ at day 126 (Figure 5.10B)).

The results presented here suggest that CpG can be combined with cationic liposomes and antigen to produce a high level of antibody response. Previous studies (Kinman et al 1999) have found that TLR 9 ligands such as CpG stimulate and cause a signaling cascade that culminates in the maturation, differentiation and proliferation of T-cells, monocytes/macrophages and natural killer cells. With regards to targeting TLR 3, some liposomal formulations containing the TLR 3 agonist poly(I:C) have the ability to cross-present antigen and therefore stimulate CD8⁺ T cell responses (Zaks et al 2006; Mastelic et al 2010). However, in this case it was found that poly(I:C) did not increase antigen-specific antibody responses (Figure 5.10).

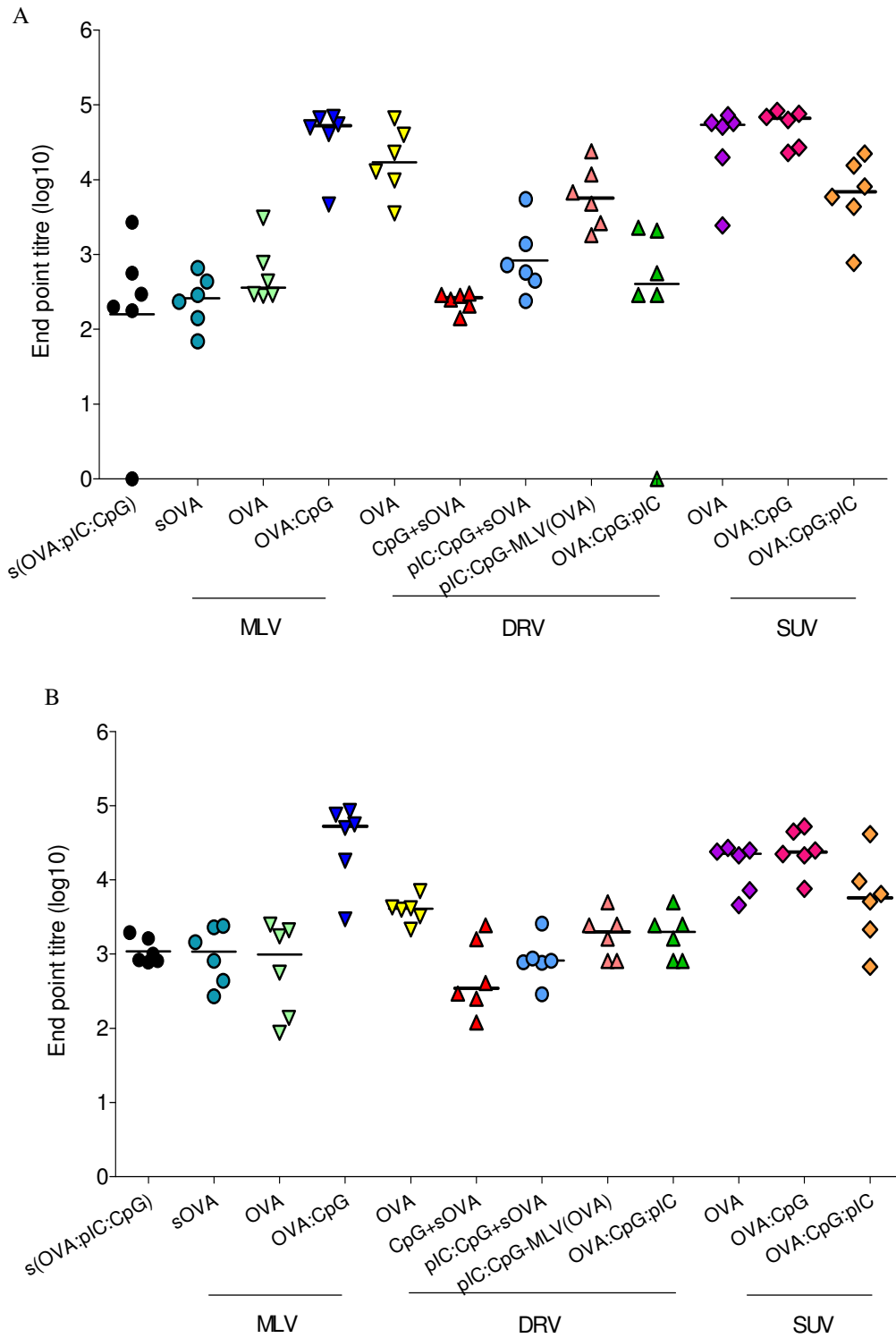


Figure 5.10 Total IgG antibody responses. Responses measured in the sera of vaccinated mice at various time-points. Titres measured at days (A) 42 and (B) 126 (2 weeks and 14 weeks post last vaccination, respectively) are shown. Experiment conducted at the Jenner Institute, University of Oxford.

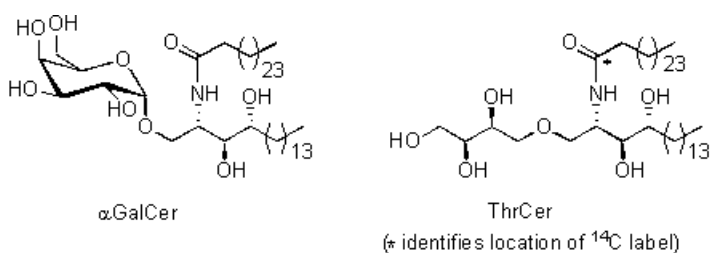
5.5 Conclusion

Many of the novel subunit vaccines require adjuvants in order to induce immune responses to vaccine antigens and enhance their protective efficacy. However, many of the potent immunogenic adjuvants also display unacceptable local or systemic reactogenicity. Liposomes, in particular cationic DDA:TDB vesicles, have been shown in animal models to induce strong humoral responses to the associated antigen without increased reactogenicity, and are currently being tested in human clinical trials. Several modifications of DDA:TDB liposomes including size, antigen association and addition of TLR agonists for immunogenic capacity as vaccine adjuvants using OVA as a model protein vaccine were explored. Cationic DDA:TDB liposomes, prepared as either MLVs, SUVs or DRVs were combined with OVA protein and TLR agonists CpG oligonucleotide (TLR 9 ligand) and poly(I:C) (TLR 3 ligand). OVA and TLR agonists were either entrapped within the vesicles or adsorbed onto the liposome surface. C57BL/6 mice were given three homologous vaccinations two weeks apart, and cellular and humoral responses measured at several time points up to ten weeks post last immunisation. SUVs showed significantly increased capacity for inducing IFN- γ CD8⁺ responses in peripheral blood and spleen, compared to larger MLV liposomes. The peak antigen-specific antibody responses were also higher with SUVs and the adsorption of TLR 9 agonist increased the adjuvanticity of MLVs but not SUVs.

Chapter 6

Preparation, characterisation and entrapment of a non-glycosidic threitol ceramide into liposomes for presentation to invariant natural killer T cells

Graphical Abstract:



Very few compounds have been found that stimulate *i*NKT cells and of these the best-characterised is the glycolipid α -galactosylceramide (α -GalCer) and the α -GalCer analogue, threitol ceramide (ThrCer). Within this chapter ThrCer is incorporated into liposomal systems.

Some of the results presented in this chapter have been published in the paper;

Kaur, R., Chen, J., Dawoodji, A., Cerundolo, V., Garcia-Diaz, Y. R., Wojno, J., Cox, L. R., Besra, G. S., Moghaddam, B., Perrie, Y. (2011) Preparation, characterisation and entrapment of a non-glycosidic threitol ceramide into liposomes for presentation to invariant natural killer T cells. *Journal of Pharmaceutical Sciences*. Accepted.

6.1 Introduction

Invariant natural killer T (*i*NKT) cells are unique lymphocytes defined by their co-expression of surface markers associated with NK cells along with a T-cell antigen receptor (Schmiege et al 2005). They recognise amphipathic ligands such as glycolipids or phospholipids presented in the context of the non-polymorphic, major histocompatibility complex (MHC) class I-like molecule CD1d (Godfrey et al 2000). To date, relatively few compounds have been found that stimulate *i*NKT cells. Of these, α -galactosylceramide 1 (α -GalCer) (Figure 6.1) is one of the most potent agonists, and has the ability to induce CD1d-restricted NKT cells specifically to produce high levels of both IL-4 (Th_2) and IFN- γ (Th_1) *in vitro* and *in vivo* once α GalCer binds with the CD1d protein (Kawano et al 1997; Spada et al 2000; Matsuda et al 2000).

*i*NKT cells in different situations display both tolerogenic and immunostimulatory functions *in vivo* following α GalCer administration. Unfortunately for therapeutic applications, α GalCer leads to overstimulation of *i*NKT cells; more specifically, it has been shown that a single injection of mice with 1 - 2 μ g of α GalCer induces long-term (> 30 days) anergy of *i*NKT cells (Parekh et al 2009; Silk et al 2008). During this hyporesponsive state, further activation of *i*NKT cells with α GalCer is unsuccessful. The production of both Th_1 and Th_2 cytokines and the “unresponsive state” of *i*NKT cells, after activation with α GalCer renders this glycolipid of limited therapeutic use as a direct activator of *i*NKT cells, and has encouraged the development of α GalCer analogues that circumvent some of these problems. It has been demonstrated that the α GalCer analogue, threitol ceramide (ThrCer) (Figure 6.1), successfully activates *i*NKT cells and overcomes

the problematic *i*NKT cell activation-induced anergy associated with α GalCer (Silk et al 2008). ThrCer is a promising agonist for *i*NKT cells and may have therapeutic application. It has been previously demonstrated that this glycolipid, whilst preventing α GalCer-dependent *i*NKT cell over-stimulation, ensures effective dendritic cell (DC) maturation, minimises *i*NKT cell-dependent DC lysis, and promotes optimal expansion of antigen-specific T cell responses (Silk et al 2008). Thus, by minimising *i*NKT cell over-stimulation and *i*NKT cell-dependent DC lysis, ThrCer rectifies some of the deficiencies of α GalCer. ThrCer also possesses the advantage over α GalCer, that the polar head group is bound to the ceramide base via an ether bond, which is more stable towards acidic hydrolysis and biodegradation than the glycosidic bond of α GalCer. This increased stability should extend the time that ThrCer persists in the cell compartments, increasing the chances of it being loaded on to CD1d for presentation.

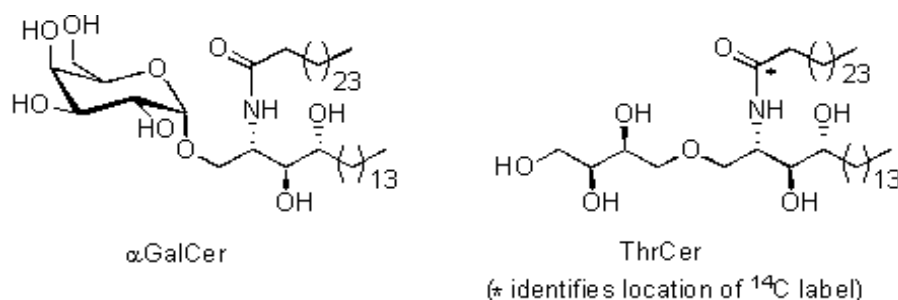


Figure 6.1 CD1d agonists α GalCer and ThrCer.

ThrCer is lipid-based with a molecular weight of 800 g/mol; it displays poor water solubility. Based on the ability of liposomes to be taken up and stimulate antigen presenting cells (APC), e.g. macrophages, the potential of using liposomes as a delivery system of ThrCer was investigated in an effort to both formulate this low solubility moiety and hence improve the delivery of this immunostimulatory agent, ThrCer.

6.1.1 Incorporation of ThrCer into liposomes

As noted previously liposomes are generally described as phospholipid vesicles consisting of one or several concentric lipid bilayers, enclosing many aqueous compartments (Bangham et al 1965). Liposomes based on dimethyldioctadecylammonium bromide (DDA) as discussed previously in chapter 5 have been evaluated as carriers for drugs (Carmona-Ribeiro et al 1997), as antimicrobial agents (Lincopan et al 2003) and as adjuvants (Dzata et al 1991) for a range of vaccines for both parenteral and mucosal delivery. In recent years, they have been used as part of more complex adjuvant systems for experimental subunit vaccines (e.g. Hilgers & Snippe 1992; Kirby et al 2008a).

Recent studies provide support for this notion by showing that if DDA is replaced with a neutral lipid such as 1,2-distearoyl-*sn*-glycero-3-phosphocholine (DSPC), the neutralisation of the surface charge of the liposomes diminishes their immunogenicity (Henriksen-Lacey et al 2010). Whilst the effect of cationic liposomes on dendritic cells (DCs) is not well characterised in the literature it is however, well known that cationic amphiphiles can be used as liposome carriers for nucleic acids and thus enhance the transfection efficiency of cells in general (Dass 2004).

6.2 Aims and objectives

Within this chapter, the aim of the studies was to incorporate ThrCer into the bilayers of liposomes composed of the cationic lipid DDA or the zwitterionic lipid DSPC. These systems were prepared both as multilamellar vesicles (MLV) and small unilamellar vesicles (SUV). To achieve this, the objectives were:

- To initially look at the physiochemical characterisation i.e. vesicle size, entrapment efficiency and stability of incorporated ThrCer.
- To carry out release studies; ThrCer release from liposomes stored in simulated *in vivo* conditions was determined using liposomes entrapping ¹⁴C-radiolabelled ThrCer.
- To investigate the packaging of ThrCer with the DDA or DSPC using surface pressure/area isotherms of monolayers of the lipids on their own or in combination.
- To investigate the uptake of the immunostimulatory agent, ThrCer by DCs, and presentation on CD1d molecules to *i*NKT cells.
- Finally, *in vivo* studies were carried out to assess DC maturation *in vivo*.

6.3 Materials and Methods

6.3.1 Materials

Chemicals	Supplier
Chloroform (HPLC grade)	Fisher Scientific (Leicestershire, UK)
Ethanol (HPLC grade)	Fisher Scientific (Leicestershire, UK)
Foetal bovine serum (Heat-Inactivated)	Invitrogen, Paisley, UK
Hydrochloric acid	Fisher Scientific (Leicestershire, UK)
Methanol (HPLC grade)	Fisher Scientific (Leicestershire, UK)
Tris-base	IDN Biomedical, Inc (Aurora, Ohio)
Ultima Gold scintillation fluid	Perkin Elmer (Waltham, MA)
Lipids	Supplier
1,2-distearoyl- <i>sn</i> -glycero-3-phosphocholine (DSPC)	Avanti Polar Lipids, Inc. (Alabaster, AL)
Dimethyldioctadecylammonium bromide (DDA)	Avanti Polar Lipids, Inc. (Alabaster, AL)

Threitol ceramide (ThrCer) and radiolabelled ThrCer, ^{14}C -ThrCer, was prepared as previously described (Garcia-Diaz et al 2009) and were supplied by Professor Besra, Birmingham University.

6.3.2 Methods

6.3.2.1 Preparation of liposomes

DDA and DSPC liposomes with and without the addition of ThrCer were prepared by the lipid hydration method (as described previously in Figure 4.4) (Bangham et al 1965). Briefly the lipids and ThrCer used in these experiments were dissolved in chloroform:methanol (2:1 v/v). DDA or DSPC (30 μL of a 10 mg ml^{-1} solution) and ThrCer (60 μL of a 1 mg ml^{-1} solution) were placed in a 50 ml round-bottom Quick-fit flask and the organic solvent was removed by rotary evaporation at about 37 $^{\circ}\text{C}$ to yield a thin lipid film on the walls of the flask, which was flushed with oxygen-free nitrogen (N_2) in order to ensure complete removal of solvent. The vesicles were formed by hydrating the lipid film in Tris buffer at pH 7.4 (600 μl of a 10 mM solution). The lipid film was hydrated for 20 minutes at a temperature of 10 $^{\circ}\text{C}$ above the main phase transition of either DDA ($T_c \sim 47^{\circ}\text{C}$) or DSPC ($T_c \sim 55^{\circ}\text{C}$) respectively to ensure complete hydration.

For the generation of small unilamellar vesicles (SUV), the multilamellar vesicles (MLV) produced were disrupted by sonication using a probe sonicator (Soniprep 150), to fracture the large liposomes into smaller structures. The DSPC liposomes were sonicated for 1 minute, whereas the DDA liposomes were sonicated for 30 seconds to produce SUV.

6.3.2.2 Measuring entrapment of ThrCer in DSPC and DDA liposomes

The degree of ThrCer incorporated in the liposomes was determined by tracking ^{14}C -labelled ThrCer. ^{14}C -Radiolabelled ThrCer (10 μl of a 1 mg ml^{-1} solution) was added to liposomes prepared as described above. The DSPC or DDA ^{14}C -ThrCer liposomes (400

µl) were placed into dialysis tubing (molecular weight cut off (MWCO) of 12,000 daltons or greater), and transferred into tris buffer (500 ml of a 10 mM solution, pH 7.4). At various time-points up to 28 days, ThrCer incorporation and release from the liposome formulations was determined by removing 1 ml sample from liposome suspension, which was subsequently replaced with 1 ml Tris buffer, in order to maintain sink conditions. Incorporation of ThrCer was determined on the basis of ¹⁴C-labelled ThrCer remaining in the liposome suspension after dialysis.

6.3.2.3 ThrCer retention in simulated in vivo conditions

ThrCer release from liposomes stored in simulated *in vivo* conditions was determined using liposomes entrapping ¹⁴C-radiolabelled ThrCer prepared as described in Section 6.3.2.1. Aliquots of each formulation were diluted (1:5) using 50 % FCS in Tris buffer and incubated in a shaking water bath at 37 °C for 28 days. At time intervals, samples were centrifuged (125000 ×g, 4 °C, 1 h), resuspended in Tris buffer and centrifuged again to ensure removal of all non-incorporated ThrCer. The ¹⁴C-ThrCer recovery in the pooled supernatant after two washes (non-incorporated ThrCer) and the pellet (incorporated ThrCer) was measured. The percentage of ThrCer entrapped was calculated as a percentage of the total radioactivity recovered from both supernatant and pellet.

6.3.2.4 Determination of liposome size

The vesicle size of DDA and DSPC liposomes with and without the inclusion of ThrCer was determined using the photon correlation spectroscopy (PCS) technique. The measurements were performed at 25 °C using a ZetaPlus (Brookhaven Instrument

Corporation, USA). Polystyrene size standards 220 ± 6 nm (Duke scientific corp, Duke, NC) was used as a control. The samples were diluted with 10 mM Tris buffer at pH 7.4 to achieve the optimal vesicle concentration.

6.3.2.5 Langmuir-Blodgett isotherms

An automated controlled film balance apparatus (KSV Langmuir Mini-trough, KSV Instruments Ltd, Helsinki, Finland) equipped with a platinum Wilhemy plate and placed on a vibration-free table was used to collect the surface pressure-area isotherms as previously reported (Christensen et al 2008). The size of the trough was $24,225.0 \text{ mm}^2$ enclosing a total volume of approximately 220 ml; the subphase was composed of filtered double-distilled water. The compounds (at fixed total concentration of 1 mg ml^{-1}) were dissolved in chloroform and $20 \text{ }\mu\text{l}$ of each solution was spread onto the air/water interface with a Hamilton microsyringe, precise to $\pm 0.2 \text{ }\mu\text{l}$. After spreading, the monolayers were left for 10 minutes to allow the chloroform to evaporate. Thereafter, the molecules underwent constant compression (10 mm s^{-1}) until the required surface pressure of less than 0.2 mN/m was attained. The spread monolayer was then compressed or expanded symmetrically with the two barriers until the desired surface pressure was reached with accuracy within 0.1 mN/m . The temperature of the subphase was kept constant at 20 ± 1 °C by means of an external water bath circulation system. Each experiment was only compressed once and was performed three times with monolayers prepared from different solutions. KSV software (KSV Instruments Ltd, Helsinki, Finland) was used for data analysis.

6.3.2.6 Liposome presentation to invariant natural killer T cells

Peripheral blood mononuclear cells (PBMCs) were isolated from healthy donors' buffy coats by density gradient centrifugation over Lymphoprep (Nycomed, Birmingham, UK). Monocytes were positively selected using anti-CD14 mAb-coated magnetic beads (MACS; Miltenyi Biotec, Surrey, UK) and were then cultured in 6-well plates in either X-Vivo 15 + 2 % Human AB serum with 800 U ml^{-1} granulocyte monocyte colony stimulating factor (GM-CSF) and 500 U ml^{-1} IL-4 for 4 days to produce immature DCs. On day 4, liposomes (100 ng ml^{-1} or $1 \mu\text{g ml}^{-1}$), lab grade ThrCer ($1 \mu\text{g ml}^{-1}$) and α -GalCer (100 ng ml^{-1}) were added to the immature DCs, followed by the addition of maturation cocktail (IL-1 β , IL-6, TNF- α and PGE2) after 3 hours. DCs were harvested and assayed with *i*NKT cells overnight, the supernatants were taken and an IFN- γ ELISA performed. DCs were also analysed by FACS after addition of liposomes for expression of CD80 and CD86 to see whether there is any contamination of liposomes.

6.3.2.7 IFN- γ ELISA

ELISA plates were coated with 1D1K antibody (Mabtech, Nacka Strand, Sweden) and left overnight at $4 \text{ }^{\circ}\text{C}$. Plates were washed with 0.05 % tween 20 in PBS (v/v). To eliminate any non-specific antigen binding, the plates were coated (i.e. blocked) with 200 μl of 10 % FCS in PBS (v/v) and incubated for 2 hours at $37 \text{ }^{\circ}\text{C}$. 100 μl of reaction supernatant was transferred to the ELISA plate and the standard was added starting at 50 ng ml^{-1} . The plate was then incubated at $4 \text{ }^{\circ}\text{C}$ overnight. The following day, the plates were washed with 0.05 % tween 20 in PBS and the biotinylated anti-cytokine detecting mAb was added at 50 μl /well and incubated at room temperature for 2 hours. After

incubation, the plates were washed eight times with 0.05 % tween 20 in PBS. 100 μ l of working dilution of avidin-peroxidase was added per well after which the plates were incubated at room temperature for 2 hours. Plates were once again washed eight times with 0.05 % tween 20 in PBS. 100 μ l of tetramethylbenzidine (TMB) agent was added per well. Reaction was stopped with 50 μ l solution of 0.5 M H₂SO₄ and the optical density of each well was measured immediately using a microplate reader (Bio-Rad Laboratories, model 680) set to 450 nm.

6.3.2.8 Phenotyping of APC

The maturation status of APC in response to different liposomes was assessed 36 hours after addition of the liposomes. DCs were analysed on a FACS Calibur (Becton Dickinson). In brief, 100000 DCs were stained with CD80-PE and CD86-APC in FACS buffer (PBS, 1 % FCS) at 4 °C for 30 minutes. Cells were washed three times in ice-cold PBS / 1 % FCS and analysed by flow cytometry using CellQuest software. Dead cells were excluded by forward light scattering and propidium iodide staining.

6.3.2.9 Injection of ThrCer liposome to assess DC maturation in vivo

C57BL/6 female mice or B6-NKTKO female mice were immunised with 200 μ l / mouse by the intravenous route of injection (IV). Stock solutions were made up at 5 μ g/ml (1 μ g / mouse). Mice were immunised with either: 1 μ g ml⁻¹ lab-grade α GalCer, 1 μ g ml⁻¹ lab grade ThrCer, 1 μ g ml⁻¹ each of the liposome formulations, 10 μ g ml⁻¹ LPS (50 μ g/ml in PBS). Spleens were removed the next day and blood taken by cardiac puncture to assess IFN- γ levels in the serum.

6.3.2.10 Statistical analysis

For all experiments, means and standard deviations were calculated. To determine statistical significance the one way analysis of variance (ANOVA) was performed on all data, with the statistical significance determined to 0.05 confidence intervals ($p < 0.05$). Tukey's post hoc test was conducted to determine which conditions differ significantly from each other.

6.4 Results and discussion

6.4.1 Characterisation of ThrCer liposomes

As discussed previously, cationic liposomes based on DDA have been evaluated and have shown potential as an adjuvant system for vaccines against a wide range of diseases (e.g. Davidsen et al 2005). In this study, two liposomal delivery systems composed of DDA and DSPC (a neutral alternative) were tested for their ability to enhance ThrCer delivery to DCs. Table 6.1 provides size, polydispersity and ThrCer loading of the liposomal systems with and without the inclusion of ThrCer when formulated in both multilamellar vesicles (MLV) and small unilamellar vesicles (SUV).

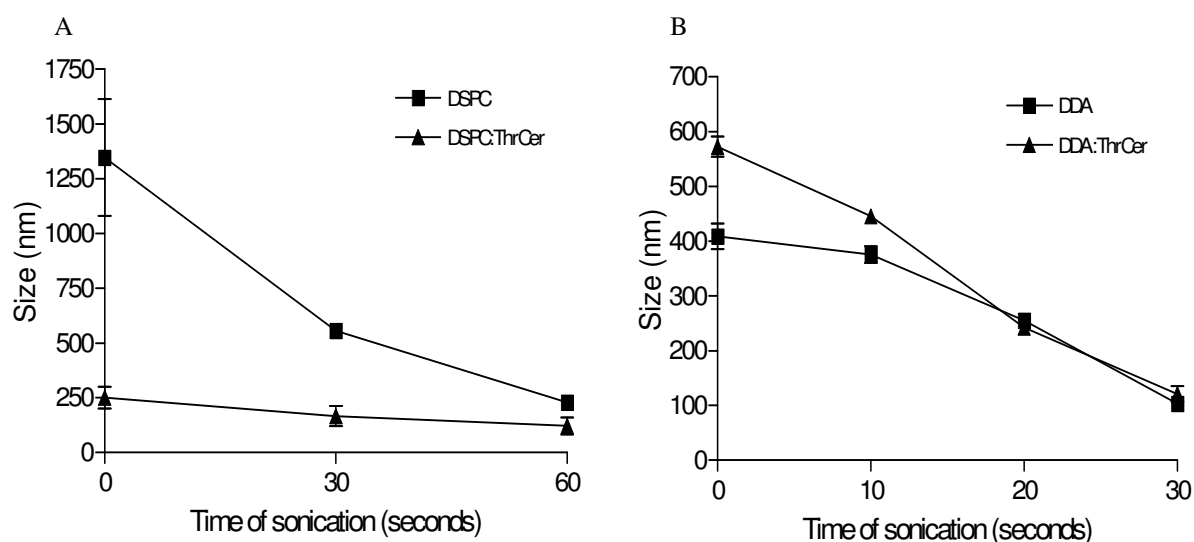


Figure 6.2 Size (nm) of (A) DSPC liposomes and (B) DDA liposomes over time of sonication. Results represent mean \pm SD of triplicate experiments.

The time required for sonication was based on these results and is dependent on concentration of lipid and sonication power used (Figure 6.2). For the DSPC based liposomes, a sonication time of 60 seconds was chosen to produce liposomes of 121.1 nm in size, whereas for the DDA based liposomes the sonication time was 30 seconds. This

may be an outcome of the cationic lipids packing less tightly into the liposome membranes such that they are more sensitive to sonication.

Table 6.1 Characterisation of MLV or SUV liposomes prepared from DSPC or DDA with and without the inclusion of ThrCer.

Formulation	MLV			SUV		
	Size (nm)	Polydispersity Index (PI)	ThrCer loading (% of amount used)	Size (nm)	Polydispersity Index (PI)	ThrCer loading (% of amount used)
DSPC	1346.6 ± 267.0	0.378 ± 0.00	-	228.4 ± 3.2	0.302 ± 0.03	-
DSPC:ThrCer	174.5 ± 3.1	0.324 ± 0.05	96 ± 2.5 %	121.1 ± 2.3	0.302 ± 0.00	94 ± 2.8 %
DDA	408.7 ± 14.9	0.345 ± 0.03	-	103.1 ± 1.4	0.296 ± 0.07	-
DDA:ThrCer	572.8 ± 18.3	0.327 ± 0.03	80 ± 1.2 %	121.2 ± 4.7	0.357 ± 0.00	74 ± 4.2 %

Size (nm) and polydispersity (PI) were measured by photon correlation spectroscopy. Results represent mean ± SD of triplicate experiments.

The addition of ThrCer to DSPC liposomes was found to significantly ($p < 0.05$) reduce the size of both MLV and SUV liposomes (Table 6.1). However in contrast, for the DDA-based liposomes a significant increase ($p < 0.05$) in size was found for MLV liposomes but no significant change in size was noted for SUV liposomes (Table 6.1). The changes in size seen in both sets of formulations suggest that ThrCer promotes a re-organisation of surfactants within the bilayers, and in the case of the DSPC liposomes promoting smaller sized vesicles. A similar effect with small-molecule drugs was found by Lopes et al (2004), where sodium diclofenac, an amphiphilic molecule, interacted with the bilayers of liposomes composed of soya phosphatidylcholine, causing a decrease in liposome size. Several other studies have also suggested that a molecular association between amphiphilic drugs and phospholipids including anti-inflammatory compounds, results in a decrease in the size of liposome structures (Schreier et al 2000; Kriwet & Muller-Goymann 1994; Stoye et al 1998). Interestingly, the effect of ThrCer on DDA liposomes

was in contrast, with its addition promoting slightly larger vesicle sizes, suggesting the charge of the lipid headgroup was playing an influencing role.

Incorporation of ThrCer was also influenced by the charge of the lipids employed, with cationic liposomes prepared from DDA having a reduced loading compared to their zwitterionic counterpart; both MLV and SUV liposomes prepared using DSPC incorporated more ThrCer than their cationic DDA counterparts (Table 6.1). This suggests that the zwitterionic lipid DSPC is better able to accommodate the ThrCer within the bilayer structure compared to DDA. This may be due to the larger head group of DDA inhibiting effective packaging of the molecules within the bilayer thereby inhibiting inclusion of ThrCer within the system.

6.4.2 Determination of vesicle stability over time

Stability was investigated in terms of changes in vesicle size over time and the 8 formulations were prepared and stored at room temperature (25 °C) for 28 days (Figure 6.3A and B). Whilst after the initial preparation, the DSPC MLV were 1346.6 ± 267.0 nm, the size of these vesicles increased rapidly on storage to 1944.2 ± 102.2 nm after 14 days and after 28 days storage visible aggregation became apparent (Figure 6.3A). In contrast, addition of ThrCer to these DSPC liposomes promoted enhanced stability with liposomes showing no significant change ($p < 0.05$) in particle size over the 28 day period with sizes remaining around 296.1 ± 39.2 nm, indicating that the presence of ThrCer in the DSPC liposome bilayers leads to improved liposome stability potentially through promoting the reduced vesicle sizes which were less likely to sediment and aggregate (Figure 6.3A).

The MLV liposomes produced with DDA alone again showed instabilities in terms of particle size when stored at room temperature with a twofold increase in size being noted over the 28 day study (Figure 6.3A). However unlike the DSPC liposomes, the addition of ThrCer did not improve the stability of DDA liposomes with vesicle size increasing by 59 % over the 28 days. These results could again suggest that the smaller vesicle size of the DSPC:ThrCer liposomes (~175 nm; Table 6.1) compared to the larger MLV DDA liposomes (~409 nm) was a factor in their improved stability. However this is not supported by stability studies of SUV formulations (Figure 6.3B). Of the four SUV formulations, again only the DSPC:ThrCer liposomes showed no significant change ($p>0.05$) in size over the 28 day period with sizes remaining around 177 nm, whilst DSPC only SUV increased by 57 % compared with their initial size (Figure 6.3B). The DDA SUV with and without ThrCer also showed size instability over time with particle sizes increasing from around 100 nm to 300 nm by day 14 with no further significant changes in size thereafter (Figure 6.3B). Therefore, whilst both liposome size and surface charge in general are known to have an influencing effect on the rate of sedimentation and potential aggregation, the change in lipid packaging with the addition of ThrCer to liposomes formulated as both MLV and SUV improved DSPC liposome stability but not those based on DDA.

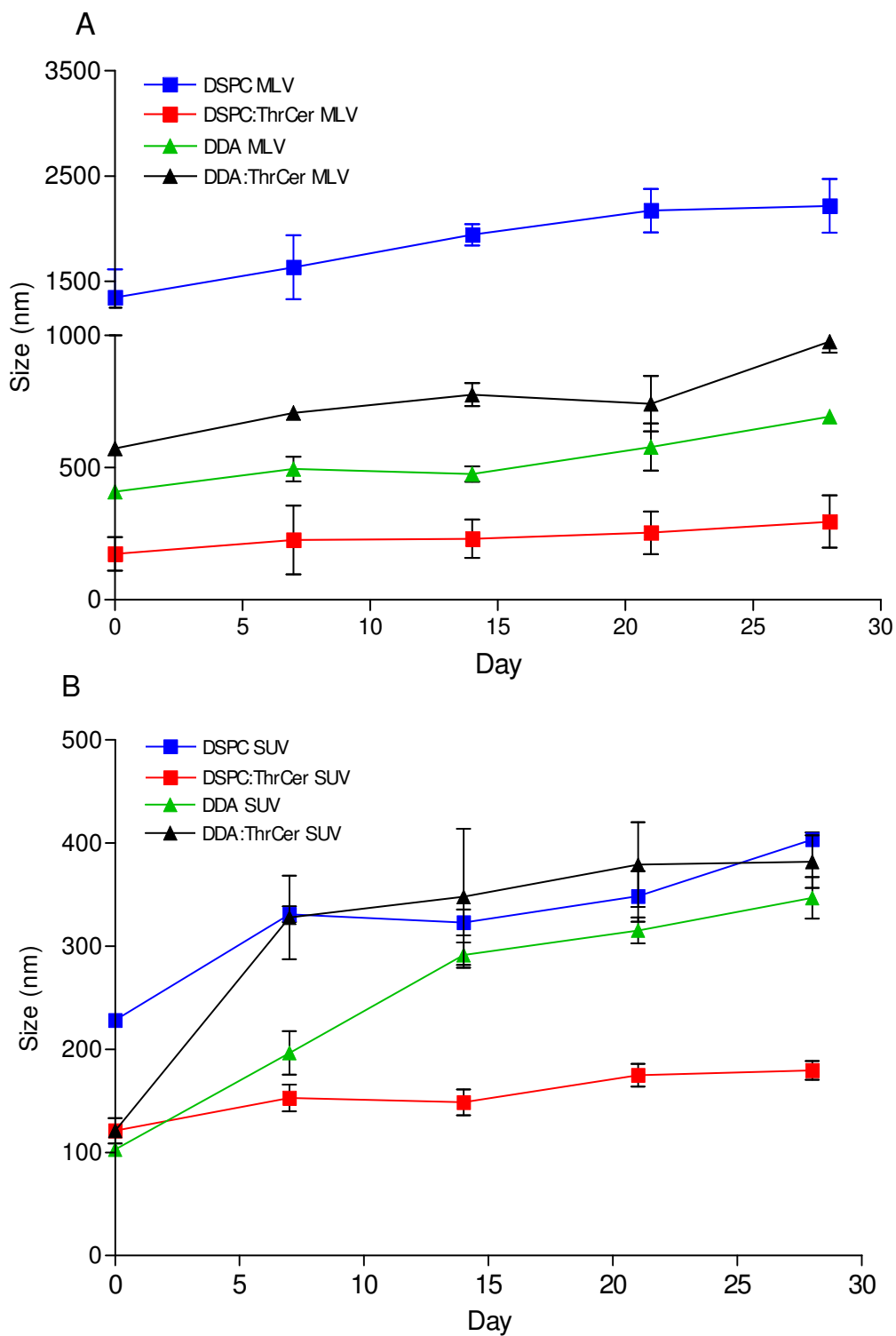


Figure 6.3 Size (nm) of (A) MLV and (B) SUV of DSPC and DDA liposomes with and without the inclusion of ThrCer represented by storage at 25 °C. Size was measured in Tris buffer (1 mM) using a Brookhaven ZetaPlus instrument. Results represent mean \pm SD of triplicate experiments.

6.4.3 ThrCer is retained in liposomes under simulated *in vivo* conditions

For therapeutic application, it is important that drugs are retained within liposomes for an appropriate time, and release kinetics may vary depending on the drug delivered, the site of action and the therapeutic application. Among the various factors that dictate the liposomal release of a drug, the bilayer composition is a key factor (Devaraj et al 2002). ThrCer retention was measured in simulated *in vivo* conditions i.e. in 50 % FCS in Tris buffer and compared to formulations in Tris buffer. The percentage of ThrCer incorporation was calculated as a percentage of the total radioactivity recovered from both supernatant and pellet in both conditions. In the case of the MLV formulations (Figure 6.4A), the DSPC:ThrCer and DDA:ThrCer MLV retained over 88 % and 80 % respectively of the initial ThrCer loading over the period of the study (Figure 6.4A) and of this 7 % was lost over the initial 24 hour period.

For the SUV-based formulations (Figure 6.4B), both the DSPC and DDA based vesicles gave significantly higher ($p<0.05$) ThrCer release in serum over time compared to the MLV, with DSPC vesicles having ThrCer retention of 63 % and DDA vesicles of 69 %. This increased instability of the SUV compared to the MLV maybe an outcome of the larger total surface area of the SUV which results in higher interactions of the lipids with the serum moieties. In general release in serum were higher than those measured for tris buffer (Figure 6.4) possibly due to the adsorption of serum proteins onto the liposomes resulting in greater release as it has been previously reported that the loss of lipids from liposomes through lipid exchange may be due to plasma high-density lipoproteins (Sulkowski et al 2005).

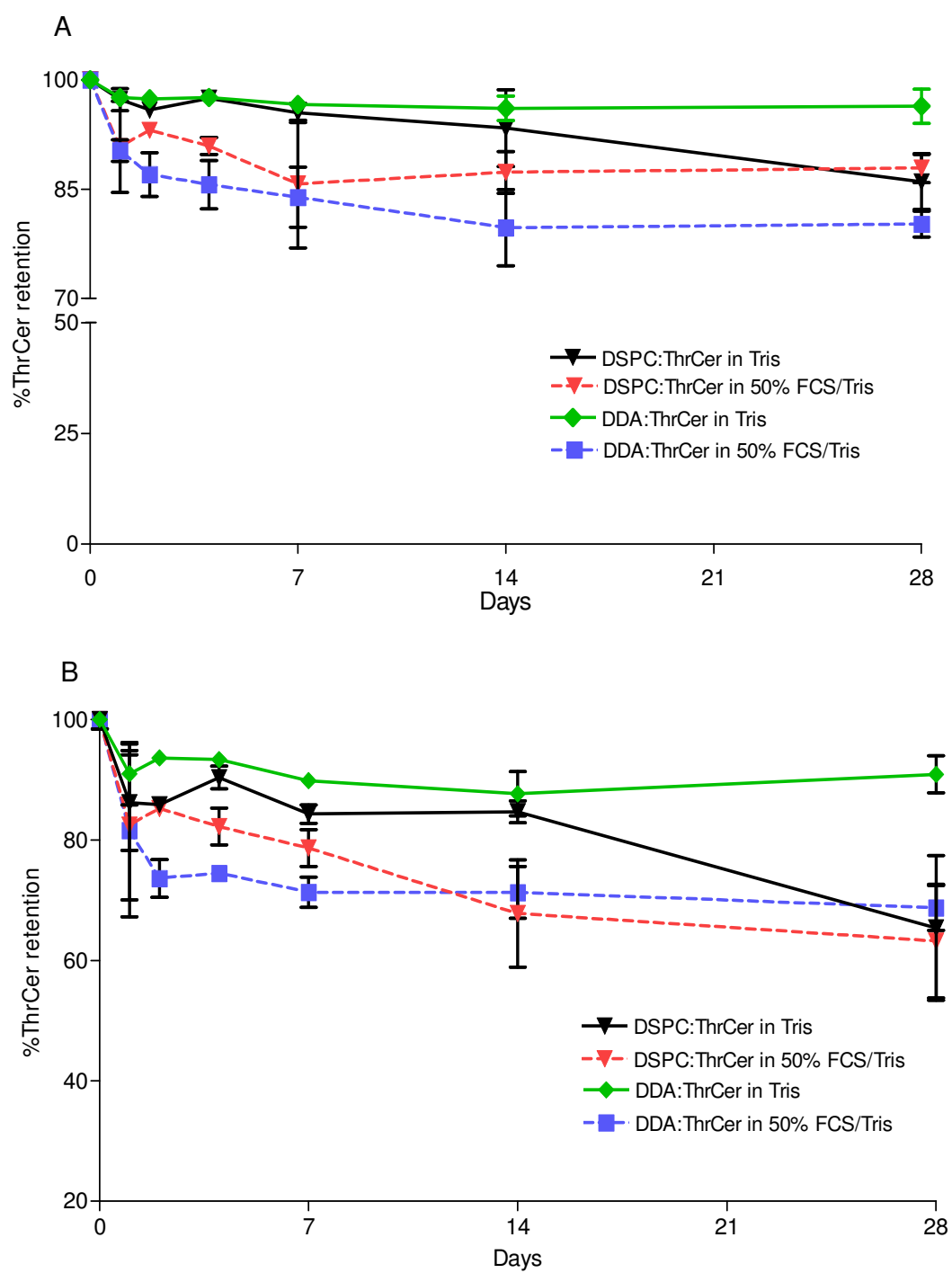


Figure 6.4 Entrapped ThrCer release profile of DSPC and DDA (A) MLV and (B) SUV. Liposomes were stored under simulated *in vivo* conditions with ThrCer (represented by storage at 37 °C in 50 % FCS). Results represent mean \pm SD of triplicate experiments.

6.4.4 Langmuir-Blodgett isotherms

To investigate the packaging of ThrCer with the DDA or DSPC surface pressure/area isotherms of monolayers of the lipids on their own or in combination were investigated. Such monolayer studies can be used to thermodynamically analyse interactions between components in mixed monolayers, allowing interactions between lipid components and their molecular arrangement at the air/water interface (Hac-Wydro et al 2007). It is clear that the structural differences of lipids influence the interactions among them and these interactions dominate the organisation of membranes (Andrade et al 2006). Many studies have been conducted on the behaviour of different lipids in mixed monolayers (e.g. Chou & Chang 2000; Gzyl & Paluch 2005), and these can be used to interpret interaction in liposome bilayers (e.g. Christensen et al 2008; Ali et al 2010). Surface properties of mixed monolayers are generally studied on the basis of surface pressure (π)/mean molecular area (A) measurements in which bidimensional phases can be detected, each separated by a phase transition. The 2D phases in increasing pressure order are (1) bidimensional gas, (2) liquid (which can be further subdivided into expanded liquid, and condensed liquid), and (3) solid. In the gas phase, the molecules are not interacting with each other (Figure 6.5). When the surface area is decreased the molecules become more closely packed and start to interact with each other. At the solid phase, the molecules are completely organised and the surface pressure increases dramatically and collapse occurs, i.e. the monolayer breaks and aggregates or multilayers are formed. Importantly, the shape and location of the isotherms are indicative of the interactions both between molecules in the monolayer and of the subphase.

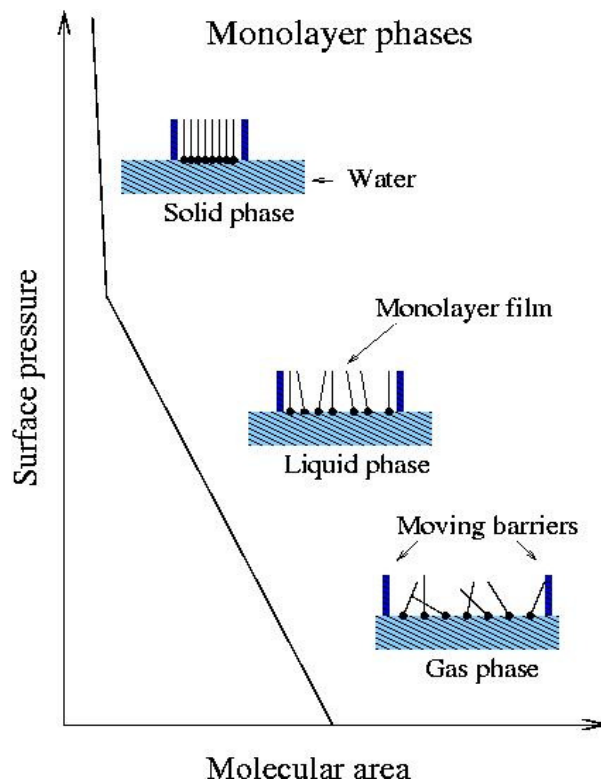


Figure 6.5 Surface pressure - area isotherm. The monolayer is formed by spreading the organic molecules on the water subphase. The molecules usually have hydrophilic (head) and hydrophobic (tail) parts, so when the film is formed the molecules stand on their heads. When the molecules first are spread on the water they are very loosely packed and form a so called gas phase. This means that the area on the water available for each molecule is rather large and the surface pressure is low. The surface pressure is usually measured using a Wilhelmy plate and a precision scale. The surface pressure can be increased by means of one or two sliding barriers. At a certain point the surface pressure starts to rise more rapidly indicating a transition to the liquid phase. As the barrier is moved even further the onset of the solid phase can be noted by an even steeper rise in the surface pressure.

To investigate the geometrical interactions between DSPC or DDA with ThrCer at the air/water interface, surface pressure studies of the various surfactants and mixtures were investigated (Figure 6.6A and B, with calculations presented in Table 6.2). The isotherm of pure DSPC (one component system) shows the molecular area as $48.1 \pm 2.7 \text{ \AA}^2$ per molecule and the condensed phase collapsing at $58.5 \pm 0.6 \text{ mN m}^{-1}$ (Figure 6.6A; Table 6.2), which are in agreement with results collated by Cardenas et al (2005). For DDA, monolayer collapse occurred at $44.8 \pm 1.9 \text{ mN m}^{-1}$, similar to literature reports of DDA on

pure water, which was found to be 45 mN m^{-1} (Hato et al 1993; Taylor et al 1996) (Figure 6.6B; Table 6.2). Of the three pure molecules, ThrCer has a smallest area/molecule (A^2) of 27.2 ± 1.3 and a collapse pressure similar to DSPC of $60.3 \pm 2.4 \text{ mN m}^{-1}$, which would be expected from this type of surfactant structure (a small headgroup and saturated tail groups; Figure 6.1).

In both cases, the isotherms of the lipid mixtures were found to lie between the ranges of those of the pure components (Figure 6.6A and B) and for both the DSPC:ThrCer and DDA:ThrCer mixtures the measured extrapolated area per molecule was significantly higher than the predicted A^2 per molecule (5 % deviation for the DSPC:ThrCer mix and 14 % for the DDA:ThrCer mix; Table 6.2). It has been suggested (Hac-Wydro & Wydro 2007) that positive deviation (which is when the experimental area is more than the ideal area) occurs with saturated lipids which stack co-operatively, and that there is no condensing effect as is noted when lipids such as DSPC are mixed with cholesterol (Ali et al 2010).

Table 6.2 The experimental extrapolated area and area compressibility of mixed and pure monolayers at the air/water interface (at 20 °C) by DSPC, DDA and ThrCer in ddH₂O.

Formulation	Extrapolated area at zero pressure ($\text{A}^2/\text{Molecule}$)	Ideal Extrapolated area at zero pressure ($\text{A}^2/\text{Molecule}$)	Deviation from ideality (%)	Collapse pressure (mN m^{-1})
DSPC	48.1 ± 2.7	-	-	58.5 ± 0.6
DDA	61.5 ± 2.7	-	-	44.8 ± 1.9
ThrCer	27.2 ± 1.3	-	-	60.28 ± 2.4
DSPC:ThrCer (1:1)	42.6 ± 2.6	37.65	+ 4.95	57.1 ± 1.1
DDA:ThrCer (1:1)	50.4 ± 2.6	44.35	+ 13.64	63.5 ± 1.5

Results represent mean \pm SD of triplicate experiments.

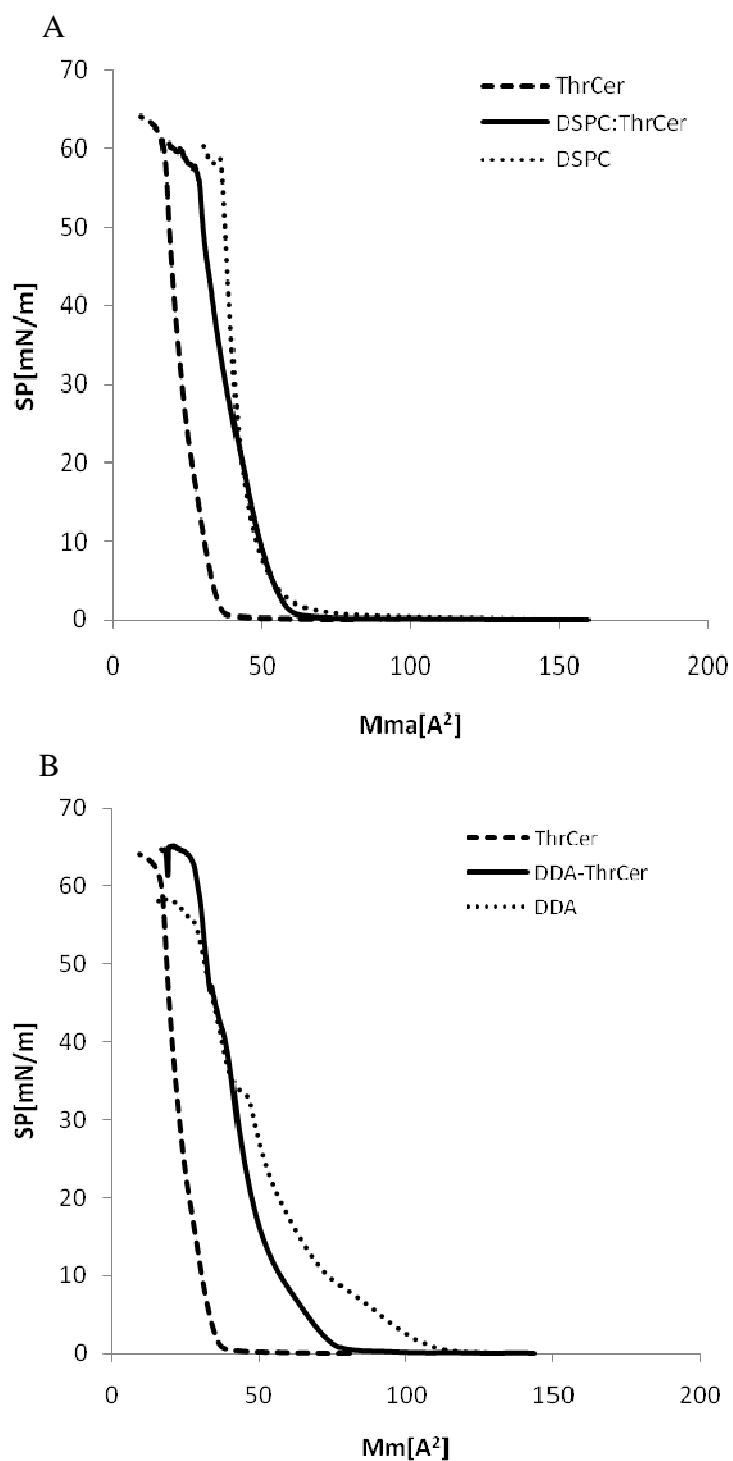


Figure 6.6 The surface pressure-area isotherms of mixed and pure monolayers at the air/water interface. The mixed and pure monolayers were of (A) DSPC, (B) DDA and ThrCer. The air/water interface was at 20 °C. Results represent mean \pm SD of triplicate experiments.

In terms of monolayer collapse pressure, the addition of ThrCer to DSPC made no significant difference to the collapse pressure of the monolayer. In contrast, ThrCer was shown to significantly increase the surface pressure at which the monolayer collapsed compared to DDA alone (increasing the collapse pressure by 8.7 mN/m; Table 6.2). Recent surface pressure studies of DDA, in combination with trehalose 6,6'-dibehenate (TDB) (Christensen et al 2008), have shown that the addition of TDB to DDA monolayers increased the collapse pressure compared to DDA alone, indicating that the attractive forces between the trehalose headgroup of TDB and water are greater than those between the quaternary ammonium head group of DDA and water. From the data in Figure 6.6, it would suggest that ThrCer is having a similar effect and improving the interaction of the monolayer mixture with water. However this did not translate into improved stability as seen in Figure 6.3. Whilst the addition of ThrCer to DSPC liposomes was seen to improve their stability, this was not the case with DDA liposomes (Figure 6.3) and it may be that higher concentrations of ThrCer than those employed in the liposomes would be required to stabilise the cationic formulations.

In general, these collapse pressures at high surface pressure and small molecular area can be attributed to the lipids (DDA, DSPC and ThrCer) used for the study, which are saturated lipids. Previous studies noted that when a lipid is unsaturated with one or more double bonds, which in most naturally occurring lipids are in the *cis* configuration, this makes the chain bend and accordingly, the more double bonds the chain has in the *cis* configuration, the more curved the chain (Hac-Wydro & Wydro 2007). This results in a decreased packaging efficiency and an increased area per molecule. In contrast, saturated

lipids are known to form straight chains resembling rods. The saturated lipids therefore occupy a smaller molecular area than unsaturated lipids and their collapse pressure is higher (Hac-Wydro et al 2007).

6.4.5 Maturation effect on DCs

To investigate whether the adjuvant activity of liposomes with ThrCer was associated with the ability to induce maturation of DCs, the maturation status of DCs (Figure 6.7) in response to different liposomes was assessed 36 hours after addition of the liposomes. DCs were analysed on a FACS Calibur. The DCs had a distinct immature profile, which was not affected by the stimulation with the liposomes because the surface expression of CD80 and CD86 was unchanged. Figure 6.7 shows that none of the liposome formulations can mature DC, which means that the liposomes were very pure with no lipopolysaccharides (LPS) contamination (Figure 6.7). Work described in here was done in collaboration with Prof Vincenzo Cerundolo at the Weatherall Institute of Molecular Medicine, University of Oxford.

6.4.6 Uptake of ThrCer by DCs

The uptake of the immunostimulatory agent, ThrCer by DCs, and presentation on CD1d molecules to *i*NKT cells were determined by measuring IFN- γ release (Figure 6.8). Previous studies have shown that ThrCer efficiently activates *i*NKT cells, resulting in DC maturation and activated *i*NKT cells rapidly produce IFN- γ (Silk et al 2008). To examine whether both the cationic and neutral ThrCer-containing liposomes were able to enhance this action, secretion of IFN- γ by *i*NKT cells stimulated with different concentrations

(100 ng ml⁻¹ and 1 µg ml⁻¹) and of liposomes was measured, which were loaded on to DCs. The results (Figure 6.8) show that both types of ThrCer-containing liposomes could sufficiently activate *i*NKT cells. When comparing concentration of ThrCer, 100 ng ml⁻¹ and 1 µg ml⁻¹, a higher IFN-γ secretion was found at higher concentrations for all formulations.

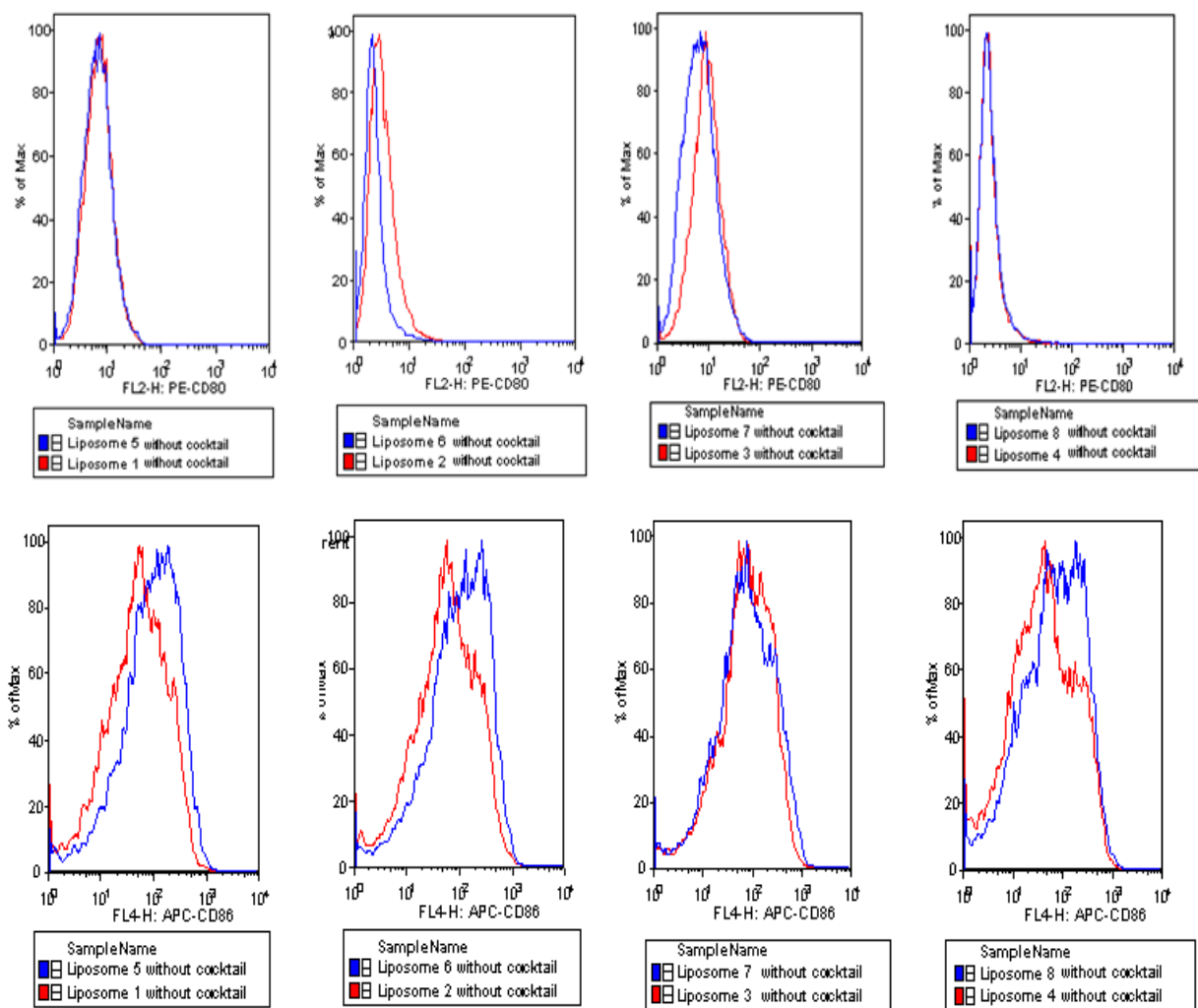


Figure 6.7 The maturation status of APC in response to different liposomes was assessed 36 hours after addition of the liposomes. DCs were analysed on a FACS Calibur (Becton Dickinson). Liposomes in the presence and absence of ThrCer were compared as follows: Liposome 1 = DDA:ThrCer MLV with Liposome 5 = DDA MLV, Liposome 2 = DSPC:ThrCer MLV with Liposome 6 = DSPC MLV, Liposome 3 = DDA:ThrCer SUV with Liposome 7 = DDA SUV, Liposome 4 = DSPC:ThrCer SUV with Liposome 8 = DSPC SUV. Experiment conducted at the Weatherall Institute of Molecular Medicine, University of Oxford.

In particular the DDA SUV based liposome formulation was found to produce a higher IFN- γ secretion at both concentrations compared to the neutral DSPC based liposomes. In all cases, the control liposomes (not containing ThrCer) induced minimal levels of IFN- γ secretion (Figure 6.8). Only a few compounds stimulate *i*NKT cells and the best characterised is the glycolipid α -GalCer, which stimulates the production of large quantities of IFN- γ and IL-4 by these cells. However, α GalCer leads to overstimulation of *i*NKT cells. ThrCer successfully activates *i*NKT cells and overcomes the problematic *i*NKT cell activation-induced anergy associated with α GalCer 1 (Garcia-Diaz et al 2009). From Figure 6.8, it has been demonstrated that the IFN- γ secretion was higher for the DDA SUV based formulation, suggesting that ThrCer encapsulation in this liposome formulation resulted in a higher uptake by dendritic cells.

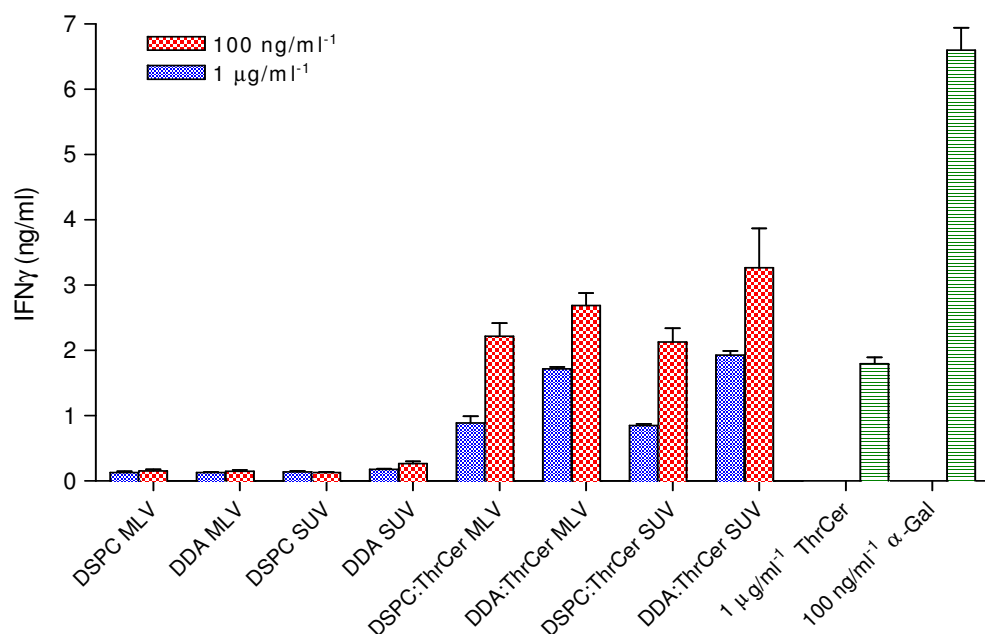


Figure 6.8 IFN- γ release from *i*NKT cells co-cultured with DCs pulsed with liposomes prepared as MLV or SUV with and without the inclusion of ThrCer. Results represent mean \pm SD of triplicate experiments. Experiment conducted at the Weatherall Institute of Molecular Medicine, University of Oxford.

6.4.7 DC maturation *in vivo*

DC maturation refers to an intricate differentiation process whereby DCs respond rapidly to an environmental stimulus and become capable of eliciting adaptive immunity. The type of stimulus determines the program of DC differentiation and the subsequent host immune response. DCs can directly sense pathogen components via TLRs, and respond to this recognition by up-regulating surface co-stimulatory molecules, secreting cytokines and chemokines, enhancing antigen presentation, and migrating to secondary lymphoid tissues (Iwasaki & Medzhitov 2004).

In this study, C57BL/6 female mice and B6-NKTKO female mice were immunised with $1\mu\text{g ml}^{-1}$ of one of the four liposome formulations and the levels of IFN- γ was assessed in the serum. LPS was used as a positive control and from Figure 6.9 the mean fluorescence intensity (an indicator of IFN- γ) for the control was found to be similar for both of the mouse strains. However, a better expression of IFN- γ was found with the B6-NKTKO mouse strain compared to the C57BL/6. When comparing the formulations, the mean fluorescence intensity, was higher for all the liposomal formulations containing ThrCer compared to ThrCer alone thereby showing a synergistic action/effectively delivery promoted by the liposomal system. The liposome formulations without ThrCer failed to produce any IFN- γ . Interestingly, DDA SUV gave the highest levels of IFN- γ suggesting a pro-inflammatory response by this formulation. The high IFN- γ levels suggest that this formulation was taken up by DCs and presented on CD1d molecules to NK T cells.

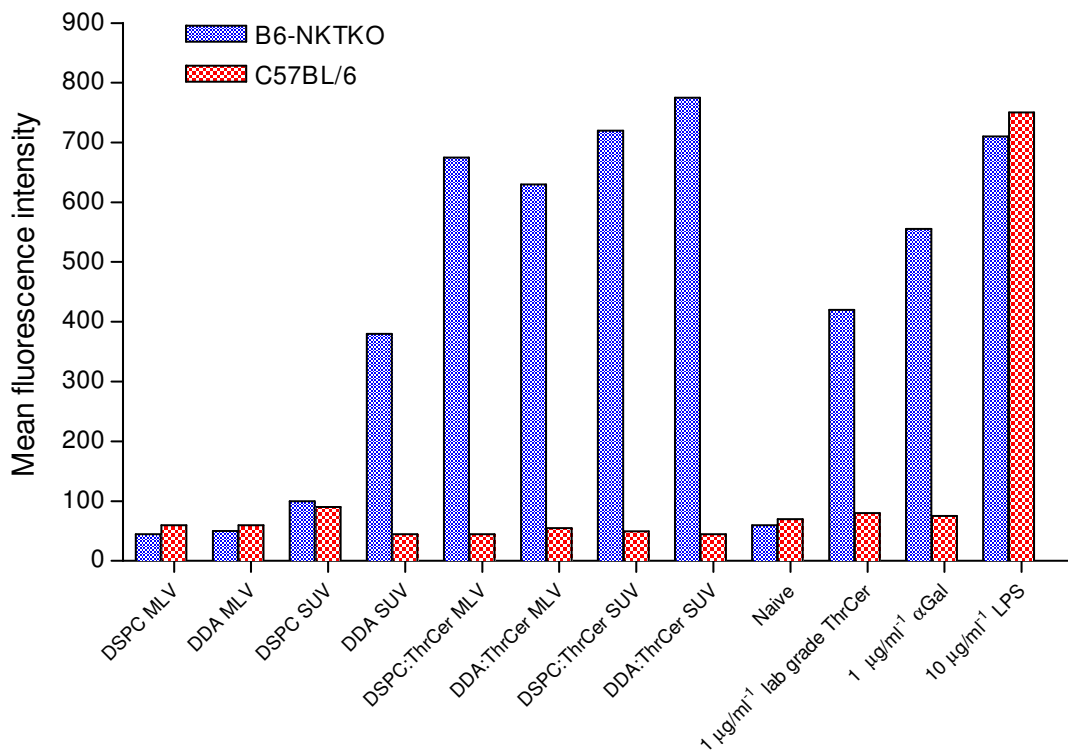


Figure 6.9 Mean fluorescence intensity. C57BL/6 female mice or B6-NKTKO female mice (n=3 per group) were immunised as follows with 200 µl / mouse by IV injection. Mice were immunised with either: 1 µg ml⁻¹ lab-grade αGalCer, 1 µg ml⁻¹ lab grade ThrCer, 1 µg ml⁻¹ each of the liposome formulations, 10 µg ml⁻¹ LPS. Spleens were removed the next day and blood taken by cardiac puncture to assess IFN-γ levels in the serum. Experiment conducted at the Weatherall Institute of Molecular Medicine, University of Oxford.

The *in vitro* studies (Figure 6.8) showed that IFN-γ secretion was higher for the DDA SUV based formulation, suggesting that ThrCer encapsulation in this liposome formulation resulted in a higher uptake by dendritic cells. The *in vivo* results confirm this, as a higher expression of ThrCer was found with this formulation (Figure 6.9). Previous studies have shown that DDA is an effective type of adjuvant promoting a cell-mediated immune response against the intracellular pathogen *M. tuberculosis* (Hilgers & Snippe 1992). A number of studies have looked at DDA and other immunomodulating agents (Stanfield et al 1973, Andersen 1994). Administration of Arquad 2HT, which comprises

DDA, in humans was promising and did not induce apparent side effects (Stanfield et al 1973). An experimental vaccine based on culture filtrate proteins from *M. tuberculosis* and DDA generated a protective immune response against TB in mice (Andersen 1994). Moreover, DDA has been used as an adjuvant for a DNA vaccine against pseudorabies virus leading to enhanced T-cell responses and antiviral immunity (van Rooij et al 2002).

6.5 Conclusion

Although previous studies (Sullivan & Kronenberg 2005) have demonstrated that α GalCer is an effective and very powerful activator of the immune system, it has also been found that after a single activation event with α GalCer, *i*NKT cells display a long period of anergy. During this period the *i*NKT cell population diminishes to nearly undetectable levels and are unresponsive when pulsed with further doses of α GalCer.

In a study by Silk et al (2008), it was discovered that replacing the galactosyl polar-head group with a truncated galactose moiety addressed some of the problems associated with α GalCer, including the long period of anergy after a single activation and the propensity to induce *i*NKT cell-dependent lysis of DCs. One of the analogues was ThrCer. In this study ThrCer has been entrapped in DSPC and DDA liposomes, formulated as both MLV and SUV. The entrapment efficiency of ThrCer within the lipid bilayers was high for both zwitterionic (DSPC) and cationic (DDA) liposomes. The release of ThrCer from liposomes was measured in Tris and 50 % FCS (to simulate *in vivo* conditions) and it was found that both the MLV based formulations had a higher ThrCer retention compared to

the SUV counterparts. In terms of ThrCer packaging it was found that the addition of ThrCer improved the stability of the DSPC liposomes. However, this was not the case for the DDA-based liposomes and it may be that higher concentrations of ThrCer than those employed in the liposomes would be required to stabilise the cationic formulations. For the *in vitro* work, it was demonstrated that the IFN- γ secretion was higher for the DDA SUV liposome formulation ($p < 0.05$), suggesting that whilst these systems had reduced stability compared to their DSPC counterparts, ThrCer encapsulation in this liposome formulation resulted in a higher uptake by dendritic cells. The *in vitro* data was supported by the *in vivo* results as a higher expression and up regulation of ThrCer by DCs was found with the DDA:ThrCer SUV formulation.

Chapter 7

General discussion

7.1 Magnetic resonance imaging (MRI) contrast agent for imaging of fluid pressure

MRI is a powerful technique to non-invasively produce images of objects exhibiting NMR signal, such as the human body, and is of particular relevance to medical imaging. The technique is particularly suited to imaging fluid (e.g. blood) concentration and fluid flow. The technique is, however, virtually insensitive to fluid pressure, although such measurements would be extremely relevant to medical imaging as well as for the investigation of fluid flow in heterogeneous porous media. Gas bubbles in liquids have been suggested in order to measure fluid pressure with MRI. The technique has been experimentally demonstrated *in vitro*, but theoretical calculations show that the method cannot be used *in vivo*, because it requires too high concentration of gas.

In chapter 2 of the thesis, the aim was to prepare a MRI contrast agent for imaging of fluid pressure using liposomes that contain the gas (lipid-coated microbubbles). Gas filled microbubbles have seen applications predominantly as ultrasound contrast agents (for which they are commercially available), as they greatly enhance radiation scattering (Duncan & Needham 2004). They have also been demonstrated as pressure sensors for non-invasive manometry using magnetic resonance imaging (MRI) (Alexander et al 1996). More recently these microbubbles have been used to spatially resolve the pressure of a liquid saturating a porous medium which has potential applications to improving oil recovery (Vangala et al 2007a). In the present work, initial studies compared four different methods of producing lipid-coated microbubbles in terms of stability and physico-chemical characteristics. The potential formulations identified from the initial characterisation studies were then further investigated as contrast agents for fluid pressure. It was found that both the formulation of the microbubble shell and the gas

incorporated were shown to influence stability and sensitivity: the addition of 5 % PEG and/or cholesterol was shown to stabilise the structures in terms of microbubble size. However, an overall decrease in foam volume was noted with such formulations and therefore microbubbles formulated from DSPC alone were adopted for further studies. In order to produce a liquid contrast agent exhibiting large MRI sensitivity to fluid pressure changes, whilst keeping micron sized gas filled bubbles homogeneously dispersed in the liquid, an aqueous solution of weakly concentrated polysaccharide gels as a liquid medium accommodating the phospholipid microbubbles was used. The inclusion of microbubbles into polysaccharide gel counteracted their intrinsic buoyancy without reducing NMR sensitivity. Furthermore, for the microbubbles formulated from DSPC, it was found that the sensitivity of these systems could be improved using nitrogen rather than air within the microbubbles.

Smaller *F*-GPC microbubbles were also prepared which can withstand higher pressures than the DSPC microbubbles. Further refinement to improve the stability of *F*-GPC microbubbles will allow their biomedical application to include echocardiography and other diagnostic ultrasound techniques, whilst the large microbubble systems may also be suitable for petrochemical applications or in the imaging of various pressure regions within joints and chronic joint disorders. The work demonstrates an important step forward in the design of MRI contrast agents for human blood pressure monitoring and imaging, although the inclusion of paramagnetic agents in the shell of the bubbles is probably a necessity for such an agent to exhibit high enough sensitivity.

7.2 Lipid-coated microbubbles as vaccine adjuvants

Liposome systems are well reported for their activity as vaccine adjuvants; however novel lipid-based microbubbles have also been reported to enhance the targeting of antigens into DCs in cancer immunotherapy (Suzuki et al 2009). The aim of this chapter was to investigate the formulation of lipid coated microbubbles and assess their potential activation of macrophages using *in vitro* models. Cell viability and phagocytic activity was measured using the MTS and NAG assays, respectively. From the results, it was found that none of the formulations tested within the concentrations tested influenced either of the activities measured. In terms of the application of the lipid-coated microbubbles this demonstrates their further potential in diagnostic imaging given these lipid-coated microbubbles were demonstrated in chapter 2 to act as potential contrast agents that allow stable MRI measurements of fluid pressure over time. The preliminary studies with regard to uptake within macrophages were not encouraging to support further investigations into their application in this respect. Therefore, further studies into the development of vaccine adjuvants then focused on aqueous-filled liposome systems.

7.3 Aqueous-filled liposomes as vaccine adjuvants

The use of liposomes as vaccine adjuvants has been investigated extensively over the last few decades. In particular, cationic liposomal adjuvants have drawn attention, with DDA liposomes as a prominent candidate. However cationic liposomes are, in general, not sufficiently immunostimulatory, and therefore a range of immunostimulatory agents have been added to these formulations. One such combination consists of liposomes formed of DDA stabilised with the synthetic mycobacterial immunomodulator, TDB inserted into

the lipid bilayers at a molar ratio of 5:1. This cationic liposome system was developed to mediate protection against tuberculosis (TB) but, in addition, has shown promising protective efficacy against other infectious diseases requiring different immunological profiles (Christensen et al 2009). One of the proposed mechanism behind the immunostimulatory effect obtained with DDA:TDB is the 'depot effect' in which the liposomal carrier helps to retain the antigen at the injection site, thereby increasing the time of vaccine exposure to the immune cells (Henriksen-Lacey et al 2010). The depot effect has been suggested to be primarily due to their cationic nature. In this chapter, the aim of the study was to further test this hypothesis by investigating whether sterically stabilising the DDA:TDB system with PEG reduces aggregation, and subsequently influences the formation of a depot at the site of injection and the immune response.

Results reported within this thesis demonstrate that higher levels of PEG i.e. 25 % was able to significantly inhibit the formation of a liposome depot at the injection site and also severely limit the retention of antigen at the site therefore resulting in a faster drainage of the liposomes from the site of injection. This was reflected by the immunisation study, where lower levels of IgG2b antibody, IFN- γ , and IL-2 was found compared to the DDA:TDB formulation, and higher level of IL-5 cytokine suggesting that the pegylated formulations stimulate a Th₂ type immune response. This study further supports the hypothesis that the depot formation is due to electrostatic forces between the net negatively charged protein and the positively charged liposomes i.e. aggregation between the cationic liposomes and serum proteins, thereby causing a liposomal net which retains the antigen.

7.4 Addition of immunostimulatory components CpG and poly(I:C)

The versatility of cationic liposomes based on DDA:TDB in combination with different immunostimulatory ligands including, poly(I:C) a TLR 3 ligand, and CpG a TLR 9 ligand, either entrapped within the vesicles or adsorbed onto the liposome surface was investigated in this chapter. Poly(I:C) (TLR 3) is a synthetic double-stranded (ds) RNA and CpG (TLR 9) is an immunomodulating synthetic oligonucleotide. Small unilamellar DDA:TDB vesicles (20 - 100 nm native size) with protein antigen adsorbed to the vesicle surface were the most potent in inducing both T cell (7-fold increase) and antibody (up to 2 log increase) antigen specific responses. It was found that the addition of TLR agonists poly(I:C) and CpG to SUV liposomes had a small or no effect on their adjuvanticity.

7.5 Incorporation of ThrCer into liposomes for presentation to *i*NKT cells

DCs are able to present glycolipids to *i*NKT cells *in vivo* and very few compounds have been found that stimulate *i*NKT cells. Of these the best-characterised is the glycolipid α -galactosylceramide (α -GalCer). It has been demonstrated that the α GalCer analogue, ThrCer, successfully activates *i*NKT cells and overcomes the problematic *i*NKT cell activation-induced anergy. ThrCer is a promising agonist for *i*NKT cells and may have therapeutic application. In this chapter, the aim of the study was to incorporate ThrCer into the bilayers of liposomes composed of the cationic lipid DDA or the zwitterionic lipid, DSPC, formulated as both MLV and SUV. For the *in vitro* work, the uptake of ThrCer by dendritic cells and presentation on CD1d molecules to *i*NKT cells, which respond by releasing IFN- γ , was also determined. It was demonstrated that the IFN- γ secretion was higher for DDA SUV liposome formulation ($p < 0.05$), suggesting that

whilst these systems had reduced stability compared to their DSPC counterparts, ThrCer encapsulation in this liposome formulation resulted in a higher uptake by dendritic cells. The *in vitro* data was supported by the *in vivo* results as a higher expression and up regulation of ThrCer by DCs was found with the DDA:ThrCer SUV formulation.

7.6 Further studies

Further studies can be conducted in continuation of this work. For the lipid-coated microbubbles the design of MRI contrast agents for human blood pressure monitoring and imaging will require the microbubbles to exhibit high enough sensitivity. The inclusion of paramagnetic agents in the shell of the bubbles can therefore be tested.

In vitro transfection studies could be further conducted in an appropriate macrophage cell line or dendritic cells as a preliminary screening criteria for different vesicle pegylated compositions and also obtain a better correlation with immunisation experiments. Knowledge of physico-chemical interaction between different vesicle components and the subunit antigen is essential, this could be studied effectively using langmuir trough by monitoring surface pressure isotherms with respect to time.

Finally, differential scanning calorimetry (DSC) studies can be conducted to see the change in phase transition temperature and the distribution of the lipids after incorporation of immunostimulating compounds i.e. CpG and poly(I:C) into the liposomes. This would also provide information on the stability of such systems.

Chapter 8

References

- Adamson, A. W. (1997) *Physical Chemistry of Surfaces*. New York: John Wiley.
- Agger, E. & Andersen, P. (2001) Tuberculosis subunit vaccine development: on the role of interferon-gamma. *Vaccine*. **19**: 2298-2302
- Agger, E., Rosenkrands, I., Hansen, J., Brahimi, K., Vandahl, B., Aagaard, C., Werninghaus, K., Kirschning, C., Lang, R., Christensen, D., Theisen, M., Follmann, F. & Andersen, P. (2008a) Cationic liposomes formulated with synthetic mycobacterial cordfactor (CAF01): a versatile adjuvant for vaccines with different immunological requirements. *PLoS ONE*. **3**: 3116-3126.
- Agger, E., Cassidy, J., Brady, J., Korsholm, K., Vingsbo-Lundberg, C. & Andersen, P. (2008b) Adjuvant modulation of the cytokine balance in Mycobacterium tuberculosis subunit vaccines; immunity, pathology, and protection. *Immunology*. **124**: 175-185.
- Aguilar, J. & Rodriguez, E. (2007) Vaccine adjuvants revisited. *Vaccine*. **25**: 3752-3762.
- Ahn, S., Costa, J. & Emanue, U. (1996) PicoGreen quantitation of DNA: effective evaluation of samples pre- or post-PCR. *Nucleic Acids Res*. **24**: 2623-2625.
- Ahsan, F., Rivas, I., Khan, M., & Torres-Suarez, A. I. (2002). Targeting to macrophages: role of physicochemical properties of particulate carriers liposomes and microspheres on the phagocytosis by macrophages. *J Control Release*. **79**: 29-40.
- Alberts, B., Johnson, A., Lewis, J., Raff, M., Roberts, K. & Walter, P. (2002) *Molecular Biology of the Cell*. New York: Garland Publishing.
- Alexander, A., McCreery, T., Barrette, T., Gmitro, A. & Unger, E. (1996) Microbubbles as novel pressure-sensitive MR contrast agents. *Magn Reson Med*. **35**: 801-806.
- Ali, M., Kirby, D., Mohammed, A. & Perrie, Y. (2010) Solubilisation of drugs within liposomal bilayers: alternatives to cholesterol as a membrane stabilising agent. *J Pharm Pharmacol*. **62**: 1646-1655.
- Allen, C., Dos, S., Gallagher, R., Chiu, G., Shu, Y., Li, W., Johnstone, S., Janoff, A., Mayer, L. & Webb, M. (2002) Controlling the physical behavior and biological performance of liposome formulations through use of surface grafted poly(ethylene glycol). *Biosc Rep*. **22**: 225-250.
- Allen, T., Austin, G., Chonn, A., Lin, L. & Lee, K. (1991a) Uptake of liposomes by cultured mouse bone marrow macrophages: influence of liposome composition and size. *Biochim Biophys Acta*. **1061**: 56-64.
- Allen, T., Hansen, C., Martin, F., Redemann, C. & Yau-Young, A. (1991b) Liposomes containing synthetic lipid derivatives of poly(ethylene glycol) show prolonged circulation half-lives *in vivo*. *Biochim Biophys Acta*. **1066**: 29-36.

- Allison, A. & Byars, N. (1991) Immunological adjuvants: desirable properties and side effects. *Mol Immunol.* **28**: 279-284.
- Allison, A. & Gregoriadis, G. (1974) Liposomes as immunological adjuvants. *Nature.* **252**: 252.
- Allison, S., Molina, M. & Anchordoquy, T. (2000) Stabilisation of lipid DNA complexes during the freezing step of the lyophilization process: the particle isolation hypothesis. *Biochim Biophys Acta.* **1468**: 127-138.
- Alving, C. (1991) Liposomes as carriers of antigens and adjuvants. *J Immunol Methods.* **140**: 1-13.
- Andersen, P. (1994) Effective vaccination of mice against *Mycobacterium tuberculosis* infection with a soluble mixture of secreted mycobacterial proteins. *Infect Immun.* **62**: 2536-2544.
- Andrade, C., Santos-Magalhaes, N. & de Melo, C. (2006) Thermodynamic characterization of the prevailing molecular interactions in mixed floating monolayers of phospholipids and usnic acid. *J Colloid Interf Sci.* **298**: 145-153.
- Aramaki, Y., Takano, S. & Tsuchiya, S. (1999) Introduction of apoptosis in macrophages in cationic liposomes. *FEBS Lett.* **460**: 472-476.
- Arvin, A. & Greenberg, H. (2006) New viral vaccines. *Virology.* **344**: 240-249.
- Asahi-Ozaki, Y., Itamura, S., Ichinohe, T., Strong, P., Tamura, S. & Takahashi, H. (2006) Intranasal administration of adjuvant-combined recombinant influenza virus HA vaccine protects mice from the lethal H5N1 virus infection. *Microbes Infect.* **8**: 2706-2714.
- Avanti (2008) L-alpha-Dioleoyl Phosphatidylethanolamine (DOPE) Available from: <http://www.avantilipids.com/SyntheticDOPE>. [Accessed 27th June 2008].
- Bangham, A., Standish, M. & Watkins, J. (1965) Diffusion of univalent ions across the lamellae of swollen phospholipids. *J Mol Biol.* **13**: 238-252.
- Bannard, O., Kraman, M. & Fearon, D. (2009) Pathways of memory CD8⁺ T-cell development. *Eur J Immunol.* **39**: 2083-2087.
- Barbour, W. & Hopwood, D. (1983) Uptake of cationized ferritin by colonic epithelium. *J Pathol.* **139**: 167-178.
- Bauer, A. & Solbiati, L. (2003) Ultrasound contrast agents. In Solbiati, L., Martegani, A., Leen, E., Correas, J., Burns, P. & Becker, D. (Eds.) *Contrast-Enhanced Ultrasound of Liver Diseases*. Italy: Springer.

- Beaudette, T., Bachelder, E., Cohen, J., Obermeyer, A., Broaders, K. & Frechet, J. (2009) *In vivo* studies on the effect of co-encapsulation of CpG DNA and antigen in acid-degradable microparticle vaccines. *Mol Pharm.* **6**: 1160-1169.
- Bencsik, M. & Ramanathan, C. (2001) Direct measurement of porous media local hydrodynamical permeability using gas MRI. *Magn Reson Imaging.* **19**: 378-383.
- Berman, P., Gregory, T., Riddle, L., Nakamura, G., Champe, M., Porter, J., Wurm, F., Hershberg, R., Cobb, E. & Eichberg, J. (1990) Protection of chimpanzees from infection by HIV-1 after vaccination with recombinant glycoprotein gp120 but not gp160. *Nature.* **345**: 622-625.
- Bingham, C. O. (2008) Basic Immunology for the Non-Immunologist: From Pathophysiology to Therapeutics. Available from: http://www.medscape.com/viewarticle/579121_3. [Accessed 30 March 2011].
- Bird, A., Taggart, M., Nicholls, R. & Higgs, D. (1987) Non-methylated CpG-rich islands at the human alpha-globin locus: implications for evolution of the alpha-globin pseudogene. *EMBO J.* **6**: 999-1004.
- Brandt, L., Elhay, M., Rosenkrands, I., Lindblad, E. & Andersen, P. (2000) ESAT-6 subunit vaccination against Mycobacterium tuberculosis. *Infect Immun.* **68**: 791-795.
- Brewer, J., Pollock, K., Tetley, L. & Russell, D. (2004) Vesicle size influences the trafficking, processing, and presentation of antigens in lipid vesicles. *J Immunol.* **173**: 6143-6150.
- Brgles, M., Jurasin, D., Sikiric, M., Frkanec, R. & Tomasic, J. (2008) Entrapment of ovalbumin into liposomes-factors affecting entrapment efficiency, liposome size, and zeta potential. *J Liposome Res.* **18**: 235-248.
- Brunei, F., Darbouret, A. & Ronco, J. (1999) Cationic lipid DC-Chol induces an improved and balanced immunity able to overcome the unresponsiveness to the hepatitis B vaccine. *Vaccine.* **17**: 2192-2203.
- Brutkiewicz, R. (2006) CD1d Ligands: The good, the bad, and the ugly. *J Immunol.* **177**: 769-775.
- Caliceti, P. & Veronese, F. (2003) Pharmacokinetic and biodistribution properties of poly(ethylene glycol)-protein conjugates. *Adv Drug Del Rev.* **55**: 1261-1277.
- Campanha, M., Mamizuka, E. & Carmona-Ribeiro, A. (1999) Interactions between cationic liposomes and bacteria: the physical-chemistry of the bactericidal action. *J Lipid Res.* **40**: 1495-1500.

- Caprette, D. (2010) Introduction to SDS-PAGE. Available from: <http://www.ruf.rice.edu/~bioslabs/studies/sds-page/gellab2.html>. [Accessed 3rd October 2010].
- Cardenas, M., Nylander, T., Jonsson, B. & Lindman, B. (2005) The interaction between DNA and cationic lipid films at the air-water interface. *J Colloid Interf Sci.* **286**: 166-175.
- Carmona-Ribeiro, A., Ortis, F., Schumacher, R. & Armelin, M. (1997) Interactions between cationic vesicles and cultured mammalian cells. *Langmuir.* **13**: 2215-2218.
- Carstens, M. (2007) Self-assembling PEG-oligoesters. The Netherlands: OctoPlus.
- Chen, F., Scher, D., Clancy, R., Vera-Yu, A. & DiCesare, P. (1999) *In vitro* and *in vivo* activation of polymorphonuclear leukocytes in response to particulate debris. *Biomed Mater Res.* **48**: 904-912.
- Chin, D., Straubinger, R., Acton, S., Nathke, I. & Brodsky, F. (1989) 100 kDa polypeptides in peripheral clathrin-coated vesicles are required for receptor-mediated endocytosis. *Proc Natl Acad Sci USA.* **86**: 9289-9293.
- Chou, T.-H. & Chang, C.-H. (2000) Thermodynamic behavior and relaxation processes of mixed DPPC:cholesterol monolayers at the air:water interface. *Colloid Surface B.* **17**: 71-79.
- Chrai, S., Murari, R. & Ahmed, I. (2002) Drug Delivery Systems. Available from: http://upload_repository2/info_request/0929022128liposome.pdf. [Accessed 9th October 2008].
- Christensen, D., Agger, E., Andreasen, L., Kirby, D., Andersen, P. & Perrie, Y. (2009) Liposome-based cationic adjuvant formulations (CAF): Past, present, and future. *J Liposome Res.* **19**: 2-11.
- Christensen, D., Kirby, D., Foged, C., Agger, E., Andersen, P., Perrie, Y. & Nielsen, H. (2008) alpha, alpha'-trehalose 6,6'-dibehenate in non-phospholipid-based liposomes enables direct interaction with trehalose, offering stability during freeze-drying. *Biochim Biophys Acta.* **1778**: 1365-1373.
- Claassen, E., de Leeuw, W., de Greeve, P., C, H. & Boersma, W. (1992) Freund's complete adjuvant: an effective but disagreeable formula. *Res Immunol.* **143**: 478-483.
- Cohen, J. & Marshall, E. (2001) Bioterrorism. Vaccines for biodefense: a system in distress. *Science.* **294**: 498-501.
- Cooper, A., Dalton, D., Stewart, T., Griffin, J., Russell, D. & Orme, I. (1993) Disseminated tuberculosis in interferon gamma gene-disrupted mice. *J Exp Med.* **178**: 2243-2247.

- Cory, H., Owen, T., Barltrop, J. & Cory, J. (1991) Use of an aqueous soluble tetrazolium/formazan assay for cell growth assays in culture. *Cancer Commun.* **3**: 207-212.
- Cox, R., Brokstad, K. & Ogra, P. (2004) Influenza virus: immunity and vaccination strategies. Comparison of the immune response to inactivated and live, attenuated influenza vaccines. *Scand J Immuno.* **59**: 1-15.
- Crommelin, D. (1984) Influence of lipid composition and ionic strength on the physical stability of liposomes. *J Pharm Sci.* **73**: 1559-1563.
- Crowe, J. & Clegg, J. (1973) Anhydrobiosis. Stroudsburg: Dowden, Hutchinson & Ross.
- Crowe, L., Crowe, J., Rudolph, A., Womersley, C. & Appel, L. (1985) Preservation of freeze-dried liposomes by trehalose. *Archives of Biochemistry and Biophysics.* **242**: 240-247.
- Crowe, L., Crowe, J., Carpenter, J., Rudolph, A., Wistrom, C., Spargo, B. & Anchordoguy, T. (1988) Interaction of sugars with membranes. *Biochim Biophys Acta.* **947**: 367-384.
- Curtiss, R. (2002) Bacterial infectious disease control by vaccine development. *J Clin Invest.* **110**: 1061-1066.
- Dass, C. (2004) Lipoplex-mediated delivery of nucleic acids: factors affecting *in vivo* transfection. *J Mol Med.* **82**: 579-591.
- Davidson, J., Rosenkrands, I., Christensen, D., Vangala, A., Kirby, D., Perrie, Y., Agger, E. & Andersen, P. (2005) Characterization of cationic liposomes based on dimethyldioctadecylammonium and synthetic cord factor from *M. tuberculosis* (trehalose 6,6 dibehenate) a novel adjuvant inducing both strong CMI and antibody responses. *Biochim Biophys Acta.* **1718**: 22-31.
- Davis, D. & Gregoriadis, G. (1987) Liposomes as adjuvants with immunopurified tetanus toxoid: influence of liposomal characteristics. *Immunology.* **61**: 229-234.
- de Jong, N. & Ten Cate, F. (1996) New ultrasound contrast agents and technological innovations. *Ultrasonics.* **34**: 587-590.
- Deamer, D. & Bangham, A. (1976) Large volume liposomes by an ether vaporization method. *Biochim Biophys Acta.* **443**: 629-634.
- Deamer, D. & Barchfield, G. (1982) Encapsulation of macromolecules by lipid vesicles under simulated prebiotic conditions. *J Mol Evol.* **18**: 203-206.

Devaraj, G., Parakh, S., Devraj, R., Apte, S., Rao, B. & Rambhau, D. (2002) Release studies on niosomes containing fatty alcohols as bilayer stabilisers instead of cholesterol. *J Colloid Interf Sci.* **251**: 360-365.

Dopico, A. (2007) *Methods in Membrane Lipids (Methods in Molecular Biology)*. USA: Humana Press.

Douce, G., Turcotte, C., Copley, I., Roberts, M., Pizza, M., Domenghini, M., Rappuoli, R. & Dougan, G. (1995) Mutants of *Escherichia coli* heat-labile toxin lacking ADP ribosyltransferase activity act as nontoxic, mucosal adjuvants. *Proc Natl Acad Sci USA.* **92**: 1644-1648.

Dreborg, S. & Akerblom, E. (1990) Immunotherapy with monomethoxypolyethylene glycol modified allergenes. *Crit Rev Ther Drug Carrier Syst.* **6**: 315-365.

Duncan, B. & Needham, D. (2004) Test of the Epstein-Plesset model for gas microparticle dissolution in aqueous media: Effect of surface tension and gas undersaturation in solution. *Langmuir.* **20**: 2567-2578.

Dzata, G., Wyckoff, J. & Confer, A. (1991) Immunopotential of cattle vaccinated with a soluble *Brucella abortus* antigen with low LPS content: an analysis of cellular and humoral immune responses. *Vet Microbiol.* **29**: 15-26.

Edlich, R., Diallo, A., Buchanan, L. & Martin, M. (2003) Hepatitis B virus: a comprehensive strategy for eliminating transmission in the United States. *Long Term Eff Med Implant.* **13**: 117-125.

Eisen, D., Liley, H. & Minchinton, R. (2004) Alternatives to conventional vaccines—mediators of innate immunity. *Curr Drug Targets.* **5**: 89-105.

Esposito, E., Sebben, S., Cortesi, R., Menegatti, E. & Nastruzzi, C. (1999) Preparation and characterization of cationic microspheres for gene delivery. *Int J Pharm.* **189**: 29-41.

Etzler, F. & Deanne, R. (1997) Particle Size Analysis: A Comparison of Various Methods. *Part Part Syst Char.* **14**: 278-282.

Fattal, E. & Barratt, G. (2009) Nanotechnologies and controlled release systems for the delivery of antisense oligonucleotides and small interfering RNA. *Br J Pharmacol.* **157**: 179-194.

Fearon, D. (1997) Seeking wisdom in innate immunity. *Nature.* **388**: 323-324.

Fidler, I. (1988) Targeting of immunomodulators to mononuclear phagocytes for therapy of cancer. *Adv Drug Deliv Rev.* **2**: 69-106.

- Fidler, I. (1992) Systemic macrophage activation with liposome entrapped immunomodulators for therapy of cancer metastasis. *Res Immunol.* **143**: 199-203.
- Fiore, A., Wasley, A. & Bell, B. (2006) Prevention of hepatitis A through active or passive immunization: recommendations of the Advisory Committee on Immunization Practices (ACIP). *MMWR Recomm Rep.* **55**: 1-23.
- Florence, A. & Attwood, D. (2005) *Physicochemical Principles of Pharmacy*. London: Pharmaceutical Press.
- Flynn, J., Chan, J., Triebold, K., Dalton, D., Stewart, T. & Bloom, B. (1993) An essential role for interferon gamma in resistance to *Mycobacterium tuberculosis* infection. *J Exp Med.* **178**: 2249-2254.
- Foged, C., Brodin, B., Frokjaer, S. & Sundblad, A. (2005) Particle size and surface charge affect particle uptake by human dendritic cells in an in vitro model. *Int J Pharm.* **298**: 315-322.
- Fortin, A., Shahum, E., Krzystyniak, K. & Therien, H-M. (1996) Differential Activation of Cell-Mediated Immune Functions by Encapsulated and Surface-Linked Liposomal Antigens. *Cell Immunol.* **169**: 208-217.
- Fox, F. & Herzfield, K. (1954) Gas bubbles with organic skin as cavitation nuclei. *J Acoust Soc Am.* **26**: 1984-1989.
- Frezard, F. (1999) Liposomes: from biophysics to the design of peptide vaccines. *Braz J Med Biol Res.* **32**: 181-189.
- Gall, D. (1966) The adjuvant activity of aliphatic nitrogenous bases. *Immunology.* **11**: 369-386.
- Gammon, B., Virden, J. & Berg, J. (1989) The aggregation kinetics of an electrostatically stabilized dipalmitoyl phosphatidylcholine system. *J Colloid Interface Sci.* **132**: 125-138.
- Garbuzenko, O., Barenholz, Y. & Prie, A. (2005) Effect of grafted PEG on liposome size and compressibility and packing of lipid bilayer. *Chem Phys Lipids.* **135**: 117-129.
- Garcia-Diaz, Y., Wojno, J., Cox, L. & Besra, G. (2009) Synthesis of threitol ceramide and [14C] threitol ceramide, non-glycosidic analogues of the potent CD1 antigen α -galactosyl ceramide. *Tetrahedron: Assymetr.* **20**: 747-753.
- Garcia-Pedrero, J., Kiskinis, E., Parker, M. & Belandia, B. (2007) The SWI/SNF chromatin remodeling subunit BAF57 is a critical regulator of estrogen receptor function in breast cancer cells. *J Biol Chem.* **281**: 22656-22664.

- Gerber, F., Krafft, M., Waton, G. & Vandamme, T. (2006) Microbubbles with exceptionally long life-synergy between shell and internal phase components. *New J Chem.* **30**: 524-527.
- Glenny, A., Pope, C., Waddington, H. & Wallace, V. (1926) The antigenic value of toxoid precipitated by potassium-alum. *J Path Bact.* **29**: 38-45.
- Goldsby, R. A., Kindt, T.J., Osborne, B.A., Kuby, J. (2003) Immunology. W. H. Freeman and Company: New York.
- Godfrey, D., Hammond, K., Poulton, L., Smyth, M. & Baxter, A. (2000) NKT cells: facts, functions and fallacies. *Immunol Today.* **21**: 573-583.
- Gregoriadis, G. & Ryman, B. (1971) Liposomes as carriers of enzymes or drugs: a new approach to the treatment of storage diseases. *Biochem Journal.* **124**: 58.
- Gregoriadis, G. (1979) Drug Carriers in Biology and Medicine: London: Academic Press.
- Gregoriadis, G. (1985) Liposomes for drugs and vaccines. *Trends Biotechnol.* **3**: 235-241.
- Gregoriadis, G. (1988) Liposomes as Drug Carriers. Chichester: John Wiley.
- Gregoriadis, G. (1990) Immunological adjuvants: a role for liposomes. *Immunol Today.* **11**: 89-97.
- Gregoriadis, G. & Florence, A. (1993) Liposomal drug delivery systems: clinical, diagnostic and ophthalmic applications. *Drugs.* **45**: 15-28.
- Gregoriadis, G., Saffie, R. & Hart, S. (1996) High yield incorporation of plasmid DNA within liposomes: effect on DNA integrity and transfection. *J Drug Targeting.* **3**: 469-475.
- Gregoriadis, G., Saffie, R. & de Souza, B. (1997) Liposome-mediated DNA vaccination. *FEBS Lett.* **402**: 107-110.
- Gregoriadis, G. (1998) Genetic vaccines: strategies for optimisation. *Pharmaceut Res.* **15**: 661-670.
- Gregoriadis, G., McCormack, B., Obrenovic, M., Saffie, R., Zadi, B. & Perrie, Y. (1999) Vaccine Entrapment in Liposomes. *Methods.* **19**: 156-162.
- Gregoriadis, G., Bacon, A., Caparros-Wanderley, W. & McCormack, B. (2002) A role for liposomes in genetic vaccination. *Vaccine.* **3462**: 1-9.
- Gun'ko, V., Klyueva, A., Levchuk, Y. & Leboda, R. (2003) Photon correlation spectroscopy investigations of proteins. *Adv Colloid Interface Sci.* **105**: 201-328.

- Gupta, R., Relyveld, E., Lindblad, E., Bizzini, B., Ben-Efraim, S. & Gupta, C. (1993) Adjuvants - a balance between toxicity and adjuvanticity. *Vaccine*. **11**: 293-306.
- Gupta, R. (1998) Aluminum compounds as vaccine adjuvants. *Adv Drug Deliv Rev*. **32**: 155-172.
- Gurumoorthy, A. V. P & Khan, K. H. (2011) Polymers at interfaces: biological and non-biological applications. *Recent Research in Science and Technology*. **3**: 80-86.
- Gzyl, B. & Paluch, M. (2005) Mixed monolayers of dipalmitoyl phosphatidylcholine and ethyl palmitate at the air/water interface. *Appl Surf Sci*. **246**: 356-361.
- Hac-Wydro, K. & Wydro, P. (2007) The influence of fatty acids on model cholesterol/phospholipid membranes. *Chem Phys Lipids*. **150**: 66-81.
- Hac-Wydro, K., Wydro, P., Jagoda, A. & Kapusta, J. (2007) The study on the interaction between phytosterols and phospholipids in model membranes. *Chem Phys Lipids*. **150**: 22-34.
- Hames, B. D. & Hooper, N. M. (2000) Biochemistry. Abingdon: BIOS Scientific.
- Harper, S., Fukuda, K., Cox, N. & Bridges, C. (2003) Using live, attenuated influenza vaccine for prevention and control of influenza: supplemental recommendations of the Advisory Committee on Immunization Practices (ACIP). *MMWR Recomm Rep*. **52**: 1-8.
- Harris, J. (1992) Poly(ethylene glycol) chemistry: biotechnical and biomedical applications. New York: Plenum Press.
- Hasik, M., Kim, D., Howle, L., Needham, D. & Prush, D. (2002) Evaluation of synthetic phospholipid ultrasound contrast agents. *Ultrasonics*. **40**: 973-982.
- Hato, M., Minamikawa, H., Okamoto, K. & Iwahashi, M. (1993) Monolayers of [omega] hydroxyalkyldimethyloctadecylammonium bromide at water-air interface. *J Colloid Interf Sci*. **161**: 155-162.
- Heldt, N., Gauger, M., Zhao, J., Slack, G., Pietryka, J. & Li, Y. (2001) Characterization of a polymer-stabilized liposome system. Reactive and Functional Polymers. *React Funct Polym*. **48**: 181-191.
- Hennig, J., Nauerth, A. & Friedburg, H. (1986) RARE imaging: a fast imaging method for clinical MR. *Magn Reson Med*. **3**: 823-833.
- Henriksen-Lacey, M., Bramwell, V., Christensen, D., Agger, E., Andersen, P. & Perrie, Y. (2010) Liposomes based on dimethyldioctadecylammonium promote a depot effect and enhance immunogenicity of soluble antigen. *J Control Release*. **142**: 180-186.

- Hiemenz, P. C., Rajagopalan, R. (1997) Principle of Colloid and Surface Chemistry. New York: Marcel Dekker.
- Hilgers, L., Snippe, H., Jansze, M. & Willers, J. M. (1985) Combination of two synthetic adjuvants: synergistic effects of a surfactant and a polyanion on the humoral response. *Cell Immunol.* **92**: 203-209.
- Hilgers, L. & Snippe, H. (1992) DDA as an immunological adjuvant. *Res Immunol.* **143**: 494-503.
- Hoff, L. (1996) Acoustic properties of ultrasonic contrast agents. *Ultrasonics.* **34**: 591-593.
- Hoffmann, J., Kafatos, F., Janeway, C. & Ezekowitz, R. (1999) Phylogenetic perspectives in innate immunity. *Science.* **284**: 1313-1318.
- Holten-Andersen, L., Doherty, T., Korsholm, K. & Andersen, P. (2004) Combination of the cationic surfactant dimethyldioctadecylammonium bromide and synthetic mycobacterial cord factor as an efficient adjuvant for tuberculosis subunit vaccines. *Infect Immun.* **72**: 1608-1617.
- Horisawa, E., Kubota, K., Tuboi, I., Sato, K., Yamamoto, H., Takeuchi, H. & Kawashima, Y. (2002) Size-dependency of DL-lactide/glycolide copolymer particulates for intra-articular delivery system on phagocytosis in rat synovium. *Pharm Res.* **19**: 132-139.
- Hsu, M. & Juliano, R. (1982) Interactions of liposomes with the reticuloendothelial system. II: Nonspecific and receptor-mediated uptake of liposomes by mouse peritoneal macrophages. *Biochim Biophys Acta.* **720**: 411-419.
- Huang, C. (1969) Studies of phosphatidylcholine vesicles. Formation and physical characteristics. *Biochemistry.* **8**: 344-351.
- Huang, Y., Chen, J., Chen, X., Gao, X. & Liang, W. (2008) PEGylated synthetic surfactant vesicles (Niosomes): novel carriers for oligonucleotides. *J Mater Sci Mater Med.* **19**: 607-614.
- Huntington, J. & Stein, P. (2001) Structure and properties of ovalbumin. *J Chromatogr B.* **756**: 189-198.
- Immordino, M. L., Dosio, F. & Cattell, L. (2006) Stealth Liposomes: Review of the Basic Science, Rationale, and Clinical Applications, Existing and Potential. *Int J Nanomed.* **1**: 297-315.
- Ivanov, V., Preobrazhensky, S., Tsibulshy, V., Babaev, V., Repin, V. & Smirnov, V. (1985) Liposome uptake by cultured macrophages mediated by modified low-density lipoproteins. *Biochim Biophys Acta.* **846**: 76-84.

- Iwasaki, A. & Medzhitov, R. (2004) Toll-like receptor control of the adaptive immune responses. *Nat Immunol.* **5**: 987-995.
- Janeway, C. (1989) Immunogenicity signals 1,2,3 ... and 0. *Immunol Today.* **10**: 283-286.
- Johnson, S., Bangham, A., Hill, M. & Korn, E. (1971) Single bilayer liposomes. *Biochim Biophys Acta.* **233**: 820-826.
- Jubeh, T., Barenholz, Y. & Rubinstein, A. (2004) Differential adhesion of normal and inflamed rat colonic mucosa by charged liposomes. *Pharm Res.* **21**: 447-453.
- Kahl, L., Scott, C., Lelchuk, R., Gregoriadis, G. & Liew, F. (1989) Vaccination against murine cutaneous leishmaniasis by using *Leishmania major* antigen/liposomes. Optimization and assessment of the requirement for intravenous immunization. *J Immunol.* **142**: 4441-4449.
- Kaisho, T. & Akira, S. (2002) Toll-like receptors as adjuvant receptors. *Biochim Biophys Acta.* **1589**: 1-13.
- Katragadda, A., Bridgman, R. & Betageri, G. (2000) Effect of liposome composition and cholesterol on the cellular uptake of stavudine by human monocytes/macrophages. *Cell Mol Biol Lett.* **5**: 483-493.
- Kawano, T., Cui, J., Koezuka, Y., Toura, I., Kaneko, Y., Motoki, K., Ueno, H., Nakagawa, R., Sato, H. & Kondo, E. e. a. (1997) CD1d-Restricted and TCR-Mediated Activation of V9 (alpha) 14 NKT Cells by Glycosylceramides. *Science.* **278**: 1626-1629.
- Keller, B. C., Lasic, D. D. (2005) Self-forming, thermodynamically stable liposomes and their applications. Available from: <http://www.patentstorm.us/patents/7150883/description.html> [Accessed 15 October 2008].
- Kenworthy, A., Hristova, K., Needham, D. & McIntosh, T. (1995) Range and magnitude of the steric pressure between bilayers containing phospholipids with covalently attached poly(ethylene glycol). *Biophys J.* **68**: 1921-1936.
- Kirby, C. & Gregoriadis, G. (1984a) Dehydration-rehydration vesicles (DRV): A new method for high yield drug entrapment in liposomes. *Biotechnology.* **2**. 979-984.
- Kirby, C. & Gregoriadis, G. (1984b) Preparation of liposomes containing factor VIII for oral treatment of haemophilia. *J Microencapsul.* **1**: 33-45.
- Kirby, D., Rosenkrands, I., Agger, E., Andersen, P., Coombes, A. & Perrie, Y. (2008a) PLGA microspheres for the delivery of a novel subunit TB vaccine. *J Drug Target.* **16**: 282-293.

- Kirby, D., Rosenkrands, I., Agger, E., Andersen, P., Coombes, A. & Perrie, Y. (2008b) Liposomes act as stronger subunit vaccine adjuvants when compared to microspheres. *J Drug Target*. **16**: 543-554.
- Klinguer, C., Beck, A., De-Lys, P., Bussat, M., Blaecke, A., Derouet, F., Bonnefoy, J., Nguyen, T., Corvaia, N. & Velin, D. (2001) Lipophilic quaternary ammonium salt acts as a mucosal adjuvant when co-administered by the nasal route with vaccine antigens. *Vaccine*. **19**: 4236-4244.
- Klinman, D., Conover, J. & Coban, C. (1999) Repeated administration of synthetic oligodeoxynucleotides expressing CpG motifs provides long-term protection against bacterial infection. *Infect Immun*. **67**: 5658-5663.
- Korsholm, K., Agger, E., Foged, C., Christensen, D., Dietrich, J., Andersen, C.-S., Geisler, C. & Andersen, P. (2007) The adjuvant mechanism of cationic dimethyldioctadecylammonium liposomes. *Immunology*. **121**: 216-226.
- Korsholm, K., Petersen, R., Agger, E. & Andersen, P. (2010) T-helper 1 and T-helper 2 adjuvants induce distinct differences in the magnitude, quality and kinetics of the early inflammatory response at the site of injection. *Immunology*. **129**: 75-86.
- Krieg, A. (2006) Therapeutic potential of Toll-like receptor 9 activation. *Nat Rev Drug Discov*. **5**: 471-484.
- Kriwet, K. & Muller-Goymann, C. (1994) Mutual interactions between diclofenac diethylamine and phospholipids – investigation on the microstructure of the arisen systems. *Pharmazie*. **49**: 187-191.
- Krug, A., Towarowski, A., Britsch, S., Rothenfusser, S., Hornung, V., Bals, R., Giese, T., Engemann, H., Endres, S., Krieg, A. & Hartmann, G. (2001) Toll-like receptor expression reveals CpG DNA as a unique microbial stimulus for plasmacytoid dendritic cells which synergizes with CD40 ligand to induce high amounts of IL-12. *Eur J Immuno*. **31**: 3026-3037.
- Kuhl, T., Leckband, D., Lasic, D. & Israelachvili, J. (1994) Modulation of interaction forces between bilayers exposing short-chained ethylene oxide headgroups. *Biophys J*. **66**: 1479-1488.
- Lahiria, A., Dasa, P. & Chakravorty, D. (2008) Engagement of TLR signaling as adjuvant: Towards smarter vaccine and beyond. *Vaccine*. **26**: 6777-6783.
- Langermans, J., Doherty, T., Vervenne, R., Laan, T., Lyaschchenko, K., Greenwald, R., Agger, E., Aagaard, C., Weiler, H., Soolingen, D., Dalemans, W., Thomas, A. & Andersen, P. (2005) Protection of macaques against Mycobacterium tuberculosis infection by a subunit vaccine based on a fusion protein of antigen 85B and ESAT-6. *Vaccine*. **23**: 2740-2750.

- Lasic, D. & Martin, F. (1995) *Stealth Liposomes*. Boca Raton, FL: CRC Press.
- Lasic, D. & Papahadjopoulos, D. (1995) Liposomes revisited. *Science*. **267**: 1275-1276.
- Lee, K.-D., Nir, S. & Papahadjopoulos, D. (1993) Quantitative analysis of liposome-cell interactions *in vitro*: rate constants of binding and endocytosis with suspension and adherent J774 cells and human monocytes. *Biochemistry*. **32**: 889-899.
- Leen, E. & Horgan, P. (2003) Ultrasound contrast agents for hepatic imaging with nonlinear modes. *Curr Probl Diagn Radiol*. **32**: 66-87.
- Lees, I. (2008) The determination of the phase diagram for a dmpc/dspc lipid mixture using ²H NMR difference spectroscopy. Available from: <http://www.vavasour.ca/irene/bsc.pdf>. [Accessed 29th October 2011].
- Leserman, L., Machy, P. & Barbet, J. (1981) Cell-specific drug transfer from liposomes bearing monoclonal antibodies. *Nature*. **293**: 226-228.
- Levchenko, T., Rammohan, R., Lukyanov, A., Whiteman, K. & Torchilin, V. (2002) Liposome clearance in mice: the effect of a separate and combined presence of surface charge and polymer coating. *Int J Pharm*. **240**: 95-102.
- Levine, L., Stone, J. & Wyman, L. (1955) Factors affecting the efficiency of the aluminum adjuvant in diphtheria and tetanus toxoids. *J Immunol*. **75**: 301-307.
- Liang, C. H. & Chou, T. H. (2009) Effect of chain length on physicochemical properties and cytotoxicity of cationic vesicles composed of phosphatidylcholines and dialkyldimethylammonium bromides. *Chem Phys Lipids*. **158**: 81-90.
- Lima, K., Aparecida dos Santos, S., Rodrigues, J. J. & Silva, C. (2004) Vaccine adjuvant: it makes the difference. *Vaccine*. **22**: 2374-2379.
- Lincopan, N., Mamizuka, E. & Carmona-Ribeiro, A. (2003) *In vivo* activity of a novel amphotericin B formulation with synthetic cationic bilayer fragments. *J Antimicrob Chemoth*. **52**: 412-418.
- Lindblad, E., Elhay, M., Silva, R., Appelberg, R. & Andersen, P. (1997) Adjuvant modulation of immune responses to tuberculosis subunit vaccines. *Infect Immun*. **65**: 623-629.
- Lindenstrom, T., Agger, E., Korsholm, K., Darrah, P., Aagaard, C. & Seder, R. (2009) Tuberculosis subunit vaccination provides long-term protective immunity characterised by multifunctional CD4 memory T cells. *J Immunol*. **182**: 8047-8055.

Liu, D., Chen, W. Y., Tasi, L. M., & Yang, S. P. (2000) The effects of cholesterol on the release of free lipids and the physical stability of lecithin liposomes. *J Chin Inst Chem Eng.* **31**: 269-276.

Liu, R., Wei, X., Yao, Y., Chai, Q., Chen, Y. & Xu, Y. (2005) The preparation and characterisation of gas bubble containing liposomes. *Engineering in Medicine and Biology 27th Annual Conference.* Shanghai.

Lopes, L., Scarpa, M., Silva, G., Rodrigues, D., Santilli, C. & Oliveira, A. (2004) Studies on the encapsulation of diclophenac in small unilamellar liposomes of soya phosphatidylcholine. *Colloid Surface B.* **39**: 151-158.

Lorenz, M., Holzapfel, V., Musyanovych, A., Nothelfer, K., Walther, P., Frank, H., Landfester, K., Schrezenmeier, H., & Mailander V. (2006) Uptake of functionalized, fluorescent-labeled polymeric particles in different cell lines and stem cells. *Biomaterials.* **27**: 2820-2828.

Mackett, M. & Williamson, J. D. (1995) *Human Vaccines and Vaccination.* Oxford: BIOS Scientific Publishers Ltd.

Madigan, M., Martinko, J. & Parker, J. (2000) *Biology of Microorganisms.* New Jersey: Prentice-Hall.

Magee, W., Goff, C., Schoknecht, J., Smith, M. & Cherian, K. (1974) The interaction of cationic liposomes containing horseradish peroxidase with cells in culture. *J Cell Biol.* **63**: 492-504.

Majumdar, S., Flasher, D., Friend, D., Nassos, P., Yajko, D., Hadley, W. & Duzgunes, N. (1992) Efficacies of liposome-encapsulated streptomycin and ciprofloxacin against *Mycobacterium avium-M.intracellulare* complex infections in human peripheral blood monocyte/macrophages. *Antimicrob Agents Chemother.* **36**: 2808-2815.

Malcharek, S., Hinz, A., Hilterhaus, L. & Galla, H. (2005) Multilayer structures in lipid monolayer films containing surfactant protein C: effects of cholesterol and POPE. *Biophys J.* **88**: 2638-2649.

Malvern Instruments Ltd (2008) The use of zeta potential measurements to study sterically stabilized liposomes using Malvern Instruments. Available from: <http://www.azonano.com/details.asp?ArticleID=1214>. [Accessed 10th February 2009].

Malvern Instruments Ltd (2009) Analyzing Light Scattering Data. Available from: http://www.malvern.co.uk/LabEng/technology/laser_diffraction/what_is_particle_size.htm. [Accessed 30 November 2008].

- Mann, J., Shakir, E., Carter, K., Mullen, A., Alexander, J. & Ferro, V. (2009) Lipid vesicle size of an oral influenza vaccine delivery vehicle influences the Th1/Th2 bias in the immune response and protection against infection. *Vaccine*. **27**: 3643-3649.
- Marx, P., Compans, R., Gettie, A., Staas, J., Gilley, R., Mulligan, M., Yamshchikov, G., Chen, D. & Eldridge, J. (1993) Protection against vaginal SIV transmission with microencapsulated vaccine. *Science*. **260**: 1323-1327.
- Mastelic, B., Ahmed, S., Egan, W. M., Del Giudice, G., Golding, H., Gust, I., Neels, P., Reed, S., Sheets, R., Siegrist, C. & Lambert, P. (2010) Mode of action of adjuvants: Implications for vaccine safety and design. *Biologicals*. **38**: 594-601.
- Matsuda, J., Naidenko, O., Gapin, L., Nakayama, T., Taniguchi, M., Wang, C., Koezuka, Y. & Kronenberg, M. (2000) Tracking the response of natural killer T cells to a glycolipid antigen using CD1d tetramers. *J Exp Med*. **192**: 741-753.
- McElrath, M. (1995) Selection of potent immunological adjuvants for vaccine construction. *Semin Cancer Biol*. **6**: 375-385.
- McNeil, S. & Perrie, Y. (2006) Gene Delivery using cationic lipids. *Expert Opin in Ther Pat*. **16**: 1371-1382.
- Medscape (2010) Monograph - Doxorubicin Hydrochloride. Available from: <http://www.medscape.com/druginfo/monograph?cid=med&drugid=7750&drugname=Doxorubicin+IV&monotype=monograph&secid=9>. [Accessed 30th March 2011].
- Medzhitov, R., Preston-Hurlburt, P. & Janeway, C. J. (1997) A human homologue of the Drosophila Toll protein signals activation of adaptive immunity. *Nature*. **388**: 394-397.
- Miller, C., Bondurant, B., McLean, S., McGovern, K. & O'Brien, D. (1998) Liposome-cell interactions *in vitro*: effect of liposome surface charge on the binding and endocytosis of conventional and sterically stabilized liposomes. *Biochemistry*. **37**: 12875-12883.
- Mohammed, A. R., Perrie, Y. (2005) Liposome solutions for poorly soluble drugs. Drug delivery report. *Technology overviews*. Available from: www.drugdeliveryreport.com/articles/ddr_w2005_article14.pdf. [Accessed 23th November 2008].
- Moghimi, S. & Szebeni, J. (2003) Stealth liposomes and long circulating nanoparticles: critical issues in pharmacokinetics, opsonization and protein-binding properties. *Progress in Lipid Research*. **42**: 463-478.
- Morris, R., Vangala, A., Bencsik, M. & Perrie, Y. (2007) Three dimensional fluid pressure mapping in porous media using magnetic resonance imaging with gas filled liposomes. *Magn Reson Imaging*. **25**: 509-512.

- Morris, R., Bencsik, M., Nestle, N., Galvosas, P., Fairhurst, D., Vangala, A., Perrie, Y. & McHale, G. (2008) Robust spatially resolved pressure measurements using MRI with novel buoyant advection-free preparations of stable microbubbles in polysaccharide gels. *J Magn Reson.* **193**: 159-167.
- Mosmann, T. & Sad, S. (1996) The expanding universe of T-cell subsets: Th1, Th2 and more. *Immunol Today.* **17**: 138-146.
- Murata, J., Kitamoto, T., Ohya, Y. & Ouchi, T. (1997) Effect of dimerization of the Dglucose analogue of muramyl dipeptide on stimulation of macrophage-like cells. *Carbohydr Res.* **297**: 127-133.
- Needham, D., McIntosh, T. & Lasic, D. (1992) Repulsive interactions and mechanical stability of polymer-grafted lipid membranes. *Biochim Biophys Acta.* **1108**: 40-48.
- Needham, D. & Kim, D. (2001) Methods for producing gas microbubbles having lipid-containing shells formed thereon. Duke University (Durham, NC) patent, 09/451627, US.
- New, R. R. C., Black, C. D. V., Parker, R. J., Puri, A., Scherphof, G. L. (1990) Preparation of liposomes. In New, R. (Ed.) *Liposomes, a practical approach*. Oxford University Press.
- Nichol, K., Mendelman, P., Mallon, K., Jackson, L., Gorse, G., Belshe, R., Glezen, W. & Wittes, J. (1999) Effectiveness of live, attenuated intranasal influenza virus vaccine in healthy, working adults: a randomized controlled trial. *Jama.* **282**: 137-144.
- Nisbet, A., Saundry, R., Moir, A., Fothergill, L. & Fothergill, J. (1981) The complete amino acid sequence of hen ovalbumin. *Eur J Biochem.* **115**: 335-345.
- Northfelt, D., Dezube B. J., Thommes J. A., Miller B. J., Fischl M. A., Friedman-Kien, A., Kaplan, L. D., Du Mond, C., Mamelok, R. D. & Henry, D. H. (1998) Pegylated-liposomal doxorubicin versus doxorubicin, bleomycin, and vincristine in the treatment of AIDS-related Kaposi's sarcoma: results of a randomized phase III clinical trial. *J Clin Oncol.* **16**: 2445-2451.
- O'Doherty, M. (2004) What are liposomes? *Nanobiotechnology and Bioanalysis Group*. Available from: http://www.etseq.urv.es/dinamic/catala/places/liposome_lit_review.doc [Accessed 12th October 2008].
- O'Hare, T., Walters, D., Stoffregen, E., Sherbenou, D., Heinrich, M., Deininger, M. & Druker, B. (2005) Combined Abl Inhibitor Therapy for Minimizing Drug Resistance in Chronic Myeloid Leukemia: Src/Abl Inhibitors Are Compatible with Imatinib. *Clin Cancer Res.* **11**: 6987-6993.
- Ohlerth, S. & O'Brien, R. (2007) Contrast ultrasound: General principles and veterinary clinical applications. *Vet J.* **174**: 501-512.

- Olds, G., Chedid, L., Lederer, E. & Mahmoud, A. (1980) Induction of Resistance to *Schistosoma-Mansoni* by Natural Cord Factor and Synthetic Lower Homologs. *J Infect Dis.* **141**: 473-478.
- Olsen, A., Pinxteren, L., Okkels, L., Rasmussen, P. & Andersen, P. (2001) Protection of mice with a tuberculosis subunit vaccine based on a fusion protein of antigen 85B and ESAT-6. *Infect Immun.* **69**: 2773-2778.
- Opanasopit, P., Nishikawa, M. & Hashida, M. (2002) Factors affecting drug and gene delivery: effects of interaction with blood components. *Crit Rev Ther Drug Carrier Syst.* **19**: 191-233.
- Oussoren, C., Zuidema, J., Crommelin, D. & Storm, G. (1997) Lymphatic uptake and biodistribution of liposomes after subcutaneous injection. II. Influence of liposomal size, lipid composition and lipid dose. *Biochem Biophys Acta.* **1328**: 261-272.
- Parekh, V., Lalani, S., Kim, S., Halder, R., Azuma, M., Yagita, H., Kumar, V., Wu, L. & Van Kaer, L. (2009) PD-1/PD-L Blockade Prevents Anergy Induction and Enhances the Anti-Tumor Activities of Glycolipid-Activated Invariant NKT Cells. *J Immunol.* **182**: 2816-2826
- Parham, P. (2009) The immune system. Oxford: Taylor & Francis.
- Pashine, A., Valiante, N. & Ulmer, J. (2005) Targeting the innate immune response with improved vaccine adjuvants. *Nat Med Supplement.* **11**: 63-68.
- Perrie, Y. & Gregoriadis, G. (2000a) Liposomal DNA vaccines: Structural Characteristics. In Gregoriadis, G. & McCormack, B. (Eds.) *Targeting of drugs: strategies for gene constructs and delivery*. IOS Press.
- Perrie, Y. & Gregoriadis, G. (2000b) Liposome-entrapped plasmid DNA: characterisation studies. *Biochim Biophys Acta.* **1475**: 125-132.
- Perrie, Y., Frederik, P. & Gregoriadis, G. (2001) Liposome-mediated DNA vaccination: the effect of vesicle composition. *Vaccine.* **19**: 3301-3310.
- Perrie, Y., McNeil, S. & Vangala, A. (2003) Liposome-mediated DNA immunisation via the subcutaneous route. *J Drug Target.* **11**: 555-563.
- Perrie, Y. (2005) How pharmaceutical scientists are going prospecting for black gold. *Pharm J.* **275**: 809.
- Perrie, Y. (2006) Vaccines: an overview and update. *Pharm J.* **276**: 209-213.
- Petrovsky, N. & Aguilar, J. C. (2004) Vaccine adjuvants: Current state and future trends. *Immunol Cell Biol.* **82**: 488-496.

- Pettis, R. (2000) Aerosol Delivery of Muramyl Dipeptide to Rodent Lungs. *AAPS Pharmsci.* **2**: 1-9.
- Phillips, D., Chen, X., Baggs, R., Rubens, D., Violante, M. & Parker, K. (1998) Acoustic backscatter properties of the particle/bubber ultrasound contrast agent. *Ultrasonics.* **36**: 883-892.
- Pimm, M., Baldwin, R., Polonsky, J. & Lederer, E. (1979) Immunotherapy of an ascitic rat hepatoma with cord factor (trehalose-6, 6'-dimycolate) and synthetic analogs. *Int J Cancer.* **24**: 780-785.
- Pitt, W. & Hussein, G. (2008) On bubbles and liposomes. *J Control Release.* **125**: 174-177.
- Playfair, J. & Bancroft, G. (2004) *Infection and Immunity.* Oxford: Oxford University Press.
- Poste, G. (1983) Liposome targeting *in vivo*: problems and opportunities. *Biology of the Cell.* **47**: 19-38.
- Powell, G. (1980) Polyethylene glycol. In Davidson, R. (Ed.) *Handbook of water soluble gums and resins.* McGraw-Hill.
- Quaia, E. (2005) *Contrast Media in Ultrasonography: Basic Principles and Clinical Applications (Medical Radiology / Diagnostic Imaging).* New York: Springer Berlin Heidelberg.
- Rahman, A., Kessler, A., More, N., Sikic, B., Rowden, G., Woolley, P. & Schein, P. (1980) Liposome production of adriamycin-induced cardiotoxicity in mice. *Cancer Res.* **40**: 1532-1537.
- Ramon, G. (1926) Procédres pour accroître la production des antitoxines. *Annual Institut Pasteur.* **40**: 1-10.
- Ramon, G. (1959) Certain works presented at the Academie Nationale de Medecine (Paris) from 1925 to 1950. *Rev Immunol Ther Antimicrob.* **23**: 359-401.
- Rao, M. & Alving, C. (2000) Delivery of lipids and liposomal proteins to the cytoplasm and Golgi of antigen-presenting cells. *Adv Drug Deliv Rev.* **41**: 171-188.
- Rao, M., Bray, M., Alving, C., Jahrling, P. & Matyas, G. (2002) Induction of immune responses in mice and monkeys to ebola virus after immunization with liposome encapsulated irradiated ebola virus: protection in mice requires CD4⁺ T cells. *J Virol.* **76**: 9176-9185.

Ratner, S., Schroit, A., Vinson, S. & Fidler, I. (1986) Analogous recognition of phospholipids by insect phagocytes and mammalian macrophages. *Proc Soc Exp Biol Med.* **182**: 272-276.

Raz, A., Bucana, C., Fogler, W., Poste, G. & Fidler, I. (1981) Biochemical, morphological and ultrastructural studies on the uptake of liposomes by murine macrophages. *Cancer Res.* **41**: 487-494.

Reddy, S., van der Vlies, A., Simeoni, E., Angeli, V., Randolph, G., O'Neil, C., Lee, L., Swartz, M. & Hubbell, J. (2007) Exploiting lymphatic transport and complement activation in nanoparticle vaccines. *Nature Biotech.* **25**: 1169-1164.

Rentech (2009) Carbon Dioxide. Available from: <http://www.rentechinc.com/carbonDioxide.php>. [Accessed 5th November 2010].

Riess, J. (2001) Oxygen carriers (blood substitutes) chemistry and some physiology. *Chem Rev.* **101**: 2797-2920.

Robinson, R., DeVita, V., Levy, H., Baron, S., Hubbard, S. & Levine, A. (1976) A phase I-II trial of multiple-dose polyriboinosic-polyribocytidylic acid in patients with leukemia or solid tumors. *J Natl Cancer Inst.* **57**: 599-602.

Rongen, H., Bult, A. & van Bennekom, W. (1997) Liposomes and immunoassays. *J Immunol Methods.* **204**: 105-133.

Rosenkrands, I., Agger, E., Olsen, A., Korsholm, K., Andersen, C., Jensen, K. & Andersen, P. (2005) Cationic liposomes containing mycobacterial lipids - a new powerful Th1 adjuvant system. *Infect Immun.* **73**: 5817-5826.

Salem, M., El-Naggar, S., Kadima, A., Gillanders, W. & Cole, D. (2006) The adjuvant effects of the toll-like receptor 3 ligand polyinosinic-cytidylic acid poly (I:C) on antigen-specific CD8+ T cell responses are partially dependent on NK cells with the induction of a beneficial cytokine milieu. *Vaccine.* **24**: 5119-5132.

Scherphof, G. & Kamps, J. (1998) Receptor vs non-receptor mediated clearance of liposomes. *Adv Drug Delivery Rev.* **32**: 81-97.

Scherphof, G., Kuipers, F., Derksen, J., Spanjer, H. & Vonk, R. (1987) Liposomes *in vivo*; conversion of liposomal cholesterol to bile salts. *Biochem Soc Trans.* **15**: 625-628.

Scherphof, G., Velinova, M., Kamps, J., Donga, J., Want, H., Kuipers, F., Havekes, L. & Daemen, T. (1997) Modulation of pharmacokinetic behavior of liposomes. *Adv Drug Delivery Rev.* **24**: 179-191.

Schiffelers, R., Crommelin, D. & Storm, G. (2006) Silencing proteins. In Torchilin, V. (Ed.) *Delivery of Protein and Peptide Drugs in Cancer*. London: Imperial College Press.

- Schmieg, J., Yang, G., Franck, R., Van Rooijen, N. & Tsuji, M. (2005) Glycolipid presentation to natural killer T cells differs in an organ-dependent fashion. *P Natl Acad Sci USA*, **102**: 1127-1132.
- Schneider, M. (1999) Characteristics of SonoVue trade mark. *Echocardiography*. **16**: 743-746.
- Schreier, S., Malleiros, S. & de Paula, E. (2000) Surface active drugs: self-association and interaction with membranes and surfactants. Physicochemical and biological aspects. *Biochim Biophys Acta*. **1508**: 210-234.
- Schwendener, R., Lagocki, P. & Rahman, Y. (1984) The effects of charge and size on the interaction of unilamellar liposomes with macrophages. *Biochim Biophys Acta*. **772**: 93-101.
- Shahum, E. & Therien, H. M. (1988) Immunopotential of the humoral response by liposomes: encapsulation versus linkage. *Immunology*. **65**: 315-317.
- Shaw, D. J. (1992) Introduction to Colloid and Surface Chemistry. Oxford: Butterworth-Heinemann.
- Shek, P. & Sabiston, B. (1982) Immune response mediated by liposome-associated protein antigens. II. Comparison of the effectiveness of vesicle-entrapped and surface-associated antigens in immunopotential. *Immunology*. **47**: 627-632.
- Shrestha, L., Acharya, D., Sharma, S., Aramaki, K., Asaoka, H., Ihara, K., Tsunehiro, T. & Kunieda, H. (2006) Aqueous foam stabilised by dispersed surfactant solid and lamellar liquid crystalline phase. *J Colloid Interface Sci*. **301**: 274-281.
- Silk, J., Salio, M., Reddy, B., Shepherd, D., Gileadi, U., Brown, J., Masri, S., Polzella, P., Ritter, G. & Besra, G. (2008) Nonglycosidic CD1d lipid ligands activate human and murine invariant NKT cells. *J Immunol*. **180**: 6452-6456
- Silverstein, S., Steiman, R. & Cohn, Z. (1977) Endocytosis. *Annu Rev Biochem*. **46**: 669-772.
- Singer, V., Jones, L., Yue, S. & Haugland, R. (1997) Characterization of PicoGreen reagent and development of a fluorescence-based solution assay for double-stranded DNA quantitation. *Anal Biochem*. **249**: 228-238.
- Singh, M., Ott, G., Kazzaz, J., Ugozzoli, M., Briones, M., Donnelly, J. & O'Hagan, D. (2001) Cationic microparticles are an effective delivery system for immune stimulatory CpG DNA. *Pharm Res*. **18**: 1476-1479.
- Skarba, M. (2008) Interactions of Colloidal Particles with Simple Electrolytes and Polyelectrolytes. Available from: <http://www.unige.ch>. [Accessed 25th March 2011].

- Smith Korsholm, K., Agger, E., Foged, C., Christensen, D., Dietrich, J., Andersen, C., Geisler, C. & Andersen, P. (2007) The adjuvant mechanism of cationic dimethyldioctadecylammonium liposomes. *Immunology*. **121**: 216-226.
- Snippe, H., de Reuver, M., Beunder, J., van der Meer, J., van Wichen, D. & Willers, J. (1982) Delayed-type hypersensitivity in rabbits. Comparison of the adjuvants dimethyl dioctadecyl ammonium bromide and Freund's complete adjuvant. *Int Arch Allergy Appl Immunol*. **67**: 139-144.
- Spack, E. & Sorgi, F. (2001) Developing non-viral DNA delivery systems for cancer and infectious disease. *Drug Discov Today*. **6**: 186-197.
- Spada, F., Borriello, F., Sugita, M., Watts, G., Koezuka, Y. & Porcelli, S. (2000) Low expression level but potent antigen presenting function of CD1d on monocyte lineage cells. *Eur J Immunol*. **30**: 3468-3477.
- Stanfield, J., Gall, D. & Bracken, P. (1973) Single-dose antenatal tetanus immunisation. *Lancet*. **1**: 215-219.
- Stewart-Tull, D. (1991) The assessment and use of adjuvants. New York: Plenum Press.
- Storm, G. & Crommelin, D. (1998) Liposomes: quo vadis? *Pharm Sci Techn Today*. **1**: 19-31.
- Stoye, I., Schroder, K. & Muller-Goymann, C. (1998) Transformation of a liposomal dispersion containing ibuprofen lysinate and phospholipids into mixed micelles physicochemical characterization and influence on drug permeation through excised human stratum corneum. *Eur J Pharm Biopharm*. **46**: 191-200.
- Strasberg, M. (1959) Onset of ultrasonic cavitation in tap water. *J Acoust Soc Am*. **31**: 163-176.
- Straubinger, R., Hong, K., Friend, D. & Papahadjopoulos, D. (1983) Endocytosis of liposomes and intracellular fate of encapsulated contents: encounter with a low-pH compartment after internalization in coated vesicles. *Cell*. **32**: 1069-1079.
- Stuart-Harris, C. H. (1969) Adjuvant influenza vaccines. *Bull WHO*. **41**: 617-621.
- Stumpo, R., Kauer, M., Martin, S. & Kolb, H. (2003) IL-10 induces gene expression in macrophages: partial overlap with IL-5 but not with IL-4 induced genes. *Cytokine*. **24**: 46-56.
- Sudhakar, P., Subramani, P. (2005) Mechanisms of Bacterial Pathogenesis and Targets for Vaccine Design. Available from: <http://www.jyi.org/research/re.php?id=610>. [Accessed 24th November 2010].

- Sulkowski, W., Pentak, D., Nowak, K. & Sulkowska, A. (2005) The influence of temperature, cholesterol content and pH on liposome stability. *J Mol Struct.* **744**: 737-747.
- Sullivan, B. & Kronenberg, M. (2005) Activation or anergy: NKT cells are stunned by alpha-galactosylceramide. *J Clin Invest.* **115**: 2328-2329.
- Suzuki, Y., Shibata, K., Kikkawa, F., Kajiyama, H., Ino, K. & Nomura, S. (2003) Possible role of placental leucine aminopeptidase (P-LAP) in the antiproliferative effect of oxytocin in human endometrial adenocarcinoma. *Clin Cancer Res.* **9**: 1528-1534.
- Suzuki, R., Takizawa, T., Negishi, Y., Hagsisawa, K., Tanaka, K., Sawamura, K., Utoguchi, N., Nishioka, T. & Maruyama, K. (2007) Gene delivery by combination of novel liposomal bubbles with perfluoropropane and ultrasound. *J Control Release.* **117**: 130-136.
- Suzuki, R., Oda, Y., Utoguchi, N., Namaia, E., Taira, Y., Okadab, N., Kadowakic, N., Kodamad, T., Tachibanae, K. & Maruyama, K. (2009) A novel strategy utilizing ultrasound for antigen delivery in dendritic cell-based cancer immunotherapy. *J Control Release.* **133**: 198-205.
- Szoka, F. & Papahadjopoulos, D. (1978) Procedure for preparation of liposomes with large internal aqueous space and high capture by reverse-phase evaporation. *P Natl Acad Sci USA.* **75**: 4194-4198.
- Szoka, F. & Papahadjopoulos, D. (1980) Comparative properties and methods of preparation of lipid vesicles (liposomes). *Annu Rev Biophys Bioeng.* **9**: 467-508.
- Takeda, K., Kaisho, T. & Akira, S. (2003) Toll-like receptors. *Annu Rev Immunol.* **21**: 335-376.
- Tanford, C. (Ed.) (1980) *The Hydrophobic Effect: Formation of Micelles and Biological Membranes.* New York: John Wiley and Sons.
- Taylor, D., Dong, Y. & Jones, C. (1996) Characterization of monolayers and LB multilayers of dioctadecyldimethylammonium chloride. *Thin Solid Films Seventh International Conference on Organized Molecular Films.*
- Therien, H. M. & Shahum, E. (1996) Differential biodistribution of encapsulated and surface-linked liposomal antigens. *Biochim Biophys Acta.* **1280**: 91-97.
- Thoelen, S., Van Damme, P., Mathei, C., Leroux-Roels, G., Desombere, L., Safary, A., Vandepapeliere, P., Slaoui, M. & Ehues, A. (1998) Safety and immunogenicity of a hepatitis B vaccine formulated with a novel adjuvant system. *Vaccine,* **16**: 708-714.

- Torchilin, V. (1985) Liposomes as targetable drug carriers. *Crit Rev Ther Drug Carrier Syst.* **2**: 65-115.
- Torchilin, V. P., Zhou, F. & Huang, L. (1993) pH-Sensitive liposomes. *J Liposome Res.* **3**: 201-255.
- Torchilin, V., Omelyanenko, V., Papisov, M., Bogdanov, A. J., Trubetskoy, V., Herron, J. & Gentry, C. (1994) Poly(ethylene glycol) on the liposome surface: on the mechanism of polymer-coated liposomes longevity. *Biochim Biophys Acta.* **1195**: 11-20.
- Torchilin, V. (1996) Liposomes as delivery agents for medical imaging. *Mol Med Today.* 242-249.
- Torchilin, V. (1997) Surface-modified liposomes in gamma and MR-imaging. *Adv Drug Deliv Rev.* **24**: 301-313.
- Tran, T., Roger, S., Le Guennec, J., Tranquart, F. & Bouakaz, A. (2007) Effect of ultrasound-activated microbubbles on the cell electrophysiological properties. *Ultrasound Med Biol.* **33**: 158-163.
- Tscharnutter, W. (2000) Photon Correlation Spectroscopy in Particle Sizing. In Meyers, R. (Ed.) *Encyclopaedia of Analytical Chemistry*. John Wiley & Sons.
- Uhumwangho, M. & Okor, R. (2005) Current trends in the production and biomedical applications of liposomes: a review. *J Med Biomed Res.* **4**: 9-21.
- Ulanova, M., Tarkowski, A., Hahn-Zoric, M. & Hanson, L. (2001) The common vaccine adjuvant aluminum hydroxide up-regulates accessory properties of human monocytes via an interleukin-4-dependent mechanism. *Infect Immun.* **69**: 1151-1159.
- Ulrich, J. & Myers, K. (1995) Monophosphoryl lipid A as an adjuvant. In Vaccine design: the subunit and adjuvant approach. New York: Plenum Press.
- Unger, E., Fritz, T., Matsunaga, T., Ramaswami, V., Yellowhair, D. & Wu, G. (1999) Methods of preparing gas-filled liposomes. ImaRx Pharmaceutical Corp. (Tucson, AZ) patent, 08/758179 US.
- Unger, E., Porter, T., Culp, W., Labell, R., Matsunaga, T. & Zutshi, R. (2004) Therapeutic applications of lipid-coated microbubble. *Adv Drug Deliv Rev.* **56**: 1291-1314.
- van Duin, D., Medzhitov, R. & Shaw, A. (2006) Triggering TLR signaling in vaccination. *Trends Immunol.* **27**: 49-55.

- van Rooij, E., Glansbeek, H., Hilgers, L., Te Lintelo, E., De Visser, Y., Boersma, W., Haagmans, B. & Bianchi, A. (2002) Protective antiviral immune responses to pseudorabies virus induced by DNA vaccination using dimethyldioctadecylammonium bromide as an adjuvant. *J Virol.* **76**: 10540-10545.
- van Slooten, M., Boerman, O., Romoren, K., Kedar, E., Crommelin, D. & Storm, G. (2001) Liposomes as sustained release system for human interferon-Q: biopharmaceutical aspects. *Biochem Biophys Acta.* **1530**: 134-145.
- van Vlerken, L., Vyas, T. & Amiji, M. (2007) Poly(ethylene glycol)-modified nanocarriers for tumor-targeted and intracellular delivery. *Pharm Res.* **24**: 1405-1414.
- Vangala, A., Kirby, D., Rosenkrands, I., Agger, E., Andersen, P. & Perrie, Y. (2006) A comparative study of cationic liposome and niosome-based adjuvant systems for protein subunit vaccines: characterisation, environmental scanning electron microscopy and immunisation studies in mice. *J Pharm Pharmacol.* **58**: 787-799.
- Vangala, A., Morris, R., Bencsik, M. & Perrie, Y. (2007a) Preparation and characterisation of gas-filled liposomes: Can they improve oil recovery? *J Liposome Res.* **17**: 263-272.
- Vangala, A., Bramwell, V., McNeil, S., Christensen, D., Agger, E. & Perrie, Y. (2007b) Comparison of vesicle based antigen delivery systems for delivery of hepatitis B surface antigen. *J Control Release.* **119**: 102-110.
- Van-Oss, C. (1978) Phagocytosis as a surface phenomenon. *Annu Rev Microbiol.* **32**: 19-39.
- Vertut-Doi, A., Ishiwata, H. & Miyajima, K. (1996) Binding and uptake of liposomes containing a poly(ethylene glycol) derivative of cholesterol (stealth liposomes) by the macrophage cell line J774: influence of PEG content and its molecular weight. *Biochim Biophys Acta.* **1278**: 19-28.
- Vieira, D. & Camona-Ribeiro, A. (2006) Cationic lipids and surfactants as antifungal agents: mode of action. *J Antimicrob Chemother.* **58**: 760-767.
- Vogel, F. (1995) Immunologic adjuvants for modern vaccine formulations. *Ann N Y Acad Sci.* **754**: 153-160.
- Waag, D., McCluskie, M., Zhang, N. & Krieg, A. (2006) A CpG oligonucleotide can protect mice from a low aerosol challenge dose of *Burkholderia mallei*. *Infect Immun.* **74**: 1944-1948.
- Wagner, H. (2004) The immunobiology of the TLR9 subfamily. *Trends Immunol.* **25**: 381-386.

Walsh, G. (2007) *Pharmaceutical Biotechnology, Concepts and Applications*. Chichester: John Wiley & Sons.

Wassef, N., Roerdink, F., Richardson, E. & Alving, C. (1984) Suppression of phagocytic function and phospholipid metabolism in macrophages by phosphatidylinositol liposomes. *Proc Natl Acad Sci USA*. **81**: 2655-2659.

Weiner, N., Martin, F. & Riaz, M. (1989) Liposomes as a drug delivery system. *Drug Dev Ind Pharm*. **15**: 1523-1554.

Weiner, G. J., Hsin-Ming, L., Wooldridge, J. E., Dahle, C. E. & Krieg, A. M. (2007) Immunostimulatory oligodeoxynucleotides containing the CpG motif are effective as immune adjuvants in tumor antigen immunization. *Proc Natl Acad Sci USA*. **94**: 10833-10837.

Weinstein, J. (1981) Liposomes as targeted drug carrier: a physical chemical perspective. *Pure Appl Chem*. **53**: 2241-2254.

Werling, D. & Jungi, T. W. (2003) Toll-like receptors linking innate and adaptive immune response. *Vet Immunol Immunopathol*. **91**: 1-12.

Win, K. & Feng, S. (2005) Effects of particle size and surface coating on cellular uptake of polymeric nanoparticles for oral delivery of anticancer drugs. *Biomaterials*. **26**: 2713-2722.

Yamagami, H., Matsumoto, T., Fujiwara, N., Arakawa, T., Kaneda, K., Yano, I. & Kobayashi, K. (2001) Trehalose 6,6'-Dimycolate (cord factor) of *Mycobacterium tuberculosis* induces foreign-body- and hypersensitivity-type granulomas in mice. *Infect Immun*. **69**: 810-815.

Yamaoka, T., Tabata, Y. & Ikada, Y. (1994) Distribution and tissue uptake of poly(ethylene glycol) with different molecular weights after intravenous administration in mice. *J Pharm Sci*. **83**: 601-606.

Yoshida, A., Hashizaki, K., Yamauchi, H., Hideki, S., Yokoyama, S. & Abe, M. (1999) Effect of lipid with covalently attached poly(ethylene glycol) on the surface properties of liposomal bilayer membranes. *Langmuir*. **15**: 2333-2337.

Zadi, B. & Gregoriadis, G. (2000) A novel method for the high-yield entrapment of solutes into small liposomes. *J Liposome Res*. **10**: 73-80.

Zagzebski, J. (1996) *Essentials of ultrasound physics*. St. Louis: Mosby.

Zaks, K., Jordan, M., Guth, A., Sellins, K., Kedl, R., Izzo, A., Bosio, C. & Dow, S. (2006) Efficient immunization and cross-priming by vaccine adjuvants containing TLR3 or TLR9 agonists complexed to cationic liposomes. *J Immunol*. **176**: 7335-7345.

Zee-Cheng, R. & Cheng, C. (1989) Delivery of anticancer drugs. *Meth Find Exp Clin Pharmacol.* **11**, 439-529.

Zhang, Y.-P., Ceh, B. & Lasic, D. (2002) Liposomes in Drug Delivery. In Dumitriu, S. (Ed.) *Polymeric Biomaterials*. New York: Marcel Dekkel.

Zhang, L., Gu, F., Chan, J., Wang, A., Langer, R. & Farokhzad, O. (2008) Nanoparticles in Medicine: Therapeutic Applications and Developments. *Clinical Pharmacol Ther.* **83**: 761-769.

Zhu, B., Qie, Y., Wang, J., Zhang, Y., Wang, Q., Xu, Y. & Wang, H. (2007) Chitosan microspheres enhance the immunogenicity of an Ag85B-based fusion protein containing multiple T-cell epitopes of *Mycobacterium tuberculosis*. *Eur J Pharm Biopharm.* **66**: 318-326.

Zimmermann, S., Dalpke, A. & Heeg, K. (2008) CpG oligonucleotides as adjuvant in therapeutic vaccines against parasitic infections. *Int J Med Microbiol.* **298**: 39-44.